VOLUME 18 NOVEMBER, 1930 NUMBER 11

PROCEEDINGS
of
The Institute of Radio Engineers

Form for Change of Mailing Address or Business Title on Page XLIII

Institute of Radio Engineers

Forthcoming Meetings

CINCINNATI SECTION

November 18, 1930
December 16, 1930

DETROIT SECTION

November 21, 1930

LOS ANGELES SECTION

November 17, 1930

NEW YORK MEETING

A Summary of High-Frequency Developments by H. H. Beverage
RCA Communications, New York City

December 3, 1930

PHILADELPHIA SECTION

November 18, 1930

ROCHESTER FALL MEETING

November 21, 1930

SAN FRANCISCO SECTION

November 19, 1930
December 17, 1930

DR. A. W. HULL

ALBERT WALLACE HULL
Morris Liebmann Memorial Prize Recipient for 1930

Dr. Albert W. Hull was born in Southington, Conn., April 19, 1880. After being graduated from the Torrington, Conn., High School he obtained his A. B. degree in 1905 and his Ph. D. degree in 1909 from Yale University. He received the degree of Sc. D. from Union College in 1930.

He became an instructor in physics at the Worcestor Polytechnic Institute in 1909, assuming an assistant professorship in 1912.

In 1914 he joined the Research Laboratory of the General Electric Company at Schenectady as a physicist and in the succeeding years has been responsible for a number of important developments in the field of electronics. He is the inventor of the dynatron, magnetron, screen-grid pliotron, and phanotron.

In 1923 he was the recipient of the Howard N. Potts medal of the Franklin Institute for work on X-ray crystal analysis.

He was awarded the Morris Liebmann Memorial Prize of the Institute of Radio Engineers for 1930 in recognition of the many advances in vacuum tube development which were due to his fundamental researches in the field of electronics.

October Meeting of the Board of Direction

The October meeting of the Board of Direction of the Institute was held on October 1st at the office of the Institute, 33 West 39th Street, New York City, the following being in attendance: Alfred N. Goldsmith, acting chairman; Melville Eastham, treasurer; R. A. Heising, J. V. L. Hogan, L. M. Hull, R. H. Manson, R. H. Marriott, A. F. Van Dyck, and H. P. Westman, secretary.

Seventy-eight applications for Associate membership and five applications for Junior membership were approved.

An invitation of the American Standards Association for the Institute to become a member body of that organization was accepted. This affiliation will assist the Institute greatly in the prosecution of its present standardization program, particularly in so far as the Institute's sponsorship of the Sectional Committee on Radio which operates under A. S. A. procedure is concerned.

Proceedings Binders

For the benefit of those who desire some method whereby they may preserve their copies of the Proceedings as they are received, special binders have been prepared. These binders may be obtained in two sizes, the smaller of which will accommodate yearly sets of Proceedings issued prior to 1929. The larger size is capable of holding the yearly issues for 1929 and 1930.

When ordering be sure to specify the size binder desired. The smaller size is available at $1.50 while the larger costs $1.75. The member's name will be stamped on the binder for 50¢ additional.

Associate Application Form

For the benefit of members who desire to have available each month an application form for Associate membership, there is printed in the PROCEEDINGS a condensed Associate form. In this issue this application will be found on page XXXIII of the advertising section.

Application forms for the Member or Fellow grades may be obtained upon application to the Institute office.

The Committee on Membership asks that members of the Institute bring the aims and activities of the Institute to the attention of desirable and eligible nonmembers. The condensed form in the advertising section of the PROCEEDINGS each month may be helpful.

Radio Signal Transmissions of Standard Frequency

The following is a schedule of radio signals of standard frequencies for use by the public in calibrating frequency standards and transmitting and receiving apparatus as transmitted from station WWV of the Bureau of Standards, Washington, D. C.

Further information regarding these schedules and how to utilize the transmissions can be found on pages 10 and 11 of the January, 1930, issue of the PROCEEDINGS, and in the Bureau of Standards Letter Circular No. 171, which may be obtained by applying to the Bureau of Standards, Washington, D. C.

Eastern Standard Time	Nov. 20	Dec. 22
10:00 P.M.	4000	550
10:12	4400	600
10:24	4800	700
10:36	5200	800
10:48	5800	1000
11:00	6400	1200
11:12	7000	1400
11:24	7600	1500

Committee Work

COMMITTEE ON ADMISSIONS AND COMMITTEE ON MEMBERSHIP

A joint meeting of the Committee on Admissions and the Committee on Membership was held at 7 P.M. on Tuesday, September 30th, 1930, at the office of the Institute, 33 West 39th Street, New York City.

At this meeting recommendations made by the Committee on Membership for transferring members of the Institute to higher grades of membership were considered and thirty-four transfers to the Member grade and three transfers to the Fellow grade were approved. After approval by the Board of Direction, these members will be requested to submit applications for transfer to higher grades. Such applications will not require the listing of sponsors as the members involved have already been investigated and approved for the transfers.

Those present at the above meeting were as follows, the members of the Committee on Admissions being listed first: R. A. Heising, chairman, Committee on Admissions; C. N. Anderson, J. S. Smith, E. R. Shute, and A. F. Van Dyck. The representatives of the Committee on Membership were I. S. Coggeshall, chairman; H. Gawler, S. R. Montcalm, A. F. Murray, C. R. Rowe, A. M. Trogner. H. P. Westman, secretary, was also in attendance.

Committee on Broadcasting

A meeting of the Committee on Broadcasting was held at 1 P.M. on Wednesday, October 1st, at the office of the Institute. It was attended by L. M. Hull, chairman; P. A. Greene, Raymond Guy, J. V. L. Hogan, C. W. Horn, and E. L. Nelson.

Report No. 10 dealing with the service areas of broadcast stations was completed.

Committee on Constitution and Laws

A meeting of the Committee on Constitution and Laws was held at 5 P.M. in the office of the Institute on September 30th. It was attended by R. H. Marriott, chairman; Melville Eastham, W.G.H. Finch, and H. E. Hallborg. Another meeting of the committee was held at 11 A.M. the following morning, R. H. Marriott, chairman, W. G. H. Finch, H. E. Hallborg, and R. A. Heising being present.

STANDARDIZATION

Committee on Standardization

Two meetings of the main Committee on Standardization of the Institute were held to pass upon a portion of the work which has already been accomplished by the various technical committees and subcommittees of the technical committees. Material which is approved by the Committee of Standardization is then submitted to the Board of Direction for final approval prior to its being published in the next report of the Committee on Standardization which will probably be contained in the 1931 Year Book.

The first meeting of the Committee to pass upon the reports made by the various technical committees was held at 9:30 A.M. on October 3rd at the office of the Institute, the following being in attendance: J. H. Dellinger, chairman; L. G. Bostwick (representing H. A. Frederick), E. L. Bowles, Stuart Ballantine, T.A.M. Craven, T. McL. Davis, E. T. Dickey, P. H. Evans, C. B. Huffman (representing A. B. DuMont), E. L. Nelson, Haraden Pratt, A. F. Rose, H. M. Turner, J. C. Warner, Donald Whiting, L. E. Whittemore, Adney Wyeth (representing L. G. Pacent), H. P. Westman, secretary, and B. Dudley, assistant secretary.

The second day's session which was held at 9:30 on October 4th was attended by J. H. Dellinger, chairman; L. G. Bostwick (representing H. A. Frederick), E. L. Bowles, T. McL. Davis, E. T. Dickey, Haraden Pratt, H. M. Turner, Donald Whiting, L. E. Whittemore,

Adney Wyeth (representing L. G. Pacent), H. P. Westman, secretary, and B. Dudley, assistant secretary.

A large number of definitions and other items regarding methods of tests and provisions for safety were discussed. Practically all were approved as submitted by the technical committees although minor changes were made in a few instances and a small number were referred back to the technical committees for further consideration. It is anticipated that final reports of all the technical committees will be available shortly and will be considered at a subsequent meeting of the Committee on Standardization.

Technical Committee on Radio Receivers—I.R.E.

A meeting of the Technical Committee on Radio Receivers of the I.R.E. was held at 10 A.M. on September 30th at the office of the Institute, the following being present: E. T. Dickey, chairman; C. M. Burrill, Malcolm Ferris, V. F. Greaves, W. A. MacDonald, E. J. T. Moore, F. X. Rettenmeyer, and B. Dudley, secretary.

Technical Committee on Radio Transmitters and Antennas—I.R.E.

The above technical committee met at 10 A.M. on September 12th at the office of the Institute. Those in attendance were Haraden Pratt, chairman; H. E. Hallborg, D. G. Little, W. Wilson, and B. Dudley, secretary.

Subcommittee on Nomenclature of the Technical Committee on Radio Transmitters and Antennas.—I.R.E.

The Subcommittee on Nomenclature, operating under the Technical Committee on Radio Transmitters and Antennas held a meeting at 10 A.M. on Thursday, October 2nd, with the following in attendance; Haraden Pratt, chairman; R. M. Wilmotte, and W. Wilson.

Technical Committee on Vacuum Tubes—I.R.E.

At 9:30 A.M. on Thursday, October 2nd, a meeting of the Technical Committee on Vacuum Tubes was held. It was attended by Stuart Ballantine, chairman; H. F. Dart, F. H. Engel, K. Henney (nonmember), M. J. Kelly, C. G. McIlwraith, Dayton Ulrey, J. C. Warner, K. S. Weaver (representing B. E. Shackelford), and B. Dudley secretary.

Technical Committee on Vacuum Tubes—A.S.A.

A meeting of the Technical Committee on Vacuum Tubes, operating under the Sectional Committee on Radio of the American Stan-

dards Association was held at 3:30 P.M. on Thursday, October 2nd. Those in attendance were J. C. Warner, chairman; A. B. DuMont, F. H. Engel, M. J. Kelly, Ernest Krause, K. S. Weaver (representing B. E. Shackelford), Paul Watson, P. T. Weeks, R.E.A. Putnan, and B. Dudley, secretary.

Institute Meetings

New York Meeting

The October New York meeting of the Institute was held on October 1st in the Engineering Societies Building, 33 West 39th Street, New York City. The paper presented at the meeting was "Ten Years of Radio Broadcasting" by C. W. Horn, General Engineer, National Broadcasting Co., New York City. The summary of the paper follows:

"The history of the development of broadcasting is briefly reviewed. The outstanding points in connection with the development of both transmitting and receiving broacast apparatus are presented, together with some discussion illustrating the tendency in design as influenced by practical operating conditions. A brief review is made of the history of network broadcasting and its influence on the industry as a whole. The influence of broadcasting on other radio developments is portrayed, as well as the influence of broadcasting on modern customs and culture. Some comments are made as to research and advance development work in radio."

Atlanta Section

The September meeting of the Atlanta Section was held on the 12th of the month in the Roof Garden of the Cecil Hotel, Harry F. Dobbs, chairman, presiding.

Although no regular paper was scheduled for this meeting a general discussion of various transmitting circuits was participated in by those present.

The election of officers for the forthcoming year resulted as follows: chairman, Harry F. Dobbs; vice chairman, H. L. Wills; and secretary-treasurer, P. C. Bangs.

The attendance at the meeting was fourteen.

Cincinnati Section

Ralph H. Langley, chairman of the Cincinnati Section, presided at the September 16th meeting of the Section.

Two papers were delivered at this meeting, the first of which by C. E. Kilgour, chief research engineer of the Crosley Radio Corpora-

tion, covered the subject of "Graphical Analysis of Output Tube Performance." The method of drawing a line representing the load resistance curve on a family of curves of plate current against plate voltage which is suitable for use with a simple resistance load was described. In addition, an accurate application of the graphic method when the load resistance is coupled to the tube by a transformer, or a choke and condenser was given. Slides and diagrams were employed to illustrate typical examples.

The second paper of the evening on the "Performance of Output Pentodes" was presented by J. M. Glessner of the research division of the Crosley Radio Corporation. In this paper the performance and distortion of output pentodes was compared with that of corresponding triodes. The following important factors were considered: power output, power sensitivity, a-c/d-c economy and fidelity. A brief description of the method and apparatus employed was included. Tables summarizing the results were distributed in addition to other illustrations projected from slides.

Messrs. Austin, Israel, Loftis, Osterbrock, and Rockwell of the sixty members and guests in attendance entered into the discussion of the papers.

Detroit Section

A meeting of the Detroit Section was held in the Detroit News Conference Room on September 19th, L. N. Holland, chairman, presiding.

A paper on the requisites essential for a successful radio manufacturer was presented by J. A. Frye, president of Frye-Glasser, Inc., of Detroit, Mich.

The meeting was attended by fifty members and guests.

Pittsburgh Section

A meeting of the Pittsburgh Section held on September 16th was presided over by A. J. Buzzard, chairman of the Section, twenty-six members being in attendance.

A paper on "Construction and Testing of Vacuum Tubes and Details of the 230,-231,-and 232-Type Tubes" was delivered by Roger M. Wise of the Sylvania Products Co.

In his paper, Mr. Wise discussed the methods used for testing materials required in tube manufacturing, the essential limits to which the product must conform and showed a series of slides illustrating the manufacturing operations and equipment employed in a tube factory.

The new two-volt series of tubes were described and the meeting

was then opened to general discussion which was participated in by Messrs. Donbar, Hetznecker, Mag, McKinley, Storm, Sunnergren, Sutherlin, and Terven.

A report on the Toronto convention was submitted by J. G. Allen and read by L. A. Terven due to the absence of Mr. Allen.

San Francisco Section

A meeting of the San Francisco Section was held on July 2nd at the Engineers' Club, Walter D. Kellogg, presiding.

Dr. Lee deForest, President of the Institute, read an interesting paper on the history, development and trend of the radio industry.

Fifty members and guests attended the meeting.

The September meeting of the San Francisco Section was held in the Engineers' Club on the 17th of the month, Walter D. Kellogg, chairman, presiding.

A paper on "The Boeing Communication System" was presented by Robert H. Freeman who described the communication system used by the Boeing Air lines both as a systems problem and as a radio engineering problem. The ignition shielding equipment was described and a set of shielded spark plugs showing the development in this field from some of the earlier experimental models to the latest types was displayed. A receiver of the type used in the planes was demonstrated by the reception of plane and ground telephone transmissions.

In addition to the above paper, Arthur Batcheller, a Manager of the Institute, who was visiting San Francisco gave a short sketch of his work in the Department of Commerce as a traveling Supervisor of Radio.

A report on the Toronto convention was made by Ralph Heintz who attended it.

Washington Section

At the September 11th meeting of the Washington Section, presided over by L. P. Wheeler, chairman, Malcolm P. Hanson, chief radio engineer of the Byrd Antarctic Expedition delivered a paper on the part radio played in the Byrd Expedition to the South Pole.

Many detailed lantern slides were shown to illustrate the conditions under which the expedition worked. The value of radio communication was pointed out and experiences obtained with electrical equipment other than radio were mentioned.

Oscillograms showing values of signal strength as received from a constant amplitude wave sent from Bellevue indicating rapid fluctuations with periods as short as 1/40 second were presented. Oscillo-

grams of reflections as well as of reception of phone signals from the United States show that fading due to a displacement of the Heaviside layer is much greater in winter than in summer due to the lack of ionization during the long winter night.

Fading records were kept of many stations on different frequencies and many hundreds of oscillograms will have to be analyzed before all of the accumulated information can be correlated and made of greatest usefulness.

The meeting was attended by one hundred and seventy members and guests.

Personal Mention

George N. Allaway, formerly engineer in charge of the Durban Broadcasting Station in Durban, South Africa, is now a radio engineer for the Phillips South African Electric Corporation at Durban.

Prescott N. Arnold, previously a research associate with the Bureau of Standards has left there for Harvard University where he is now a graduate student.

Stuart L. Bailey has left the Bureau of Lighthouses where he was employed as a radio engineer to become a partner with Professor C. M. Jansky, Jr. in the firm of Jansky & Bailey, National Press Building, Washington, D.C. Jansky and Bailey specialize in the technical problems of allocation and broadcast coverage.

Major L. B. Bender has been assigned to duty at the Army War College in Washington, D.C. He was previously located at Fort Monmouth, Oceanport, N.J.

K. Charlton Black formerly a physicist at the Boonton Research Corporation has entered the Bell Telephone Laboratory at 180 Varick Street, New York City, as an engineer.

Paul Brake has recently joined the technical staff of the Bell Telephone Laboratories at 463 West St., New York City.

Charles A. Brokaw has left the General Electric Company at Schenectady to become a radio engineer for the RCA-Victor Company at Camden, N.J.

Formerly a radio engineer for the RCA-Victor Company at Camden, I. F. Byrnes is now an engineer for the Radiomarine Corporation at 66 Broad St., New York City.

Robert W. Clark has left the RCA station at Bolinas, Calif., to become recording engineer for the Pathé Sound News at San Francisco.

Formerly a radio engineer of the Radio Corporation of America,

Murray G. Crosby has taken a similar position with RCA Communicacations, Inc., at Riverhead, N.Y.

Previously in the engineering department of the Wireless Specialty Apparatus Company, Edwin B. Dallin is now an engineer for the Submarine Signal Company at 160 State St., Boston, Mass.

Roy Dally is now a sound engineer for the Webster Electric Company at Racine, Wis., previously being with the General Motors Radio Corporation.

Daniel R. Donovan, formerly with the Westinghouse Lamp Company is now vice president of the Radio Products Company at Newark, N. J.

Formerly a government radio inspector at Saskatoon, Canada, K. M. Durkee has joined the radio department of the General Electric Company at Schenectady.

Formerly in the research laboratory of the National Carbon Company, John T. Filgate has entered the engineering department of the General Motors Radio Corporation at Dayton, Ohio.

William J. Gillule, has joined the staff of the Mackay Radio and Telegraph Company at 33 S. William St., New York City, as a radio compass engineer. He was formerly in the engineering department of the Kolster Radio Corporation at Newark, N.J.

Ralph A. Hackbusch has left the engineering department of Canadian Brandes, Ltd., to join the radio engineering staff of the Stromberg-Carlson Telephone Manufacturing Company at 211 Geary Avenue, Toronto, Ont., Canada.

Norman L. Jacklin has entered the radio transmitter department of the General Electric Company at Schenectady.

Previously superintendent of lighthouses in Detroit, W. E. Jackson has become a radio engineer in the airways division of the Department of Commerce.

Lieutenant C. M. Johnson has been transferred from the USS Bridge to the Naval Air Station at Lakehurst, N. J.

Arthur G. Manke, formerly with the Earl Radio Corporation has entered the engineering department of the RCA-Victor Company at Camden.

John F. Maxwell has been transferred from the Oakland, Calif., branch of the General Electric Company to Schenectady, N.Y.

Formerly engineer in charge of WMU of the Southern Radio Corporation, W. G. McConnel has joined the staff of the DeForest Radio Tube Company of Passaic as design engineer.

Vern D. Mills, has left the Radio Corporation of America to become field engineer for the National Broadcasting Company in their Chicago district.

William H. Moore is now a radio engineer for the Canadian Marconi Company at Montreal, having previously been a demonstrator in the physics department of McGill University.

Howard K. Morgan has left the radio engineering department of the General Electric Company at Schenectady to join the staff of the RCA-Victor Company at Camden as a radio engineer.

Harry J. Nichols has left the radio engineering department of the Westinghouse Electric and Manufacturing Company at East Pittsburgh to become chief engineer for the General Motors Radio Corporation at Dayton, Ohio.

Noel C. Olmstead has joined the staff of the American Telephone and Telegraph Company as an engineer.

Nils Johann Oman, formerly with the Bell Telephone Laboratories has joined the engineering staff of Wired Radio, Inc., at Newark, N.J.

Philip A. Richards has joined the development laboratory staff of RCA Radiotrons at Harrison, N.J., previously having been a vacuum tube engineer with the General Electric Company in Chicago.

Previously with the Radio Corporation of America, George Rodwin, has joined the technical staff of Bell Telephone Laboratories.

Another of those who has left the radio department of the General Electric Company at Schenectady to go with RCA-Victor at Camden, is Arnold J. Rohner.

C. R. Rowe is now a radio engineer for Wired Radio, Inc., at Ampere, N. J. He was formerly with the Kolster Radio Corporation.

Peter C. Sandretto is now a radio development engineer for the Bell Telephone Laboratories.

Garold D. Sears, previously manager of KGFF is now a radio engineer for the Transcontinental Air Transport-Maddux Air Lines at Waynoka, Okla.

Leaving the radio section of the Bureau of Standards, Robert S. Shankland has become an instructor in physics at the Case School of Applied Science at Cleveland, Ohio.

Kenneth S. Sherman is now a radio engineer for RCA-Victor, previously being with the General Electric Company at Schenectady.

Henry Tholstrup has left the radio engineering department of the Westinghouse Electric and Manufacturing Company at Chicopee Falls, Mass., to become a radio engineer for the General Motors Radio Corporation at Dayton, Ohio.

Previously with the General Electric Company at Schenectady, W. A. Tolson, has joined the staff of the RCA-Victor Company at Camden as a television engineer.

Kenneth G. Tyler is now with the radio engineering department of the RCA-Victor Company at Camden, having previously been a member of the radio engineering department of the General Electric Company at Schenectady.

Winfield G. Wagener, formerly a radio engineer for the Federal Telegraph Company at Palo Alto, Calif. is now on the radio engineering staff of Heintz & Kaufman, Ltd., South San Francisco, Calif.

Don C. Wallace is now zone manager for the General Motors Radio Corporation at Los Angeles, Calif.

Donald G. Ward has left RCA Communications at New Brunswick to join the engineering department of the RCA-Victor Company at Camden.

Edwin L. White has joined the engineering staff of the Federal Radio Commission, formerly being a radio engineer in the signal office headquarters at Ft. Shafter, Hawaii.

John A. Willoughby, formerly a radio engineer for Aladdin Industries, Inc., is now a senior radio engineer under the Federal Radio Commission at Washington.

Proceedings of the Institute of Radio Engineers
Volume 18, Number 11 *November, 1930*

ADDRESS OF WELCOME*

By

Dr. Lee de Forest

(President, Institute of Radio Engineers)

FELLOW members of the Institute, Friends of the Radio Manufacturers' Association, and other guests:

It is with befitting pride that we open the fifth National, the first International, Convention, of the Institute. It is a striking indication of the magnitude and genuine worth of our past history, and a significant augury of our world destiny, that we have thus already outgrown national boundaries. And since no instrumentality of man's creation has achieved more, or will more potently act, to bring the varied nations and the peoples of the earth to a common understanding and acquaintanceship than the radio broadcast and radio communication it is indeed appropriate that we assemble this year as the guests of a foreign nation.

We are proud to report that 17 per cent of our total membership of 5695, marking a very rapid increase during the past two years, is located outside of the United States. It is reasonable therefore to assume that the amazing activities of our members now so well scattered over the globe, as indicated each month in the extraordinarily high quality of papers appearing in the Proceedings of the Institute, will win more and more a deserved increase in our membership abroad and the highest pride everywhere in the technical achievements of our members.

Already the physicist, the geographer, even the astronomer, the medical investigator, and the general scientist, finds in the issues of our Proceedings papers of exceptional information and suggestive value. The same holds to an ever-increasing degree for the industrialist in almost any field of endeavor.

I regard it as highly significant of the protean province and influence of the radio art on humanity and modern civilization that this year witnessed the birth of a new, already powerful, magazine devoted wholly to the application of the electron and its tube to science and industry. That the development of radio has been almost completely responsible for this interesting state of facts cannot be disputed. We members of the Institute of Radio Engineers have just cause, therefore,

* Delivered before the Fifth Annual Convention of the Institute, Toronto, Canada, at its opening session, Monday, August 18, 1930.

for a great and growing pride in our profession. In the truest, least debatable sense of the word, we may consider ourselves benefactors.

The record of the Institute since the 1929 Convention in Washington is indeed gratifying. The report of our secretary for 1929, recently published in the 1930 Year Book, is most encouraging. I wish I could quote it at length.

Touching on the subject of Committees, Mr. Clayton writes:

"Under the direction and supervision of the Board of Direction the major activities of the Institute were carried on by twelve committees and eleven subcommittees. It is unfortunate that members of the Institute cannot be afforded the opportunity to acknowledge their debt of appreciation to these important bodies without whose continuous assistance their Institute could not conduct any of its work. These gentlemen, during 1929, have given unsparingly of their time and counsel to the variegated problems, both routine and constructive, which are involved in every phase of the carrying out of policies handed down by the Board of Direction. Members serving on any of the Institute committees are making a very direct and distinct contribution to the radio art.

"Particularly deserving of the gratitude of the Institute is the Committee on Meetings and Papers, with K. S. Van Dyke, chairman. The extensive editorial work and careful reading of a very large number of highly technical papers conducted by this committee can scarcely be estimated. Last year 185 papers were secured for publication. Of these 126 were accepted by the Board of Editors of the Proceedings under the tireless chairmanship of W. G. Cady.

"The commendable increase in our membership is chiefly due to the efficiency and energy of the Committee on Membership.

"The 1928 Committee on Standardization carried over through 1929 and has largely the same membership for this year. Eighty-five hundred copies of its report published in the 1929 Year Book of the Institute have been distributed.

"This report constitutes a contribution to technical radio literature of utmost value. Under the chairmanship of Dr. Dellinger the splendidly efficient work of this Committee is continuing with main technical committees devoted respectively to Radio Receivers, Radio Transmitters and Antennas, Vacuum Tubes, Electro-Acoustic Devices, each of these divisions functioning with several subcommittees. Our Standardization Committee is working in close collaboration with other organizations in similar fields."

The efficiency of the Program Committee for this Toronto Convention is abundantly evidenced by the fine list of technical papers

which are here for your enjoyment and instruction. In diversity and interest of topics I consider the program unusually fortunate. The Institute is deeply in debt to the authors of such capable papers.

During 1929 the Institute was represented by delegates to the Engineering Congresses or celebrations at Tokyo, Washington, Berlin, Des Moines, The Hague; and this past summer sent Dr. Dellinger as special delegate to the meeting of the International Electrotechnical Commission at Stockholm and Copenhagen.

This fall marks the eighteenth anniversary of the Institute. Its personnel therefore may claim to combine the experience of age with the energy of youth. For in an industry rushing forward with the ever-increasing speed, the ever-expanding scope of radio eighteen years is indeed an age, while a never tiring enthusiasm seems to distinguish the ever young in this game to a far more marked degree than in any other profession. If one cannot say that radio engineering did not exist prior to the foundation of the Institute it is indisputable that practically all of the radio and sound-projection sciences as they exist today have been brought to application by men who are members of this international organization of engineers.

The quality which more than any other distinguishes radio from the other branches of engineering is its human relationship, its peculiar and intimate contact with and influence upon the human mind, the intimate daily home life, nay, the very spiritual life of man. In this respect, in the ability of radio to influence the mind of man, to mold his daily manner of life and thinking, his mode of entertainment, even his religious habits—we have created, all unintentionally perhaps, but none the less effectively, an instrumentality the like of which all history showeth not.

Therefore it well behooves us members of the Institute of Radio Engineers to pause occasionally in the midst of our hurried hours with slide rule and frequency measurements, and fascinating inventive frenzy, to consider calmly and frankly the civic, the humanitarian, and the moral aspects and influences of Radio upon our people and our civilization.

For, after all, this it is which so deeply intrigues most of us in our work, and has so keenly fastened upon us the unflagging interest of all the modern world. We may little realize such to be the case, but it is none the less true.

It is therefore our duty, as well as rare privilege, to consider frankly and critically the manner of use and application which is being made of this magnificent means of human contact and influence, which we chiefly are responsible for having created and developed.

I sadly deplore the attitude of some radio engineers that since ours is an engineering organization we should "stick to our knitting," should occupy ourselves wholly with the engineering aspects of radio, and leave to the manufacturers and the outside business men who have recently come into the picture to direct this great growing thing, the radio broadcast.

With this attitude and tendency I have scant patience. For it there might be much justification in ordinary lines of electrical and other engineering. But we have invented, created, and caused to grow up not merely a marvellous electrical device to lighten man's labor, like electric power, or to lengthen his waking hours by electric light—we have created something finer, more powerful—farther reaching than all these—dealing intimately with every phase and age and strata of home and family and society. Therefore we members of this Institute should be jealous of the good name, regardful of a wise supervision of this broadcast institution.

In my inaugural address last January I sought to point out a very real danger to the fullest usefulness and enjoyment which radio has power to confer, a menace steadily growing greater, more ruthless, more deserving of suspicion, and more generally detested—the use of the broadcast for direct and blatant advertising—in larger and longer doses. Subsequent observation and active inquiry has convinced me that the warning to the radio industry then sounded was not a needless fear.

If we consider the prosperity of the industry alone, the possibly lessened sales of sets, the unquestionably lessened hours of listening by the public resulting from this abuse by direct advertising—we engineers, dependent on radio for our livelihood, have ample ground for emphatic protest. But there are higher, less selfish considerations which may well inspire a fear in our minds—the thought that short-sighted avarice is at work to curtail the usefulness, the beneficence of radio, in the home, in the school, as a means of entertainment, of education, of uplift generally. Unless this evil is voluntarily cured (and without earnest organized protest it won't be cured), we are headed straight for government regulation, with taxation, possibly censorship, and all the evils and all the benefits of government control. Already certain states are framing radio taxation measures—Canada, our host, has followed her mother country, and now levies a tax on each radio receiver.

Or else the present deplorable and worse-becoming conditions in the States will rapidly hasten the entry of wired-radio into our homes—entertainment freed from interference, static, fading, and purged of all

advertising. I am willing to stake seriously what reputation I may have as a prophet on this prediction. The wired-radio era lies ahead, in any event. It rests largely with the attitude of the radio advertiser and the broadcaster how rapidly this situation will come upon us.

Therefore, as loyal citizens of the state, regardful of the best interests of all its citizens, and as engineers of radio, jealous of its highest good, let us protest this situation, and protect its future.

This year of our first International Convention coincides with the gratifying progress made in international broadcasting, and calls attention of engineers the world over to the manifold problems of short wave communication yet to be solved. Multiple receiving antennas, a common receiver and automatic volume control, possibly combined with double polarized transmitted waves of greater power, will shortly bring to pass the nightly exchange of foreign programs.

We already have the international language, music, and we shall learn much to our advantage from many foreign programs. Then, indeed, will be realized the benign power of the radio broadcast to draw together into a common fellowship of understanding the varied peoples of the earth, strangers and enemies no longer.

Ten years ago commercial radio broadcasting began. Ten years ago this month the Detroit Daily News opened the first daily newspaper radio broadcast service at station WWD, which station has since remained steadily in operation, the real pioneer of all existing broadcasters. The influence of radio on the Press has now become profound. The problem of the relations of newspapers and broadcasters claimed the close attention of five hundred newspaper publishers at a recent convention in New York. While agreeing that radio can never supersede the newspaper, a basis was earnestly sought as to how to deal fairly and reasonably with the new medium which is at once a source of news and of commercial competition. While its inherent limitations will never permit it to supplant newsprint, yet radio has largely eliminated extras on prize fight results, and has shown a curtailment of interest in baseball news. But radio has this limitation, that it must present its programs when the broadcasters choose and not when the listeners desire it.

Radio's debt to the newspaper, for daily program notices, program reviews, and for their generous radio sections, is beyond all computation. Unquestionably it was this astonishing interest on the part of the press in broadcasting during its early struggling days, ten years ago, which alone enabled it to survive those crucial years until an awakened popular interest made radio self-supporting. I sincerely feel therefore that the debt today lies heavily on radio's side of the

ledger—a debt which will be partially repaid only when certain forms of advertising most obviously ill-suited for radio's medium go back to the printed sheet.

Toronto! This city has a special appeal to me, who can never forget the terrific difficulties experienced in the winter of 1903 in establishing the first wireless communication down frozen Lake Ontario to Hamilton only 40 miles away. And three years later when by stringing a short antenna wire between two telegraph poles along the railroad near Hamilton I demonstrated the correctness of my theory that all such wires acted as a wave-chute and gathered in radio waves from great distances; when I picked up strong signals from Toronto and Ottawa. This was, I believe, the first demonstration of "wired-wireless." And in 1919 over the power wires of the Dominion Hydro-electric system between Toronto and Hamilton in coöperation with the Automatic Telephone Company we operated what I believe was the first complete two-way carrier-current telephone service over power wires, using radio frequencies. Thus Toronto has played an early rôle in important developments in radio.

And today Toronto stands high among the leading cities in America in the engineering development and manufacture of radio equipment. Second only to London as a radio center in all the vast British Empire her radio establishments are deservedly objects of pride throughout the Dominion.

A glance at the unusually varied program of papers provided for this Convention is convincing that we members of the Institute will indeed be well repaid for our visit to Toronto. Among all the topics listed however that one which appeals most eloquently to me (for reasons which my earlier remarks surely make clear)—is entitled: "The Rôle of Radio in the Growth of International Communication." That this title might well be expanded to read: "In the Growth of International Friendship and Good Will" will, I firmly believe, be clearly evidenced by the success of this our First International Convention.

Part II
TECHNICAL PAPERS

Proceedings of the Institute of Radio Engineers
Volume 18, Number 11 *November, 1930*

THE DIURNAL AND SEASONAL PERFORMANCE OF HIGH-FREQUENCY RADIO TRANSMISSION OVER VARIOUS LONG DISTANCE CIRCUITS*

By

M. L. PRESCOTT

(Radio Engineering Department, General Electric Co., Schenectady, N. Y.)

Summary—*This paper presents a quantity of radio wave propagation data that has been obtained during the past six years by the General Electric Company through the use of its developmental transmission facilities at South Schenectady, New York.*

Nineteen radio circuits which radiate in various directions from Schenectady are treated. These circuits range in length from 2300 to 11,400 miles. Data are given which will aid in determining the proper frequency to use in any high-frequency radio circuit from 1000 to 10,000 miles in length.

It is shown that the daylight-darkness distribution over the path of propagation largely determines the diurnal and seasonal performance of high-frequency transmissions.

FOR some time, particularly during the last two or three years, constantly increasing needs have been evidenced for data that are readily applicable to the solution of practical radio transmission problems that involve frequency selection, consideration of diurnal and seasonal variations, etc. These needs have originated largely from the demand for the establishment of long distance high-frequency commercial circuits and have more recently been stimulated by the advent of transoceanic developmental relay broadcasting.

Through the treatment herein of a number of typical long radio circuits, it is believed that data are presented which will provide:

(1) A source of high-frequency radio propagation data for use in the treating of long distance high-frequency radio circuits.

(2) Data that will show the diurnal and seasonal performance of the high-frequency broadcast transmissions from the General Electric stations W2XAD (15,340kc) and W2XAF (9530kc).

It is a fairly well established fact that the reception characteristics of signals from high-frequency radio transmitters (i.e., about 6000kc to the highest frequency now in commercial use) are subject to wide day-to-day variations. So pronounced are these variations that the

* Decimal classification: R113.2. Original manuscript received by the Institute, July 16, 1930.

over-all utility of the signal becomes a variable quantity whose value cannot be predetermined accurately. This factor of uncertainty is an appreciable handicap when dealing with high-frequency transmission since it does not readily permit of an accurate predetermination of the performance that will be rendered by a particular frequency at a given time.

When working with terminal apparatus interconnected by a metallic circuit, it is possible to set up and maintain relatively constant conditions over the circuit. In a radio circuit where the terminal transmitting and receiving equipments are separated in space, the interlinking medium is, of course, no longer provided metallically but by an intervening medium of ether, the conductivity of which is apparently variable, thereby making it almost impossible to maintain constant circuit conditions except for brief intervals.

Some of the Factors That Influence the Propagation of High-Frequency Radio Transmission

1. Ionization of the Earth's Atmosphere.

Relatively little is known regarding the changes that occur in the ethereal medium of propagation which exert such a great influence on high-frequency radio transmission.

During recent years, particularly since the advent of high-frequency transmission, much study has been accorded the earth's atmosphere with the view of determining the extent to which it affects the medium. The phenomenon of transmission around the globe which could not be explained by the diffraction theory apparently first led to the suggestions that the atmosphere may have some influence on the propagation as well as the absorption of radio waves. As investigations have progressed, it has become more and more evident that all radio transmission (particularly high-frequency transmission) over long distances is dependent upon the atmosphere and atmospheric phenomena to a hitherto unsuspected degree.

The theory has been advanced and is now generally accepted that the earth's atmosphere is subject to ionization by the sun and that many of the changes which occur in the propagating characteristics of the medium are produced by changes in the degree of ionization and the ionization gradient of the atmosphere. This theory affords a very logical explanation of many of the phenomena associated with high-

frequency radio propagation which would otherwise be difficult to explain. It appears, therefore, that many of the diurnal and seasonal variations in high-frequency radio transmission may be accounted for, either directly or indirectly, by variations in the ionization of the earth's atmosphere.

2. Length of Circuit.

In any radio circuit, the distance over which transmission is to be effected is an important factor. This is particularly true when utilizing high-frequency transmissions since there is a definite relationship between the length of the circuit and the frequency (or frequencies) to be utilized for the rendering of optimum service.

3. Direction of Transmission.

When dealing with high-frequency radio transmission, it is important that consideration be given to the direction of the receiving point from the transmitting station. North-south circuits differ from east-west circuits in that a higher degree of ionization normally prevails over the north-south circuit. This condition will cause the service range of a particular frequency to be dependent upon the direction of transmission. For instance, in a north-south circuit, the service range of a particular frequency may be from 2000 to 3000 miles. If this same frequency is utilized in an east-west circuit, the service range might begin at 2500 miles and extend to 4000 miles because of the difference in atmospheric ionization that prevails over the two paths.

Since the degree of ionization and the ionization gradient of the earth's atmosphere are produced mainly, either directly or indirectly by the sun, it follows that the daylight-darkness distribution of any long radio circuit is a matter of prime importance. In north-south circuits, the daylight-darkness distribution is usually such that the path of propagation is covered by complete daylight or complete darkness except for brief periods around sunrise and sunset, when the path may be part in daylight and part in darkness. In east-west circuits, the time during which the path is covered by all daylight or all darkness is generally much less than that for a north-south circuit of the same length; while the period during which the path is covered by part daylight and part darkness is correspondingly greater than for north-south circuits. These differences in daylight-darkness distribution not only cause the north-south and east-west circuit performances to differ, but are instrumental in making it necessary to use more frequencies for maintaining 24-hour service over east-west circuits than for 24-hour service over north-south circuits of corresponding length.

Daylight-Darkness Distribution Charts

Since this report deals mainly with the effect of daylight and darkness on the propagation of high-frequency radio transmissions, daylight-darkness distribution charts for each of the circuits considered in this paper have been prepared. These charts, as will be observed, have as an abscissa the 24 hours of the day, while the ordinate is the earth's circumference which is considered as being 24,900 miles. It is assumed that in traveling between any two points on the earth's surface, a radio signal follows a great circle path. It is probable that this is not always the case, but if there are deviations of a radio signal from the great circle path during propagation it appears that more data in this connection must be obtained before this phase can be treated in a paper of this nature. After radiation from the transmitting antenna, a radio signal may reach the receiving point by traversing either the short or long great circle path, or both. In the preparation of the daylight-darkness charts, provision has been made for showing the daylight-darkness distribution over both of these paths. In cases where the length of the circuit approaches the magnitude of one-half of the earth's circumference it is particularly important that both paths be considered since the signal is very likely to traverse both during the course of a day.

There are two ways in which to obtain the data from which daylight-darkness charts may be prepared. The first and more accurate method is to make the calculations through the use of spherical trigonometric formulas. However, this method is not practical because too much time is required to make the calculations. The second and more feasible method is to utilize a globe equipped with special features which permit the necessary data to be taken off directly.

A great circle projection map of the world with Schnectady as the center was also found very useful for facilitating the taking of data from the specially equipped globe.

Types of Daylight-Darkness Distribution Charts

Two types of daylight-darkness distribution charts are utilized in this paper.

1. Charts showing diurnal and seasonal daylight-darkness distribution.

In presenting the diurnal and seasonal performance of different frequencies over long radio circuits, it is very helpful if data are available for showing the daylight-darkness distribution over the circuit. By

utilizing the special globe previously mentioned these daylight-darkness data were obtained and plotted in suitable chart form. In order to show seasonal variation, four charts were prepared for each circuit. By reference to the various figures which appear on the following pages it will be observed that the season covered by each chart differs somewhat from the corresponding yearly seasons. This difference was purposely introduced as will be understood by reference to the following paragraphs.

In the temperate zones there are four seasons: spring, summer, autumn, and winter, beginning respectively at the vernal equinox, the summer solstice, the autumnal equinox, and the winter solstice, for which, in the north temperate zone, the approximate dates are March 20th, June 20th, September 20th, and December 20th.

Since Schenectady is located in the north temperate zone, its seasons are approximately as follows:

Season	Duration
Spring	March 20th to June 20th
Summer	June 20th to September 20th
Autumn	September 20th to December 20th
Winter	December 20th to March 20th

In the preparation of seasonal daylight-darkness charts, a chart was made up for the dates of March 20th, June 20th, September 20th, and December 20th. These dates, which are the dates on which the yearly seasons change, were chosen on account of the fact that the vernal and autumnal equinoxes occur on March 20th and September 20th (approximately), thereby causing the charts for these two dates to be identical (or almost identical). Also, on June 20th and December 20th the inclination of the axis of the earth from the earth's orbit is at a maximum.

Inasmuch as the daylight-darkness charts were prepared for dates on which there is a change of yearly seasons, the reception data covered by each chart are not for a particular season of the year, but rather a "radio season" that includes a part of two yearly seasons. The duration of the "radio seasons" is tabulated below:

Date of D-D Seasonal Chart	Radio Season Covered
March 20th	February 1st to May 1st
June 20th	May 1st to August 1st
September 20th	August 1st to November 1st
December 20th	November 1st to February 1st

2. Charts Showing Seasonal Daylight-Darkness Distribution.

While the daylight-darkness data contained in the charts just discussed are quite complete, they can, nevertheless, be arranged in a different manner so as to present a somewhat clearer picture of the daylight-darkness distribution that exists over a radio circuit from season to season. In this connection, a chart has been prepared for each of the circuits treated herein which shows graphically the number of hours of "all daylight," "all darkness," "daylight-darkness," etc., that exist over the great circle path of each circuit. Both the short and long great circle paths are treated on these charts.

From a study of daylight-darkness distribution data, it has been learned that there are six different daylight-darkness conditions that may exist over the great circle path of a radio circuit (provided both the short and long paths are considered). These are:

1. All daylight
2. All darkness
3. Daylight to darkness
4. Darkness to daylight
5. Daylight to darkness to daylight
6. Darkness to daylight to darkness

These conditions, together with their duration for each of the four yearly seasons, are shown on the chart for each circuit treated.

By having available both types of the daylight-darkness distribution charts, the problem of choosing the proper frequencies for maintaining 24-hour service over a long radio circuit is greatly simplified. For instance, suppose that it is desired to establish a 24-hour radio service between Schenectady and Manila. The distance over the short great circle path is approximately 8200 miles. If a specific date is taken, December 20th for example, it is found that the daylight-darkness distribution over this path is:

Daylight to darkness	9.2 hours
Darkness to daylight	10.4 hours
All darkness	4.4 hours
All daylight	0.0 hours
Total	24.0 hours

On the same date the daylight-darkness distribution over the long great circle path of 16,700 miles is:

Daylight to darkness to daylight	0.0 hours
Darkness to daylight to darkness	4.0 hours
Daylight to darkness	9.2 hours
Darkness to daylight	10.8 hours
Total	24.0 hours

It is possible, and entirely probable, that a radio transmission in going from Schenectady to Manila will follow the short path during one period of the day and that twelve hours or so later it will follow the long path. If this happens, it will be noted that there are six different daylight-darkness conditions through which the transmission may travel during a 24-hour day (December 20th) in reaching Manila.

In order to determine the frequencies and power necessary to maintain 24-hour service over the Schenectady-Manila circuit, it is necessary to know how various frequencies perform when propagated through the daylight-darkness conditions that are encountered over this circuit. It is believed that, due to the recent advent of high-frequency transmission, no data are anywhere available which are sufficiently accurate to meet *fully* this demand. However, some of the most authentic data that are available may be analyzed and adapted to this circuit so as to permit a determination of the "probable optimum frequencies" for rendering 24-hour service during each of the seasons. Elsewhere in this paper are tabulations giving this "probable optimum frequency data" for the Schenectady-Manila circuit; consequently, they will not be reproduced here.

Transmission Charts

For each of the circuits with which this paper deals, there have been prepared four transmission charts—a chart for each of the seasons. These charts show the degree of reception that may normally be obtained from broadcasts of W2XAD and W2XAF at any hour of the day and any season of the year. They also give the approximate value of the frequencies that would be required in order to render the "optimum" 24-hour service. The frequencies given are applicable to the circuit regardless of the type of transmission that it is desired to employ.

Optimum Frequencies

By "optimum frequency" is meant the frequency that, at a given power output and at a particular time of the day, is capable of delivering the most usable signal at the receiving terminal of a radio circuit.

On the transmission charts previously discussed there are tabulated a quantity of optimum frequency data covering diurnal and seasonal conditions.

Optimum Frequency Charts

From the optimum frequency data contained on the transmission charts, "optimum frequency charts" were prepared.

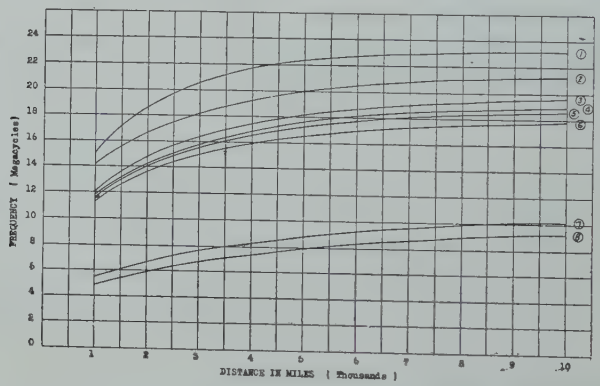

Fig. 1—Optimum frequencies for day-night, north-south, and east-west long distance transmission.

(1) North-south (day)
(2) East-west (day)
(3) North-south (50 per cent day—50 per cent night)
(4) North-south (50 per cent night—50 per cent day)
(5) East-west (50 per cent day—50 per cent night)
(6) East-west (50 per cent night—50 per cent day)
(7) North-south (night)
(8) East-west (night)

These charts, of which there is one for each of the circuits treated, have as their abscissa the time of the day, while the ordinate shows the proper frequencies to utilize in order to maintain a 24-hour service over the circuit.

It will be observed that the midday and midnight optimum frequencies listed have the same value for both summer and winter. In a number of the circuits treated herein it is not practical to give a different optimum frequency for each of these seasons since summer

at the transmitting terminal corresponds to winter at the receiving terminal, and vice versa. In the shorter circuits where similar seasons occur simultaneously at both terminals, it may be found that the midday and midnight "optimum frequencies" shown by the family of curves on Fig. 1 are subject to a correcting factor. However, since the data available are insufficient for determining the value of this factor accurately, and, furthermore, since the shortest circuit treated is more than two thousand miles in length, it is probably of minor importance and has, therefore, been neglected.

In the majority of circuits treated herein the direction of the receiving terminal from Schnectady is neither in a true north-south nor east-west direction. By obtaining the true bearing and interpolating between the north-south and east-west frequency values shown on Fig. 1, the midday and midnight optimum frequency values are obtained. The value of the frequencies for intermediate periods are obtained from a survey of the daylight-darkness distribution over the short path of the great circle, together with a study of the actual reception data available for these periods.

Source of Data

The data which are presented herein were deduced mainly from a study of the high frequency radio propagation data that are available to the General Electric Company as a result of (1) propagation transmission utilizing various frequencies and powers, and (2) the transmission of broadcast programs on high frequencies, utilizing stations W2XAD and W2XAF.

The major portion of these data was obtained when using power outputs of the order of 10 kw. Accordingly, the performances given herein are based on a power output of 10 kw—except in the case of W2XAF, where the power is 16 kw.

On Fig. 1, which incorporates much of the above data, will be found a family of curves that show the optimum frequency for use over day-night, north-south, and east-west transmission circuits.

Circuits Treated

This paper treats of the following nineteen radio circuits which radiate in various directions from Schenectady, and range in length from 2300 to 11,400 miles.

Circuit	Length (Miles)
Schenectady to Perth, West Australia	11,400
Schenectady to Sydney, East Australia	9,970
Schenectady to Palmerston North, New Zealand	8,900
Schenectady to Manila, Philippine Islands	8,200
Schenectady to Johannesburg, South Africa	7,900
Schenectady to Calcutta, India	7,800
Schenectady to Shanghai, China	7,100
Schenectady to Tokio, Japan	6,600
Schenectady to Buenos Aires, Argentina	5,400
Schenectady to Rio de Janeiro, Brazil	4,900
Schenectady to Honolulu, Hawaiian Islands	4,900
Schenectady to Moscow, U.S.S.R.	4,400
Schenectady to Berlin, Germany	3,850
Schenectady to Paris, France	3,500
Schenectady to London, England	3,400
Schenectady to Fairbanks, Alaska	3,100
Schenectady to Bogotá, Colombia	2,700
Schenectady to Oakland, California	2,545
Schenectady to Panama, Canal Zone	2,300

Each circuit is treated independently and includes the following:

a. Brief discussion of the circuit
b. Five daylight-darkness distribution charts
c. Four transmission charts
d. One optimum frequency chart

Schenectady–Perth (West Australia) Circuit

The distance from Schenectady to Perth, as measured in the plane of the great circle, is about 11,400 miles. The bearing of Perth from Schenectady is such that in traversing the great circle path, a Schenectady-Perth transmission will pass over the southerly portion of Alaska, thence across the Pacific Ocean and over new Guinea and Northern Australia.

The radio wave propagation data available for this circuit indicate that seasonal variation is not very pronounced. (Figs. 6 to 9.) Best reception of transmission from Schenectady should be obtained during the months of June, July, August, and September, since atmospheric interference in Western Australia is at a minimum during this period.

Since the earth's antipodes, with respect to Schenectady, is located in the Indian Ocean to the southwest of Perth, it follows that the

TIME			DAYLIGHT-DARKNESS DISTRIBUTION OVER GREAT CIRCLE PATH	PROBABLE RECEPTION OBTAINABLE FROM		PROBABLE OPTIMUM
GMT	W.Aus.	Local		W2XAD	W2XAF	FREQUENCY
				13660 K.C.	9550 K.C.	Short Path
1100	7 P.M.	6 A.M.		Fair	Good-Fair	9600 K.C.
1200	8 P.M.	7 A.M.		Fair-Poor	Good-Fair	9600 K.C.
1300	9 P.M.	8 A.M.		Fair-Poor	Fair-Poor	11000 K.C.
1400	10 P.M.	9 A.M.		Fair-Poor	Poor	14000 K.C.
1500	11 P.M.	10 A.M.		Poor	Unsat.	15600 K.C.
1600	12 M.	11 A.M.		Poor-Unsat.	Unsat.	16400 K.C.
1700	1 A.M.	12 N.		Unsat.	Nil	16900 K.C.
1800	2 A.M.	1 P.M.		Unsat.	Nil	17300 K.C.
1900	3 A.M.	2 P.M.		Unsat.	Nil	17700 K.C.
2000	4 A.M.	3 P.M.		Nil	Nil	18300 K.C.
2100	5 A.M.	4 P.M.		Nil	Nil	20800 K.C.
2200	6 A.M.	5 P.M.		Unsat.	Unsat.	22000 K.C.
2300	7 A.M.	6 P.M.		Poor	Unsat.	21900 K.C.
0000	8 A.M.	7 P.M.		Poor	Unsat.	21700 K.C.
0100	9 A.M.	8 P.M.		Poor-Unsat.	Unsat.	21400 K.C.
0200	10 A.M.	9 P.M.		Poor-Unsat.	Nil	20800 K.C.
0300	11 A.M.	10 P.M.		Unsat.	Nil	20300 K.C.
0400	12 N.	11 P.M.		Unsat.	Nil	19700 K.C.
0500	1 P.M.	12 M.		Unsat.	Nil	19000 K.C.
0600	2 P.M.	1 A.M.		Unsat.	Nil	18300 K.C.
0700	3 P.M.	2 A.M.		Unsat.	Nil	17200 K.C.
0800	4 P.M.	3 A.M.		Unsat.-Poor	Unsat.	16000 K.C.
0900	5 P.M.	4 A.M.		Poor-Fair	Unsat.-Poor	14400 K.C.
1000	6 P.M.	5 A.M.		Poor-Fair	Poor-Fair	11200 K.C.

Fig. 2—Schenectady—West Australia transmission chart. Winter season (November 1 to February 1). Distance from Schenectady to Perth 11,400 miles (approx.).

TIME			DAYLIGHT-DARKNESS DISTRIBUTION OVER GREAT CIRCLE PATH	PROBABLE RECEPTION OBTAINABLE FROM		PROBABLE OPTIMUM
GMT	W.Aus.	Local		W2XAD	W2XAF	FREQUENCY
				13660 K.C.	9550 K.C.	Short Path
1100	7 P.M.	6 A.M.		Fair	Good-Fair	9600 K.C.
1200	8 P.M.	7 A.M.		Fair-Poor	Fair	10200 K.C.
1300	9 P.M.	8 A.M.		Fair-Poor	Poor	12600 K.C.
1400	10 P.M.	9 A.M.		Poor	Unsat.	15000 K.C.
1500	11 P.M.	10 A.M.		Poor-Unsat.	Nil	16100 K.C.
1600	12 M.	11 A.M.		Unsat.	Nil	17000 K.C.
1700	1 A.M.	12 N.		Unsat.	Nil	17800 K.C.
1800	2 A.M.	1 P.M.		Nil	Nil	18300 K.C.
1900	3 A.M.	2 P.M.		Nil	Nil	19000 K.C.
2000	4 A.M.	3 P.M.		Unsat.	Nil	20000 K.C.
2100	5 A.M.	4 P.M.		Unsat.	Unsat.	21000 K.C.
2200	6 A.M.	5 P.M.		Fair	Poor-Fair	22000 K.C.
2300	7 A.M.	6 P.M.		Fair-Good	Fair-Good	22000 K.C.
0000	8 A.M.	7 P.M.		Fair	Good-Fair	21900 K.C.
0100	9 A.M.	8 P.M.		Fair-Poor	Fair	21800 K.C.
0200	10 A.M.	9 P.M.		Poor	Fair-Poor	21600 K.C.
0300	11 A.M.	10 P.M.		Poor-Unsat.	Poor-Unsat.	21200 K.C.
0400	12 N.	11 P.M.		Poor-Unsat.	Unsat.	20800 K.C.
0500	1 P.M.	12 M.		Unsat.	Unsat.	20300 K.C.
0600	2 P.M.	1 A.M.		Unsat.	Unsat.	19300 K.C.
0700	3 P.M.	2 A.M.		Unsat.-Poor	Unsat.	18200 K.C.
0800	4 P.M.	3 A.M.		Poor-Fair	Unsat.	16000 K.C.
0900	5 P.M.	4 A.M.		Fair	Poor	14400 K.C.
1000	6 P.M.	5 A.M.		Fair-Good	Fair-Good	9600 K.C.

Fig. 3—Schenectady—West Australia transmission chart. Spring season (February 1 to May 1). Distance from Schenectady to Perth 11,400 miles (approx.)

TIME			DAYLIGHT-DARKNESS DISTRIBUTION OVER GREAT CIRCLE PATH	PROBABLE RECEPTION OBTAINABLE FROM		PROBABLE OPTIMUM FREQUENCY
GMT	W.Aus.	Local		W2XAD	W2XAF	
				13660 K.C.	9550 K.C.	Short Path
1100	7 P.M.	6 A.M.		Fair-Poor	Nil	14000 K.C.
1200	8 P.M.	7 A.M.		Poor-Unsat.	Nil	15100 K.C.
1300	9 P.M.	8 A.M.		Unsat.	Nil	16000 K.C.
1400	10 P.M.	9 A.M.		Unsat.	Nil	17000 K.C.
1500	11 P.M.	10 A.M.		Nil	Nil	17600 K.C.
1600	12 M.	11 A.M.		Nil	Nil	18100 K.C.
1700	1 A.M.	12 N.		Nil	Nil	18600 K.C.
1800	2 A.M.	1 P.M.		Nil	Nil	18900 K.C.
1900	3 A.M.	2 P.M.		Nil	Nil	19200 K.C.
2000	4 A.M.	3 P.M.		Unsat.	Nil	19800 K.C.
2100	5 A.M.	4 P.M.		Unsat.-Poor	Unsat.	20600 K.C.
2200	6 A.M.	5 P.M.		Poor-Fair	Unsat.-Poor	21500 K.C.
2300	7 A.M.	6 P.M.		Fair-Good	Good	22000 K.C.
0000	8 A.M.	7 P.M.		Fair	Good-Fair	22000 K.C.
0100	9 A.M.	8 P.M.		Fair-Poor	Good-Fair	22000 K.C.
0200	10 A.M.	9 P.M.		Fair-Poor	Fair-Poor	21900 K.C.
0300	11 A.M.	10 P.M.		Poor	Poor	21800 K.C.
0400	12 N.	11 P.M.		Poor-Unsat.	Poor-Unsat.	21700 K.C.
0500	1 P.M.	12 M.		Poor-Unsat.	Unsat.	21600 K.C.
0600	2 P.M.	1 A.M.		Poor-Unsat.	Unsat.	21300 K.C.
0700	3 P.M.	2 A.M.		Unsat.	Nil	20600 K.C.
0800	4 P.M.	3 A.M.		Unsat.	Nil	19200 K.C.
0900	5 P.M.	4 A.M.		Poor-Fair	Unsat.	15000 K.C.
1000	6 P.M.	5 A.M.		Fair-Poor	Good-Fair	10000 K.C.

Fig. 4—Schenectady—West Australia transmission chart. Summer season (May 1 to August 1). Distance from Schenectady to Perth 11,400 miles (approx.).

TIME			DAYLIGHT-DARKNESS DISTRIBUTION OVER GREAT CIRCLE PATH	PROBABLE RECEPTION OBTAINABLE FROM		PROBABLE OPTIMUM FREQUENCY
GMT	W.Aus.	Local		W2XAD	W2XAF	
				13660 K.C.	9550 K.C.	Short Path
1100	7 P.M.	6 A.M.		Fair	Good-Fair	9600 K.C.
1200	8 P.M.	7 A.M.		Fair-Poor	Good-Fair	10200 K.C.
1300	9 P.M.	8 A.M.		Fair-Poor	Poor	12600 K.C.
1400	10 P.M.	9 A.M.		Poor	Unsat.	15000 K.C.
1500	11 P.M.	10 A.M.		Poor-Unsat.	Nil	16100 K.C.
1600	12 M.	11 A.M.		Unsat.	Nil	17000 K.C.
1700	1 A.M.	12 N.		Unsat.	Nil	17800 K.C.
1800	2 A.M.	1 P.M.		Nil	Nil	18300 K.C.
1900	3 A.M.	2 P.M.		Nil	Nil	19000 K.C.
2000	4 A.M.	3 P.M.		Unsat.	Nil	20000 K.C.
2100	5 A.M.	4 P.M.		Unsat.-Poor	Unsat.	21000 K.C.
2200	6 A.M.	5 P.M.		Poor	Poor-Fair	22000 K.C.
2300	7 A.M.	6 P.M.		Poor-Fair	Fair-Good	22000 K.C.
0000	8 A.M.	7 P.M.		Fair	Good-Fair	21900 K.C.
0100	9 A.M.	8 P.M.		Fair-Poor	Good-Fair	21800 K.C.
0200	10 A.M.	9 P.M.		Poor	Fair-Poor	21600 K.C.
0300	11 A.M.	10 P.M.		Poor-Unsat.	Poor	21200 K.C.
0400	12 N.	11 P.M.		Poor-Unsat.	Unsat.	20800 K.C.
0500	1 P.M.	12 M.		Poor-Unsat.	Unsat.	20300 K.C.
0600	2 P.M.	1 A.M.		Unsat.	Unsat.	19300 K.C.
0700	3 P.M.	2 A.M.		Unsat.	Unsat.	18200 K.C.
0800	4 P.M.	3 A.M.		Poor	Unsat.	16000 K.C.
0900	5 P.M.	4 A.M.		Poor-Fair	Poor-Fair	14400 K.C.
1000	6 P.M.	5 A.M.		Poor-Fair	Fair-Good	9600 K.C.

Fig. 5—Schenectady—West Australia transmission chart. Fall season (August 1 to November 1). Distance from Schenectady to Perth 11,400 miles (approx.)

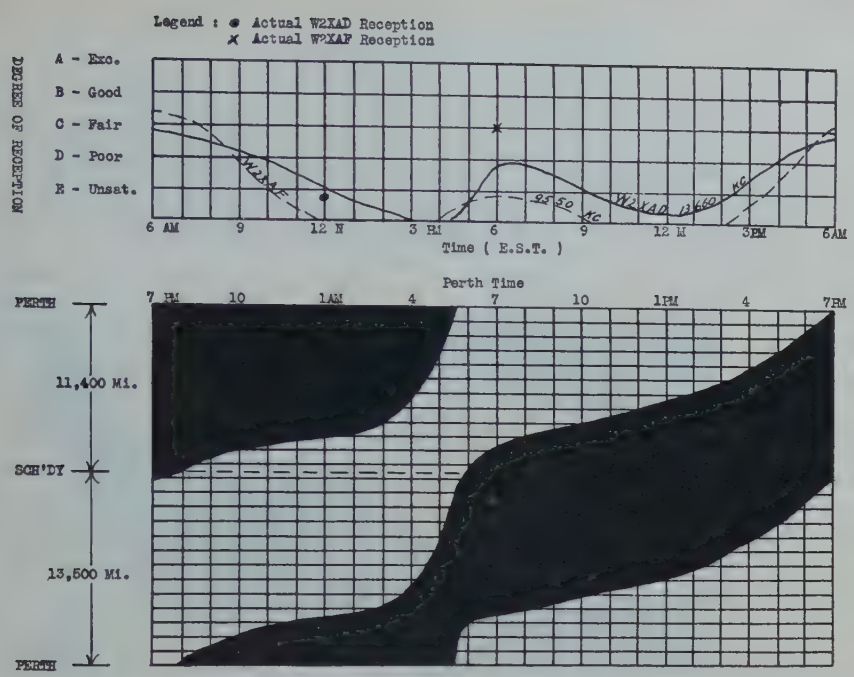

Fig. 6—West Australia reception from November 1 to February 1. Daylight-darkness distribution over great circle path from Schenectady to Perth, Australia, as of December 20.

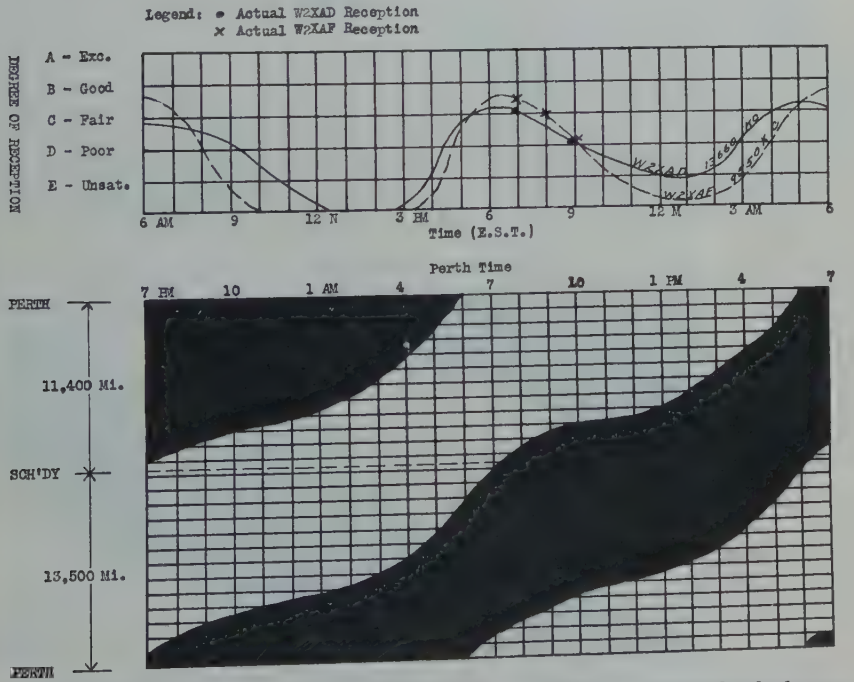

Fig. 7—West Australia reception from February 1 to May 1. Daylight-darkness distribution over great circle path from Schenectady to Perth, Australia, as of March 20.

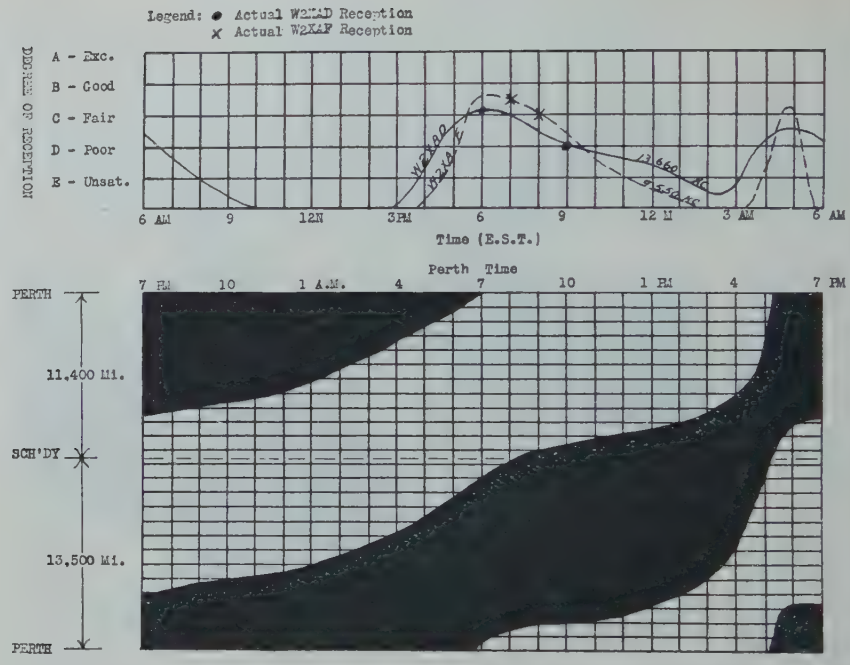

Fig. 8—West Australia reception from May 1 to August 1. Daylight-darkness distribution over great circle path from Schenectady to Perth, Australia, as of June 20.

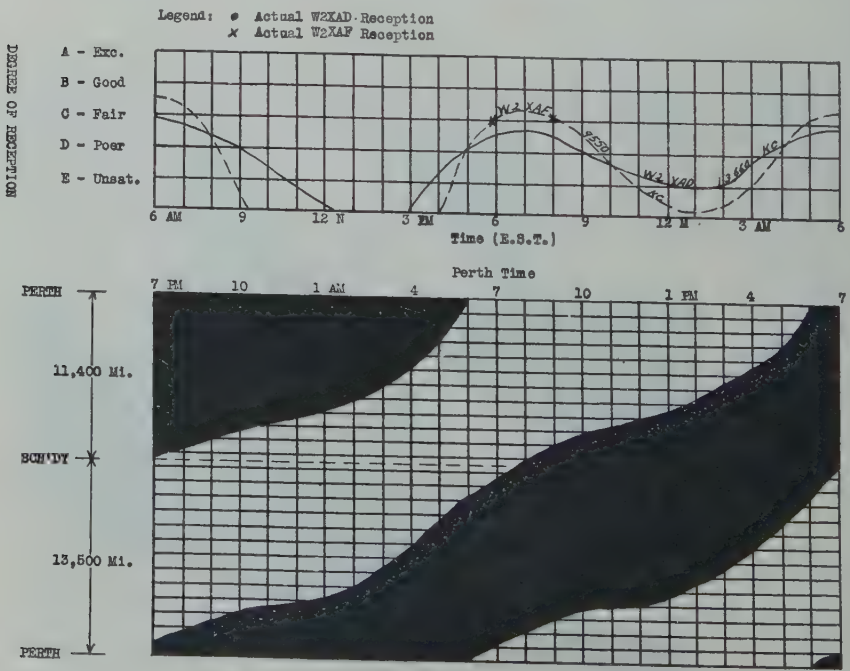

Fig. 9—West Australia reception from August 1 to November 1. Daylight-darkness distribution over great circle path from Schenectady to Perth, Australia, as of September 20.

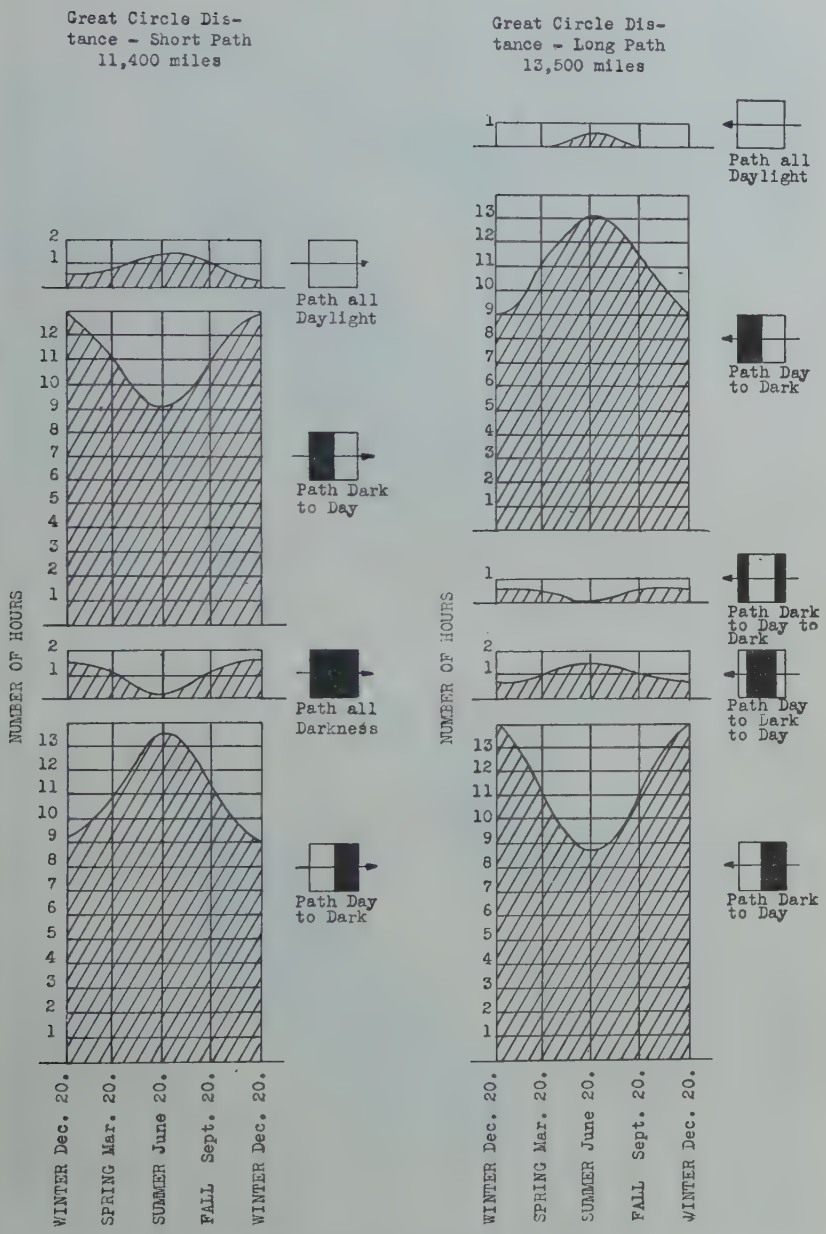

Fig. 10—Daylight-darkness distribution between Schenectady and Perth, West Australia.

Schenectady-Perth circuit is the longest international circuit that can be established, so long as Schenectady is the transmitting terminal.

Further reference to Figs. 6 to 9, and by noting Figs. 2 to 5, an understanding should be obtained of the diurnal and seasonal reception that is normally obtained from W2XAD and W2XAF in Perth and vicinity. In this connection it is interesting to note best reception usually occurs from 5:00 to 7:00 A.M., E.S.T. and from 5:00 to 7:00 P.M., E.S.T. Since W2XAD and W2XAF render maximum performance

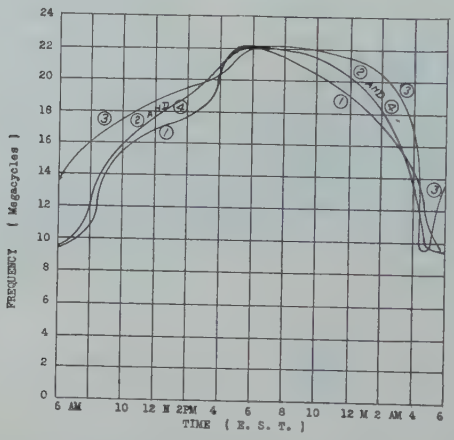

Fig. 11—Optimum frequency chart—Schenectady to Perth, Australia.
(1) Winter—November 1 to February 1.
(2) and (4)—Spring and Fall—February 1 to May 1 and August 1 to November 1.
(3) Summer—May 1 to August 1.

over this circuit when it is mostly in darkness, it appears that during the morning, the transmission is over the short great circle path, while during the evening it traverses the long path. This apparent change in the path of propagation is further substantiated by the fact that listeners in South Africa can receive the evening transmissions but are unable to receive those of the morning.

Fig. 11 shows the optimum frequency to use in transmitting from Schenectady to Perth at any hour of the day and during the different seasons of the year.

TIME			DAYLIGHT-DARKNESS DISTRIBUTION OVER GREAT CIRCLE PATH	PROBABLE RECEPTION OBTAINABLE FROM		PROBABLE OPTIMUM
GMT	E.Aus.	Local		W2XAD	W2XAF	FREQUENCY
				13660 K.C.	9550 K.C.	Short Path
1100	9 P.M.	6 A.M.		Fair	Good	9000 K.C.
1200	10 P.M.	7 A.M.		Fair-Poor	Good-Fair	10200 K.C.
1300	11 P.M.	8 A.M.		Fair	Fair	12500 K.C.
1400	12 M.	9 A.M.		Fair	Poor	15000 K.C.
1500	1 A.M.	10 A.M.		Fair-Poor	Unsat.	17200 K.C.
1600	2 A.M.	11 A.M.		Poor-Unsat.	Nil	19000 K.C.
1700	3 A.M.	12 N.		Unsat.	Nil	20100 K.C.
1800	4 A.M.	1 P.M.		Unsat.-Poor	Nil	20700 K.C.
1900	5 A.M.	2 P.M.		Poor-Fair	Unsat.	21000 K.C.
2000	6 A.M.	3 P.M.		Fair	Fair	21000 K.C.
2100	7 A.M.	4 P.M.		Fair	Fair-Good	21000 K.C.
2200	8 A.M.	5 P.M.		Fair-Poor	Good	21000 K.C.
2300	9 A.M.	6 P.M.		Fair-Poor	Good-Fair	20900 K.C.
0000	10 A.M.	7 P.M.		Poor	Fair-Poor	20600 K.C.
0100	11 A.M.	8 P.M.		Poor-Unsat.	Poor	20200 K.C.
0200	12 N.	9 P.M.		Unsat.	Unsat.	19600 K.C.
0300	1 P.M.	10 P.M.		Unsat.-Poor	Unsat.-Nil	18700 K.C.
0400	2 P.M.	11 P.M.		Poor-Fair	Unsat.	17800 K.C.
0500	3 P.M.	12 M.		Fair-Good	Poor	16000 K.C.
0600	4 P.M.	1 A.M.		Fair-Good	Poor-Fair	14200 K.C.
0700	5 P.M.	2 A.M.		Fair-Good	Fair	11400 K.C.
0800	6 P.M.	3 A.M.		Fair-Good	Fair-Good	9400 K.C.
0900	7 P.M.	4 A.M.		Fair	Good	9000 K.C.
1000	8 P.M.	5 A.M.		Fair	Good	9000 K.C.

Fig. 12—Schenectady-East Australia transmission chart. Winter season (November 1 to February 1). Distance from Schenectady to Sydney 9970 miles (approx.).

TIME			DAYLIGHT-DARKNESS DISTRIBUTION OVER GREAT CIRCLE PATH	PROBABLE RECEPTION OBTAINABLE FROM		PROBABLE OPTIMUM
GMT	E.Aus.	Local		W2XAD	W2XAF	FREQUENCY
				13660 K.C.	9550 K.C.	Short Path
1100	9 P.M.	6 A.M.		Fair	Good	9000 K.C.
1200	10 P.M.	7 A.M.		Fair-Poor	Good-Fair	9800 K.C.
1300	11 P.M.	8 A.M.		Fair-Good	Fair	12300 K.C.
1400	12M.	9 A.M.		Fair-Good	Poor-Unsat.	15000 K.C.
1500	1 A.M.	10 A.M.		Fair-Poor	Unsat.-Nil	17000 K.C.
1600	2 A.M.	11 A.M.		Poor-Unsat.	Unsat.-Nil	18600 K.C.
1700	3 A.M.	12 N.		Unsat.	Unsat.-Nil	19600 K.C.
1800	4 A.M.	1 P.M.		Unsat.-Poor	Unsat.-Nil	20300 K.C.
1900	5 A.M.	2 P.M.		Poor	Unsat.-Nil	20800 K.C.
2000	6 A.M.	3 P.M.		Fair	Unsat.	21000 K.C.
2100	7 A.M.	4 P.M.		Fair-Good	Fair	21000 K.C.
2200	8 A.M.	5 P.M.		Fair-Good	Fair-Good	21000 K.C.
2300	9 A.M.	6 P.M.		Fair-Good	Good-Fair	21000 K.C.
0000	10 A.M.	7 P.M.		Fair	Fair-Poor	20900 K.C.
0100	11 A.M.	8 P.M.		Fair-Poor	Poor	20700 K.C.
0200	12 N.	9 P.M.		Poor	Poor-Unsat.	20000 K.C.
0300	1 P.M.	10 P.M.		Poor-Unsat.	Unsat.	19000 K.C.
0400	2 P.M.	11 P.M.		Poor-Unsat.	Unsat.	17800 K.C.
0500	3 P.M.	12 M.		Poor-Unsat.	Unsat.	16400 K.C.
0600	4 P.M.	1 A.M.		Poor-Fair	Unsat.-Poor	14800 K.C.
0700	5 P.M.	2 A.M.		Fair	Unsat.-Poor	12500 K.C.
0800	6 P.M.	3 A.M.		Fair	Poor	10600 K.C.
0900	7 P.M.	4 A.M.		Fair	Fair	9000 K.C.
1000	8 P.M.	5 A.M.		Fair	Good	9000 K.C.

Fig. 13—Schenectady-East Australia transmission chart. Spring season (February 1 to May 1). Distance from Schenectady to Sydney 9970 miles (approx.).

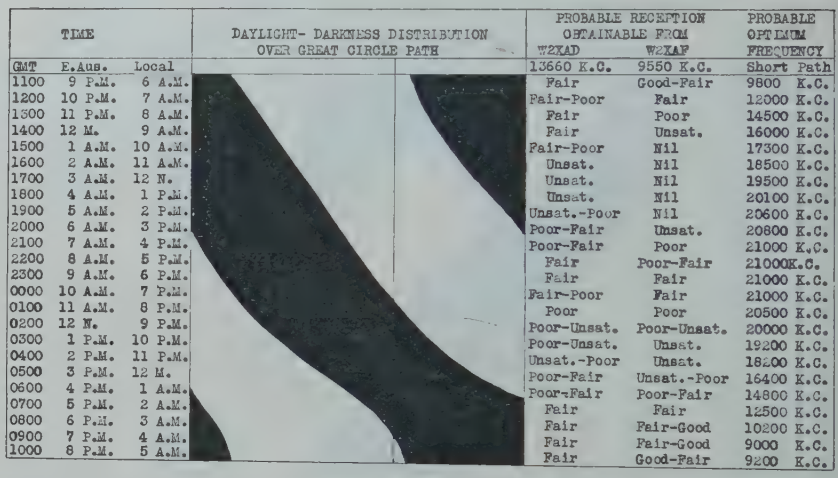

Fig. 14—Schenectady-East Australia transmission chart. Summer season (May 1 to August 1). Distance from Schenectady to Sydney 9970 miles (approx.).

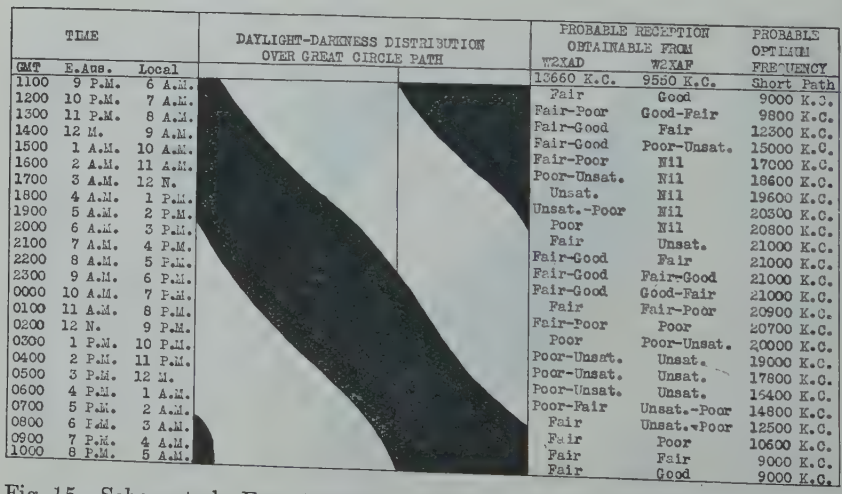

Fig. 15—Schenectady-East Australia transmission chart. Fall season (August 1 to November 1). Distance from Schenectady to Sydney 9970 miles (approx.).

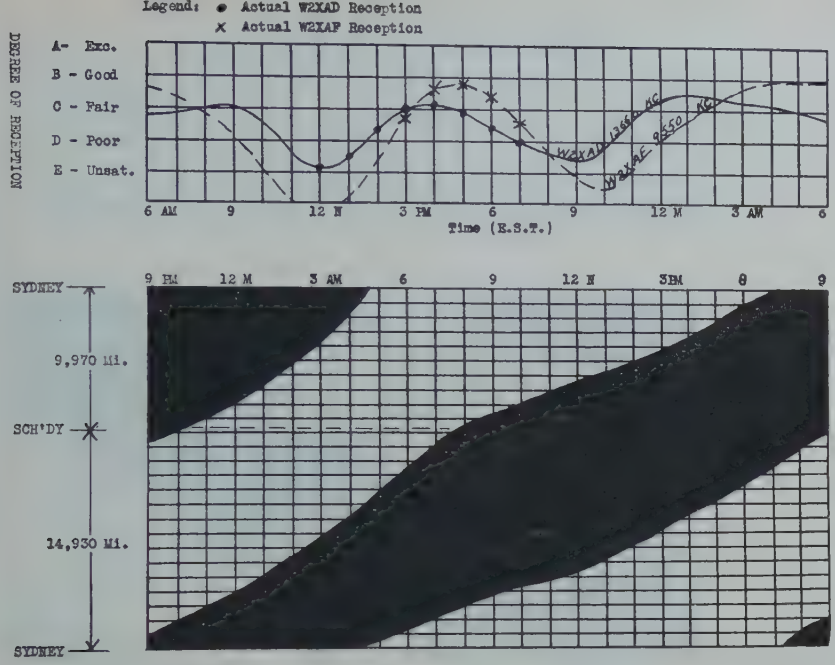

Fig. 16—East Australia reception from November 1 to February 1. Daylight-darkness distribution over great circle path from Schenectady to Sydney, Australia, as of December 20.

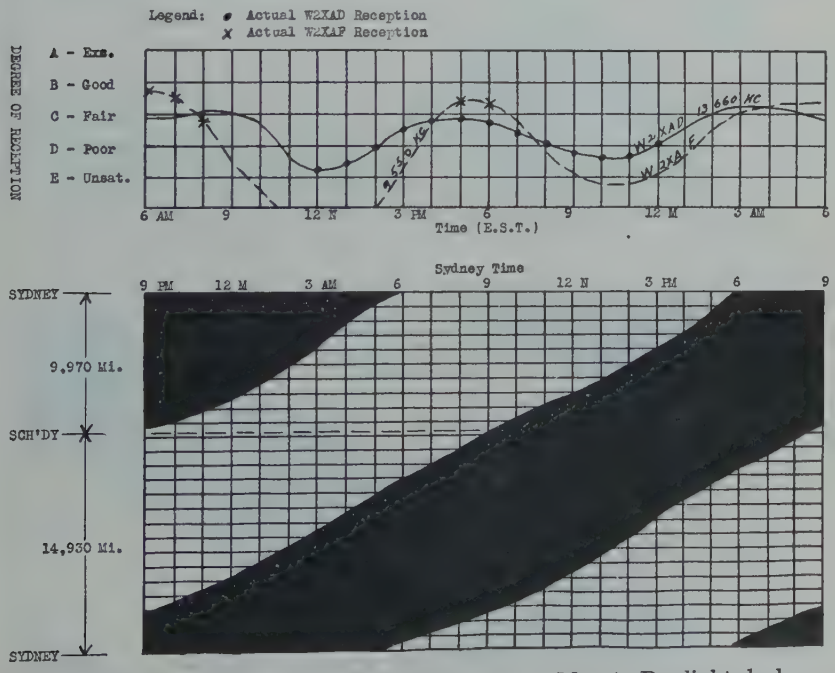

Fig. 17—East Australia reception from February 1 to May 1. Daylight-darkness distribution over great circle path from Schenectady to Sydney, Australia, as of March 20.

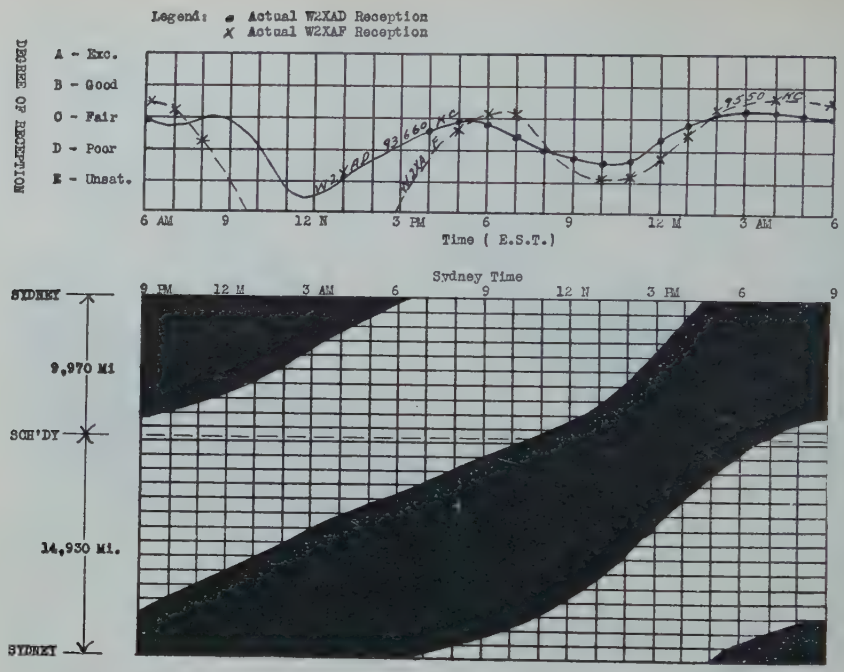

Fig. 18—East Australia reception from May 1 to August 1. Daylight-darkness distribution over great circle path from Schenectady to Sydney, Australia, as of June 20.

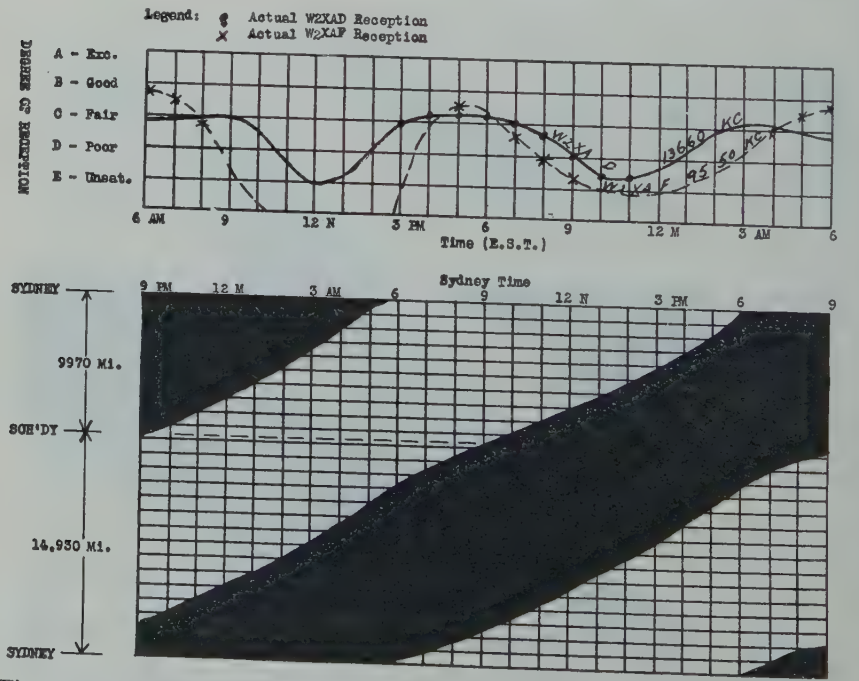

Fig. 19—East Australia reception from August 1 to November 1. Daylight-darkness distribution over great circle path from Schenectady to Sydney, Australia, as of September 20.

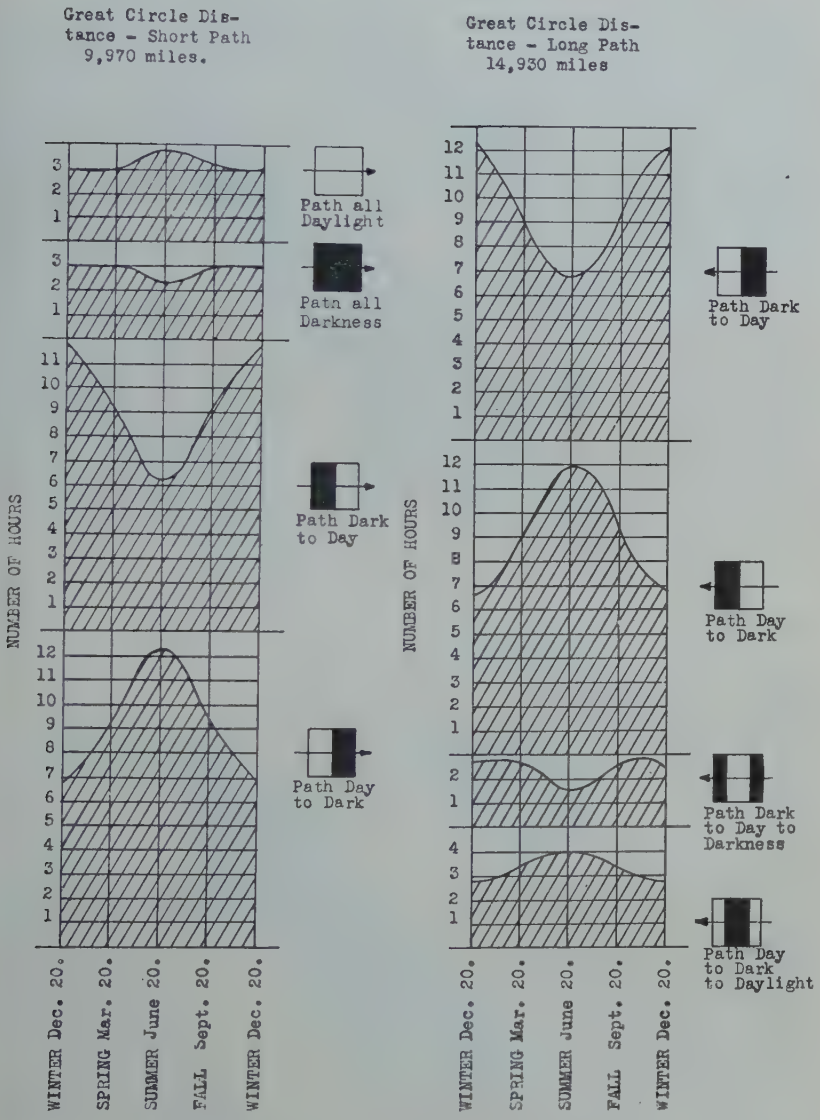

Fig. 20—Daylight-darkness distribution between Schenectady and Sydney, Australia.

Schenectady–Sydney (East Australia) Circuit

The length of the Schenectady-Sydney circuit is 9970 miles. A transmission from Schenectady will travel across the United States, pass over Southern California, and across the Pacific Ocean before reaching Sydney.

Reference to Figs. 16, 17, 18, and 19 will show that "seasonal variation" over this circuit is not very pronounced. As is true in the case of the Schenectady-Perth circuit, best reception should be effected during the months of June, July, August, and September.

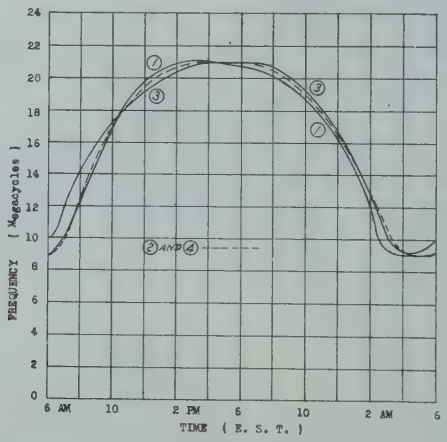

Fig. 21—Optimum frequency chart—Schenectady to Sydney Australia.
(1) Winter—November 1 to February 1.
(2) and (4)—Spring and Fall—February 1 to May 1 and August 1 to November 1.
(3) Summer—May 1 to August 1.

From a survey of Figs. 16 to 19, inclusive, the degree of reception that is normally obtained in Sydney and vicinity from W2XAD and W2XAF may be determined. It will be observed that best reception is obtained during the periods from about 1:00 to 9:00 A.M., E.S.T. and 3:00 to 6:00 P.M., E.S.T. It is probable that the 3:00 to 6:00 P.M. reception is made possible by transmission over the long great circle path since during this interval the short path is too well covered with daylight to allow the effective traversal of 15,340- or 9530-kc transmissions.

Optimum transmission frequency curves are shown on Fig. 21.

TIME			DAYLIGHT-DARKNESS DISTRIBUTION OVER GREAT CIRCLE PATH	PROBABLE RECEPTION OBTAINABLE FROM		PROBABLE OPTIMUM FREQUENCY
				W2XAD	W2XAF	
GMT	N.Zeland	Local		13660 K.C.	9550 K.C.	Short Path
1100	10:30 P.M.	6 A.M.		Fair	Good-Fair	9200 K.C.
1200	11:30 P.M.	7 A.M.		Fair	Good-Fair	9200 K.C.
1300	12:30 A.M.	8 A.M.		Fair	Fair-Poor	14000 K.C.
1400	1:30 A.M.	9 A.M.		Fair-Poor	Poor-Unsat.	16600 K.C.
1500	2:30 A.M.	10 A.M.		Poor	Unsat.	18400 K.C.
1600	3:30 A.M.	11 A.M.		Poor-Unsat.	Unsat.	20000 K.C.
1700	4:30 A.M.	12 N.		Poor	Unsat.	21700 K.C.
1800	5:30 A.M.	1 P.M.		Poor-Fair	Unsat.	21700 K.C.
1900	6:30 A.M.	2 P.M.		Poor-Fair	Unsat.-Poor	21700 K.C.
2000	7:30 A.M.	3 P.M.		Poor-Fair	Poor	21700 K.C.
2100	8:30 A.M.	4 P.M.		Poor-Unsat.	Poor-Fair	21700 K.C.
2200	9:30 A.M.	5 P.M.		Poor-Unsat.	Poor-Fair	21700 K.C.
2300	10:30 A.M.	6 P.M.		Poor-Unsat.	Poor	20800 K.C.
0000	11:30 A.M.	7 P.M.		Poor-Unsat.	Unsat.	20500 K.C.
0100	12:30 P.M.	8 P.M.		Poor-Unsat.	Unsat.	20000 K.C.
0200	1:30 P.M.	9 P.M.		Poor-Unsat.	Unsat.	19100 K.C.
0300	2:30 P.M.	10 P.M.		Poor	Unsat.	17800 K.C.
0400	3:30 P.M.	11 P.M.		Poor-Fair	Unsat.	16000 K.C.
0500	4:30 P.M.	12 M.		Fair-Good	Unsat.-Poor	14200 K.C.
0600	5:30 P.M.	1 A.M.		Fair-Good	Poor-Fair	12500 K.C.
0700	6:30 P.M.	2 A.M.		Fair-Good	Fair	10600 K.C.
0800	7:30 P.M.	3 A.M.		Fair-Good	Fair-Good	9200 K.C.
0900	8:30 P.M.	4 A.M.		Fair	Fair-Good	9200 K.C.
1000	9:30 P.M.	5 A.M.		Fair	Good	9200 K.C.

Fig. 22—Schenectady-New Zealand transmission chart. Winter season (November 1 to February 1). Distance from Schenectady to Palmerston North 8900 miles (approx.).

TIME			DAYLIGHT-DARKNESS DISTRIBUTION OVER GREAT CIRCLE PATH	PROBABLE RECEPTION OBTAINABLE FROM		PROBABLE OPTIMUM FREQUENCY
				W2XAD	W2XAF	
GMT	N.Zeland	Local		13660 K.C.	9550 K.C.	Short Path
1100	10:30 P.M.	6 A.M.		Fair	Good-Fair	9200 K.C.
1200	11:30 P.M.	7 A.M.		Fair-Good	Good-Fair	11500 K.C.
1300	12:30 A.M.	8 A.M.		Fair-Good	Good-Fair	14000 K.C.
1400	1:30 A.M.	9 A.M.		Fair-Good	Fair-Poor	15800 K.C.
1500	2:30 A.M.	10 A.M.		Fair-Good	Poor	17500 K.C.
1600	3:30 A.M.	11 A.M.		Fair-Poor	Unsat.	18800 K.C.
1700	4:30 A.M.	12 N.		Poor	Unsat.-Nil	20000 K.C.
1800	5:30 A.M.	1 P.M.		Poor-Unsat.	Nil-Unsat.	21700 K.C.
1900	6:30 A.M.	2 P.M.		Poor	Unsat.Poor	21700 K.C.
2000	7:30 A.M.	3 P.M.		Poor-Fair	Poor	21700 K.C.
2100	8:30 A.M.	4 P.M.		Fair	Fair	21700 K.C.
2200	9:30 A.M.	5 P.M.		Fair-Poor	Fair	21700 K.C.
2300	10:30 A.M.	6 P.M.		Fair-Poor	Fair	21700 K.C.
0000	11:30 A.M.	7 P.M.		Poor-Unsat.	Poor-Fair	20400 K.C.
0100	12:30 P.M.	8 P.M.		Poor-Unsat.	Poor	20000 K.C.
0200	1:30 P.M.	9 P.M.		Unsat.-Poor	Poor-Unsat.	19000 K.C.
0300	2:30 P.M.	10 P.M.		Poor	Poor-Unsat.	18000 K.C.
0400	3:30 P.M.	11 P.M.		Poor-Fair	Poor	16400 K.C.
0500	4:30 P.M.	12 P.M.		Fair	Poor-Fair	14400 K.C.
0600	5:30 P.M.	1 A.M.		Fair	Fair-Good	12000 K.C.
0700	6:30 P.M.	2 A.M.		Fair	Fair-Good	9200 K.C.
0800	7:30 P.M.	3 A.M.		Fair	Fair-Good	9200 K.C.
0900	8:30 P.M.	4 A.M.		Fair	Good	9200 K.C.
1000	9:30 P.M.	5 A.M.		Fair	Good	9200 K.C.

Fig. 23—Schenectady-New Zealand transmission chart. Spring season (February 1 to May 1). Distance from Schenectady to Palmerston North 8900 miles (approx.).

TIME			DAYLIGHT-DARKNESS DISTRIBUTION OVER GREAT CIRCLE PATH	PROBABLE RECEPTION OBTAINABLE FROM		PROBABLE OPTIMUM FREQUENCY
GMT	N.Zeland	Local		W2XAD	W2XAF	
				13660 K.C.	9550 K.C.	Short Path
1100	10:30 P.M.	6 A.M.		Fair	Good-Fair	10000 K.C.
1200	11:30 P.M.	7 A.M.		Fair	Good-Fair	11000 K.C.
1300	12:30 A.M.	8 A.M.		Fair-Good	Good-Fair	14300 K.C.
1400	1:30 A.M.	9 A.M.		Fair-Good	Fair	16700 K.C.
1500	2:30 A.M.	10 A.M.		Fair-Good	Fair-Poor	18300 K.C.
1600	3:30 A.M.	11 A.M.		Fair-Poor	Poor	19100 K.C.
1700	4:30 A.M.	12 N.		Poor	Poor-Unsat.	19700 K.C.
1800	5:30 A.M.	1 P.M.		Poor-Unsat.	Unsat.	20800 K.C.
1900	6:30 A.M.	2 P.M.		Poor-Unsat.	Unsat.	21700 K.C.
2000	7:30 A.M.	3 P.M.		Unsat.-Poor	Unsat.	21700 K.C.
2100	8:30 A.M.	4 P.M.		Poor	Unsat.-Poor	21700 K.C.
2200	9:30 A.M.	5 P.M.		Poor-Fair	Poor	21700 K.C.
2300	10:30 A.M.	6 P.M.		Poor-Fair	Poor	21700 K.C.
0000	11:30 A.M.	7 P.M.		Fair-Poor	Poor	21700 K.C.
0100	12:30 P.M.	8 P.M.		Fair-Poor	Poor-Unsat.	21700 K.C.
0200	1:30 P.M.	9 P.M.		Poor	Poor-Unsat.	19800 K.C.
0300	2:30 P.M.	10 P.M.		Poor	Unsat.-Poor	17000 K.C.
0400	3:30 P.M.	11 P.M.		Poor-Fair	Poor	14500 K.C.
0500	4:30 P.M.	12 M.		Poor-Fair	Fair	9200 K.C.
0600	5:30 P.M.	1 A.M.		Fair	Fair-Good	9200 K.C.
0700	6:30 P.M.	2 A.M.		Fair	Good	9200 K.C.
0800	7:30 P.M.	3 A.M.		Fair	Good-Fair	9200 K.C.
0900	8:30 P.M.	4 A.M.		Fair	Good-Fair	9200 K.C.
1000	9:30 P.M.	5 A.M.		Fair	Good-Fair	9500 K.C.

Fig. 24—Schenectady-New Zealand transmission chart. Summer season (May 1 to August 1). Distance from Schenectady to Palmerston North 8900 miles (approx.).

TIME			DAYLIGHT-DARKNESS DISTRIBUTION OVER GREAT CIRCLE PATH	PROBABLE RECEPTION OBTAINABLE FROM		PROBABLE OPTIMUM FREQUENCY
GMT	N.Zeland	Local		W2XAD	W2XAF	
				13660 K.C.	9550 K.C.	Short Path
1100	10:30 P.M.	6 A.M.		Fair	Good	9200 K.C.
1200	11:30 P.M.	7 A.M.		Fair-Good	Good-Fair	11500 K.C.
1300	12:30 A.M.	8 A.M.		Fair-Good	Good-Fair	14000 K.C.
1400	1:30 A.M.	9 A.M.		Fair-Good	Fair	15800 K.C.
1500	2:30 A.M.	10 A.M.		Fair-Good	Poor	17500 K.C.
1600	3:30 A.M.	11 A.M.		Fair-Poor	Unsat.	18800 K.C.
1700	4:30 A.M.	12 N.		Poor	Unsat.-Nil	20000 K.C.
1800	5:30 A.M.	1 P.M.		Poor-Unsat.	Nil-Unsat.	21700 K.C.
1900	6:30 A.M.	2 P.M.		Poor	Unsat.-Poor	21700 K.C.
2000	7:30 A.M.	3 P.M.		Poor-Fair	Poor-Fair	21700 K.C.
2100	8:30 A.M.	4 P.M.		Fair	Fair	21700 K.C.
2200	9:30 A.M.	5 P.M.		Fair-Poor	Fair	21700 K.C.
2300	10:30 A.M.	6 P.M.		Fair-Poor	Fair-Poor	21700 K.C.
0000	11:30 A.M.	7 P.M.		Poor-Unsat.	Poor	20400 K.C.
0100	12:30 P.M.	8 P.M.		Poor-Unsat.	Poor-Unsat.	20000 K.C.
0200	1:30 P.M.	9 P.M.		Poor-Unsat.	Poor-Unsat.	19000 K.C.
0300	2:30 P.M.	10 P.M.		Poor	Poor-Unsat.	18000 K.C.
0400	3:30 P.M.	11 P.M.		Poor-Fair	Poor	16400 K.C.
0500	4:30 P.M.	12 M.		Fair	Poor-Fair	14400 K.C.
0600	5:30 P.M.	1 A.M.		Fair	Fair-Good	12000 K.C.
0700	6:30 P.M.	2 A.M.		Fair	Fair-Good	9200 K.C.
0800	7:30 P.M.	3 A.M.		Fair	Fair-Good	9200 K.C.
0900	8:30 P.M.	4 A.M.		Fair	Good	9200 K.C.
1000	9:30 P.M.	5 A.M.		Fair	Good	9200 K.C.

Fig. 25—Schenectady-New Zealand transmission chart. Fall season (August 1 to November 1). Distance from Schenectady to Palmerston North 8900 miles (approx.).

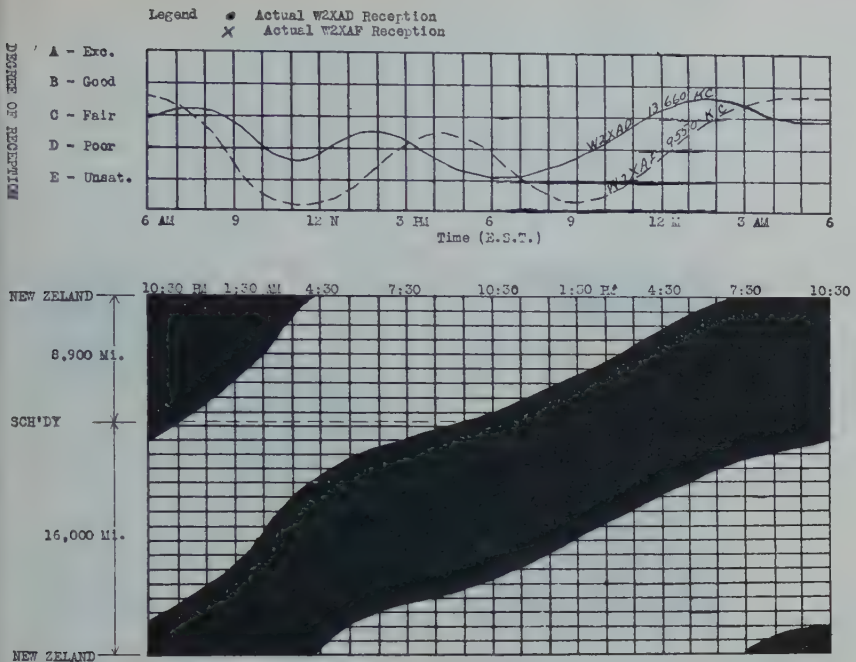

Fig. 26—New Zealand reception from November 1 to February 1. Daylight-darkness distribution over great circle path from Schenectady to Palmerston North, N. Z., as of December 20.

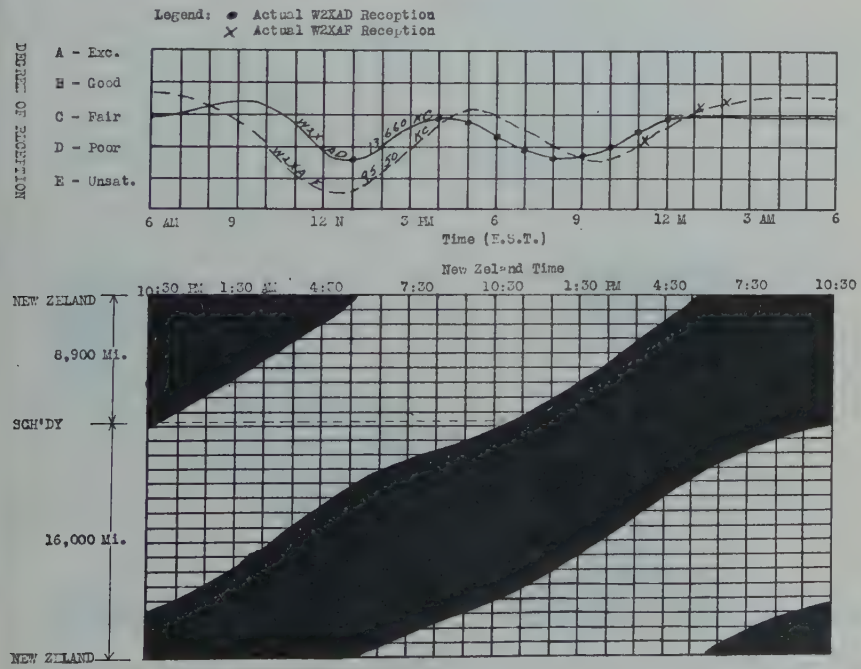

Fig. 27—New Zealand reception from February 1 to May 1. Daylight-darkness distribution over great circle path from Schenectady to Palmerston North, N. Z., as of March 20.

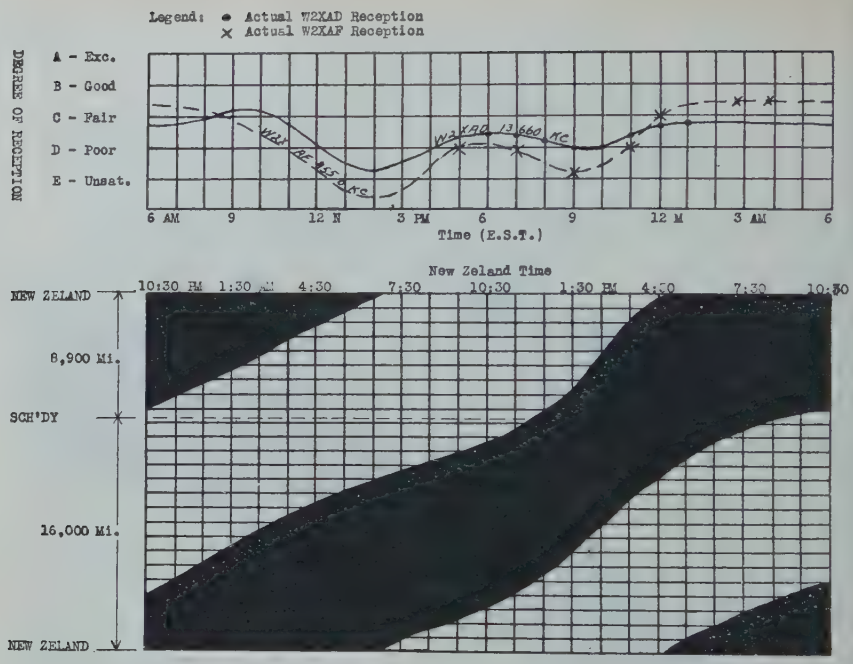

Fig. 28—New Zealand reception from May 1 to August 1. Daylight-darkness distribution over great circle path from Schenectady to Palmerston North, N. Z., as of June 20.

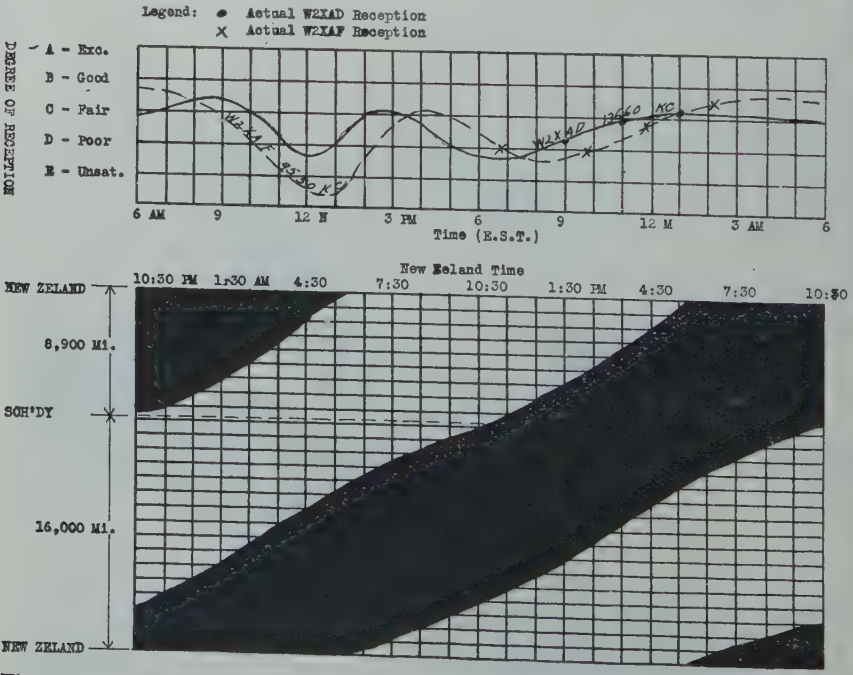

Fig. 29—New Zealand reception from August 1 to November 1. Daylight-darkness distribution over great circle path from Schenectady to Palmerston North, N. Z., as of September 20.

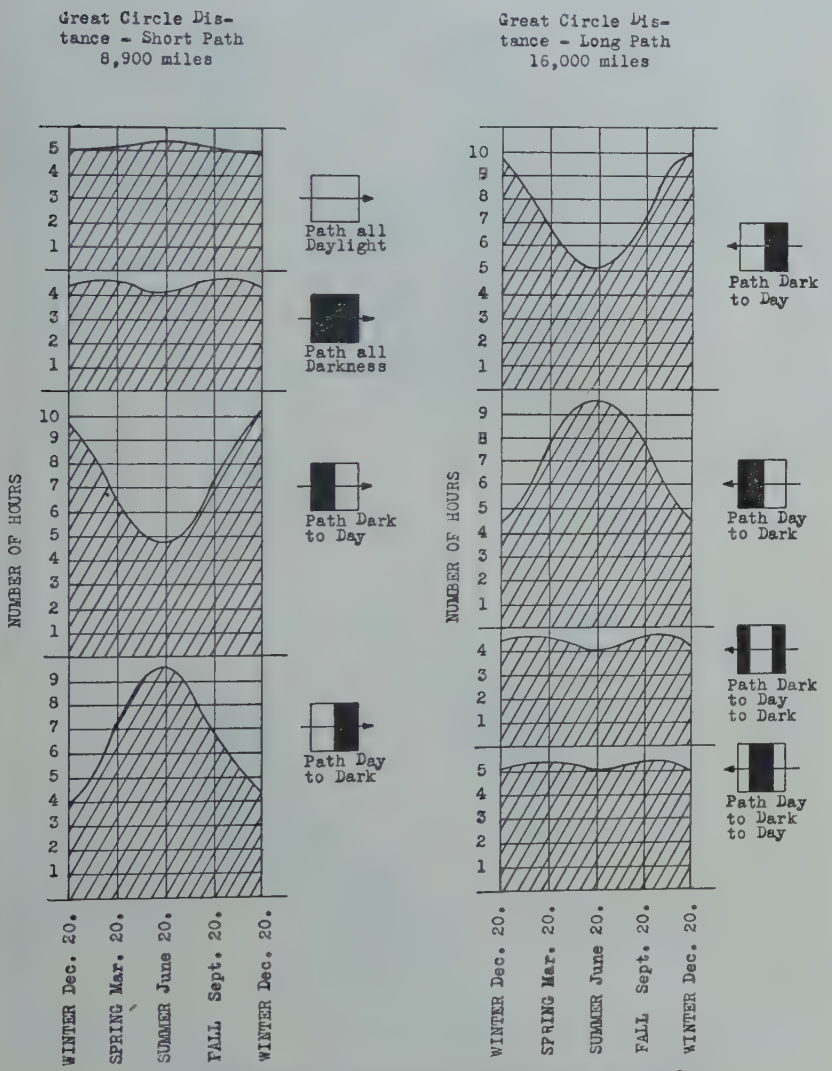

Fig. 30—Daylight-darkness distribution. Schenectady to Palmerston North, New Zealand.

Schenectady–Palmerston North (New Zealand) Circuit

The great circle distance from Schenectady to Palmerston North, New Zealand, is approximately 8900 miles. The direction of Palmerston North from Schenectady is such that in traversing the great circle path, a transmission from Schenectady will leave the United States in the vicinity of El Paso, Texas, pass over the northern portion of Mexico, and cross the Pacific to New Zealand.

The seasonal variation over this circuit is not very appreciable, although it is somewhat greater than that for the circuits already discussed. (Refer to Figs. 26, 27, 28, and 29.)

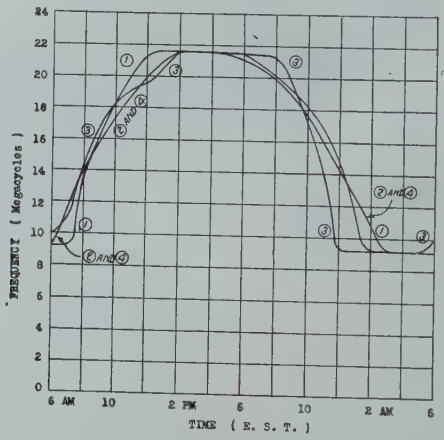

Fig. 31—Optimum frequency chart—Schenectady to Palmerston North, New Zealand.
(1) Winter—November 1 to February 1.
(2) and (4)—Spring and Fall—February 1 to May 1 and August 1 to November 1.
(3) Summer—May 1 to August 1.

From these figures, it will be seen that best reception from W2XAD and W2XAF is obtained during the period from 1:00 to 9:00 A.M., E.S.T. In the afternoon another peak occurs but it does not afford reception that is quite on a par with that obtainable during the morning. This peak of afternoon reception is undoubtedly produced by transmission over the long great circle path.

Data which show the hourly and seasonal degree of reception that may be expected in New Zealand from W2XAD and W2XAF transmissions are shown on Figs. 22, 23, 24, and 25. Fig. 31 gives the optimum frequency data for this circuit.

TIME			DAYLIGHT-DARKNESS DISTRIBUTION OVER GREAT CIRCLE PATH	PROBABLE RECEPTION OBTAINABLE FROM		PROBABLE OPTIMUM FREQUENCY
GMT	P.Isl.	Local		WZXAD	WZXAF	
				13660 K.C.	9550 K.C.	Short Path
1100	7 P.M.	6 A.M.		Fair-Poor	Fair	9400 K.C.
1200	8 P.M.	7 A.M.		Fair-Poor	Fair	10400 K.C.
1300	9 P.M.	8 A.M.		Poor	Poor	14500 K.C.
1400	10 P.M.	9 A.M.		Poor-Unsat.	Unsat.	15600 K.C.
1500	11 P.M.	10 A.M.		Poor-Unsat.	Unsat.	16300 K.C.
1600	12 M.	11 A.M.		Poor-Unsat.	Unsat.	16800 K.C.
1700	1 A.M.	12 N.		Unsat.-Poor	Unsat.	17000 K.C.
1800	2 A.M.	1 P.M.		Unsat.-Poor	Unsat.	16900 K.C.
1900	3 A.M.	2 P.M.		Unsat.-Poor	Unsat.	16600 K.C.
2000	4 A.M.	3 P.M.		Poor	Unsat.	15800 K.C.
2100	5 A.M.	4 P.M.		Poor-Fair	Poor	12900 K.C.
2200	6 A.M.	5 P.M.		Poor	Poor-Fair	9800 K.C.
2300	7 A.M.	6 P.M.		Poor-Unsat.	Poor	9800 K.C.
0000	8 A.M.	7 P.M.		Poor-Unsat.	Unsat.	12200 K.C.
0100	9 A.M.	8 P.M.		Poor-Unsat.	Unsat.	16000 K.C.
0200	10 A.M.	9 P.M.		Poor-Unsat.	Unsat.	17600 K.C.
0300	11 A.M.	10 P.M.		Poor-Unsat.	Unsat.	17800 K.C.
0400	12 N.	11 P.M.		Unsat.-Poor	Unsat.	17800 K.C.
0500	1 P.M.	12 M.		Unsat.-Poor	Unsat.	17700 K.C.
0600	2 P.M.	1 A.M.		Unsat.-Poor	Unsat.	17200 K.C.
0700	3 P.M.	2 A.M.		Unsat.-Poor	Unsat.	16400 K.C.
0800	4 P.M.	3 A.M.		Poor-Fair	Unsat.-Poor	15000 K.C.
0900	5 P.M.	4 A.M.		Poor-Fair	Poor	12500 K.C.
1000	6 P.M.	5 A.M.		Fair-Poor	Fair	9400 K.C.

Fig. 32—Schenectady-Philippine Islands transmission chart. Winter season (November 1 to February 1). Distance from Schenectady to Manila 8200 miles (approx.).

TIME			DAYLIGHT-DARKNESS DISTRIBUTION OVER GREAT CIRCLE PATH	PROBABLE RECEPTION OBTAINABLE FROM		PROBABLE OPTIMUM FREQUENCY
GMT	P.Isl.	Local		WZXAD	WZXAF	
				13660 K.C.	9550 K.C.	Short Path
1100	7 P.M.	6 A.M.		Fair	Fair	10500 K.C.
1200	8 P.M.	7 A.M.		Fair	Poor	12800 K.C.
1300	9 P.M.	8 A.M.		Fair-Poor	Unsat.	14500 K.C.
1400	10 P.M.	9 A.M.		Fair-Poor	Nil	16000 K.C.
1500	11 P.M.	10 A.M.		Poor-Unsat.	Nil	16600 K.C.
1600	12 M.	11 A.M.		Unsat.	Nil	17000 K.C.
1700	1 A.M.	12 N.		Unsat.	Nil	17300 K.C.
1800	2 A.M.	1 P.M.		Nil	Nil	17700 K.C.
1900	3 A.M.	2 P.M.		Nil	Nil	18200 K.C.
2000	4 A.M.	3 P.M.		Nil	Nil	18800 K.C.
2100	5 A.M.	4 P.M.		Nil	Nil	21400 K.C.
2200	6 A.M.	5 P.M.		Nil	Nil	22600 K.C.
2300	7 A.M.	6 P.M.		Nil	Nil	22600 K.C.
0000	8 A.M.	7 P.M.		Nil	Nil	22400 K.C.
0100	9 A.M.	8 P.M.		Unsat.	Nil	22300 K.C.
0200	10 A.M.	9 P.M.		Unsat.	Nil	22000 K.C.
0300	11 A.M.	10 P.M.		Unsat.	Unsat.	21500 K.C.
0400	12 N.	11 P.M.		Unsat.-Poor	Unsat.	21000 K.C.
0500	1 P.M.	12 M.		Unsat.-Poor	Unsat.	20400 K.C.
0600	2 P.M.	1 A.M.		Unsat.-Poor	Unsat.-Poor	19700 K.C.
0700	3 P.M.	2 A.M.		Poor	Poor	18800 K.C.
0800	4 P.M.	3 A.M.		Poor-Fair	Poor-Fair	17200 K.C.
0900	5 P.M.	4 A.M.		Poor-Fair	Fair	14400 K.C.
1000	6 P.M.	5 A.M.		Fair	Fair-Good	9400 K.C.

Fig. 33—Schenectady-Philippine Islands transmission chart. Spring season (February 1 to May 1). Distance from Schenectady to Manila 8200 miles (approx.).

TIME			DAYLIGHT-DARKNESS DISTRIBUTION OVER GREAT CIRCLE PATH	PROBABLE RECEPTION OBTAINABLE FROM		PROBABLE OPTIMUM FREQUENCY
GMT	P.Isl.	Local		WEXAD	WEXAF	
				13660 K.C.	9550 K.C.	Short Path
1100	7 P.M.	6 A.M.		Nil	Nil	22000 K.C.
1200	8 P.M.	7 A.M.		Nil	Nil	21600 K.C.
1300	9 P.M.	8 A.M.		Nil	Nil	21100 K.C.
1400	10 P.M.	9 A.M.		Nil	Nil	20400 K.C.
1500	11 P.M.	10 A.M.		Nil	Nil	19600 K.C.
1600	12 M.	11 A.M.		Nil	Nil	19600 K.C.
1700	1 A.M.	12 N.		Nil	Nil	20300 K.C.
1800	2 A.M.	1 P.M.		Nil	Nil	21300 K.C.
1900	3 A.M.	2 P.M.		Nil	Nil	22000 K.C.
2000	4 A.M.	3 P.M.		Nil	Nil	22600 K.C.
2100	5 A.M.	4 P.M.		Nil	Nil	22700 K.C.
2200	6 A.M.	5 P.M.		Nil	Nil	22700 K.C.
2300	7 A.M.	6 P.M.		Unsat.	Nil	22700 K.C.
0000	8 A.M.	7 P.M.		Unsat.	Nil	22700 K.C.
0100	9 A.M.	8 P.M.		Unsat.	Nil	22600 K.C.
0200	10 A.M.	9 P.M.		Unsat.	Nil	22200 K.C.
0300	11 A.M.	10 P.M.		Unsat.	Nil	21600 K.C.
0400	12 N.	11 P.M.		Unsat.	Nil	20600 K.C.
0500	1 P.M.	12 M.		Unsat.	Nil	19900 K.C.
0600	2 P.M.	1 A.M.		Unsat.	Nil	20200 K.C.
0700	3 P.M.	2 A.M.		Unsat.	Nil	21200 K.C.
0800	4 P.M.	3 A.M.		Unsat.	Nil	22000 K.C.
0900	5 P.M.	4 A.M.		Unsat.	Nil	22500 K.C.
1000	6 P.M.	5 A.M.		Unsat.	Nil	22700 K.C.

Fig. 34—Schenectady-Philippine Islands transmission chart. Summer season (May 1 to August 1). Distance from Schenectady to Manila 8200 miles (approx.).

TIME			DAYLIGHT-DARKNESS DISTRIBUTION OVER GREAT CIRCLE PATH	PROBABLE RECEPTION OBTAINABLE FROM		PROBABLE OPTIMUM FREQUENCY
GMT	P.Isl.	Local		WEXAD	WEXAF	
				13660 K.C.	9550 K.C.	Short Path
1100	7 P.M.	6 A.M.		Fair	Fair	10500 K.C.
1200	8 P.M.	7 A.M.		Fair	Poor	12800 K.C.
1300	9 P.M.	8 A.M.		Fair-Poor	Unsat.	14500 K.C.
1400	10 P.M.	9 A.M.		Fair-Poor	Nil	16000 K.C.
1500	11 P.M.	10 A.M.		Poor-Unsat.	Nil	16600 K.C.
1600	12 M.	11 A.M.		Unsat.	Nil	17000 K.C.
1700	1 A.M.	12 N.		Unsat.	Nil	17300 K.C.
1800	2 A.M.	1 P.M.		Nil	Nil	17700 K.C.
1900	3 A.M.	2 P.M.		Nil	Nil	18200 K.C.
2000	4 A.M.	3 P.M.		Nil	Nil	18800 K.C.
2100	5 A.M.	4 P.M.		Nil	Nil	21400 K.C.
2200	6 A.M.	5 P.M.		Nil	Nil	22600 K.C.
2300	7 A.M.	6 P.M.		Nil	Nil	22600 K.C.
0000	8 A.M.	7 P.M.		Nil	Nil	22400 K.C.
0100	9 A.M.	8 P.M.		Unsat.	Nil	22300 K.C.
0200	10 A.M.	9 P.M.		Unsat.	Nil	22000 K.C.
0300	11 A.M.	10 P.M.		Unsat.	Unsat.	21500 K.C.
0400	12 A.M.	11 P.M.		Unsat.	Unsat.	21000 K.C.
0500	1 P.M.	12 M.		Unsat.-Poor	Unsat.	20400 K.C.
0600	2 P.M.	1 A.M.		Unsat.-Poor	Unsat.-Poor	19700 K.C.
0700	3 P.M.	2 A.M.		Poor	Poor	18800 K.C.
0800	4 P.M.	3 A.M.		Poor-Fair	Poor-Fair	17200 K.C.
0900	5 P.M.	4 A.M.		Poor-Fair	Fair	14400 K.C.
1000	6 P.M.	5 A.M.		Fair	Fair-Good	9400 K.C.

Fig. 35—Schenectady-Philippine Islands transmission chart. Fall season (August 1 to November 1). Distance from Schenectady to Manila 8200 miles (approx.).

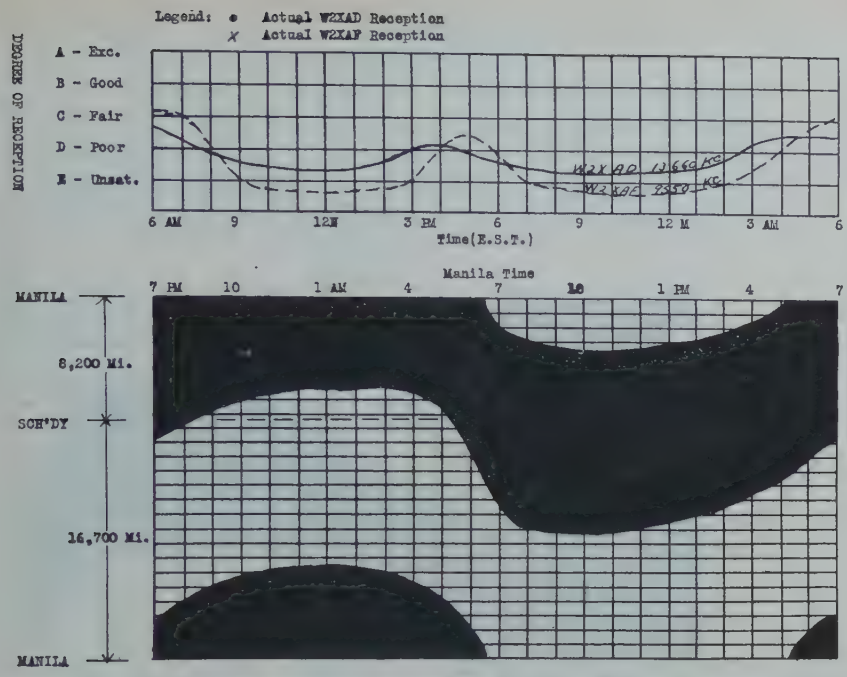

Fig. 36—Reception in Manila from November 1 to February 1. Daylight-darkness distribution over great circle path from Schenectady to Manila, Philippine Islands, as of December 20.

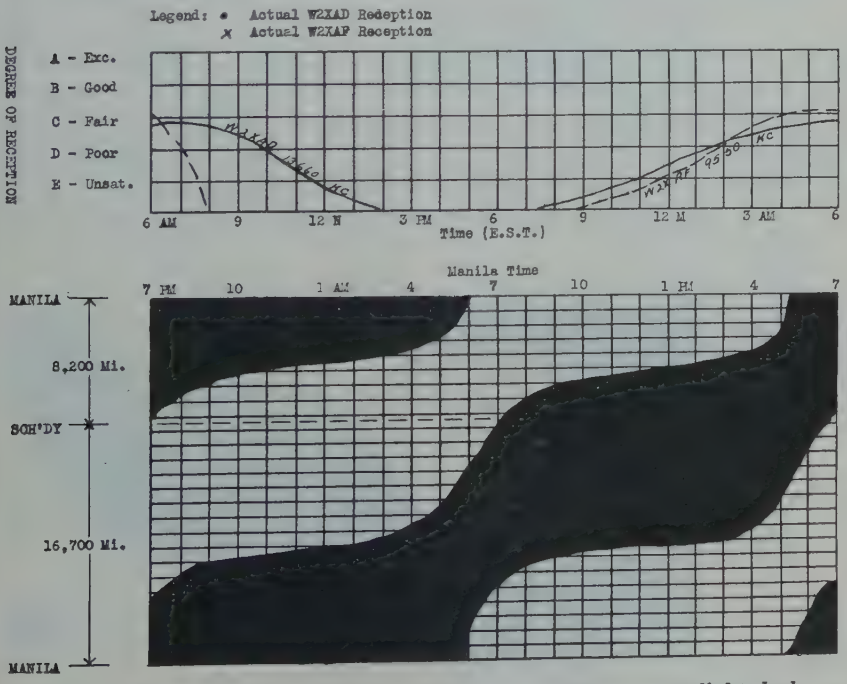

Fig. 37—Reception in Manila from February 1 to May 1. Daylight-darkness distribution over great circle path from Schenectady to Manila, Philippine Islands, as of March 20.

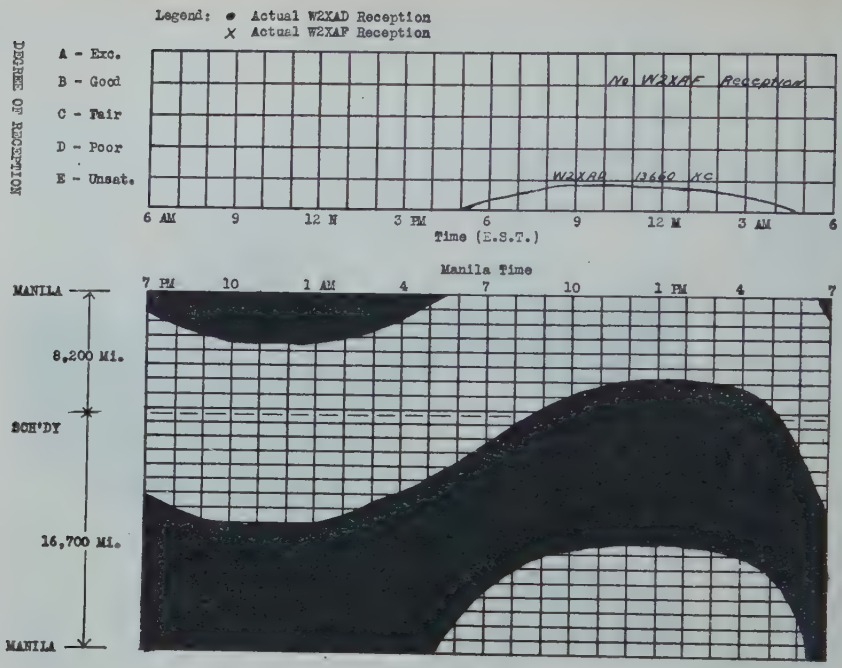

Fig. 38—Reception in Manila from May 1 to August 1. Daylight-darkness distribution over great circle path from Schenectady to Manila, Philippine Islands, as of June 20.

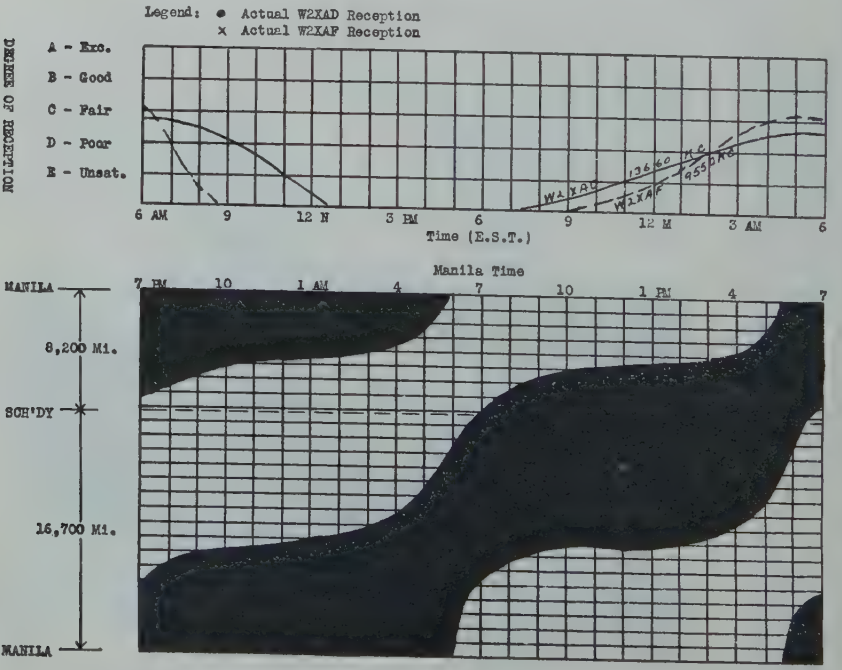

Fig. 39—Reception in Manila from August 1 to November 1. Daylight-darkness distribution over great circle path from Schenectady to Manila, Philippine Islands, as of September 20.

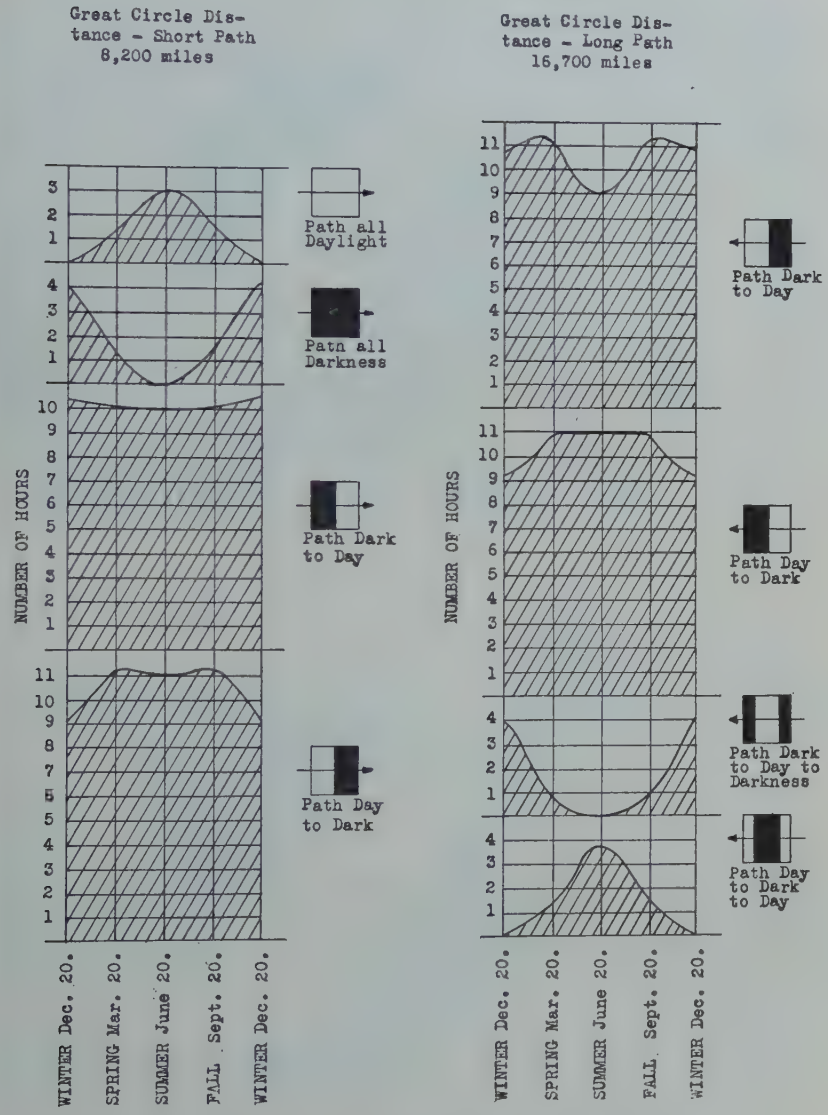

Fig. 40—Daylight–darkness distribution between Schenectady and Manila, Philippine Islands.

Schenectady–Manila (Philippine Islands) Circuit

Seasonal variation over this circuit is very pronounced as will be noted from a study of Figs. 32 to 39.

The direction of Manila from Schenectady (N 16 deg. W-approx.) is such that a transmission from Schenectady in order to reach Manila will follow a route over Hudson Bay, Siberia, and Eastern China. The length of this circuit is about 8200 miles.

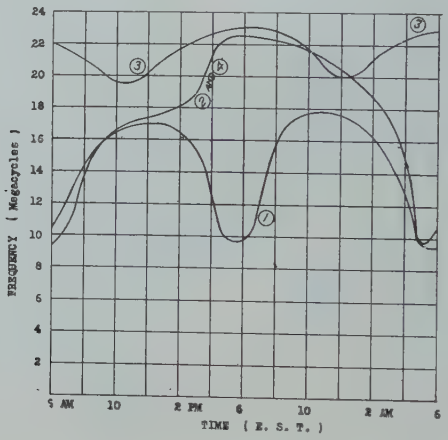

Fig. 41—Optimum frequency chart—Schenectady to Manila, Philippine Islands.
(1) Winter—November 1 to February 1.
(2) and (4)—Spring and Fall—February 1 to May 1 and August 1 to November 1.
(3) Summer—May 1 to August 1.

Only a few reception reports pertaining to General Electric transmissions have been received from the Philippine Islands. Throughout the duration of WGY's evening program when W2XAD and W2XAF are normally in operation, it appears that reception in the Philippines is very poor, or nil.

The optimum transmission frequency data for this circuit are given on Fig. 41.

Schenectady–Johannesburg (South Africa) Circuit

The distance from Schenectady to Johannesburg is about 7900 miles. In covering this distance, a transmission from Schenectady will

TIME		DAYLIGHT-DARKNESS DISTRIBUTION OVER GREAT CIRCLE PATH	PROBABLE RECEPTION OBTAINABLE FROM		PROBABLE OPTIMUM FREQUENCY
GMT	S.Africa Local		W2XAD	W2XAF	
			13660 K.C.	9550 K.C.	Short Path
1100	1 P.M. 6 A.M.		Poor-Unsat.	Nil	20000 K.C.
1200	2 P.M. 7 A.M.		Nil	Nil	20600 K.C.
1300	3 P.M. 8 A.M.		Nil	Nil	21000 K.C.
1400	4 P.M. 9 A.M.		Nil	Nil	21000 K.C.
1500	5 P.M. 10 A.M.		Nil	Nil	21000 K.C.
1600	6 P.M. 11 A.M.		Nil	Nil	21000 K.C.
1700	7 P.M. 12 N.		Nil	Nil	20500 K.C.
1800	8 P.M. 1 P.M.		Unsat.	Nil	19700 K.C.
1900	9 P.M. 2 P.M.		Unsat.	Unsat.	18400 K.C.
2000	10 P.M. 3 P.M.		Unsat.	Unsat.	17000 K.C.
2100	11 P.M. 4 P.M.		Unsat.-Poor	Poor	15000 K.C.
2200	12 M. 5 P.M.		Poor-Fair	Fair	11500 K.C.
2300	1 A.M. 6 P.M.		Poor-Fair	Fair-Good	8900 K.C.
0000	2 A.M. 7 P.M.		Fair	Fair-Good	8900 K.C.
0100	3 A.M. 8 P.M.		Fair	Good-Fair	8900 K.C.
0200	4 A.M. 9 P.M.		Fair-Poor	Fair	8900 K.C.
0300	5 A.M. 10 P.M.		Fair-Poor	Fair-Poor	10500 K.C.
0400	6 A.M. 11 P.M.		Fair-Poor	Poor	12500 K.C.
0500	7 A.M. 12 M.		Fair-Poor	Poor-Unsat.	15000 K.C.
0600	8 A.M. 1 A.M.		Poor	Unsat.	16800 K.C.
0700	9 A.M. 2 A.M.		Poor-Unsat.	Unsat.	18000 K.C.
0800	10 A.M. 3 A.M.		Unsat.	Unsat.	18800 K.C.
0900	11 A.M. 4 A.M.		Unsat.	Nil	19300 K.C.
1000	12 N. 5 A.M.		Unsat.	Nil	19700 K.C.

Fig. 42—Schenectady-South Africa transmission chart. Winter season (November 1 to February 1). Distance from Schenectady to Johannesburg 7900 miles (approx.).

TIME		DAYLIGHT-DARKNESS DISTRIBUTION OVER GREAT CIRCLE PATH	PROBABLE RECEPTION OBTAINABLE FROM		PROBABLE OPTIMUM FREQUENCY
GMT	S.Africa Local		W2XAD	W2XAF	
			13660 K.C.	9550 K.C.	Short Path
1100	1 P.M. 6 A.M.		Nil	Nil	21000 K.C.
1200	2 P.M. 7 A.M.		Nil	Nil	21000 K.C.
1300	3 P.M. 8 A.M.		Nil	Nil	21000 K.C.
1400	4 P.M. 9 A.M.		Nil	Nil	21000 K.C.
1500	5 P.M. 10 A.M.		Nil	Nil	21000 K.C.
1600	6 P.M. 11 A.M.		Nil	Nil	21000 K.C.
1700	7 P.M. 12 N.		Nil	Nil	20300 K.C.
1800	8 P.M. 1 P.M.		Nil	Nil	20000 K.C.
1900	9 P.M. 2 P.M.		Unsat.	Nil	19000 K.C.
2000	10 P.M. 3 P.M.		Unsat.	Nil	17800 K.C.
2100	11 P.M. 4 P.M.		Unsat.-Poor	Unsat.	16600 K.C.
2200	12 M. 5 P.M.		Poor	Poor	15200 K.C.
2300	1 A.M. 6 P.M.		Poor-Fair	Fair	12500 K.C.
0000	2 A.M. 7 P.M.		Poor-Fair	Fair-Good	8900 K.C.
0100	3 A.M. 8 P.M.		Poor-Fair	Fair-Good	8900 K.C.
0200	4 A.M. 9 P.M.		Fair-Poor	Good-Fair	8900 K.C.
0300	5 A.M. 10 P.M.		Fair-Poor	Fair	8900 K.C.
0400	6 A.M. 11 P.M.		Fair-Poor	Fair-Poor	8900 K.C.
0500	7 A.M. 12 M.		Fair-Poor	Poor	12000 K.C.
0600	8 A.M. 1 A.M.		Poor	Unsat.	16000 K.C.
0700	9 A.M. 2 A.M.		Poor-Unsat.	Unsat.	18400 K.C.
0800	10 A.M. 3 A.M.		Unsat.	Nil	19600 K.C.
0900	11 A.M. 4 A.M.		Unsat.	Nil	20300 K.C.
1000	12 N. 5 A.M.		Unsat.	Nil	20800 K.C.

Fig. 43—Schenectady-South Africa transmission chart. Spring Season (February 1 to May 1). Distance from Schenectady to Johannesburg 7900 miles (approx.).

TIME		DAYLIGHT-DARKNESS DISTRIBUTION OVER GREAT CIRCLE PATH	PROBABLE RECEPTION OBTAINABLE FROM		PROBABLE OPTIMUM FREQUENCY
GMT	S.Africa Local		W2XAD	W2XAF	
			13660 K.C.	9550 K.C.	Short Path
1100	1 P.M. 6 A.M.		Nil	Nil	21000 K.C.
1200	2 P.M. 7 A.M.		Nil	Nil	21000 K.C.
1300	3 P.M. 8 A.M.		Nil	Nil	21000 K.C.
1400	4 P.M. 9 A.M.		Nil	Nil	21000 K.C.
1500	5 P.M. 10 A.M.		Nil	Nil	21000 K.C.
1600	6 P.M. 11 A.M.		Nil	Nil	20800 K.C.
1700	7 P.M. 12 N.		Nil	Nil	20300 K.C.
1800	8 P.M. 1 P.M.		Nil	Nil	19600 K.C.
1900	9 P.M. 2 P.M.		Nil	Nil	18900 K.C.
2000	10 P.M. 3 P.M.		Unsat.	Nil	18000 K.C.
2100	11 P.M. 4 P.M.		Unsat.	Unsat.	17000 K.C.
2200	12 M. 5 P.M.		Poor	Unsat.	15700 K.C.
2300	1 A.M. 6 P.M.		Poor-Fair	Unsat.-Poor	14500 K.C.
0000	2 A.M. 7 P.M.		Poor-Fair	Poor	11200 K.C.
0100	3 A.M. 8 P.M.		Poor-Fair	Fair	8900 K.C.
0200	4 A.M. 9 P.M.		Poor-Fair	Fair-Good	8900 K.C.
0300	5 A.M. 10 P.M.		Fair	Good-Fair	8900 K.C.
0400	6 A.M. 11 P.M.		Fair	Good-Fair	8900 K.C.
0500	7 A.M. 12 M.		Fair-Poor	Fair-Poor	12300 K.C.
0600	8 A.M. 1 A.M.		Fair-Poor	Poor-Unsat.	17000 K.C.
0700	9 A.M. 2 A.M.		Poor	Unsat.	18800 K.C.
0800	10 A.M. 3 A.M.		Unsat.	Nil	20000 K.C.
0900	11 A.M. 4 A.M.		Nil	Nil	20600 K.C.
1000	12 N. 5 A.M.		Nil	Nil	20900 K.C.

Fig. 44—Schenectady-South Africa transmission chart. Summer season (May 1 to August 1). Distance from Schenectady to Johannesburg 7900 miles (approx.).

TIME		DAYLIGHT-DARKNESS DISTRIBUTION OVER GREAT CIRCLE PATH	PROBABLE RECEPTION OBTAINABLE FROM		PROBABLE OPTIMUM FREQUENCY
GMT	S.Africa Local		W2XAD	W2XAF	
			13660 K.C.	9550 K.C.	Short Path
1100	1 P.M. 6 A.M.		Nil	Nil	21000 K.C.
1200	2 P.M. 7 A.M.		Nil	Nil	21000 K.C.
1300	3 P.M. 8 A.M.		Nil	Nil	21000 K.C.
1400	4 P.M. 9 A.M.		Nil	Nil	21000 K.C.
1500	5 P.M. 10 A.M.		Nil	Nil	21000 K.C.
1600	6 P.M. 11 A.M.		Nil	Nil	21000 K.C.
1700	7 P.M. 12 N.		Nil	Nil	20300 K.C.
1800	8 P.M. 1 P.M.		Nil	Nil	20000 K.C.
1900	9 P.M. 2 P.M.		Unsat.	Nil	19000 K.C.
2000	10 P.M. 3 P.M.		Unsat.	Nil	17800 K.C.
2100	11 P.M. 4 P.M.		Unsat.-Poor	Unsat.	16600 K.C.
2200	12 M. 5 P.M.		Poor	Poor	15200 K.C.
2300	1 A.M. 6 P.M.		Poor-Fair	Fair	12500 K.C.
0000	2 A.M. 7 P.M.		Poor-Fair	Fair-Good	8900 K.C.
0100	3 A.M. 8 P.M.		Poor-Fair	Fair-Good	8900 K.C.
0200	4 A.M. 9 P.M.		Fair-Poor	Good-Fair	8900 K.C.
0300	5 A.M. 10 P.M.		Fair-Poor	Fair	8900 K.C.
0400	6 A.M. 11 P.M.		Fair-Poor	Fair-Poor	8900 K.C.
0500	7 A.M. 12 M.		Fair-Poor	Poor	12000 K.C.
0600	8 A.M. 1 A.M.		Poor	Unsat.	16000 K.C.
0700	9 A.M. 2 A.M.		Poor-Unsat.	Unsat.	16400 K.C.
0800	10 A.M. 3 A.M.		Unsat.	Nil	19600 K.C.
0900	11 A.M. 4 A.M.		Unsat.	Nil	20300 K.C.
1000	12 N. 5 A.M.		Unsat.	Nil	20800 K.C.

Fig. 45—Schenectady-South Africa transmission chart. Fall season (August 1 to November 1). Distance from Schenectady to Johannesburg 7900 miles (approx.)

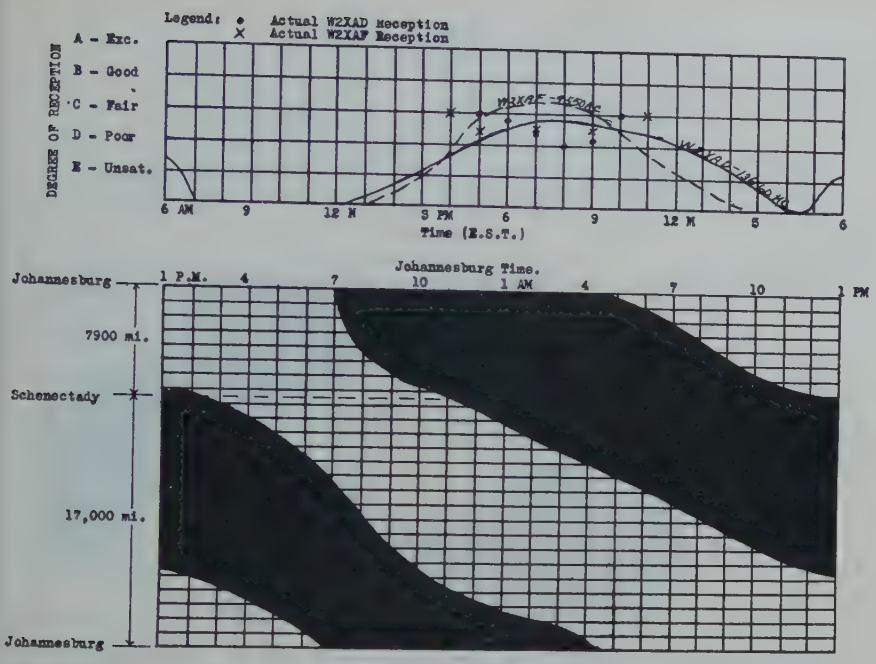

Fig. 46—Johannesburg reception from November 1 to February 1. Daylight-darkness distribution over great circle path from Schenectady to Johannesburg, South Africa, as of December 20.

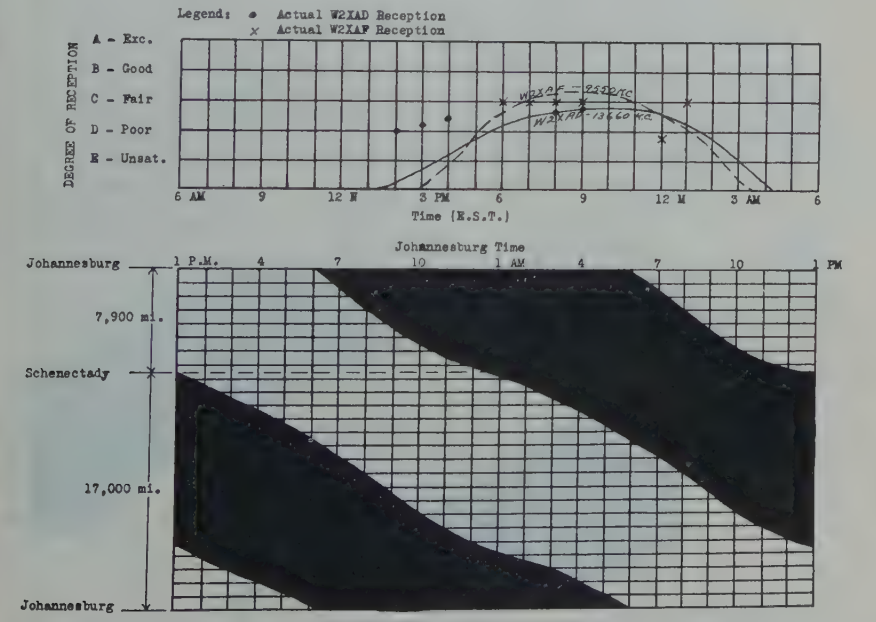

Fig. 47—Johannesburg reception from February 1 to May 1. Daylight-darkness distribution over great circle path from Schenectady to Johannesburg, South Africa, as of March 20.

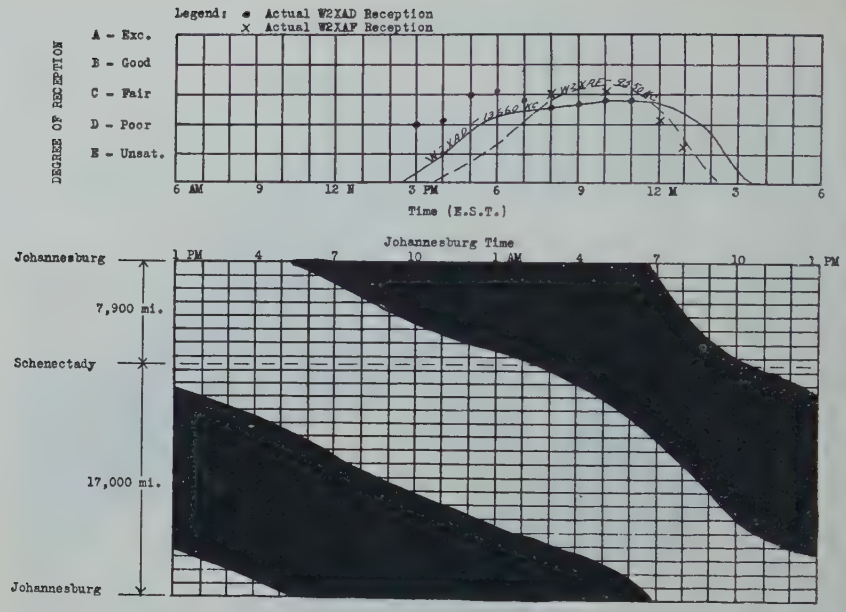

Fig. 48—Johannesburg reception from May 1 to August 1. Daylight-darkness distribution over great circle path from Schenectady to Johannesburg, South Africa, as of June 20.

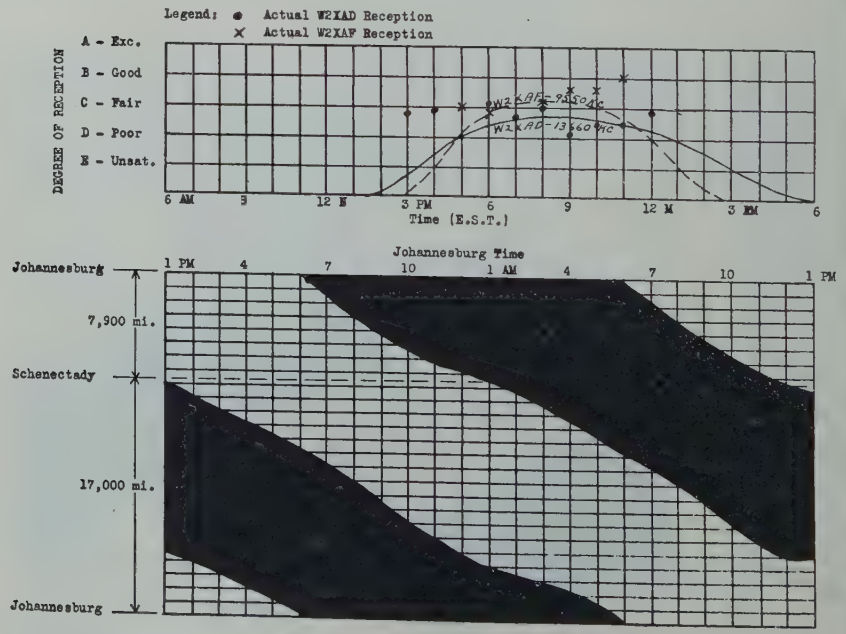

Fig. 49—Johannesburg reception from August 1 to November 1. Daylight-darkness distribution over great circle path from Schenectady to Johannesburg, South Africa, as of September 20.

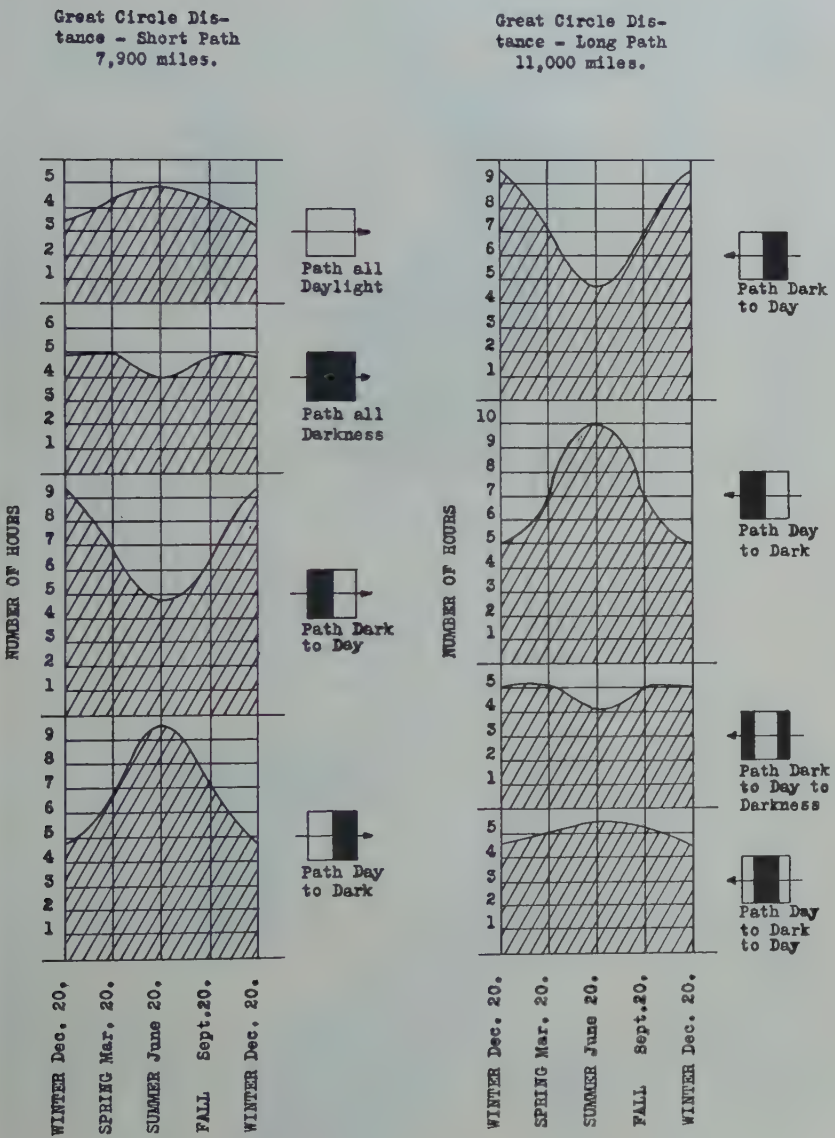

Fig. 50—Daylight-darkness distribution between Schenectady and Johannesburg, South Africa.

span the Atlantic, pass over the coast of West Africa and a part of the South Atlantic before reaching South Africa.

The diurnal and seasonal variations over this circuit are fully covered on Figs. 42 to 49.

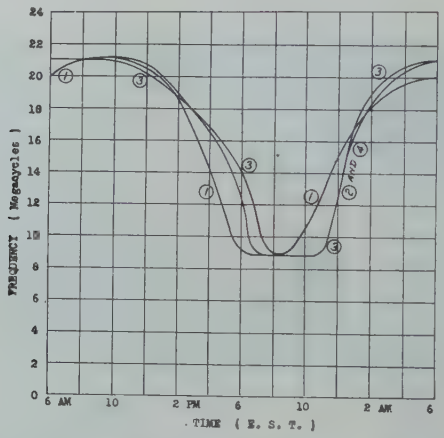

Fig. 51—Optimum frequency chart—Schenectady to Johannesburg, South Africa.
(1) Winter—November 1 to February 1.
(2) and (4)—Spring and Fall—February 1 to May 1 and August 1 to November 1.
(3) Summer—May 1 to August 1.

Seasonal daylight-darkness distribution data and the optimum frequency data are shown on Figs. 50 and 51, respectively.

Schenectady–Calcutta (India) Circuit

The length of this circuit and the direction of Calcutta from Schenectady are such that the effects of "seasonal variation" are very marked.

Reports from India on the reception of W2XAD and W2XAF are comparatively few thereby making it difficult to show the normal performances of the signals in that locality. At certain times these stations should be received fairly well. (Note Figs. 52 to 59, inclusive.)

TIME		DAYLIGHT-DARKNESS DISTRIBUTION OVER GREAT CIRCLE PATH	PROBABLE RECEPTION OBTAINABLE FROM		PROBABLE OPTIMUM
GMT	Calcutta Local		W2XAD	W2XAP	FREQUENCY
			13660 K.C.	9550 K.C.	Short Path
1100	4 P.M. 6 A.M.	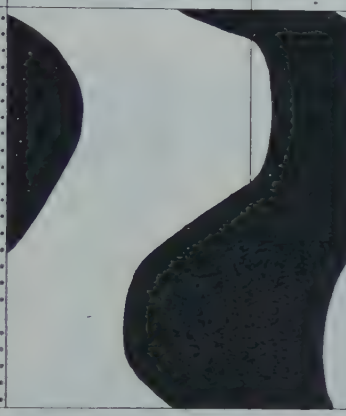	Fair-Poor	Unsat.-Poor	12500 K.C.
1200	5 P.M. 7 A.M.		Poor	Poor-Fair	10500 K.C.
1300	6 P.M. 8 A.M.		Poor	Poor-Unsat.	11500 K.C.
1400	7 P.M. 9 A.M.		Poor-Fair	Unsat.	12500 K.C.
1500	8 P.M. 10 A.M.		Poor-Fair	Unsat.	13300 K.C.
1600	9 P.M. 11 A.M.		Fair	Unsat.-Poor	14000 K.C.
1700	10 P.M. 12 A.M.		Fair-Poor	Unsat.-Poor	14500 K.C.
1800	11 P.M. 1 P.M.		Fair-Poor	Unsat.-Poor	13200 K.C.
1900	12 M. 2 P.M.		Poor	Poor	12300 K.C.
2000	1 A.M. 3 P.M.		Poor	Poor-Fair	11500 K.C.
2100	2 A.M. 4 P.M.		Poor	Poor-Fair	10400 K.C.
2200	3 A.M. 5 P.M.		Poor	Fair	9200 K.C.
2300	4 A.M. 6 P.M.		Poor	Fair	9200 K.C.
0000	5 A.M. 7 P.M.		Poor	Fair-Poor	9200 K.C.
0100	6 A.M. 8 P.M.		Poor	Fair-Poor	9200 K.C.
0200	7 A.M. 9 P.M.		Poor	Poor-Unsat.	10500 K.C.
0300	8 A.M. 10 P.M.		Poor	Unsat.	11200 K.C.
0400	9 A.M. 11 P.M.		Poor-Fair	Unsat.	11800 K.C.
0500	10 A.M. 12 M.		Poor-Fair	Unsat.	12600 K.C.
0600	11 A.M. 1 A.M.		Poor-Fair	Unsat.	13200 K.C.
0700	12 N. 2 A.M.		Fair	Unsat.	14000 K.C.
0800	1 P.M. 3 A.M.		Fair-Poor	Unsat.	14500 K.C.
0900	2 P.M. 4 A.M.		Fair-Poor	Unsat.	14600 K.C.
1000	3 P.M. 5 A.M.		Fair-Poor	Unsat.-Poor	14400 K.C.

Fig. 52—Schenectady-Calcutta transmission chart. Winter Season (November 1 to February 1). Distance from Schenectady to Calcutta 7800 miles (approx.)

TIME		DAYLIGHT-DARKNESS DISTRIBUTION OVER GREAT CIRCLE PATH	PROBABLE RECEPTION OBTAINABLE FROM		PROBABLE OPTIMUM
GMT	Calcutta Local		W2XAD	W2XAF	FREQUENCY
			13660 K.C.	9550 K.C.	Short Path
1100	4 P.M. 6 A.M.		Unsat.	Nil	22400 K.C.
1200	5 P.M. 7 A.M.		Unsat.	Nil	22400 K.C.
1300	6 P.M. 8 A.M.		Nil	Nil	22000 K.C.
1400	7 P.M. 9 A.M.		Nil	Nil	21500 K.C.
1500	8 P.M. 10 A.M.		Nil	Nil	20800 K.C.
1600	9 P.M. 11 A.M.		Nil	Nil	20000 K.C.
1700	10 P.M. 12 N.		Nil	Nil	19200 K.C.
1800	11 P.M. 1 P.M.		Nil	Nil	18400 K.C.
1900	12 M. 2 P.M.		Nnsat.	Nil	17600 K.C.
2000	1 A.M. 3 P.M.		Unsat.	Nil	16800 K.C.
2100	2 A.M. 4 P.M.		Unsat.-Poor	Unsat.	15600 K.C.
2200	3 A.M. 5 P.M.		Poor	Unsat.	14800 K.C.
2300	4 A.M. 6 P.M.		Poor-Fair	Poor	12800 K.C.
0000	5 A.M. 7 P.M.		Fair-Poor	Fair	9200 K.C.
0100	6 A.M. 8 P.M.		Fair-Poor	Fair	11800 K.C.
0200	7 A.M. 9 P.M.		Fair-Poor	Fair-Poor	15000 K.C.
0300	8 A.M. 10 P.M.		Fair-Poor	Poor-Unsat.	17200 K.C.
0400	9 A.M. 11 P.M.		Poor	Poor-Unsat.	19500 K.C.
0500	10 A.M. 12 M.		Poor-Unsat.	Unsat.	20400 K.C.
0600	11 A.M. 1 A.M.		Poor-Unsat.	Unsat.	21000 K.C.
0700	12 N. 2 A.M.		Poor-Unsat.	Nil	21500 K.C.
0800	1 P.M. 3 A.M.		Poor-Unsat.	Nil	21800 K.C.
0900	2 P.M. 4 A.M.		Unsat.	Nil	22100 K.C.
1000	3 P.M. 5 A.M.		Unsat.	Nil	22300 K.C.

Fig. 53—Schenectady-Calcutta transmission chart. Spring season (February 1 to May 1). Distance from Schenectady to Calcutta 7800 miles (approx.)

TIME		DAYLIGHT-DARKNESS DISTRIBUTION OVER GREAT CIRCLE PATH	PROBABLE RECEPTION OBTAINABLE FROM		PROBABLE OPTIMUM FREQUENCY
GMT	Calcutta Local		W2XAD	W2XAF	
			13660 K.C.	9550 K.C.	Short Path
1100	4 P.M. 6 2.M.		Nil	Nil	22400 K.C.
1200	5 P.M. 7 A.M.		Nil	Nil	22400 K.C.
1300	6 P.M. 8 A.M.		Nil	Nil	22400 K.C.
1400	7 P.M. 9 A.M.		Nil	Nil	22500 K.C.
1500	8 P.M. 10 A.M.		Nil	Nil	22200 K.C.
1600	9 P.M. 11 A.M.		Nil	Nil	21900 K.C.
1700	10 P.M. 12 N.		Nil	Nil	21500 K.C.
1800	11 P.M. 1 P.M.		Nil	Nil	21000 K.C.
1900	12 M. 2 P.M.		Nil	Nil	20000 K.C.
2000	1 A.M. 3 P.M.		Nil,	Nil	19100 K.C.
2100	2 A.M. 4 P.M.		Nil	Nil	19800 K.C.
2200	3 A.M. 5 P.M.		Nil	Nil	20900 K.C.
2300	4 A.M. 6 P.M.		Unsat.	Nil	21900 K.C.
0000	5 A.M. 7 P.M.		Unsat.	Unsat.	22400 K.C.
0100	6 A.M. 8 P.M.		Poor	Unsat.	22200 K.C.
0200	7 A.M. 9 P.M.		Poor-Unsat.	Unsat.	22000 K.C.
0300	8 A.M. 10 P.M.		Unsat.	Unsat.	21000 K.C.
0400	9 A.M. 11 P.M.		Unsat.	Unsat.	20200 K.C.
0500	10 A.M. 12 M.		Unsat.	Unsat.	19500 K.C.
0600	11 A.M. 1 A.M.		Unsat.	Unsat.	20000 K.C.
0700	12 N. 2 A.M.		Unsat.-Poor	Unsat.	21000 K.C.
0800	1 P.M. 3 A.M.		Unsat.-Poor	Unsat.	22000 K.C.
0900	2 P.M. 4 A.M.		Poor-Unsat.	Unsat.	22400 K.C.
1000	3 P.M. 5 A.M.		Poor-Unsat.	Unsat.	22400 K.C.

Fig. 54—Schenectady-Calcutta transmission chart. Summer season (May 1 to August 1). Distance from Schenectady to Calcutta 7800 miles (approx.)

TIME		DAYLIGHT-DARKNESS DISTRIBUTION OVER GREAT CIRCLE PATH	PROBABLE RECEPTION OBTAINABLE FROM		PROBABLE OPTIMUM FREQUENCY
GMT	Calcutta Local		W2XAD	W2XAF	
			13660 K.C.	9550 K.C.	Short Path
1100	4 P.M. 6 A.M.		Unsat.	Nil	22400 K.C.
1200	5 P.M. 7 A.M.		Unsat.	Nil	22400 K.C.
1300	6 P.M. 8 A.M.		Nil	Nil	22000 K.C.
1400	7 P.M. 9 A.M.		Nil	Nil	21500 K.C.
1500	8 P.M. 10 A.M.		Nil	Nil	20800 K.C.
1600	9 P.M. 11 A.M.		Nil	Nil	20000 K.C.
1700	10 P.M. 12 N.		Nil	Nil	19200 K.C.
1800	11 P.M. 1 P.M.		Nil	Nil	18400 K.C.
1900	12 M. 2 P.M.		Unsat.	Nil	17600 K.C.
2000	1 A.M. 3 P.M.		Unsat.	Nil	16800 K.C.
2100	2 A.M. 4 P.M.		Unsat.-Poor	Unsat.	15600 K.C.
2200	3 A.M. 5 P.M.		Poor	Unsat.	14800 K.C.
2300	4 A.M. 6 P.M.		Poor-Fair	Poor	12800 K.C.
0000	5 A.M. 7 P.M.		Fair-Poor	Fair	9200 K.C.
0100	6 A.M. 8 P.M.		Fair-Poor	Fair	11800 K.C.
0200	7 A.M. 9 P.M.		Fair-Poor	Fair-Poor	15000 K.C.
0300	8 A.M. 10 P.M.		Fair-Poor	Poor-Unsat.	17200 K.C.
0400	9 A.M. 11 P.M.		Poor	Poor-Unsat.	19500 K.C.
0500	10 A.M. 12 M.		Poor-Unsat.	Unsat.	20400 K.C.
0600	11 A.M. 1 A.M.		Poor-Unsat.	Unsat.	21000 K.C.
0700	12 N. 2 A.M.		Poor-Unsat.	Nil	21500 K.C.
0800	1 P.M. 3 A.M.		Poor-Unsat.	Nil	21800 K.C.
0900	2 P.M. 4 A.M.		Unsat.	Nil	22100 K.C.
1000	3 P.M. 5 A.M.		Unsat.	Nil	22300 K.C.

Fig. 55—Schenectady-Calcutta transmission chart. Fall season (August 1 to November 1). Distance from Schenectady to Calcutta 7800 miles (approx.).

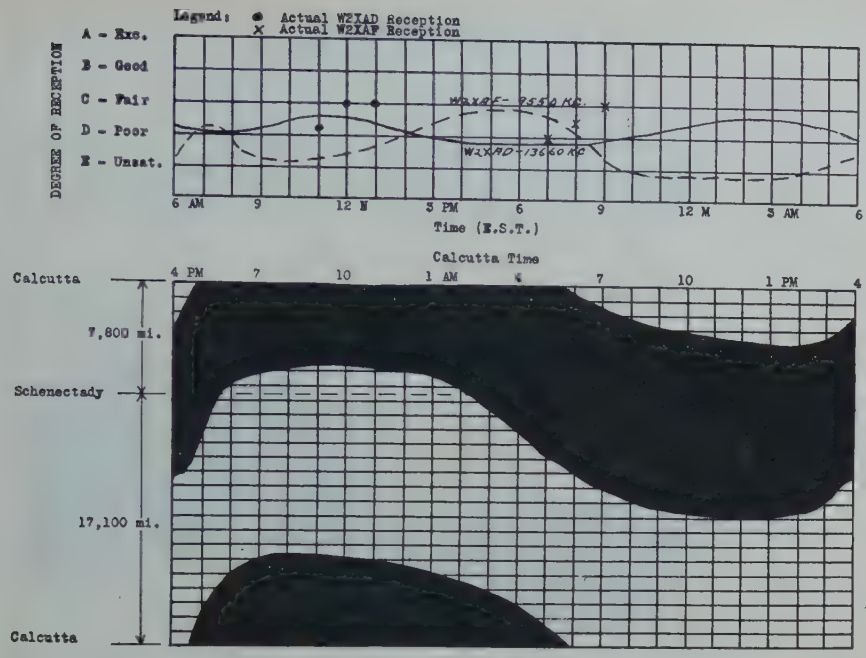

Fig. 56—Calcutta reception from November 1 to February 1. Daylight-darkness distribution over great circle path from Schenectady to Calcutta, India, as of December 20.

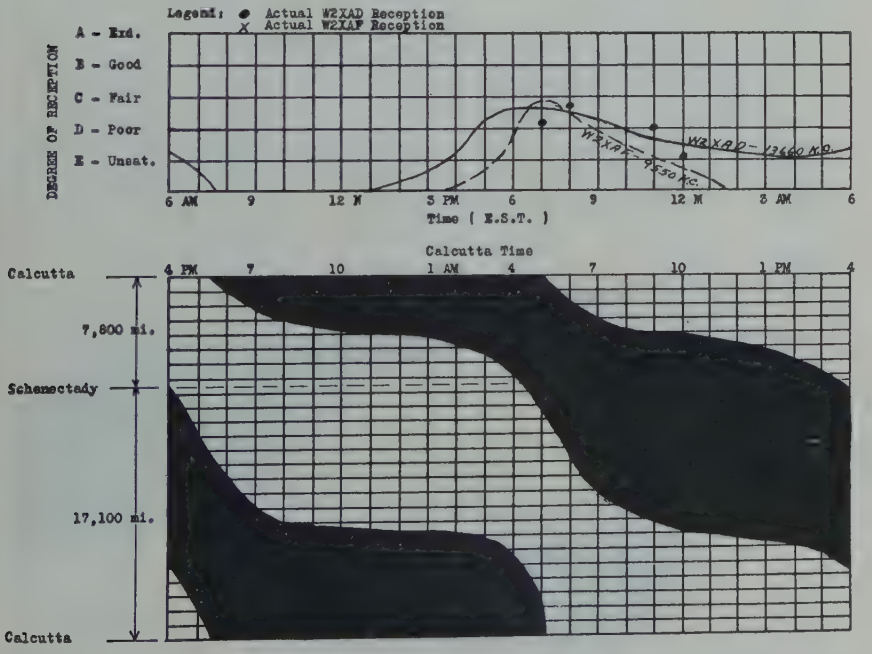

Fig. 57—Calcutta reception from February 1 to May 1. Daylight-darkness distribution over great circle path from Schenectady to Calcutta, India, as of March 20.

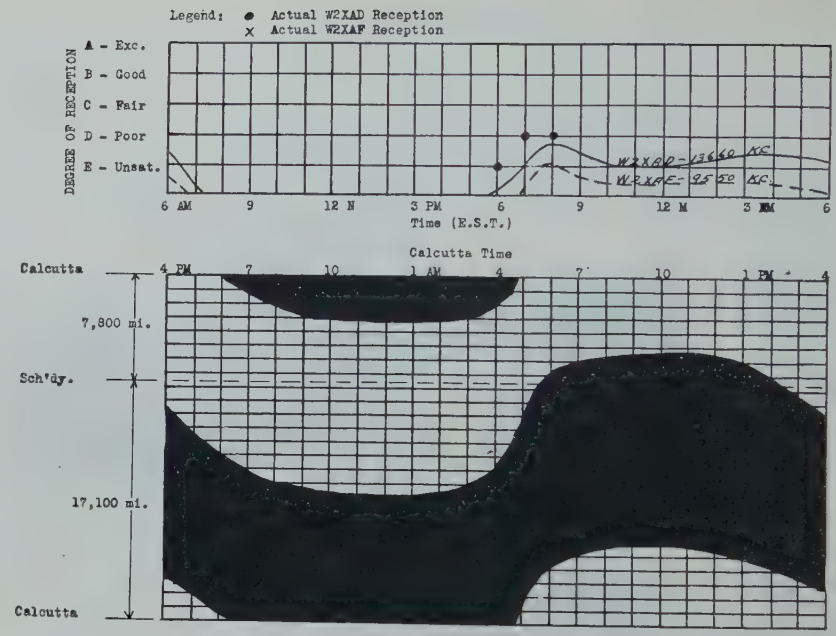

Fig. 58—Calcutta reception from May 1 to August 1. Daylight-darkness distribution over great circle path from Schenectady to Calcutta, India, as of June 20.

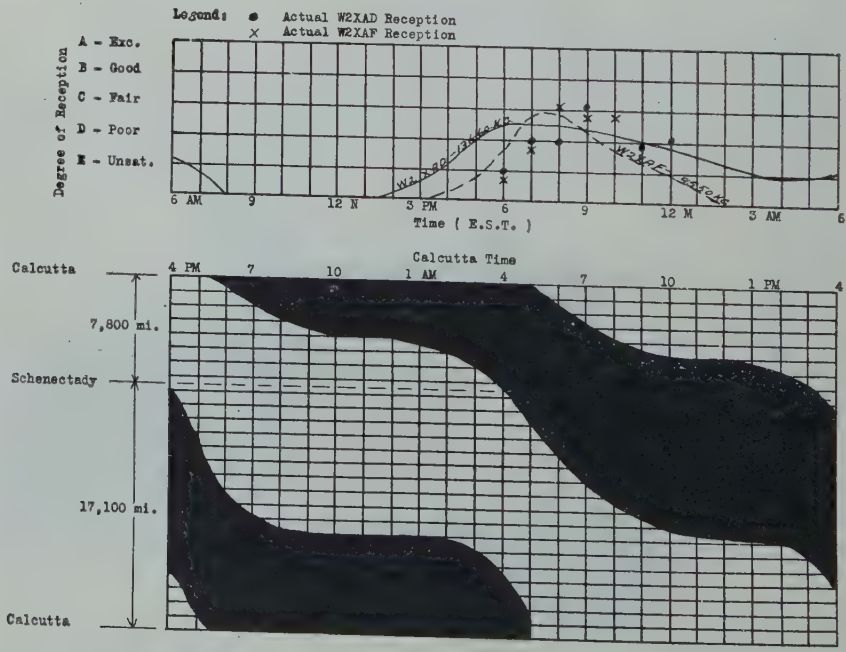

Fig. 59—Calcutta reception from August 1 to November 1. Daylight-darkness distribution over great circle path from Schenectady to Calcutta, India, as of September 20.

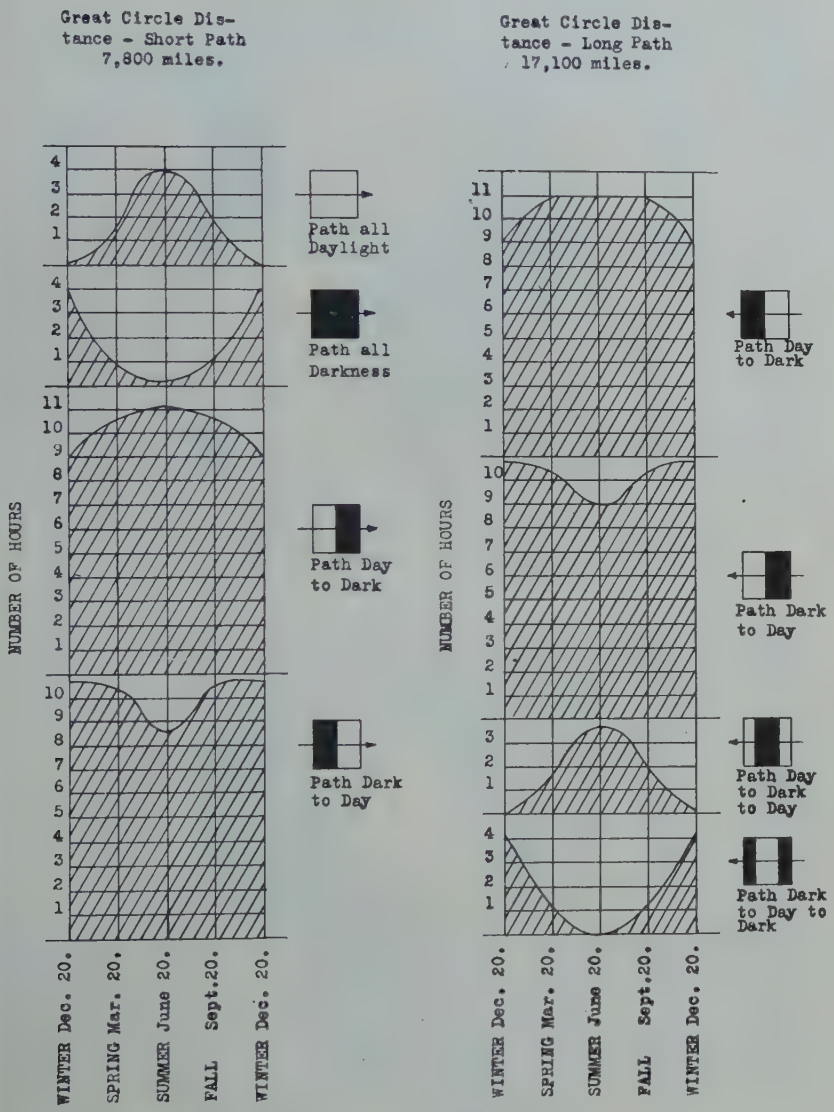

Fig. 60—Daylight-darkness distribution between Schenectady and Calcutta, India.

The reasons for more reception reports not being received are probably (1) lack of high-frequency receiving apparatus and (2) inconvenient hours for reception.

Optimum transmission frequency data for this circuit are given on Fig. 61.

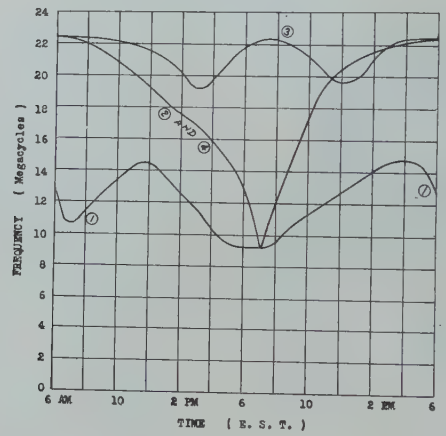

Fig. 61—Optimum frequency chart—Schenectady to Calcutta, India.
(1) Winter—November 1 to February 1.
(2) and (4)—Spring and Fall—February 1 to May 1 and August 1 to November 1.
(3) Summer—May 1 to August 1.

Schenectady–Shanghai (China) Circuit

The approximate distance over the great circle path from Schenectady to Shanghai is 7100 miles. The data available indicate that the seasonal variation over this circuit is quite pronounced. This is probably largely due to the proximity of the transmission path to the North Polar region, where six-month periods of daylight and darkness alternately prevail. For additional data see Figs. 62 to 69.

TIME		DAYLIGHT-DARKNESS DISTRIBUTION OVER GREAT CIRCLE PATH	PROBABLE RECEPTION OBTAINABLE FROM		PROBABLE OPTIMUM FREQUENCY
GMT	Shanghai Local		W2XAD	W2XAF	
			13660 K.C.	9550 K.C.	Short Path
1100	7 P.M. 6 A.M.		Poor-Fair	Good-Fair	9200 K.C.
1200	8 P.M. 7 A.M.		Poor-Fair	Good-Fair	9200 K.C.
1300	9 P.M. 8 A.M.		Fair	Fair	11000 K.C.
1400	10 P.M. 9 A.M.		Fair-Good	Fair-Poor	15400 K.C.
1500	11 P.M. 10 A.M.		Fair	Poor-Unsat.	15000 K.C.
1600	12 M. 11 A.M.		Fair-Poor	Unsat.	16200 K.C.
1700	1 A.M. 12 N.		Fair-Poor	Unsat.	17000 K.C.
1800	2 A.M. 1 P.M.		Poor	Unsat.	17000 K.C.
1900	3 A.M. 2 P.M.		Poor-Fair	Unsat.	16800 K.C.
2000	4 A.M. 3 P.M.		Fair	Unsat.	14800 K.C.
2100	5 A.M. 4 P.M.		Fair	Poor	12400 K.C.
2200	6 A.M. 5 P.M.		Fair-Poor	Poor-Fair	9200 K.C.
2300	7 A.M. 6 P.M.		Poor	Fair	11000 K.C.
0000	8 A.M. 7 P.M.		Poor-Unsat.	Poor	15000 K.C.
0100	9 A.M. 8 P.M.		Poor-Unsat.	Poor-Unsat.	16400 K.C.
0200	10 A.M. 9 P.M.		Unsat.-Poor	Poor	16800 K.C.
0300	11 A.M. 10 P.M.		Unsat.-Poor	Unsat.	17000 K.C.
0400	12 N. 11 P.M.		Unsat.-Poor	Unsat	16800 K.C.
0500	1 P.M. 12 M.		Unsat.-Poor	Unsat.-Poor	16600 K.C.
0600	2 P.M. 1 A.M.		Poor	Unsat.-Poor	16300 K.C.
0700	3 P.M. 2 A.M.		Poor-Fair	Poor	15200 K.C.
0800	4 P.M. 3 A.M.		Fair	Poor-Fair	12800 K.C.
0900	5 P.M. 4 A.M.		Fair	Fair	9200 K.C.
1000	6 P.M. 5 A.M.		Fair-Poor	Fair-Good	9200 K.C.

Fig. 62—Schenectady-Shanghai transmission chart. Winter season (November 1 to February 1). Distance from Schenectady to Shanghai 7100 miles (approx.)

TIME		DAYLIGHT-DARKNESS DISTRIBUTION OVER GREAT CIRCLE PATH	PROBABLE RECEPTION OBTAINABLE FROM		PROBABLE OPTIMUM FREQUENCY
GMT	Shanghai Local		W2XAD	W2XAF	
			13660 K.C.	9550 K.C.	Short Path
1100	7 P.M. 6 A.M.		Fair-Poor	Good-Fair	8200 K.C.
1200	8 P.M. 7 A.M.		Fair-Poor	Fair-Poor	10600 K.C.
1300	9 P.M. 8 A.M.		Fair-Poor	Unsat.	12800 K.C.
1400	10 P.M. 9 A.M.		Fair-Poor	Nil	15200 K.C.
1500	11 P.M. 10 A.M.		Poor	Nil	16000 K.C.
1600	12 M. 11 A.M.		Poor-Unsat.	Nil	17000 K.C.
1700	1 A.M. 12 N.		Poor-Unsat.	Nil	17400 K.C.
1800	2 A.M. 1 P.M.		Unsat.	Nil	17800 K.C.
1900	3 A.M. 2 P.M.		Unsat.	Nil	18500 K.C.
2000	4 A.M. 3 P.M.		Nil	Nil	20300 K.C.
2100	5 A.M. 4 P.M.		Nil	Nil	21800 K.C.
2200	6 A.M. 5 P.M.		Nil	Nil	22200 K.C.
2300	7 A.M. 6 P.M.		Nil	Nil	22200 K.C.
0000	8 A.M. 7 P.M.		Nil	Nil	22100 K.C.
0100	9 A.M. 8 P.M.		Unsat.	Nil	21900 K.C.
0200	10 A.M. 9 P.M.		Unsat.	Nil	21400 K.C.
0300	11 A.M. 10 P.M.		Unsat.	Nil	20700 K.C.
0400	12 N. 11 P.M.		Unsat.-Poor	Unsat.	20000 K.C.
0500	1 P.M. 12 M.		Poor	Unsat.	19000 K.C.
0600	2 P.M. 1 A.M.		Poor-Fair	Unsat.	17500 K.C.
0700	3 P.M. 2 A.M.		Fair	Unsat.-Poor	16000 K.C.
0800	4 P.M. 3 A.M.		Fair	Poor	14400 K.C.
0900	5 P.M. 4 A.M.		Fair	Poor-Fair	12800 K.C.
1000	6 P.M. 5 A.M.		Fair-Poor	Fair	11000 K.C.

Fig. 63—Schenectady-Shanghai transmission chart. Spring season (February 1 to May 1). Distance from Schenectady to Shanghai 7100 miles (approx.)

TIME		DAYLIGHT-DARKNESS DISTRIBUTION OVER GREAT CIRCLE PATH	PROBABLE RECEPTION OBTAINABLE FROM		PROBABLE OPTIMUM FREQUENCY
GMT	Shanghai Local		W2XAD	W2XAF	
			13660 K.C.	9550 K.C.	Short Path
1100	7 P.M. 6 A.M.		Nil	Nil	22200 K.C.
1200	8 P.M. 7 A.M.		Nil	Nil	22200 K.C.
1300	9 P.M. 8 A.M.		Nil	Nil	21700 K.C.
1400	10 P.M. 9 A.M.		Nil	Nil	21000 K.C.
1500	11 P.M. 10 A.M.		Nil	Nil	19400 K.C.
1600	12 M. 11 A.M.		Nil	Nil	19100 K.C.
1700	1 A.M. 12 N.		Nil	Nil	20000 K.C.
1800	2 A.M. 1 P.M.		Nil	Nil	21000 K.C.
1900	3 A.M. 2 P.M.		Nil	Nil	21700 K.C.
2000	4 A.M. 3 P.M.		Nil	Nil	22100 K.C.
2100	5 A.M. 4 P.M.		Nil	Nil	22000 K.C.
2200	6 A.M. 5 P.M.		Unsat.	Nil	22000 K.C.
2300	7 A.M. 6 P.M.		Unsat.	Nil	22000 K.C.
0000	8 A.M. 7 P.M.		Unsat.	Nil	22000 K.C.
0100	9 A.M. 8 P.M.		Nil	Nil	22100 K.C.
0200	10 A.M. 9 P.M.		Nil	Nil	21900 K.C.
0300	11 A.M. 10 P.M.		Unsat.	Nil	21500 K.C.
0400	12 N. 11 P.M.		Unsat.	Nil	20600 K.C.
0500	1 P.M. 12 M.		Unsat.	Nil	19000 K.C.
0600	2 P.M. 1 A.M.		Unsat.	Nil	20200 K.C.
0700	3 P.M. 2 A.M.		Unsat.	Nil	21500 K.C.
0800	4 P.M. 3 A.M.		Nil	Nil	22000 K.C.
0900	5 P.M. 4 A.M.		Nil	Nil	22100 K.C.
1000	6 P.M. 5 A.M.		Nil	Nil	22200 K.C.

Fig. 64—Schenectady-Shanghai transmission chart. Summer season (May 1 to to August 1). Distance from Schenectady to Shanghai 7100 miles (approx.)

TIME		DAYLIGHT-DARKNESS DISTRIBUTION OVER GREAT CIRCLE PATH	PROBABLE RECEPTION OBTAINABLE FROM		PROBABLE OPTIMUM FREQUENCY
GMT	Shanghai Local		W2XAD	W2XAF	
			13660 K.C.	9550 K.C.	Short Path
1100	7 P.M. 6 A.M.		Fair-Poor	Good-Fair	9200 K.C.
1200	8 P.M. 7 A.M.		Fair-Poor	Fair-Poor	10600 K.C.
1300	9 P.M. 8 A.M.		Fair-Poor	Unsat.	12800 K.C.
1400	10 P.M. 9 A.M.		Fair-Poor	Nil	15200 K.C.
1500	11 P.M. 10 A.M.		Poor	Nil	16000 K.C.
1600	12 M. 11 A.M.		Poor-Unsat.	Nil	17000 K.C.
1700	1 A.M. 12 N.		Poor-Unsat.	Nil	17400 K.C.
1800	2 A.M. 1 P.M.		Unsat.	Nil	17800 K.C.
1900	3 A.M. 2 P.M.		Unsat.	Nil	18500 K.C.
2000	4 A.M. 3 P.M.		Nil	Nil	20500 K.C.
2100	5 A.M. 4 P.M.		Nil	Nil	21800 K.C.
2200	6 A.M. 5 P.M.		Nil	Nil	22200 K.C.
2300	7 A.M. 6 P.M.		Nil	Nil	22200 K.C.
0000	8 A.M. 7 P.M.		Nil	Nil	22100 K.C.
0100	9 A.M. 8 P.M.		Unsat.	Nil	21900 K.C.
0200	10 A.M. 9 P.M.		Unsat.	Nil	21400 K.C.
0300	11 A.M. 10 P.M.		Unsat.	Nil	20700 K.C.
0400	12 N. 11 P.M.		Unsat.-Poor	Unsat.	20000 K.C.
0500	1 P.M. 12 M.		Poor	Unsat.	19000 K.C.
0600	2 P.M. 1 A.M.		Poor-Fair	Unsat.	17500 K.C.
0700	3 P.M. 2 A.M.		Fair	Unsat.-Poor	16000 K.C.
0800	4 P.M. 3 A.M.		Fair	Poor	14400 K.C.
0900	5 P.M. 4 A.M.		Fair	Poor-Fair	12800 K.C.
1000	6 P.M. 5 A.M.		Fair-Poor	Fair	11000 K.C.

Fig. 65—Schenectady-Shanghai transmission chart. Fall season (August 1 to November 1). Distance from Schenectady to Shanghai 7100 miles (approx.)

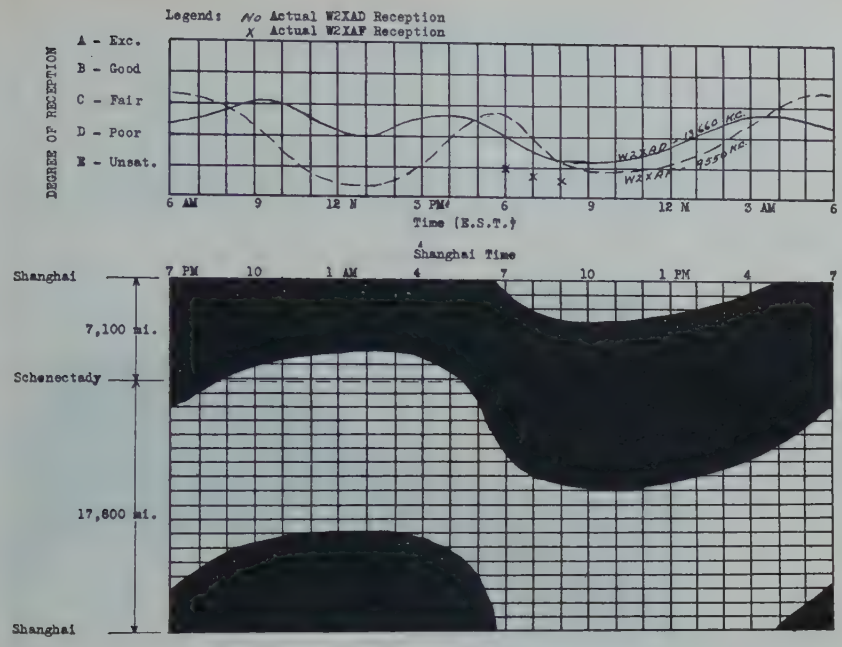

Fig. 66—Shanghai reception from November 1 to February 1. Daylight-darkness distribution over great circle path from Schenectady to Shanghai, China, as of December 20.

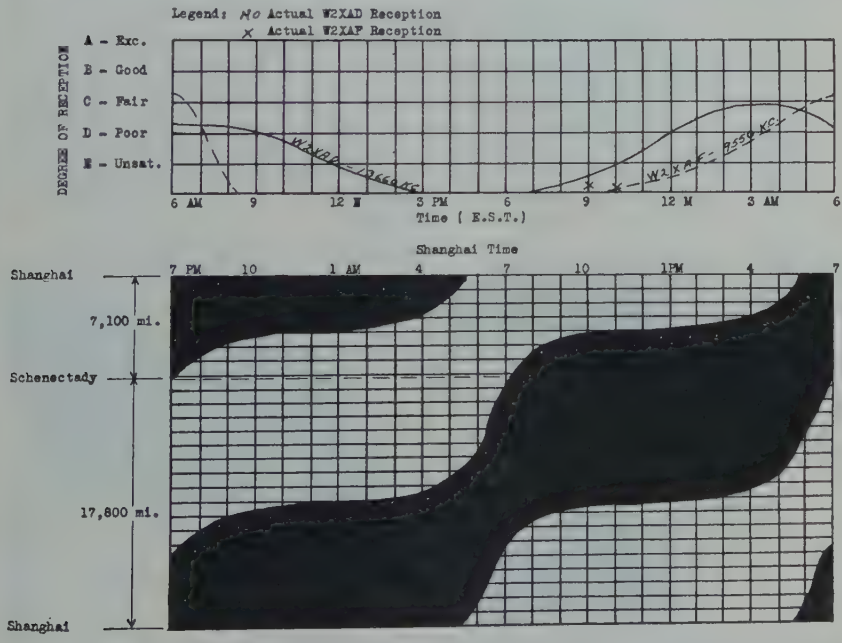

Fig. 67—Shanghai reception from February 1 to May 1. Daylight-darkness distribution over great circle path from Schenectady to Shanghai, China, as of March 20.

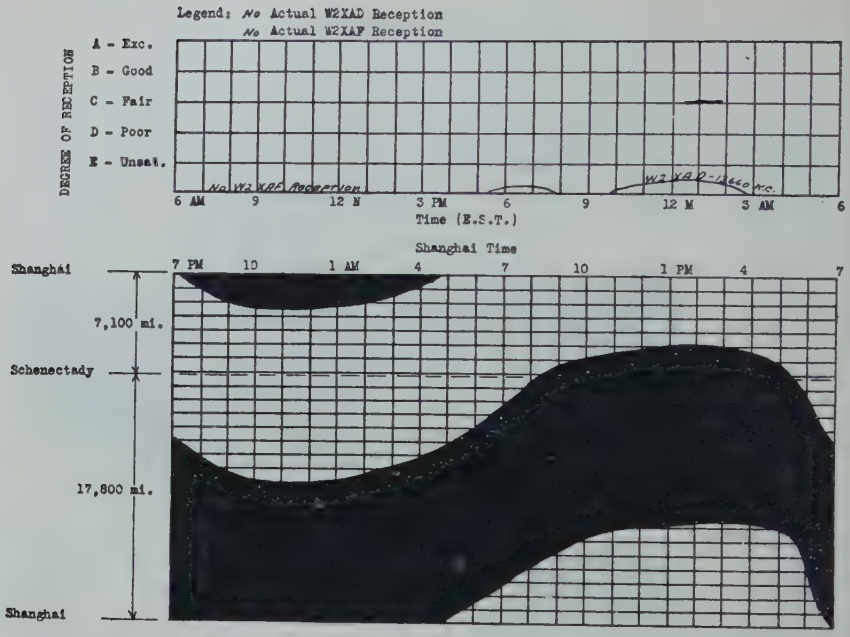

Fig. 68—Shanghai reception from May 1 to August 1. Daylight-darkness distribution over great circle path from Schenectady, to Shanghai, China, as of June 20.

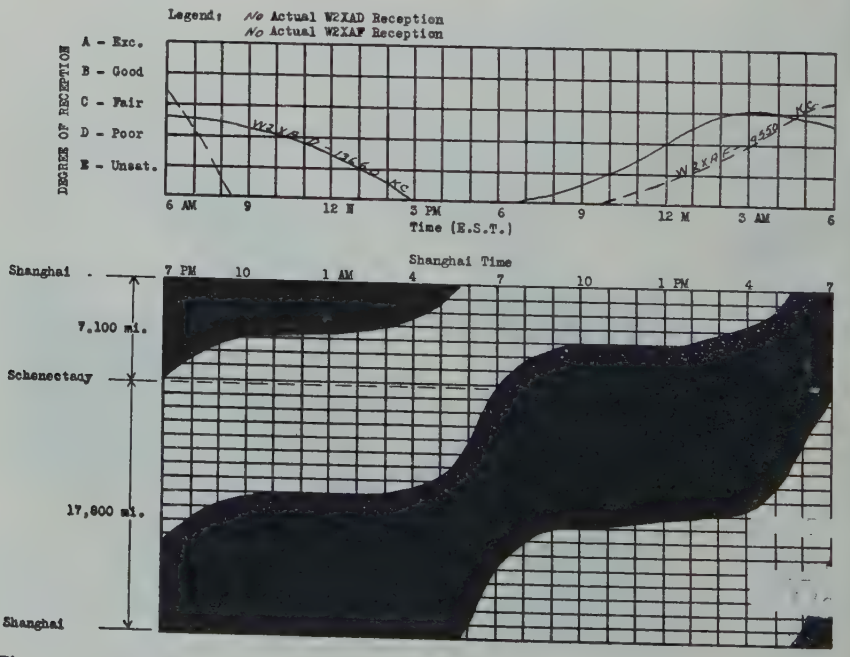

Fig. 69—Shanghai reception from August 1 to November 1. Daylight-darkness distribution over great circle path from Schenectady to Shanghai, China as of September 20.

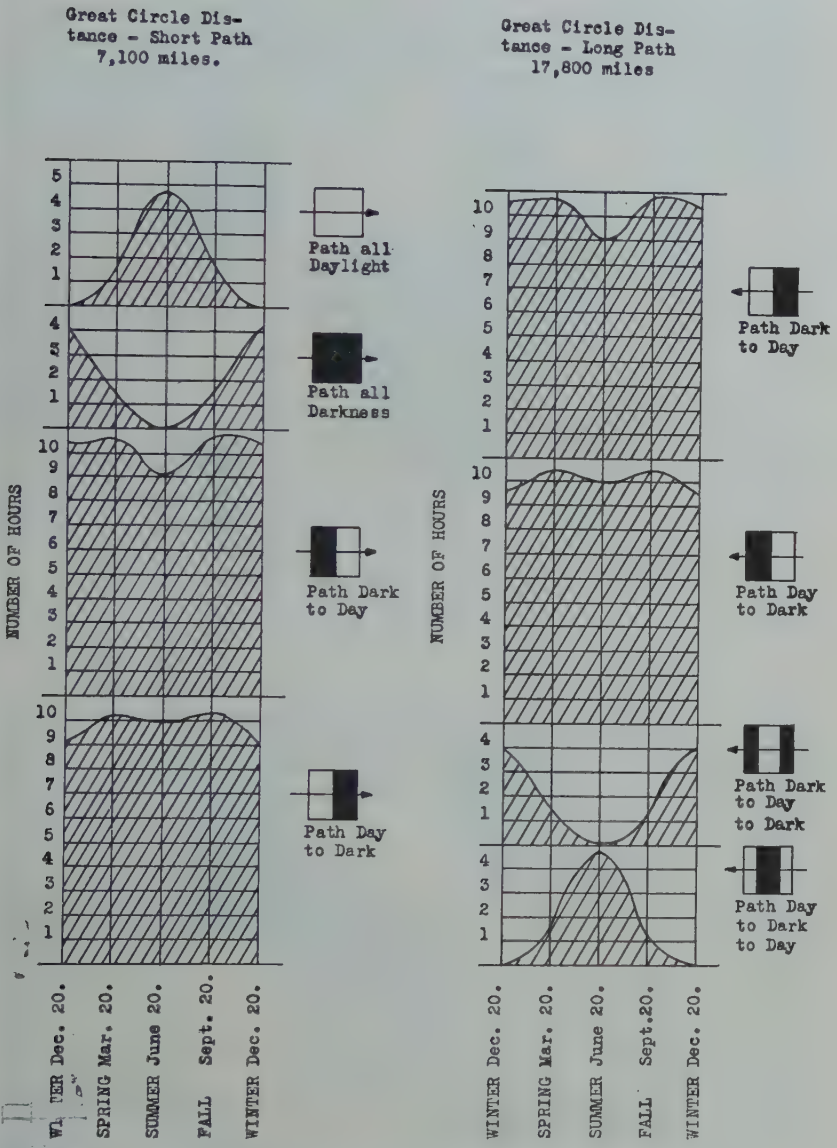

Fig. 70—Daylight-darkness distribution between Schenectady and Shanghai, China.

Comparatively few reception reports have been received from China. This is particularly true in the case of W2XAD and W2XAF. The main reason for the scarcity of W2XAD and W2XAF reception reports is that neither of these stations is well received in China during their normal hours of operation. During the summer months, no reception of W2XAD and W2XAF transmissions should normally be effected in China.

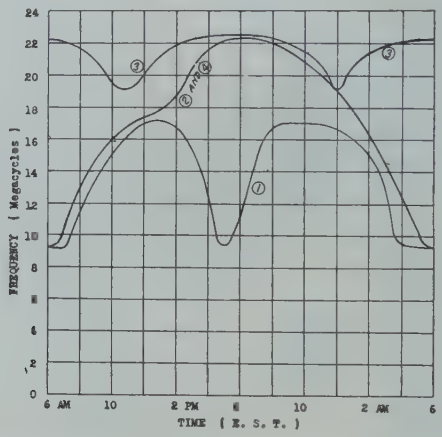

Fig. 71—Optimum frequency chart—Schenectady to Shanghai, China.
(1) Winter—November 1 to February 1.
(2) and (4)—Spring and Fall—February 1 to May 1 and August 1 to November 1.
(3) Summer—May 1 to August 1.

By referring to Fig. 71, the value of the optimum frequencies for this circuit may be obtained. This figure also shows the magnitude of the diurnal and seasonal variation.

Schenectady–Tokio (Japan) Circuit

This circuit is similar to the Schenectady–Shanghai circuit which has already been discussed.

TIME			DAYLIGHT-DARKNESS DISTRIBUTION OVER GREAT CIRCLE PATH	PROBABLE RECEPTION OBTAINABLE FORM		PROBABLE OPTIMUM FREQUENCY
GMT	Tokio	Local		W2XAD	W2XAF	
1100	6 P.M.	6 A.M.		13660 K.C.	9550 K.C.	Short Path
1200	7 P.M.	7 A.M.		Poor-Fair	Good-Fair	9000 K.C.
1300	8 P.M.	8 A.M.		Poor-Fair	Good-Fair	9000 K.C.
1400	9 P.M.	9 A.M.		Fair	Fair-Poor	11500 K.C.
1500	10 P.M.	10 A.M.		Fair	Poor	13200 K.C.
1600	11 P.M.	11 A.M.		Fair-Poor	Poor-Unsat.	15000 K.C.
1700	12 M.	12 N.		Poor-Unsat.	Unsat.	16400 K.C.
1800	1 A.M.	1 P.M.		Poor-Unsat.	Unsat.	17000 K.C.
1900	2 A.M.	2 P.M.		Poor-Unsat.	Unsat.	17600 K.C.
2000	3 A.M.	3 P.M.		Unsat.-Poor	Unsat.	16800 K.C.
2100	4 A.M.	4 P.M.		Unsat.-Poor	Unsat.	16500 K.C.
2200	5 A.M.	5 P.M.		Poor	Poor-Fair	11500 K.C.
2300	6 A.M.	6 P.M.		Poor-Unsat.	Fair-Poor	9000 K.C.
0000	7 A.M.	7 P.M.		Poor	Poor-Unsat.	14600 K.C.
0100	8 A.M.	8 P.M.		Poor-Unsat.	Unsat.	16600 K.C.
0200	9 A.M.	9 P.M.		Poor-Unsat.	Unsat.	17600 K.C.
0300	10 A.M.	10 P.M.		Unsat.	Unsat.	17800 K.C.
0400	11 A.M.	11 P.M.		Unsat.-Poor	Unsat.	17800 K.C.
0500	12 N.	12 M.		Unsat.-Poor	Unsat.	17600 K.C.
0600	1 P.M.	1 A.M.		Poor	Unsat.	17000 K.C.
0700	2 P.M.	2 A.M.		Poor-Fair	Unsat.-Poor	15800 K.C.
0800	3 P.M.	3 A.M.		Fair	Poor	14400 K.C.
0900	4 P.M.	4 A.M.		Fair	Poor-Fair	12800 K.C.
1000	5 P.M.	5 A.M.		Fair	Fair	11200 K.C.
				Fair-Poor	Fair-Good	9000 K.C.

Fig. 72—Schenectady-Tokio transmission chart. Winter season (November 1 to February 1). Distance from Schenectady to Tokio 6600 miles (approx.)

TIME			DAYLIGHT-DARKNESS DISTRIBUTION OVER GREAT CIRCLE PATH	PROBABLE RECEPTION OBTAINABLE FROM		PROBABLE OPTIMUM FREQUENCY
GMT	Tokio	Local		W2XAD	W2XAF	
1100	8 P.M.	6 A.M.		13660 K.C.	9550 K.C.	Short Path
1200	9 P.M.	7 A.M.		Fair	Good-Fair	9000 K.C.
1300	10 P.M.	8 A.M.		Fair-Poor	Fair	10400 K.C.
1400	11 P.M.	9 A.M.		Fair-Poor	Poor	12800 K.C.
1500	12 M.	10 A.M.		Fair-Poor	Unsat.	14500 K.C.
1600	1 A.M.	11 A.M.		Poor	Nil	15800 K.C.
1700	2 A.M.	12 N.		Poor-Unsat.	Nil	17200 K.C.
1800	3 A.M.	1 P.M.		Unsat.	Nil	18400 K.C.
1900	4 A.M.	2 P.M.		Unsat.	Nil	19700 K.C.
2000	5 A.M.	3 P.M.		Nil	Nil	21000 K.C.
2100	6 A.M.	4 P.M.		Nil	Nil	21700 K.C.
2200	7 A.M.	5 P.M.		Nil	Nil	22000 K.C.
2300	8 A.M.	6 P.M.		Nil	Nil	22000 K.C.
0000	9 A.M.	7 P.M.		Nil	Nil	22000 K.C.
0100	10 A.M.	8 P.M.		Nil	Nil	21800 K.C.
0200	11 A.M.	9 P.M.		Unsat.	Nil	21600 K.C.
0300	12 N.	10 P.M.		Unsat.	Nil	21000 K.C.
0400	1 P.M.	11 P.M.		Unsat.	Unsat.	19500 K.C.
0500	2 P.M.	12 M.		Unsat.-Poor	Unsat.	17500 K.C.
0600	3 P.M.	1 A.M.		Poor-Fair	Unsat.	15500 K.C.
0700	4 P.M.	2 A.M.		Poor-Fair	Unsat.-Poor	14200 K.C.
0800	5 P.M.	3 A.M.		Fair	Poor	13000 K.C.
0900	6 P.M.	4 A.M.		Fair-Poor	Poor-Fair	11800 K.C.
1000	7 P.M.	5 A.M.		Fair-Poor	Fair	11000 K.C.
				Poor-Fair	Fair-Good	10000 K.C.

Fig. 73—Schenectady-Tokio transmission chart. Spring season (February 1 to May 1). Distance from Schenectady to Tokio 6600 miles (approx.)

TIME			DAYLIGHT-DARKNESS DISTRIBUTION OVER GREAT CIRCLE PATH	PROBABLE RECEPTION OBTAINABLE FROM		PROBABLE OPTIMUM FREQUENCY
				W2XAD	W2XAF	
GMT	Tokio	Local		13660 K.C.	9550 K.C.	Short Path
1100	8 P.M.	5 A.M.		Nil	Nil	19000 K.C.
1200	9 P.M.	7 A.M.		Unsat.	Nil	18300 K.C.
1300	10 P.M.	8 A.M.		Unsat.	Nil	18000 K.C.
1400	11 P.M.	9 A.M.		Unsat.	Nil	18000 K.C.
1500	12 M.	10 A.M.		Unsat.	Nil	19200 K.C.
1600	1 A.M.	11 A.M.		Unsat.	Nil	20300 K.C.
1700	2 A.M.	12 N.		Unsat.	Nil	21300 K.C.
1800	3 A.M.	1 P.M.		Nil	Nil	21800 K.C.
1900	4 A.M.	2 P.M.		Nil	Nil	22000 K.C.
2000	5 A.M.	3 P.M.		Nil	Nil	22000 K.C.
2100	6 A.M.	4 P.M.		Nil	Nil	22000 K.C.
2200	7 A.M.	5 P.M.		Nil	Nil	22000 K.C.
2300	8 A.M.	6 P.M.		Unsat.	Nil	22000 K.C.
0000	9 A.M.	7 P.M.		Unsat.	Nil	22000 K.C.
0100	10 A.M.	8 P.M.		Unsat.	Nil	22000 K.C.
0200	11 A.M.	9 P.M.		Unsat.	Nil	21800 K.C.
0300	12 N.	10 P.M.		Unsat.	Nil	21600 K.C.
0400	1 P.M.	11 P.M.		Unsat.	Nil	21300 K.C.
0500	2 P.M.	12 M.		Unsat.	Nil	20800 K.C.
0600	3 P.M.	1 A.M.		Unsat.	Nil	20000 K.C.
0700	4 P.M.	2 A.M.		Unsat.	Nil	19000 K.C.
0800	5 P.M.	3 A.M.		Unsat.	Nil	19600 K.C.
0900	6 P.M.	4 A.M.		Poor	Nil	21400 K.C.
1000	7 P.M.	5 A.M.		Unsat.	Nil	22000 K.C.

Fig. 74—Schenectady-Tokio transmission chart. Summer season (May 1 to August 1). Distance from Schenectady to Tokio 6600 miles (approx.)

TIME			DAYLIGHT-DARKNESS DISTRIBUTION OVER GREAT CIRCLE PATH	PROBABLE RECEPTION OBTAINABLE FROM		PROBABLE OPTIMUM FREQUENCY
				W2XAD	W2XAF	
GMT	Tokio	Local		13660 K.C.	9550 K.C.	Short Pahh
1100	8 P.M.	6 A.M.		Fair	Good-Fair	9000 K.C.
1200	9 P.M.	7 A.M.		Fair-Poor	Fair	10400 K.C.
1300	10 P.M.	8 A.M.		Fair-Poor	Poor	12800 K.C.
1400	11 P.M.	9 A.M.		Fair-Poor	Unsat.	14500 K.C.
1500	12 M.	10 A.M.		Poor	Nil	15800 K.C.
1600	1 A.M.	11 A.M.		Poor-Unsat.	Nil	17200 K.C.
1700	2 A.M.	12 N.		Unsat.	Nil	18400 K.C.
1800	3 A.M.	1 P.M.		Unsat.	Nil	19700 K.C.
1900	4 A.M.	2 P.M.		Nil	Nil	21000 K.C.
2000	5 A.M.	3 P.M.		Nil	Nil	21700 K.C.
2100	6 A.M.	4 P.M.		Nil	Nil	22000 K.C.
2200	7 A.M.	5 P.M.		Nil	Nil	22000 K.C.
2300	8 A.M.	6 P.M.		Nil	Nil	22000 K.C.
0000	9 A.M.	7 P.M.		Nil	Nil	21800 K.C.
0100	10 A.M.	8 P.M.		Unsat.	Nil	21600 K.C.
0200	11 A.M.	9 P.M.		Unsat.	Nil	21000 K.C.
0300	12 N.	10 P.M.		Unsat.	Unsat.	19500 K.C.
0400	1 P.M.	11 P.M.		Unsat.-Poor	Unsat.	17500 K.C.
0500	2 P.M.	12 M.		Poor-Fair	Unsat.	15500 K.C.
0600	3 P.M.	1 A.M.		Poor-Fair	Unsat.-Poor	14200 K.C.
0700	4 P.M.	2 A.M.		Fair	Poor	13000 K.C.
0800	5 P.M.	3 A.M.		Fair-Poor	Poor-Fair	11800 K.C.
0900	6 P.M.	4 A.M.		Fair-Poor	Fair	11000 K.C.
1000	7 P.M.	5 A.M.		Poor-Fair	Fair-Good	10000 K.C.

Fig. 75—Schenectady-Tokio transmission chart. Fall season (August 1 to November 1). Distance from Schenectady to Tokio 6600 miles (approx.)

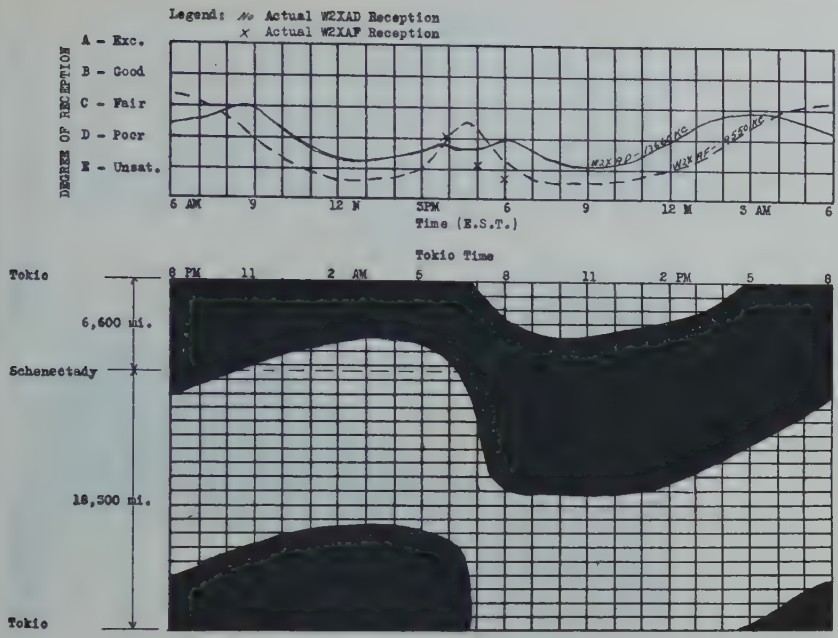

Fig. 76—Tokio reception from November 1 to February 1. Daylight-darkness distribution over great circle path from Schenectady to Tokio, Japan, as of December 20.

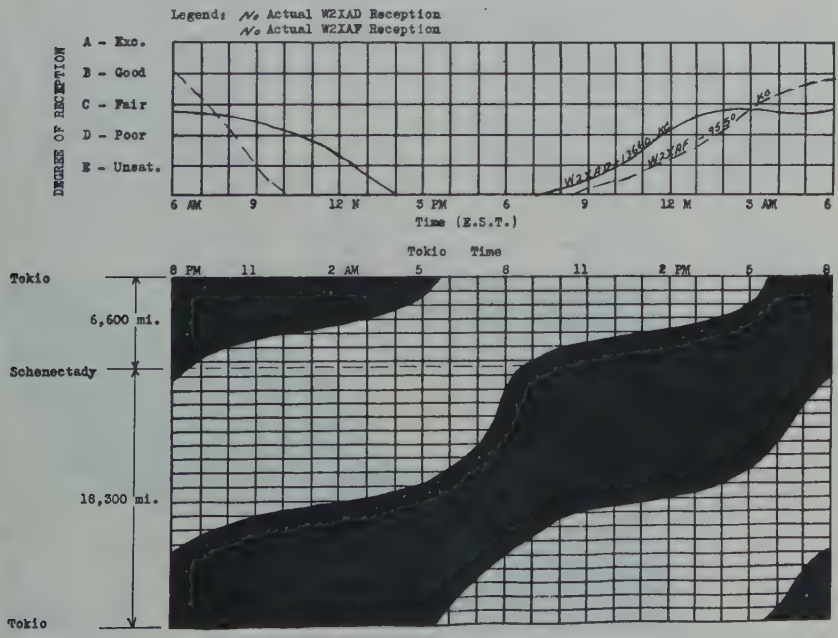

Fig. 77—Tokio reception from February 1 to May 1. Daylight-darkness distribution over great circle path from Schenectady to Tokio, Japan, as of March 20.

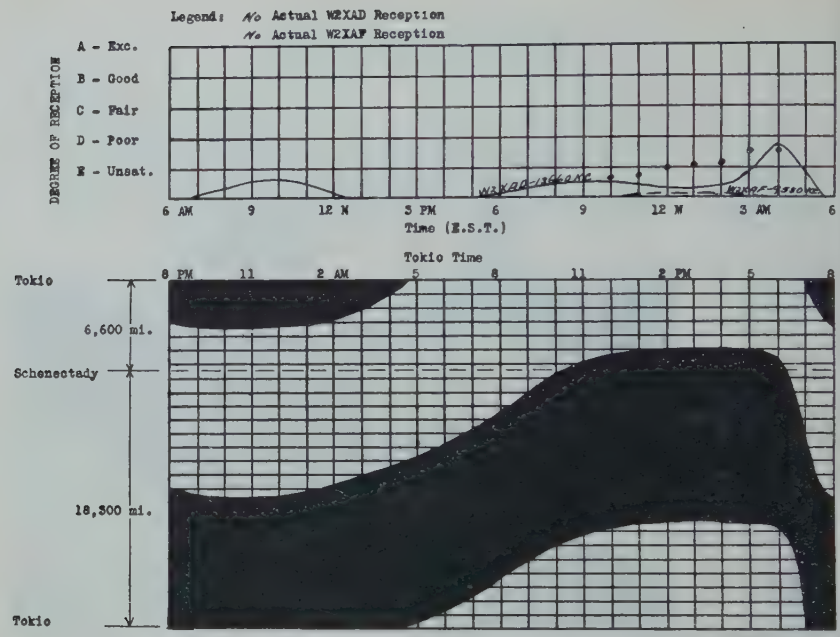

Fig. 78—Tokio reception from May 1 to August 1. Daylight-darkness distribution over great circle path from Schenectady to Tokio, Japan, as of June 20.

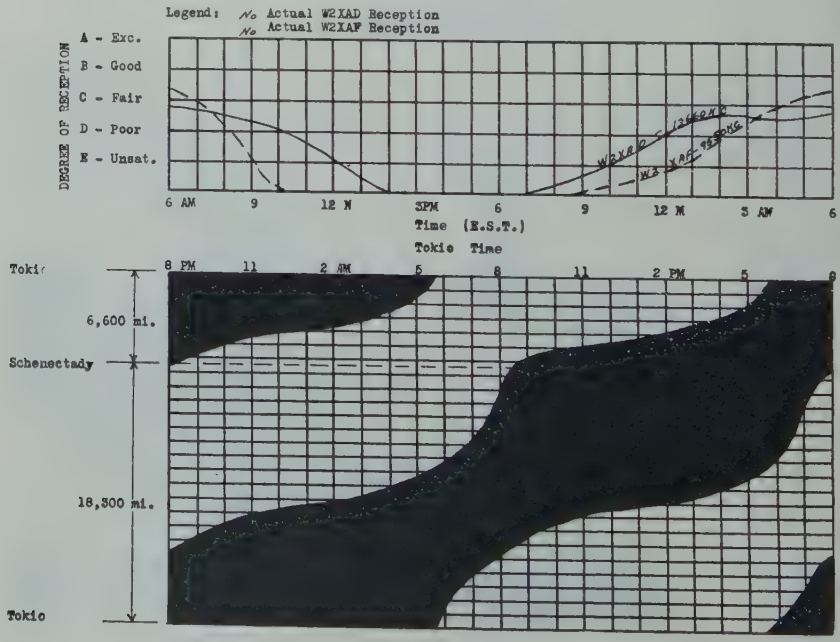

Fig. 79—Tokio reception from August 1 to November 1. Daylight-darkness distribution over great circle path from Schenectady to Tokio, Japan, as of September 20.

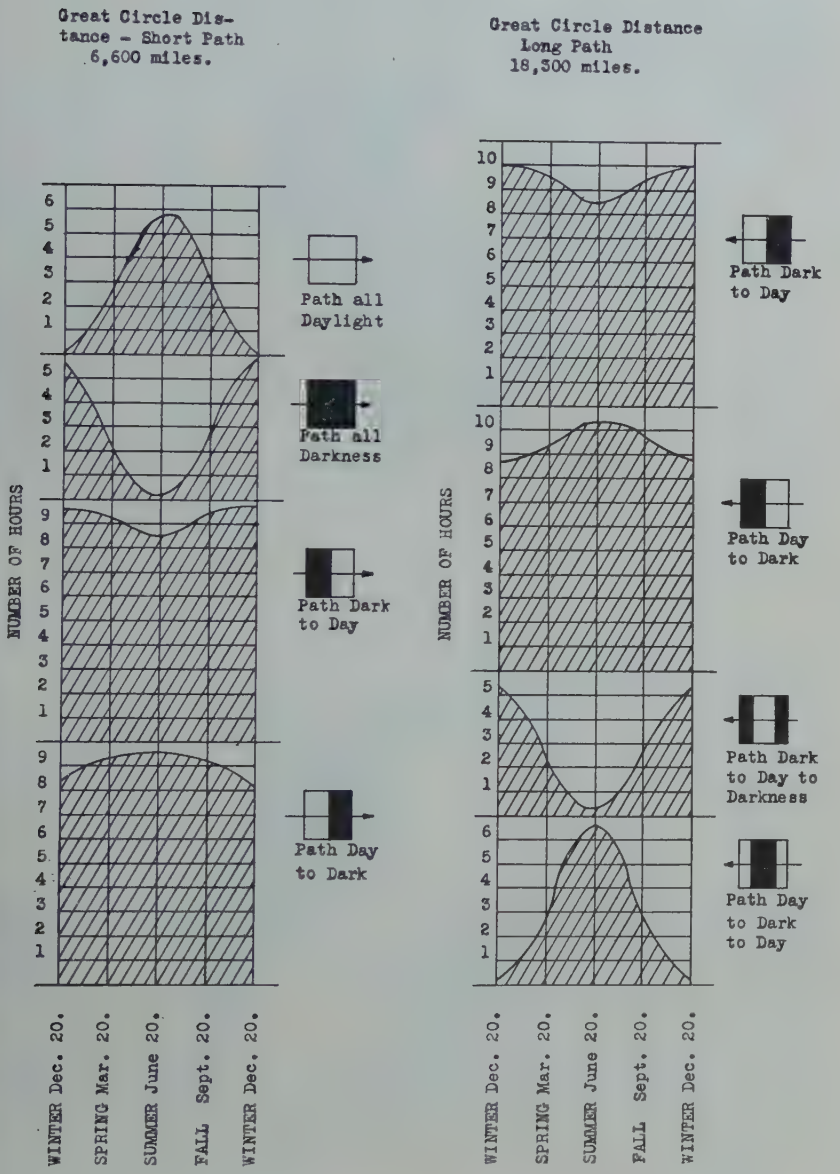

Fig. 80—Daylight-darkness distribution between Schenectady and Tokio, Japan.

The bearing of Tokio from Schenectady (N 26 deg. W-approx.) is such that in following the great circle path, a transmission originating at Schenectady will pass over Hudson Bay, the northern portion of Alaska, and across Siberia to Japan.

On Figs. 72 to 81 are data pertaining to transmission over this circuit.

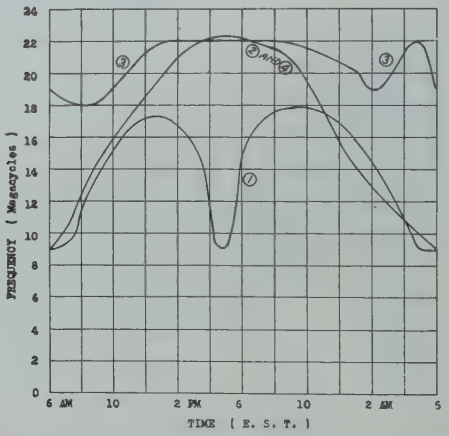

Fig. 81—Optimum frequency chart—Schenectady to Tokio, Japan.
(1) Winter—November 1 to February 1.
(2) and (4)—Spring and Fall—February 1 to May 1 and August 1 to November 1.
(3) Summer—May 1 to August 1.

Schenectady–Buenos Aires Circuit

This circuit, which is approximately 5400 miles in length, is not greatly affected by seasonal variation. (See Figs. 82 to 89. Also Fig. 91.) Best reception should be obtained during the period from June to October since atmospheric interference in the Argentine will be at a minimum.

Best reception of W2XAD and W2XAF is obtained from about 6:00 P.M. to 12:00 o'clock midnight, E.S.T. As the difference between

TIME			DAYLIGHT-DARKNESS DISTRIBUTION OVER GREAT CIRCLE PATH	PROBABLE RECEPTION OBTAINABLE FROM		PROBABLE OPTIMUM FREQUENCY
GMT	B.Aires	Local		W2XAD	W2XAF	
				13660 K.C.	9550 K.C.	Short Path
1100	7 A.M.	6 A.M.		Unsat.	Unsat.	18800 K.C.
1200	8 A.M.	7 A.M.		Unsat.	Nil	20200 K.C.
1300	9 A.M.	8 A.M.		Nil	Nil	21800 K.C.
1400	10 A.M.	9 A.M.		Nil	Nil	21800 K.C.
1500	11 A.M.	10 A.M.		Nil	Nil	21800 K.C.
1600	12 N.	11 A.M.		Nil	Nil	21800 K.C.
1700	1 P.M.	12 N.		Nil	Nil	21800 K.C.
1800	2 P.M.	1 P.M.		Nil	Nil	21800 K.C.
1900	3 P.M.	2 P.M.		Nil	Nil	21800 K.C.
2000	4 P.M.	3 P.M.		Nil	Nil	21800 K.C.
2100	5 P.M.	4 P.M.		Unsat.	Nil	20000 K.C.
2200	6 P.M.	5 P.M.		Poor-Fair	Unsat.	15400 K.C.
2300	7 P.M.	6 P.M.		Fair	Poor-Fair	11600 K.C.
0000	8 P.M.	7 P.M.		Fair	Fair	8600 K.C.
0100	9 P.M.	8 P.M.		Fair-Poor	Fair-Good	8600 K.C.
0200	10 P.M.	9 P.M.		Fair-Poor	Fair-Good	8600 K.C.
0300	11 P.M.	10 P.M.		Poor	Good	8600 K.C.
0400	12 M.	11 P.M.		Poor	Good-Fair	8600 K.C.
0500	1 A.M.	12 M.		Poor	Good-Fair	8600 K.C.
0600	2 A.M.	1 A.M.		Poor	Good-Fair	8600 K.C.
0700	3 A.M.	2 A.M.		Poor-Fair	Fair	8600 K.C.
0800	4 A.M.	3 A.M.		Fair-Poor	Poor	8600 K.C.
0900	5 A.M.	4 A.M.		Poor	Poor-Unsat.	11400 K.C.
1000	6 A.M.	5 A.M.		Poor-Unsat.	Unsat.	16400 K.C.

Fig. 82—Schenectady-Buenos Aires transmission chart. Winter season (November 1 to February 1). Distance from Schenectady to Buenos Aires 5400 miles (approx.)

TIME			DAYLIGHT-DARKNESS DISTRIBUTION OVER GREAT CIRCLE PATH	PROBABLE RECEPTION OBTAINABLE FROM		PROBABLE OPTIMUM FREQUENCY
GMT	B.Aires	Local		W2XAD	W2XAF	
				13660 K.C.	9550 K.C.	Short Path
1100	7 A.M.	6 A.M.		Unsat.	Nil	21800 K.C.
1200	8 A.M.	7 A.M.		Nil	Nil	21800 K.C.
1300	9 A.M.	8 A.M.		Nil	Nil	21800 K.C.
1400	10 A.M.	9 A.M.		Nil	Nil	21800 K.C.
1500	11 A.M.	10 A.M.		Nil	Nil	21800 K.C.
1600	12 N.	11 A.M.		Nil	Nil	21800 K.C.
1700	1 P.M.	12 N.		Nil	Nil	21800 K.C.
1800	2 P.M.	1 P.M.		Nil	Nil	21800 K.C.
1900	3 P.M.	2 P.M.		Nil	Nil	21800 K.C.
2000	4 P.M.	3 P.M.		Nil	Nil	21800 K.C.
2100	5 P.M.	4 P.M.		Nil	Nil	21800 K.C.
2200	6 P.M.	5 P.M.		Unsat.	Nil	16000 K.C.
2300	7 P.M.	6 P.M.		Poor-Fair	Poor	13000 K.C.
0000	8 P.M.	7 P.M.		Fair-Poor	Fair	10500 K.C.
0100	9 P.M.	8 P.M.		Fair-Poor	Fair	8600 K.C.
0200	10 P.M.	9 P.M.		Fair-Poor	Fair-Good	8600 K.C.
0300	11 P.M.	10 P.M.		Fair-Poor	Good-Fair	8600 K.C.
0400	12 M.	11 P.M.		Fair-Poor	Good-Fair	8600 K.C.
0500	1 A.M.	12 M.		Fair-Poor	Fair	8600 K.C.
0600	2 A.M.	1 A.M.		Poor	Fair-Poor	8600 K.C.
0700	3 A.M.	2 A.M.		Poor	Fair-Poor	8600 K.C.
0800	4 A.M.	3 A.M.		Poor	Poor	10800 K.C.
0900	5 A.M.	4 A.M.		Poor	Unsat.	12500 K.C.
1000	6 A.M.	5 A.M.		Poor-Unsat.	Unsat.	16000 K.C.

Fig. 83—Schenectady-Buenos Aires transmission chart. Spring season (February 1 to May 1). Distance from Schenectady to Buenos Aires 5400 miles (approx.)

TIME			DAYLIGHT-DARKNESS DISTRIBUTION OVER GREAT CIRCLE PATH	PROBABLE RECEPTION OBTAINABLE FROM		PROBABLE OPTIMUM FREQUENCY
GMT	B.Aires	Local		W2XAD	W2XAF	
				13660 K.C.	9550 K.C.	Short Path
1100	7 A.M.	6 A.M.		Nil	Nil	21800 K.C.
1200	8 A.M.	7 A.M.		Nil	Nil	21800 K.C.
1300	9 A.M.	8 A.M.		Nil	Nil	21800 K.C.
1400	10 A.M.	9 A.M.		Nil	Nil	21800 K.C.
1500	11 A.M.	10 A.M.		Nil	Nil	21800 K.C.
1600	12 N.	11 A.M.		Nil	Nil	21800 K.C.
1700	1 P.M.	12 N.		Nil	Nil	21800 K.C.
1800	2 P.M.	1 P.M.		Nil	Nil	21800 K.C.
1900	3 P.M.	2 P.M.		Nil	Nil	21800 K.C.
2000	4 P.M.	3 P.M.		Nil	Nil	21800 K.C.
2100	5 P.M.	4 P.M.		Nil	Nil	21800 K.C.
2200	6 P.M.	5 P.M.		Unsat.	Nil	19200 K.C.
2300	7 P.M.	6 P.M.		Unsat.	Nil	16100 K.C.
0000	8 P.M.	7 P.M.		Poor-Fair	Unsat.-Poor	14800 K.C.
0100	9 P.M.	8 P.M.		Fair	Poor-Fair	12000 K.C.
0200	10 P.M.	9 P.M.		Fair-Poor	Fair-Good	8600 K.C.
0300	11 P.M.	10 P.M.		Fair-Poor	Fair-Good	8600 K.C.
0400	12 M.	11 P.M.		Fair-Poor	Good-Fair	8600 K.C.
0500	1 A.M.	12 M.		Fair-Poor	Good-Fair	8600 K.C.
0600	2 A.M.	1 A.M.		Fair-Poor	Good-Fair	8600 K.C.
0700	3 A.M.	2 A.M.		Fair-Poor	Fair	8600 K.C.
0800	4 A.M.	3 A.M.		Fair-Poor	Fair-Poor	8600 K.C.
0900	5 A.M.	4 A.M.		Poor	Poor	11000 K.C.
1000	6 A.M.	5 A.M.		Unsat.	Unsat.	15000 K.C.

Fig. 84—Schenectady-Buenos Aires transmission chart. Summer season (May 1 to August 1). Distance from Schenectady to Buenos Aires 5400 miles (approx.)

TIME			DAYLIGHT-DARKNESS DISTRIBUTION OVER GREAT CIRCLE PATH	PROBABLE RECEPTION OBTAINABLE FROM		PROBABLE OPTIMUM FREQUENCY
GMT	B.Aires	Local		W2XAD	W2XAF	
				13650 K.C.	9550 K.C.	Short Path
1100	7 A.M.	6 A.M.		Unsat.	Nil	21800 K.C.
1200	8 A.M.	7 A.M.		Nil	Nil	21800 K.C.
1300	9 A.M.	8 A.M.		Nil	Nil	21800 K.C.
1400	10 A.M.	9 A.M.		Nil	Nil	21800 K.C.
1500	11 A.M.	10 A.M.		Nil	Nil	21800 K.C.
1600	12 N.	11 A.M.		Nil	Nil	21800 K.C.
1700	1 P.M.	12 N.		Nil	Nil	21800 K.C.
1800	2 P.M.	1 P.M.		Nil	Nil	21800 K.C.
1900	3 P.M.	2 P.M.		Nil	Nil	21800 K.C.
2000	4 P.M.	3 P.M.		Nil	Nil	21800 K.C.
2100	5 P.M.	4 P.M.		Nil	Nil	21800 K.C.
2200	6 P.M.	5 P.M.		Unsat.	Nil	18000 K.C.
2300	7 P.M.	6 P.M.		Poor-Fair	Poor	13000 K.C.
0000	8 P.M.	7 P.M.		Fair-Poor	Fair	10500 K.C.
0100	9 P.M.	8 P.M.		Fair-Poor	Fair	8600 K.C.
0200	10 P.M.	9 P.M.		Fair-Poor	Fair-Good	8600 K.C.
0300	11 P.M.	10 P.M.		Fair-Poor	Good-Fair	8600 K.C.
0400	12 M.	11 P.M.		Fair-Poor	Good-Fair	8600 K.C.
0500	1 A.M.	12 M.		Fair-Poor	Fair	8600 K.C.
0600	2 A.M.	1 A.M.		Poor	Fair-Poor	8600 K.C.
0700	3 A.M.	2 A.M.		Poor	Fair-Poor	8600 K.C.
0800	4 A.M.	3 A.M.		Poor	Poor	10800 K.C.
0900	5 A.M.	4 A.M.		Poor	Unsat.	12500 K.C.
1000	6 A.M.	5 A.M.		Poor-Unsat.	Unsat.	16000 K.C.

Fig. 85—Schenectady-Buenos Aires transmission chart. Fall season (August 1 to November 1). Distance from Schenectady to Buenos Aires 5400 miles (approx.)

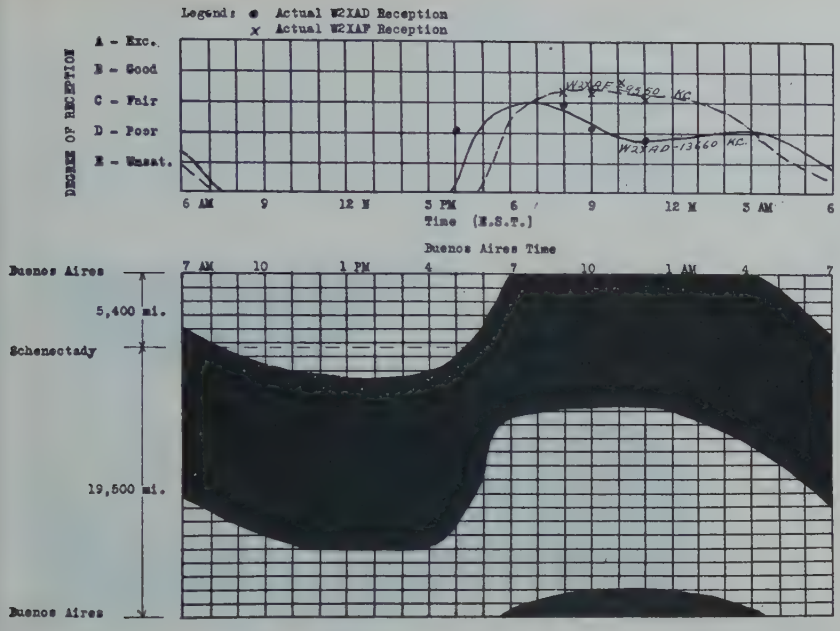

Fig. 86—Buenos Aires reception from November 1 to February 1. Daylight-darkness distribution over great circle path from Schenectady to Buenos Aires, South America, as of December 20.

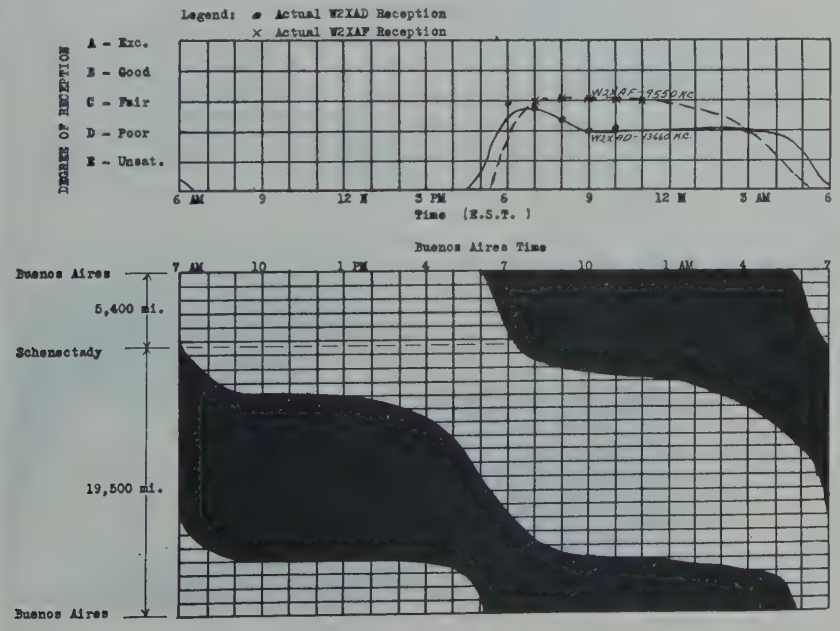

Fig. 87—Buenos Aires reception from February 1 to May 1. Daylight-darkness distribution over great circle path from Schenectady to Buenos Aires, South America, as of March 20.

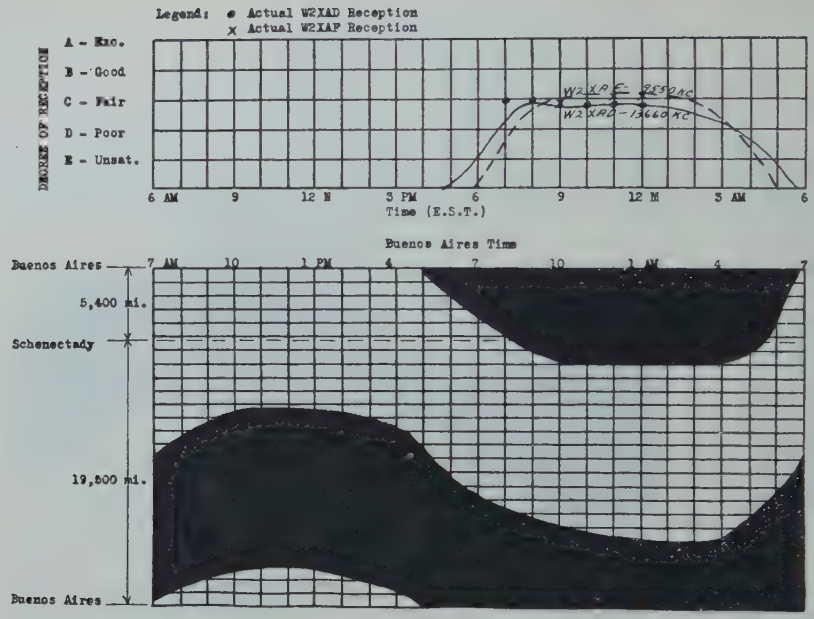

Fig. 88—Buenos Aires reception from May 1 to August 1. Daylight-darkness distribution over great circle path from Schenectady to Buenos Aires, South America, as of June 20.

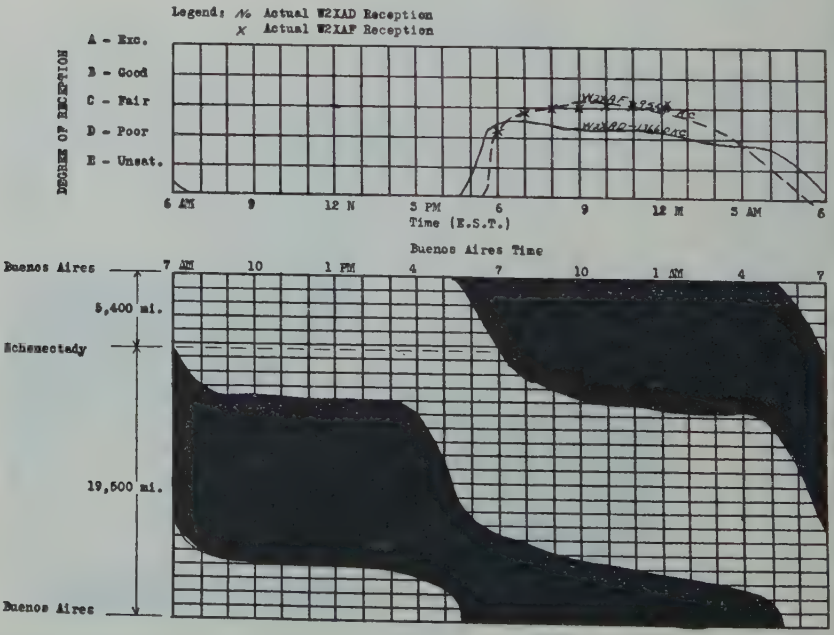

Fig. 89—Buenos Aires reception from August 1 to November 1. Daylight-darkness distribution over great circle path from Schenectady to Buenos Aires, South America, as of September 20.

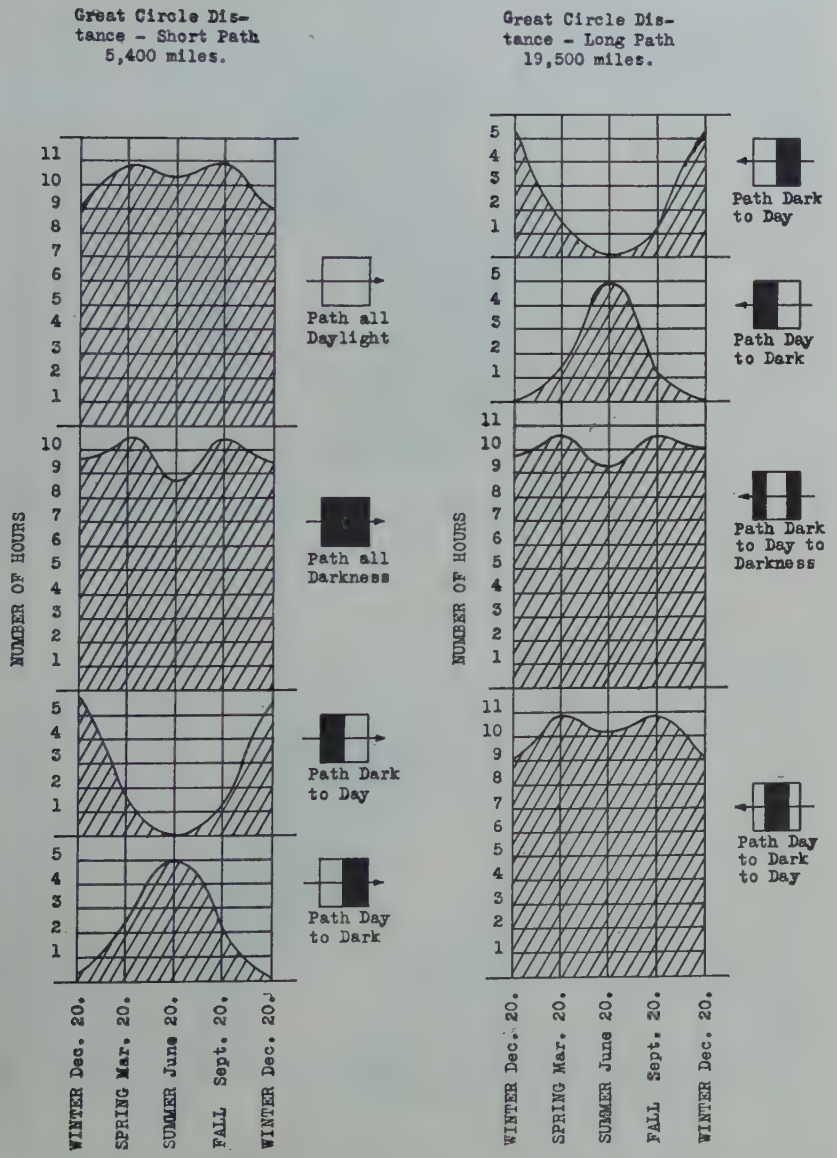

Fig. 90—Daylight-darkness distribution between Schenectady and Buenos Aires.

Eastern Standard Time and Buenos Aires time is only one hour, it is possible for entire evening programs of WGY (as relayed by W2XAD and W2XAF) to be followed conveniently by listeners in the Argentine.

Daylight-darkness distribution and optimum frequency data for this circuit are shown on Figs. 90 and 91, respectively.

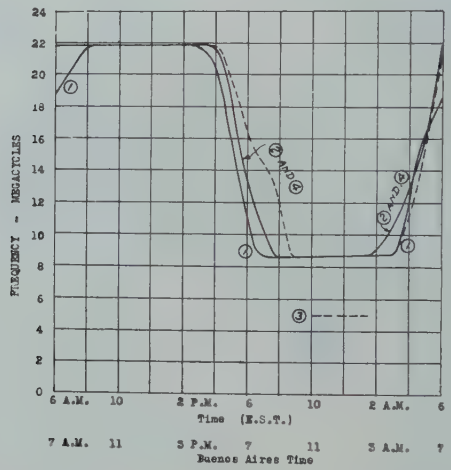

Fig. 91—Optimum frequency chart—Schenectady to Buenos Aires.
(1) Winter—November 1 to February 1.
(2) and (4)—Spring and Fall—February 1 to May 1 and August 1 to November 1.
(3) Summer—May 1 to August 1.

Schenectady–Rio de Janeiro Circuit

From a survey of the transmission and reception data pertaining to this circuit, it appears that seasonal variation will be slight. Perhaps the greatest factor that has to be considered in this connection is the height of the atmospheric interference level at the receiving terminal. Under normal conditions, this level is lowest during the months of June, July, August, and September.

TIME		DAYLIGHT-DARKNESS DISTRIBUTION OVER GREAT CIRCLE PATH	PROBABLE RECEPTION OBTAINABLE FROM		PROBABLE OPTIMUM FREQUENCY
GMT	Rio Local		W2XAD	W2XAF	
			13660 K.C.	9550 K.C.	Short Path
1100	8 A.M. 6 A.M.		Unsat.	Unsat.	18800 K.C.
1200	9 A.M. 7 A.M.		Nil	Nil	20800 K.C.
1300	10 A.M. 8 A.M.		Nil	Nil	21400 K.C.
1400	11 A.M. 9 A.M.		Nil	Nil	21400 K.C.
1500	12 N. 10 A.M.		Nil	Nil	21400 K.C.
1600	1 P.M. 11 A.M.		Nil	Nil	21400 K.C.
1700	2 P.M. 12 N.		Nil	Nil	21400 K.C.
1800	3 P.M. 1 P.M.		Nil	Nil	21400 K.C.
1900	4 P.M. 2 P.M.		Nil	Nil	21400 K.C.
2000	5 P.M. 3 P.M.		Nil	Nil	21400 K.C.
2100	6 P.M. 4 P.M.		Nil	Nil	20000 K.C.
2200	7 P.M. 5 P.M.		Unsat.	Nil	18000 K.C.
2300	8 P.M. 6 P.M.		Poor-Fair	Unsat.	15000 K.C.
0000	9 P.M. 7 P.M.		Fair	Poor-Fair	12200 K.C.
0100	10 P.M. 8 P.M.		Fair-Poor	Fair	8200 K.C.
0200	11 P.M. 9 P.M.		Fair-Poor	Fair	8200 K.C.
0300	12 M. 10 P.M.		Poor	Fair	8200 K.C.
0400	1 A.M. 11 P.M.		Poor-Unsat.	Fair	8200 K.C.
0500	2 A.M. 12 M.		Poor-Unsat.	Fair-Poor	8200 K.C.
0600	3 A.M. 1 A.M.		Unsat.-Poor	Fair-Poor	10700 K.C.
0700	4 A.M. 2 A.M.		Poor	Poor	12700 K.C.
0800	5 A.M. 3 A.M.		Poor-Fair	Poor-Unsat.	14500 K.C.
0900	6 A.M. 4 A.M.		Fair-Poor	Unsat.	16000 K.C.
1000	7 A.M. 5 A.M.		Poor	Unsat.	17500 K.C.

Fig. 92—Schenectady—Rio de Janeiro transmission chart. Winter Season (November 1 to February 1). Distance from Schenectady to Rio de Janerio 4900 miles (approx.)

TIME		DAYLIGHT-DARKNESS DISTRIBUTION OVER GREAT CIRCLE PATH	PROBABLE RECEPTION OBTAINABLE FROM		PROBABLE OPTIMUM FREQUENCY
GMT	Rio. Local		W2XAD	W2XAF	
			13660 K.C.	9550 K.C.	Short Path
1100	8 A.M. 6 A.M.		Nil	Nil	21400 K.C.
1200	9 A.M. 7 A.M.		Nil	Nil	21400 K.C.
1300	10 A.M. 8 A.M.		Nil	Nil	21400 K.C.
1400	11 A.M. 9 A.M.		Nil	Nil	21400 K.C.
1500	12 N. 10 A.M.		Nil	Nil	21400 K.C.
1600	1 P.M. 11 A.M.		Nil	Nil	21400 K.C.
1700	2 P.M. 12 N.		Nil	Nil	21400 K.C.
1800	3 P.M. 1 P.M.		Nil	Nil	21400 K.C.
1900	4 P.M. 2 P.M.		Nil	Nil	21400 K.C.
2000	5 P.M. 3 P.M.		Nil	Nil	21400 K.C.
2100	6 P.M. 4 P.M.		Nil	Nil	20000 K.C.
2200	7 P.M. 5 P.M.		Unsat.	Nil	18000 K.C.
2300	8 P.M. 6 P.M.		Poor	Unsat.	16000 K.C.
0000	9 P.M. 7 P.M.		Poor-Fair	Poor	14000 K.C.
0100	10 P.M. 8 P.M.		Fair	Poor-Fair	11500 K.C.
0200	11 P.M. 9 P.M.		Fair-Poor	Fair	8200 K.C.
0300	12 M. 10 P.M.		Fair-Poor	Fair	8200 K.C.
0400	1 A.M. 11 P.M.		Poor	Fair	8200 K.C.
0500	2 A.M. 12 M.		Poor-Unsat.	Fair	8200 K.C.
0600	3 A.M. 1 A.M.		Unsat.-Poor	Fair-Poor	8200 K.C.
0700	4 A.M. 2 A.M.		Poor	Poor	8200 K.C.
0800	5 A.M. 3 A.M.		Poor-Fair	Poor-Unsat.	11500 K.C.
0900	6 A.M. 4 A.M.		Fair-Poor	Unsat.	15000 K.C.
1000	7 A.M. 5 A.M.		Poor-Unsat.	Unsat.	18300 K.C.

Fig. 93—Schenectady-Rio de Janeiro transmission chart. Spring season (February 1 to May 1). Distance from Schenectady to Rio de Janeiro 4900 miles (approx.)

GMT	Rio.	Local	DAYLIGHT-DARKNESS DISTRIBUTION OVER GREAT CIRCLE PATH	PROBABLE RECEPTION OBTAINABLE FROM W2XAD 13660 K.C.	PROBABLE RECEPTION OBTAINABLE FROM W2XAF 9550 K.C.	PROBABLE OPTIMUM FREQUENCY Short Path
1100	8 A.M.	6 A.M.	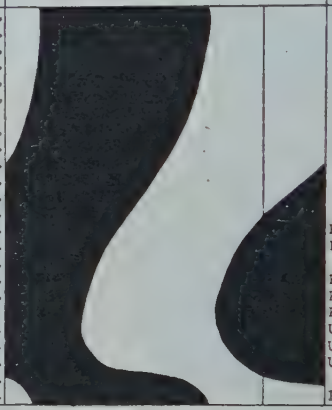	Nil	Nil	21400 K.C.
1200	9 A.M.	7 A.M.		Nil	Nil	21400 K.C.
1300	10 A.M.	8 A.M.		Nil	Nil	21400 K.C.
1400	11 A.M.	9 A.M.		Nil	Nil	21400 K.C.
1500	12 N.	10 A.M.		Nil	Nil	21400 K.C.
1600	1 P.M.	11 A.M.		Nil	Nil	21400 K.C.
1700	2 P.M.	12 N.		Nil	Nil	21400 K.C.
1800	3 P.M.	1 P.M.		Nil	Nil	21400 K.C.
1900	4 P.M.	2 P.M.		Nil	Nil	21400 K.C.
2000	5 P.M.	3 P.M.		Nil	Nil	21400 K.C.
2100	6 P.M.	4 P.M.		Nil	Nil	19800 K.C.
2200	7 P.M.	5 P.M.		Unsat.	Nil	17800 K.C.
2300	8 P.M.	6 P.M.		Poor	Unsat.	15500 K.C.
0000	9 P.M.	7 P.M.		Poor-Fair	Unsat.-Poor	13000 K.C.
0100	10 P.M.	8 P.M.		Fair-Poor	Poor-Fair	10500 K.C.
0200	11 P.M.	9 P.M.		Poor	Poor-Fair	8200 K.C.
0300	12 M.	10 P.M.		Poor-Unsat.	Fair	8200 K.C.
0400	1 A.M.	11 P.M.		Poor-Unsat.	Fair	8200 K.C.
0500	2 A.M.	12 M.		Poor-Unsat.	Fair	8200 K.C.
0600	3 A.M.	1 A.M.		Unsat.-Poor	Fair-Poor	8200 K.C.
0700	4 A.M.	2 A.M.		Unsat.-Poor	Fair-Poor	10500 K.C.
0800	5 A.M.	3 A.M.		Unsat.-Poor	Poor	12800 K.C.
0900	6 A.M.	4 A.M.		Poor	Poor-Unsat.	15200 K.C.
1000	7 A.M.	5 A.M.		Poor-Unsat.	Nil	18000,K.C.

Fig. 94—Schenectady-Rio de Janeiro transmission chart. Summer season (May 1 to August 1). Distance from Schenectady to Rio de Janeiro 4900 miles (approx.)

GMT	Rio.	Local	DAYLIGHT-DARKNESS DISTRIBUTION OVER GREAT CIRCLE PATH	PROBABLE RECEPTION OBTAINABLE FROM W2XAD 13660 K.C.	PROBABLE RECEPTION OBTAINABLE FROM W2XAF 9550 K.C.	PROBABLE OPTIMUM FREQUENCY Short Path
1100	8 A.M.	6 A.M.	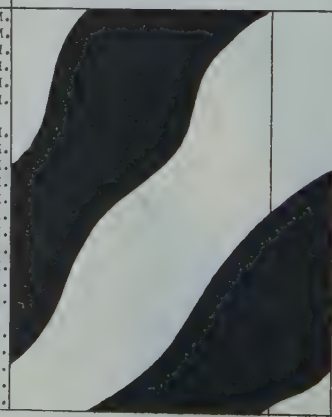	Nil	Nil	21400 K.C.
1200	9 A.M.	7 A.M.		Nil	Nil	21400 K.C.
1300	10 A.M.	8 A.M.		Nil	Nil	21400 K.C.
1400	11 A.M.	9 A.M.		Nil	Nil	21400 K.C.
1500	12 N.	10 A.M.		Nil	Nil	21400 K.C.
1600	1 P.M.	11 A.M.		Nil	Nil	21400 K.C.
1700	2 P.M.	12 N.		Nil	Nil	21400 K.C.
1800	3 P.M.	1 P.M.		Nil	Nil	21400 K.C.
1900	4 P.M.	2 P.M.		Nil	Nil	21400 K.C.
2000	5 P.M.	3 P.M.		Nil	Nil	21400 K.C.
2100	6 P.M.	4 P.M.		Nil	Nil	21400 K.C.
2200	7 P.M.	5 P.M.		Nil	Nil	21400 K.C.
2300	8 P.M.	6 P.M.		Nil	Nil	19500 K.C.
0000	9 P.M.	7 P.M.		Unsat.	Nil	18000 K.C.
0100	10 P.M.	8 P.M.		Poor	Unsat.	16000 K.C.
0200	11 P.M.	9 P.M.		Poor-Fair	Poor	14000 K.C.
0300	12 M.	10 P.M.		Fair	Poor-Fair	11500 K.C.
0400	1 A.M.	11 P.M.		Fair-Poor	Fair	8200 K.C.
0500	2 A.M.	12 M.		Fair-Poor	Fair	8200 K.C.
0600	3 A.M.	1 A.M.		Poor	Fair	8200 K.C.
0700	4 A.M.	2 A.M.		Poor-Unsat.	Fair	8200 K.C.
0800	5 A.M.	3 A.M.		Unsat.-Poor	Fair-Poor	8200 K.C.
0900	6 A.M.	4 A.M.		Poor	Poor	8200 K.C.
1000	7 A.M.	5 A.M.		Poor-Fair	Poor-Unsat.	11500 K.C.
				Fair-Poor	Unsat.	15000 K.C.
				Poor-Unsat.	Unsat.	18300 K.C.

Fig. 95—Schenectady—Rio de Janeiro transmission chart. Fall season (August 1 to November 1. Distance from Schenectady to Rio de Janeiro 4900 miles (approx.)

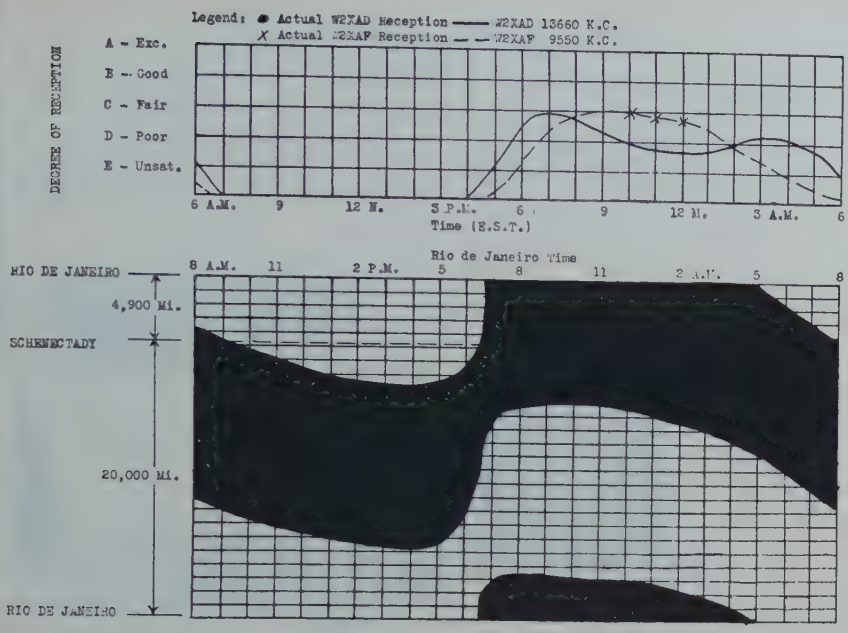

Fig. 96—Rio de Janeiro reception from November 1 to February 1. Daylight-darkness distribution over great circle distance from Schenectady to Rio de Janeiro, South America, as of December 20.

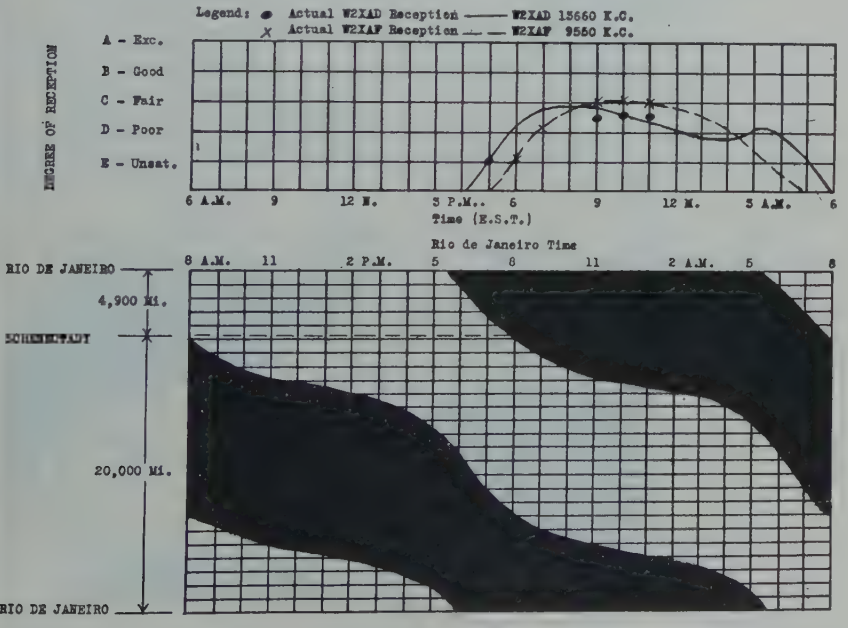

Fig. 97—Rio de Janeiro reception from February 1 to May 1. Daylight-darkness distribution over great circle distance from Schenectady to Rio de Janeiro, South America, as of March 20.

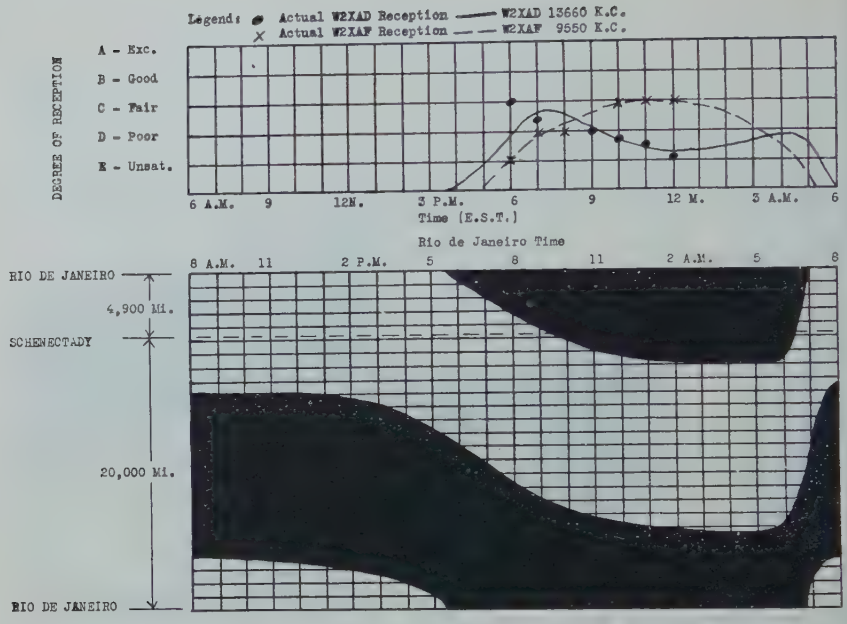

Fig. 98—Rio de Janeiro reception from May 1 to August 1. Daylight-darkness distribution over great circle distance from Schenectady to Rio de Janeiro, South America, as of June 20.

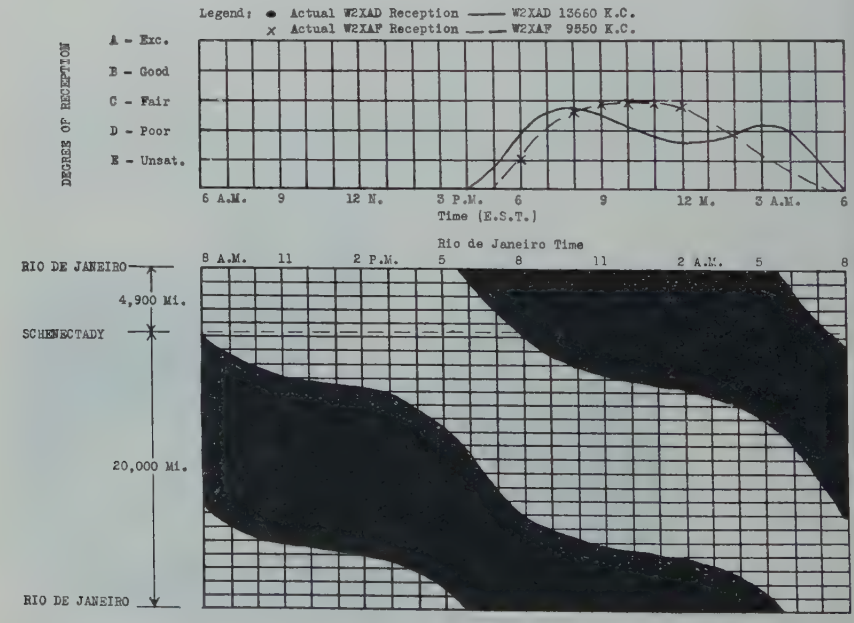

Fig. 99—Rio de Janeiro reception from August 1 to November 1. Daylight-darkness distribution over great circle distance from Schenectady to Rio de Janeiro, South America, as of September 20.

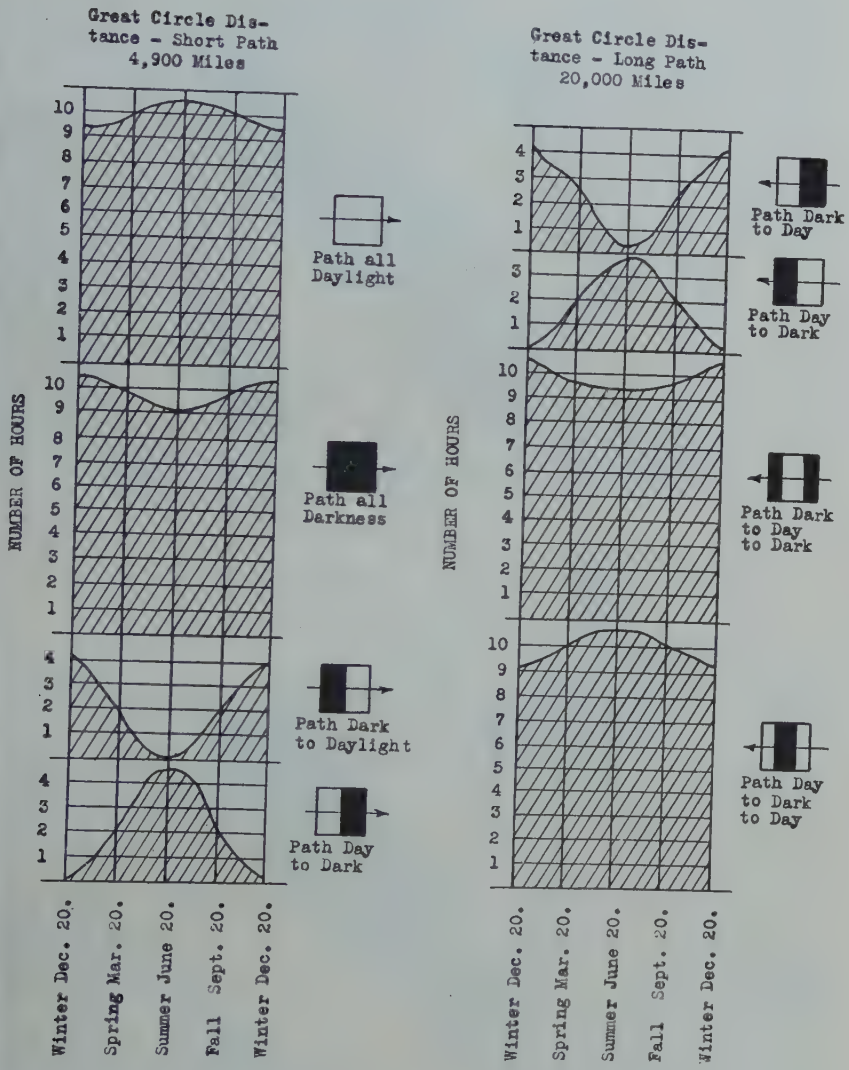

Fig. 100—Daylight-darkness distribution between Schenectady and Rio De Janeiro, South America.

Best reception of W2XAD is obtained from 6:00 to 9:00 P.M. and 3:00 to 5:00 A.M., E.S.T., while W2XAF affords best reception from about 8:00 P.M. to 12:00 midnight, E.S.T. Since the difference between Eastern Standard Time and Rio de Janeiro time is only two hours, most of the evening transmission of W2XAD and W2XAF can be conveniently followed by listeners in Rio and vicinity.

For further details relative to this circuit refer to Figs. 92 to 101.

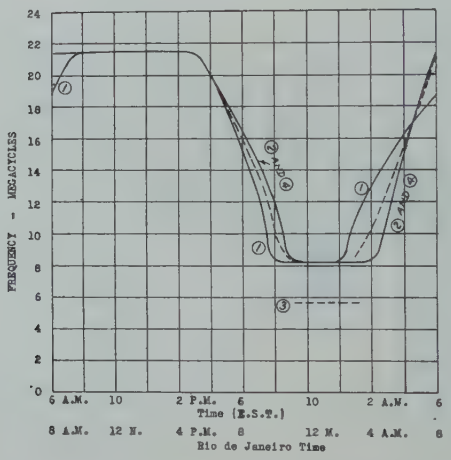

Fig. 101—Optimum frequency chart—Schenectady to Rio de Janeiro.
(1) Winter—November 1 to February 1.
(2) and (4) Spring and Fall-February 1 to May 1 and August 1 to November 1.
(3) Summer—May 1 to August 1.

Schenectady–Honolulu (Hawaii) Circuit

The length of the Schenectady–Honolulu circuit is 4900 miles—the same as that of the Schenectady–Rio de Janeiro circuit discussed in the preceding section.

Seasonal variation over this circuit is moderate as will be observed from a study of Figs. 102 to 109.

TIME			DAYLIGHT-DARKNESS DISTRIBUTION OVER GREAT CIRCLE PATH	PROBABLE RECEPTION OBTAINABLE FROM		PROBABLE OPTIMUM
GMT	Hawaii	Local		W2XAD	W2XAF	FREQUENCY
				13660 K.C.	9550 K.C.	Short Path
1100	12:30 A.M.	6 A.M.		Fair-Poor	Fair	7800 K.C.
1200	1:30 A.M.	7 A.M.		Fair-Poor	Fair	7800 K.C.
1300	2:30 A.M.	8 A.M.		Fair-Poor	Fair	7800 K.C.
1400	3:30 A.M.	9 A.M.		Poor	Fair-Poor	12000 K.C.
1500	4:30 A.M.	10 A.M.		Poor-Unsat.	Unsat.	16800 K.C.
1600	5:30 A.M.	11 A.M.		Unsat.	Nil	19000 K.C.
1700	6:30 A.M.	12 N.		Nil	Nil	20400 K.C.
1800	7:30 A.M.	1 P.M.		Nil	Nil	20400 K.C.
1900	8:30 A.M.	2 P.M.		Nil	Nil	20400 K.C.
2000	9:30 A.M.	3 P.M.		Nil	Nil	20400 K.C.
2100	10:30 A.M.	4 P.M.		Nil	Nil	20000 K.C.
2200	11:30 A.M.	5 P.M.		Nil	Nil	19400 K.C.
2300	12:30 P.M.	6 P.M.		Unsat.	Nil	18800 K.C.
0000	1:30 P.M.	7 P.M.		Unsat.-Poor	Unsat.	17600 K.C.
0100	2:30 P.M.	8 P.M.		Poor	Unsat.-Poor	16500 K.C.
0200	3:30 P.M.	9 P.M.		Poor-Fair	Poor	15200 K.C.
0300	4:30 P.M.	10 P.M.		Fair	Poor-Fair	12800 K.C.
0400	5:30 P.M.	11 P.M.		Fair-Poor	Poor-Fair	10500 K.C.
0500	6:30 P.M.	12 M.		Fair-Poor	Fair	7800 K.C.
0600	7:30 P.M.	1 A.M.		Fair-Poor	Fair	7800 K.C.
0700	8:30 P.M.	2 A.M.		Fair-Poor	Fair	7800 K.C.
0800	9:30 P.M.	3 A.M.		Fair-Poor	Fair	7800 K.C.
0900	10:30 P.M.	4 A.M.		Fair-Poor	Fair	7800 K.C.
1000	11:30 P.M.	5 A.M.		Fair-Poor	Fair	7800 K.C.

Fig. 102—Schenectady-Hawaii transmission chart. Winter season (November 1 to February 1). Distance from Schenectady to Hawaii 4900 miles (approx.)

TIME			DAYLIGHT-DARKNESS DISTRIBUTION OVER GREAT CIRCLE PATH	PROBABLE RECEPTION OBTAINABLE FROM		PROBABLE OPTIMUM
GMT	Hawaii	Local		W2XAD	W2XAF	FREQUENCY
				13660 K.C.	9550 K.C.	Short Path
1100	12:30 A.M.	6 A.M.		Fair-Poor	Fair	7800 K.C.
1200	1:30 A.M.	7 A.M.		Fair-Poor	Fair-Poor	10600 K.C.
1300	2:30 A.M.	8 A.M.		Poor	Poor-Unsat.	14800 K.C.
1400	3:30 A.M.	9 A.M.		Unsat.	Unsat.	16600 K.C.
1500	4:30 A.M.	10 A.M.		Unsat.	Nil	18200 K.C.
1600	5:30 A.M.	11 A.M.		Nil	Nil	19600 K.C.
1700	6:30 A.M.	12 N.		Nil	Nil	20400 K.C.
1800	7:30 A.M.	1 P.M.		Nil	Nil	20400 K.C.
1900	8:30 A.M.	2 P.M.		Nil	Nil	20400 K.C.
2000	9:30 A.M.	3 P.M.		Nil	Nil	20400 K.C.
2100	10:30 A.M.	4 P.M.		Nil	Nil	20400 K.C.
2200	11:30 A.M.	5 P.M.		Nil	Nil	20400 K.C.
2300	12:30 P.M.	6 P.M.		Unsat.	Nil	19800 K.C.
0000	1:30 P.M.	7 P.M.		Unsat.	Nil	18500 K.C.
0100	2:30 P.M.	8 P.M.		Unsat.-Poor	Unsat.	17000 K.C.
0200	3:30 P.M.	9 P.M.		Poor-Fair	Unsat.-Poor	15000 K.C.
0300	4:30 P.M.	10 P.M.		Fair	Poor	13200 K.C.
0400	5:30 P.M.	11 P.M.		Fair	Poor-Fair	10400 K.C.
0500	6:30 P.M.	12 M.		Fair-Poor	Fair	7800 K.C.
0600	7:30 P.M.	1 A.M.		Fair-Poor	Fair	7800 K.C.
0700	8:30 P.M.	2 A.M.		Fair-Poor	Fair	7800 K.C.
0800	9:30 P.M.	3 A.M.		Fair-Poor	Fair	7800 K.C.
0900	10:30 P.M.	4 A.M.		Fair-Poor	Fair	7800 K.C.
1000	11:30 P.M.	5 A.M.		Fair-Poor	Fair	7800 K.C.

Fig. 103—Schenectady-Hawaii transmission chart. Spring season (February 1 to May 1). Distance from Schenectady to Hawaii 4900 miles (approx.)

TIME			DAYLIGHT-DARKNESS DISTRIBUTION OVER GREAT CIRCLE PATH	PROBABLE RECEPTION OBTAINABLE FROM		PROBABLE OPTIMUM FREQUENCY
				W2XAD	W2XAF	
GMT	Hawaii	Local		13660 K.C.	9550 K.C.	Short Path
1100	12:30 A.M.	6 A.M.		Fair-Poor	Fair-Poor	12400 K.C.
1200	1:30 A.M.	7 A.M.		Fair-Poor	Poor-Unsat.	14700 K.C.
1300	2:30 A.M.	8 A.M.		Poor-Unsat.	Nil	17000 K.C.
1400	3:30 A.M.	9 A.M.		Unsat.	Nil	18700 K.C.
1500	4:30 A.M.	10 A.M.		Unsat.	Nil	19800 K.C.
1600	5:30 A.M.	11 A.M.		Nil	Nil	20400 K.C.
1700	6:30 A.M.	12 A.M.		Nil	Nil	20400 K.C.
1800	7:30 A.M.	1 P.M.		Nil	Nil	20400 K.C.
1900	8:30 A.M.	2 P.M.		Nil	Nil	20400 K.C.
2000	9:30 A.M.	3 P.M.		Nil	Nil	20400 K.C.
2100	10:30 A.M.	4 P.M.		Nil	Nil	20400 K.C.
2200	11:30 A.M.	5 P.M.		Nil	Nil	20400 K.C.
2300	12:30 P.M.	6 P.M.		Nil	Nil	20400 K.C.
0000	1:30 P.M.	7 P.M.		Nil	Nil	20400 K.C.
0100	2:30 P.M.	8 P.M.		Nil	Nil	19700 K.C.
0200	3:30 P.M.	9 P.M.		Unsat.	Nil	18200 K.C.
0300	4:30 P.M.	10 P.M.		Unsat.-Poor	Unsat.	16500 K.C.
0400	5:30 P.M.	11 P.M.		Poor-Fair	Unsat.	15000 K.C.
0500	6:30 P.M.	12 M.		Fair	Unsat.-Poor	12800 K.C.
0600	7:30 P.M.	1 A.M.		Fair	Poor-Fair	10800 K.C.
0700	8:30 P.M.	2 A.M.		Fair	Fair-Good	7800 K.C.
0800	9:30 P.M.	3 A.M.		Fair-Poor	Good-Fair	7800 K.C.
0900	10:30 P.M.	4 A.M.		Fair-Poor	Good-Fair	7800 K.C.
1000	11:30 P.M.	5 A.M.		Fair-Poor	Fair	10400 K.C.

Fig. 104—Schenectady-Hawaii transmission chart. Summer season (May 1 to August 1). Distance from Schenectady to Hawaii 4900 miles (approx.)

TIME			DAYLIGHT-DARKNESS DISTRIBUTION OVER GREAT CIRCLE PATH	PROBABLE RECEPTION OBTAINABLE FROM		PROBABLE OPTIMUM FREQUENCY
				W2XAD	W2XAF	
GMT	Hawaii	Local		13660 K.C.	9550 K.C.	Short Path
1100	12:30 A.M.	6 A.M.		Fair-Poor	Fair	7800 K.C.
1200	1:30 A.M.	7 A.M.		Fair-Poor	Fair-Poor	10600 K.C.
1300	2:30 A.M.	8 A.M.		Poor	Poor-Unsat.	14800 K.C.
1400	3:30 A.M.	9 A.M.		Unsat.	Unsat.	16600 K.C.
1500	4:30 A.M.	10 A.M.		Unsat.	Nil	18200 K.C.
1600	5:30 A.M.	11 A.M.		Nil	Nil	19600 K.C.
1700	6:30 A.M.	12 N.		Nil	Nil	20400 K.C.
1800	7:30 A.M.	1 P.M.		Nil	Nil	20400 K.C.
1900	8:30 A.M.	2 P.M.		Nil	Nil	20400 K.C.
2000	9:30 A.M.	3 P.M.		Nil	Nil	20400 K.C.
2100	10:30 A.M.	4 P.M.		Nil	Nil	20400 K.C.
2200	11:30 A.M.	5 P.M.		Nil	Nil	20400 K.C.
2300	12:30 P.M.	6 P.M.		Nil	Nil	20400 K.C.
0000	1:30 P.M.	7 P.M.		Unsat.	Nil	19800 K.C.
0100	2:30 P.M.	8 P.M.		Unsat.	Nil	18500 K.C.
0200	3:30 P.M.	9 P.M.		Unsat.-Poor	Unsat.	17000 K.C.
0300	4:30 P.M.	10 P.M.		Poor-Fair	Unsat.-Poor	15000 K.C.
0400	5:30 P.M.	11 P.M.		Fair-	Poor	13200 K.C.
0500	6:30 P.M.	12 M.		Fair	Poor-Fair	10400 K.C.
0600	7:30 P.M.	1 A.M.		Fair-Poor	Fair	7800 K.C.
0700	8:30 P.M.	2 A.M.		Fair-Poor	Fair	7800 K.C.
0800	9:30 P.M.	3 A.M.		Fair-Poor	Fair	7800 K.C.
0900	10:30 P.M.	4 A.M.		Fair-Poor	Fair	7800 K.C.
1000	11:30 P.M.	5 A.M.		Fair-Poor	Fair	7800 K.C.

Fig. 105—Schenectady-Hawaii transmission chart. Fall season (August 1 to November 1). Distance from Schenectady to Hawaii 4900 miles (approx.)

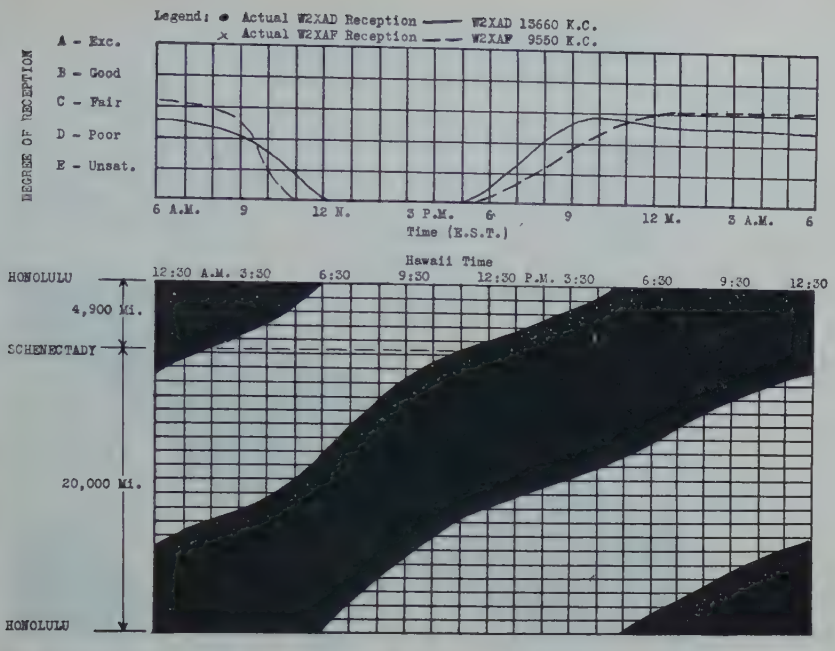

Fig. 106—Reception in Hawaii from November 1 to February 1. Daylight-darkness distribution over great circle distance from Schenctady to Hawaii, as of December 20.

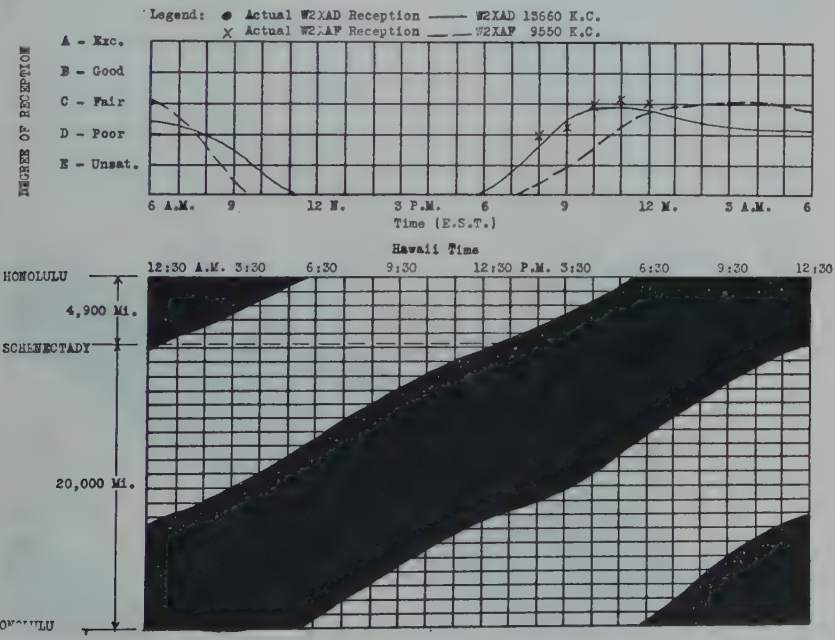

Fig. 107—Reception in Hawaii from February 1 to May 1. Daylight-darkness distribution over great circle distance from Schenectady to Hawaii, as of March 20.

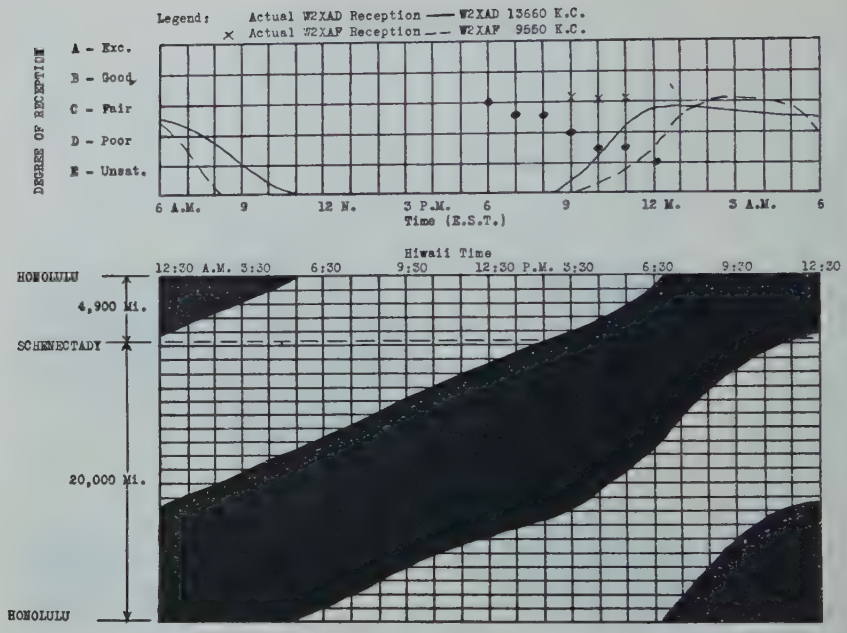

Fig. 108—Reception in Hawaii from May 1 to August 1. Daylight-darkness distribution over great circle distance from Schenectady to Hawaii, as of June 20.

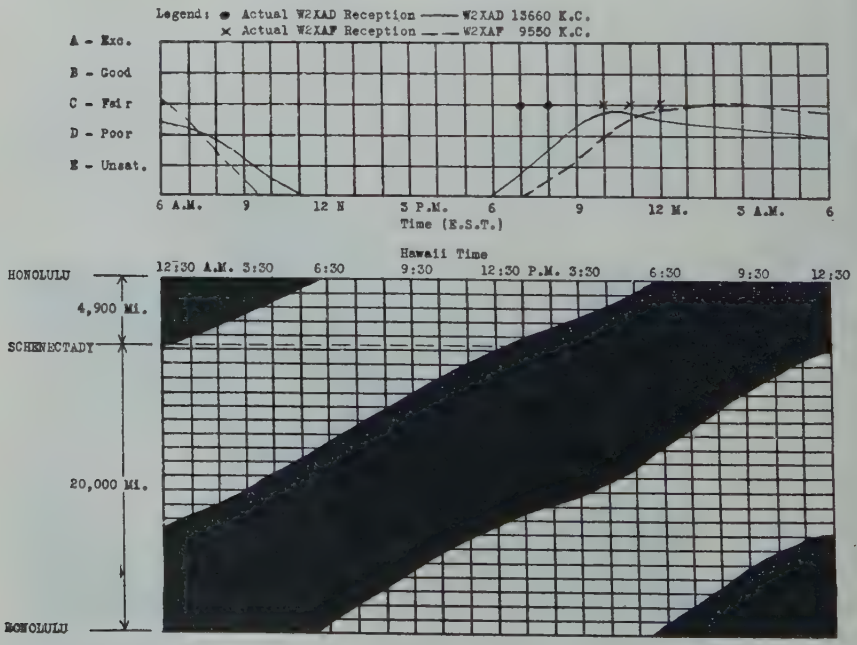

Fig. 109—Reception in Hawaii from August 1 to November 1. Daylight-darkness distribution over great circle distance from Schenectady to Hawaii, as of September 20.

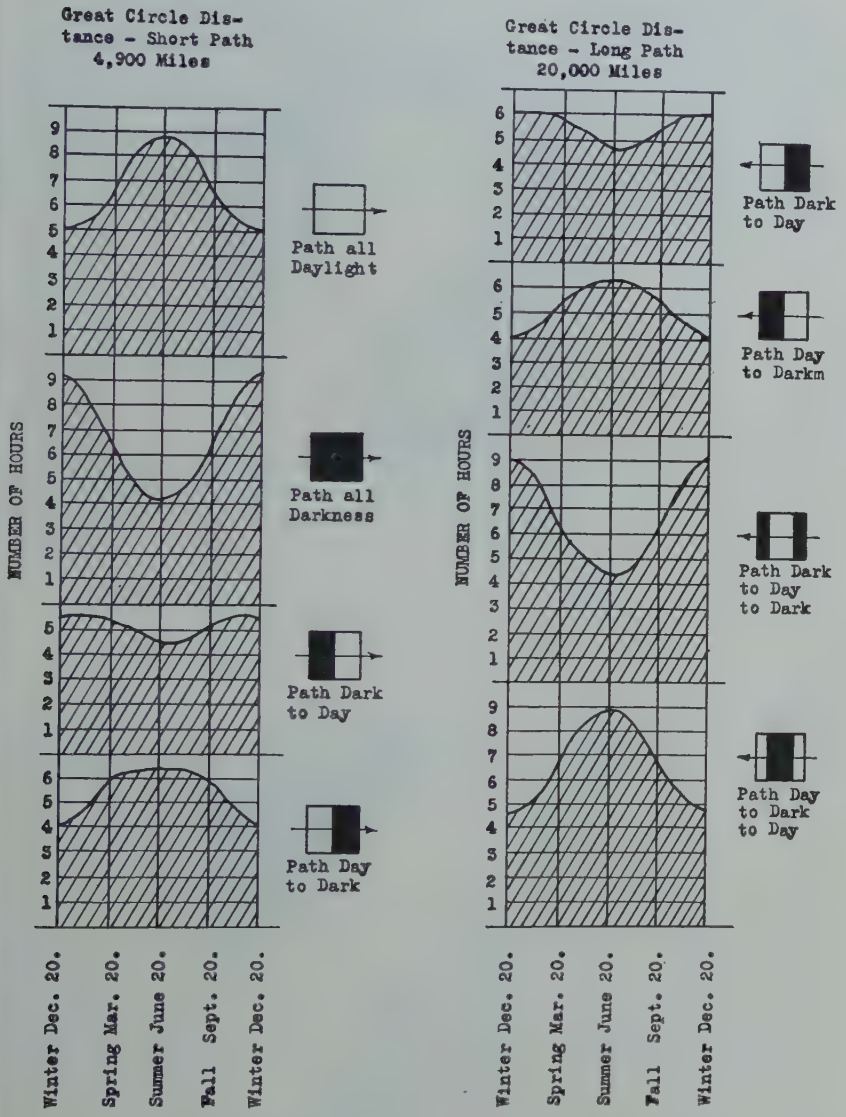

Fig. 110—Daylight-darkness distribution between Schenectady and Hawaii.

Hawaiian reception of W2XAD and W2XAF is best from 9:00 P.M. to 7:00 A.M., E.S.T. While this permits the last three hours of WGY's evening program to be received, it is probable that the size of the listening audience is very small since 9:00 P.M. to 12:00 o'clock midnight, E.S.T., corresponds with 3:30 to 6:30 P.M., Hawaii time—a period when a very small percentage of listeners are at their receivers.

Figs. 110 and 111 show the daylight-darkness distribution and optimum frequency data for the Schenectady-Honolulu circuit.

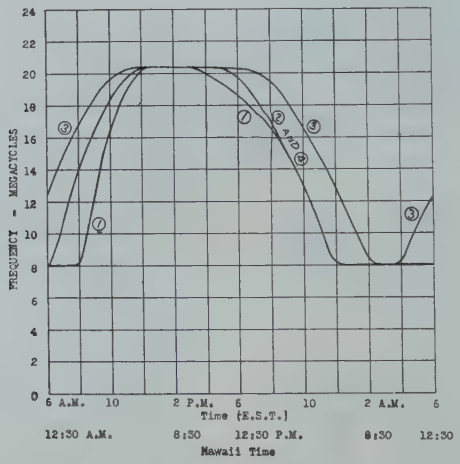

Fig. 111—Optimum frequency chart—Schenectady to Hawaii.
(1) Winter—November 1 to February 1.
(2) and (4) Spring and Fall—February 1 to May 1 and August 1 to November 1.
(3) Summer—May 1 to August 1.

Schenectady–Moscow (U.S.S.R.) Circuit

The distance from Schenectady to Moscow, as measured, in the plane of the great circle passing through these points, is approximately 4400 miles. Seasonal variation over this circuit is rather pronounced although it is not nearly as great as for some of the circuits previously discussed. (Note Figs. 116, 117, 118, 119, and 121.)

The degree of diurnal and seasonal reception normally obtainable from the transmissions of stations W2XAD and W2XAF at Schenectady may be ascertained by referring to the first four of the figures

TIME		DAYLIGHT-DARKNESS DISTRIBUTION OVER GREAT CIRCLE PATH	PROBABLE RECEPTION OBTAINABLE FROM		PROBABLE OPTIMUM FREQUENCY
GMT	Moscow Local		W2XAD	W2XAF	
			13660 K.C.	9550 K.C.	Short Path
1100	1 P.M. 6 A.M.		Fair-Poor	Poor-Unsat.	15400 K.C.
1200	2 P.M. 7 A.M.		Poor-Unsat.	Unsat.	16700 K.C.
1300	3 P.M. 8 A.M.		Nil	Nil	20400 K.C.
1400	4 P.M. 9 A.M.		Unsat.	Nil	20400 K.C.
1500	5 P.M. 10 A.M.		Unsat.	Nil	19600 K.C.
1600	6 P.M. 11 A.M.		Unsat.	Nil	18600 K.C.
1700	7 P.M. 12 N.		Unsat.-Poor	Nil	17500 K.C.
1800	8 P.M. 1 P.M.		Unsat.-Poor	Unsat.	16400 K.C.
1900	9 P.M. 2 P.M.		Poor	Unsat.	15500 K.C.
2000	10 P.M. 3 P.M.		Poor-Fair	Unsat.-Poor	14400 K.C.
2100	11 P.M. 4 P.M.		Poor-Fair	Poor	12800 K.C.
2200	12 M. 5 P.M.		Poor-Fair	Fair	11000 K.C.
2300	1 A.M. 6 P.M.		Fair	Fair-Good	9600 K.C.
0000	2 A.M. 7 P.M.		Fair	Fair-Good	8000 K.C.
0100	3 A.M. 8 P.M.		Fair	Fair-Good	8000 K.C.
0200	4 A.M. 9 P.M.		Fair	Fair-Good	8000 K.C.
0300	5 A.M. 10 P.M.		Fair	Fair-Good	8000 K.C.
0400	6 A.M. 11 P.M.		Fair-Poor	Good-Fair	8000 K.C.
0500	7 A.M. 12 M.		Fair-Poor	Fair	8000 K.C.
0600	8 A.M. 1 A.M.		Fair-Poor	Fair-Poor	8000 K.C.
0700	9 A.M. 2 A.M.		Fair-Poor	Poor	8400 K.C.
0800	10 A.M. 3 A.M.		Fair-Poor	Poor-Unsat.	11000 K.C.
0900	11 A.M. 4 A.M.		Fair-Poor	Poor-Unsat.	12500 K.C.
1000	12 N. 5 A.M.		Fair-Poor	Poor-Unsat.	14800 K.C.

Fig. 112—Schenectady-Moscow transmission chart. Winter season (November 1 to February 1). Distance from Schenectady to Moscow 4400 miles (approx.)

TIME		DAYLIGHT-DARKNESS DISTRIBUTION OVER GREAT CIRCLE PATH	PROBABLE RECEPTION OBTAINABLE FROM		PROBABLE OPTIMUM FREQUENCY
GMT	Moscow Local		W2XAD	W2XAF	
			13660 K.C.	9550 K.C.	Short Path
1100	1 P.M. 6 A.M.		Nil	Nil	20800 K.C.
1200	2 P.M. 7 A.M.		Nil	Nil	20800 K.C.
1300	3 P.M. 8 A.M.		Nil	Nil	20800 K.C.
1400	4 P.M. 9 A.M.		Nil	Nil	20800 K.C.
1500	5 P.M. 10 A.M.		Nil	Nil	20800 K.C.
1600	6 P.M. 11 A.M.		Unsat.	Nil	20400 K.C.
1700	7 P.M. 12 N.		Unsat.	Nil	20000 K.C.
1800	8 P.M. 1 P.M.		Unsat.	Nil	19200 K.C.
1900	9 P.M. 2 P.M.		Poor	Nil	18000 K.C.
2000	10 P.M. 3 P.M.		Poor-Fair	Nil	16400 K.C.
2100	11 P.M. 4 P.M.		Fair	Unsat.	15000 K.C.
2200	12 M. 5 P.M.		Fair	Unsat.	13000 K.C.
2300	1 A.M. 6 P.M.		Fair-Poor	Poor	11800 K.C.
0000	2 A.M. 7 P.M.		Fair-Poor	Poor-Fair	10200 K.C.
0100	3 A.M. 8 P.M.		Poor	Fair	8000 K.C.
0200	4 A.M. 9 P.M.		Poor-Unsat.	Fair	8000 K.C.
0300	5 A.M. 10 P.M.		Poor-Unsat.	Fair-Poor	9000 K.C.
0400	6 A.M. 11 P.M.		Unsat.-Poor	Fair-Poor	10500 K.C.
0500	7 A.M. 12 M.		Unsat.-Poor	Poor-Unsat.	11800 K.C.
0600	8 A.M. 1 A.M.		Poor-Fair	Poor-Unsat.	13000 K.C.
0700	9 A.M. 2 A.M.		Fair	Unsat.	15000 K.C.
0800	10 A.M. 3 A.M.		Fair-Poor	Unsat.	17000 K.C.
0900	11 A.M. 4 A.M.		Poor-Unsat.	Unsat.	18500 K.C.
1000	12 N. 5 A.M.		Unsat.	Nil	20500 K.C.

Fig. 113—Schenectady-Moscow transmission chart. Spring season (February 1 to May 1). Distance from Schenectady to Moscow 4400 miles (approx.)

TIME			DAYLIGHT-DARKNESS DISTRIBUTION OVER GREAT CIRCLE PATH	PROBABLE RECEPTION OBTAINABLE FROM		PROBABLE OPTIMUM FREQUENCY
				W2XAD	W2XAF	
GMT	Moscow	Local		13660 K.C.	9550 K.C.	Short Path
1100	1 P.M.	6 A.M.	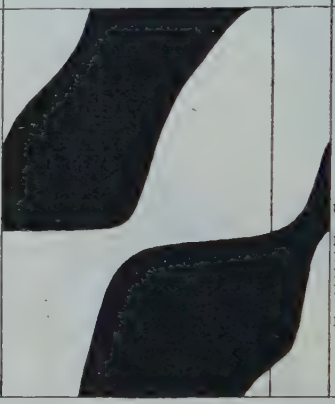	Nil	Nil	20800 K.C.
1200	2 P.M.	7 A.M.		Nil	Nil	20800 K.C.
1300	3 P.M.	8 A.M.		Nil	Nil	20800 K.C.
1400	4 P.M.	9 A.M.		Nil	Nil	20800 K.C.
1500	5 P.M.	10 A.M.		Nil	Nil	20800 K.C.
1600	6 P.M.	11 A.M.		Nil	Nil	20800 K.C.
1700	7 P.M.	12 N.		Nil	Nil	20800 K.C.
1800	8 P.M.	1 P.M.		Nil	Nil	20800 K.C.
1900	9 P.M.	2 P.M.		Nil	Nil	20800 K.C.
2000	10 P.M.	3 P.M.		Nil	Nil	20000 K.C.
2100	11 P.M.	4 P.M.		Unsat.	Nil	19000 K.C.
2200	12 M.	5 P.M.		Unsat.	Nil	18000 K.C.
2300	1 A.M.	6 P.M.		Unsat.-Poor	Nil	16500 K.C.
0000	2 A.M.	7 P.M.		Poor	Unsat.	14800 K.C.
0100	3 A.M.	8 P.M.		Poor-Fair	Fair	8500 K.C.
0200	4 A.M.	9 P.M.		Fair-Poor	Fair	9000 K.C.
0300	5 A.M.	10 P.M.		Fair-Poor	Fair-Poor	11500 K.C.
0400	6 A.M.	11 P.M.		Fair-Poor	Poor-Unsat.	14500 K.C.
0500	7 A.M.	12 M.		Poor	Unsat.	16000 K.C.
0600	8 A.M.	1 A.M.		Poor-Unsat.	Unsat.	17300 K.C.
0700	9 A.M.	2 A.M.		Unsat.	Unsat.	18800 K.C.
0800	10 A.M.	3 A.M.		Unsat.	Unsat.	19800 K.C.
0900	11 A.M.	4 A.M.		Unsat.	Nil	20600 K.C.
1000	12 N.	5 A.M.		Nil	Nil	21000 K.C.

Fig. 114—Schenectady-Moscow transmission chart. Summer season (May 1 to August 1). Distance from Schenectady to Moscow 4400 miles (approx.

TIME			DAYLIGHT-DARKNESS DISTRIBUTION OVER GREAT CIRCLE PATH	PROBABLE RECEPTION OBTAINABLE FROM		PROBABLE OPTIMUM FREQUENCY
				W2XAD	W2XAF	
GMT	Moscow	Local		13660 K.C.	9550 K.C.	Short Path
1100	1 P.M.	6 A.M.		Nil	Nil	20800 K.C.
1200	2 P.M.	7 A.M.		Nil	Nil	20800 K.C.
1300	3 P.M.	8 A.M.		Nil	Nil	20800 K.C.
1400	4 P.M.	9 A.M.		Nil	Nil	20800 K.C.
1500	5 P.M.	10 A.M.		Nil	Nil	20800 K.C.
1600	6 P.M.	11 A.M.		Nil	Nil	20400 K.C.
1700	7 P.M.	12 N.		Unsat.	Nil	20000 K.C.
1800	8 P.M.	1 P.M.		Unsat.	Nil	19200 K.C.
1900	9 P.M.	2 P.M.		Poor	Nil	18000 K.C.
2000	10 P.M.	3 P.M.		Poor-Fair	Nil	16400 K.C.
2100	11 P.M.	4 P.M.		Fair	Unsat.	15000 K.C.
2200	12 M.	5 P.M.		Fair	Unsat.	13000 K.C.
2300	1 A.M.	6 P.M.		Fair-Poor	Poor	11800 K.C.
0000	2 A.M.	7 P.M.		Fair-Poor	Poor-Fair	10200 K.C.
0100	3 A.M.	8 P.M.		Poor	Fair	8000 K.C.
0200	4 A.M.	9 P.M.		Poor-Unsat.	Fair	8000 K.C.
0300	5 A.M.	10 P.M.		Poor-Unsat.	Fair-Poor	9000 K.C.
0400	6 A.M.	11 P.M.		Unsat.-Poor	Fair-Poor	10500 K.C.
0500	7 A.M.	12 M.		Unsat.-Poor	Poor-Unsat.	11800 K.C.
0600	8 A.M.	1 A.M.		Poor-Fair	Poor-Unsat.	13000 K.C.
0700	9 A.M.	2 A.M.		Fair	Unsat.	15000 K.C.
0800	10 A.M.	3 A.M.		Fair-Poor	Unsat.	17000 K.C.
0900	11 A.M.	4 A.M.		Poor-Unsat.	Unsat.	18500 K.C.
1000	12 A.M.	5 A.M.		Unsat.	Nil	20600 K.C.

Fig. 115—Schenectady-Moscow transmission chart. Fall season (August 1 to November 1). Distance from Schenectady to Moscow 4400 miles (approx.)

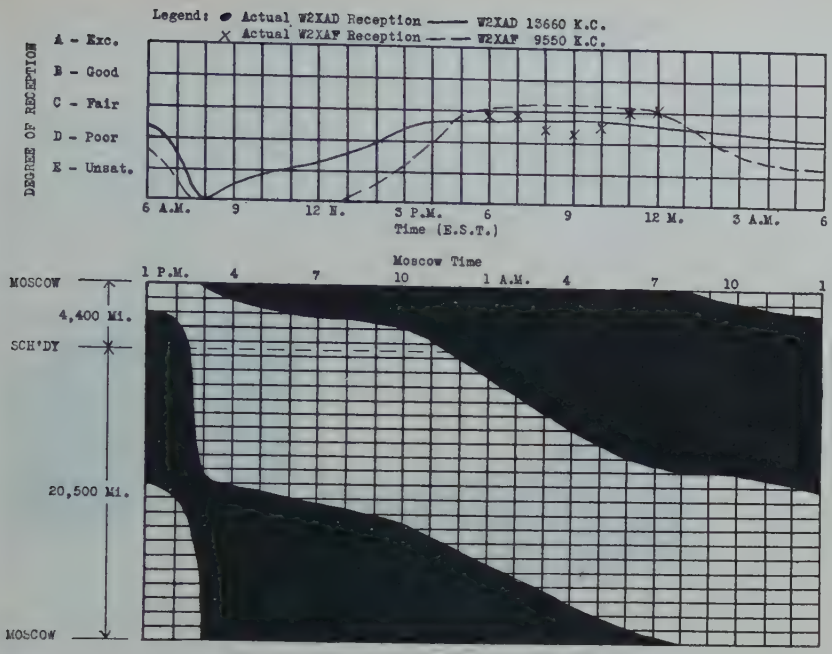

Fig. 116—Reception in Moscow from November 1 to February 1. Daylight-darkness distribution over great circle distance from Schenectady to Moscow, U.S.S.R., as of December 20.

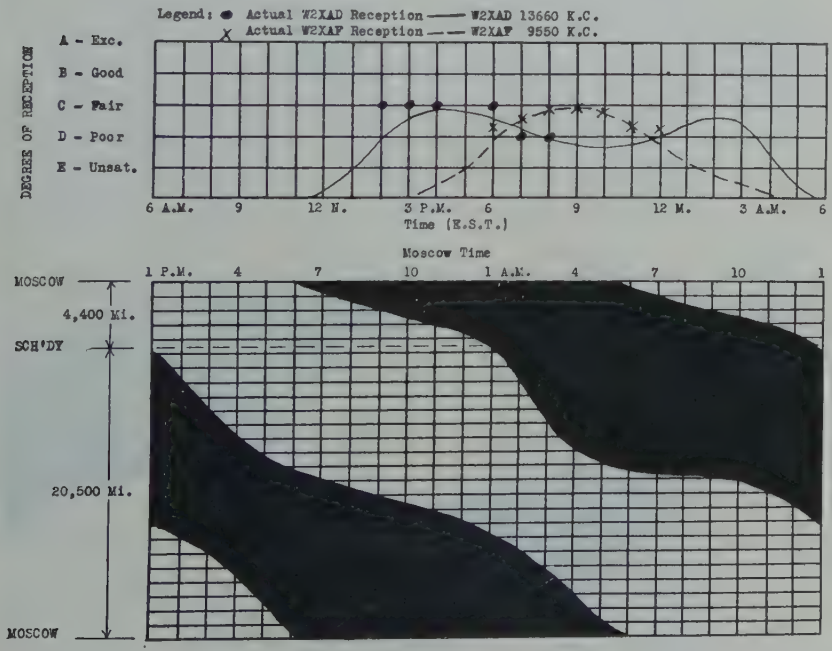

Fig. 117—Reception in Moscow from February 1 to May 1. Daylight-darkness distribution over great circle distance from Schenectady to Moscow, U. S. S. R., as of March 20.

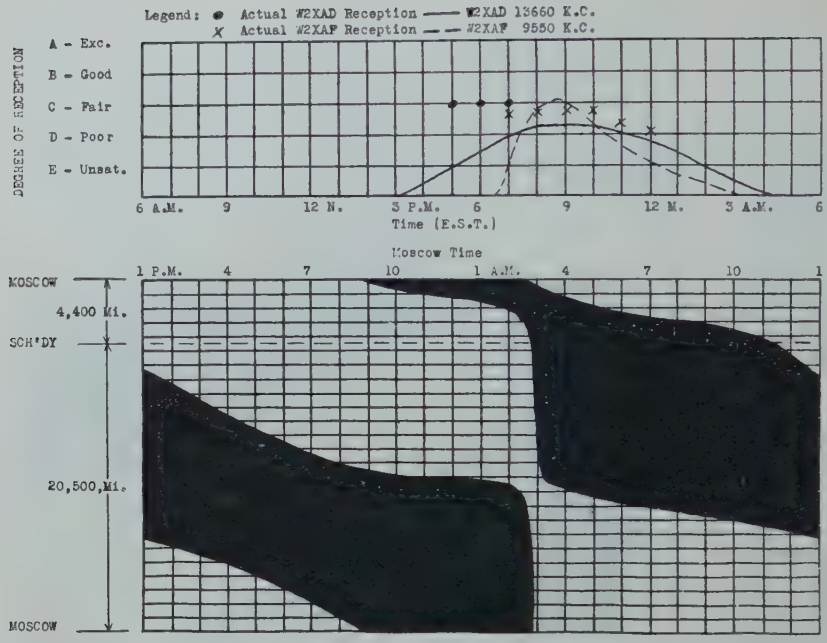

Fig. 118—Reception in Moscow from May 1 to August 1. Daylight-darkness distribution over great circle distance from Schenectady to Moscow, U.S.S.R., as of June 20.

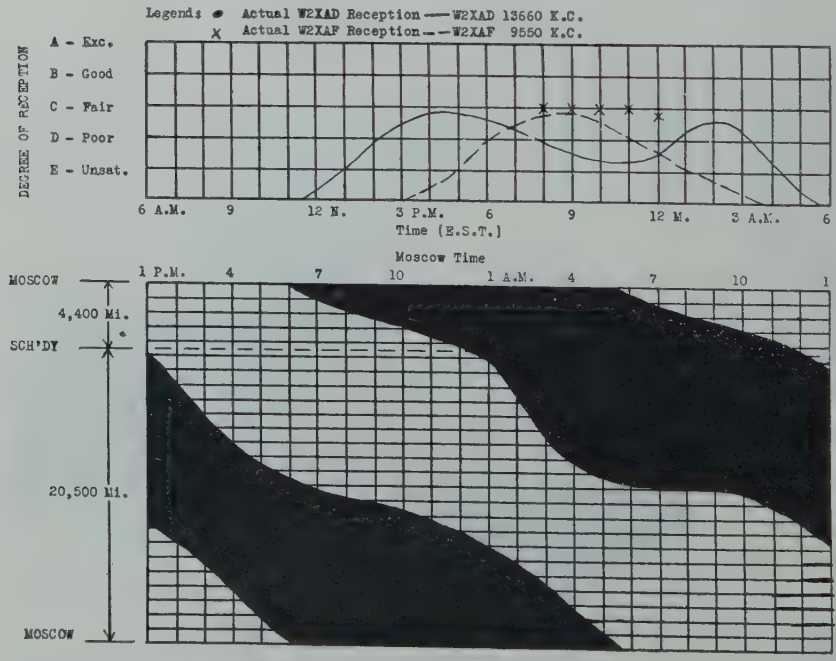

Fig. 119—Reception in Moscow from August 1 to November 1. Daylight-darkness distribution over great circle distance from Schenectady to Moscow, U.S.S.R., as of September 20.

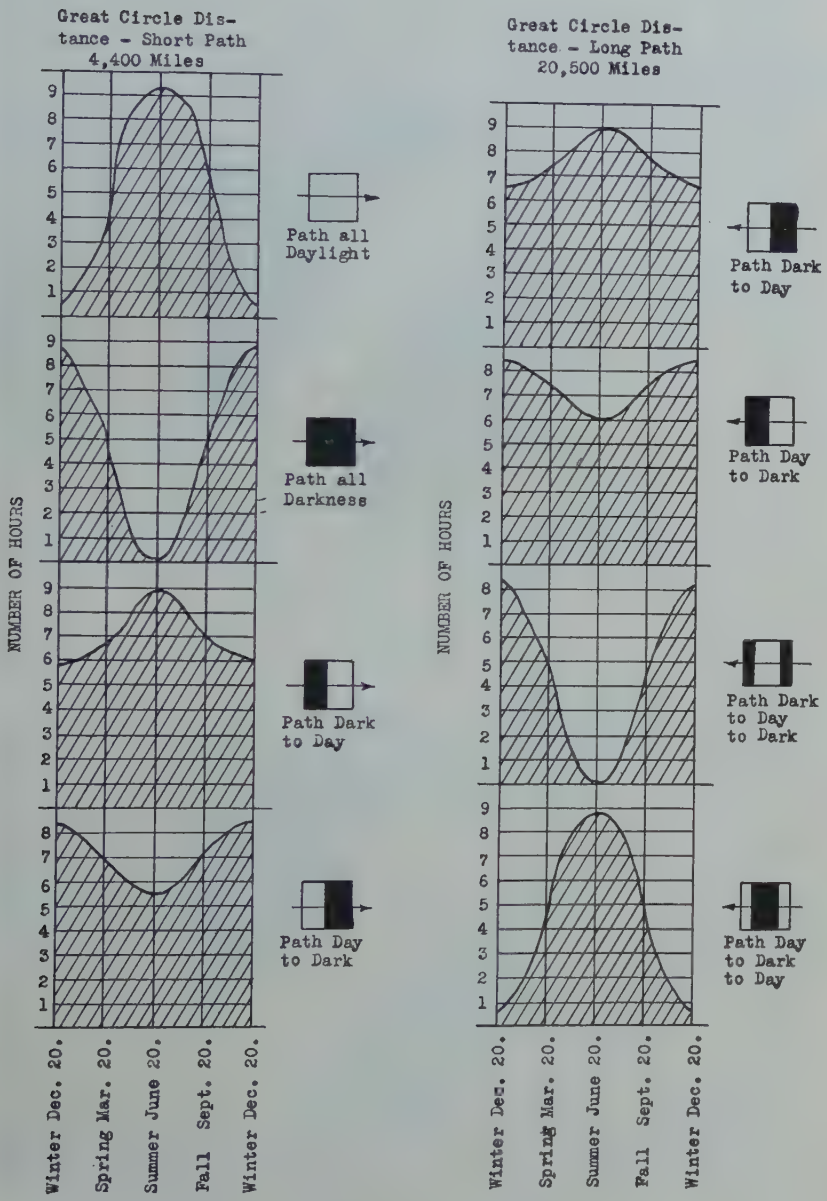

Fig. 120—Daylight-darkness distribution between Schenectady and Moscow, U.S.S.R.

mentioned above. Fig. 120, which shows the type and number of hours of daylight-darkness distribution between Schenectady and Moscow, may be of interest. From this figure it will be observed that, among other things, during the winter season, the circuit is covered by daylight for a period of less than one hour while there is a period of almost nine hours of complete darkness. Conversely, during the summer season, there is an interval of more than nine hours of daylight and

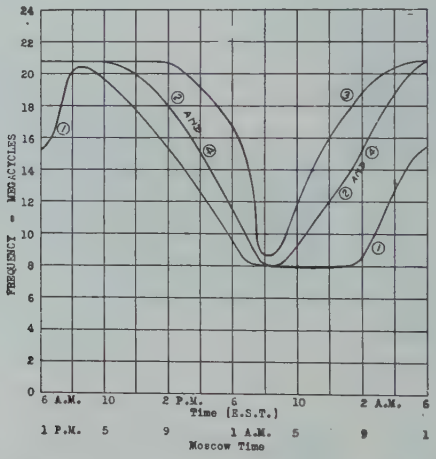

Fig. 121—Optimum frequency chart—Schenectady to Moscow.
(1) Winter—November 1 to February 1.
(2) and (4) Spring and Fall—February 1 to May 1 and August 1 to November 1.
(3) Summer—May 1 to August 1.

only about fifteen minutes of darkness. These factors will cause the diurnal performance of a given frequency to vary considerably from summer to winter.

Schenectady-Berlin (Germany) Circuit

This circuit is approximately 3850 miles in length.

Figs. 122, 123, 124, and 125 show the type of reception that may be expected in Germany from the broadcast transmissions of W2XAD and W2XAF; also, the value of the optimum frequency that should be utilized for best results in transmitting from Schenectady to Germany.

TIME			DAYLIGHT-DARKNESS DISTRIBUTION OVER GREAT CIRCLE PATH	PROBABLE RECEPTION OBTAINABLE FROM		PROBABLE OPTIMUM
GMT	Germany	Local		W2XAD	W2XAF	FREQUENCY
				13660 K.C.	9550 K.C.	Short Path
1100	12 N.	6 A.M.		Poor-Unsat.	Nil	18400 K.C.
1200	1 P.M.	7 A.M.		Unsat.	Nil	19500 K.C.
1300	2 P.M.	8 A.M.		Unsat.	Nil	20000 K.C.
1400	3 P.M.	9 A.M.		Unsat.	Nil	20000 K.C.
1500	4 P.M.	10 A.M.		Unsat.-Poor	Nil	19200 K.C.
1600	5 P.M.	11 A.M.		Poor-Fair	Nil	17800 K.C.
1700	6 P.M.	12 N.		Poor-Fair	Nil	16800 K.C.
1800	7 P.M.	1 P.M.		Fair	Nil	15500 K.C.
1900	8 P.M.	2 P.M.		Fair-Good	Unsat.	14200 K.C.
2000	9 P.M.	3 P.M.		Fair-Good	Unsat.-Poor	12800 K.C.
2100	10 P.M.	4 P.M.		Fair	Poor	11200 K.C.
2200	11 P.M.	5 P.M.		Fair	Poor-Fair	7400 K.C.
2300	12 M.	6 P.M.		Fair-Poor	Poor-Fair	7400 K.C.
0000	1 A.M.	7 P.M.		Fair-Poor	Fair	7400 K.C.
0100	2 A.M.	8 P.M.		Fair-Poor	Fair	7400 K.C.
0200	3 A.M.	9 P.M.		Poor	Fair-Good	7400 K.C.
0300	4 A.M.	10 P.M.		Poor-Unsat.	Fair-Good	7400 K.C.
0400	5 A.M.	11 P.M.		Poor-Unsat.	Good-Fair	7400 K.C.
0500	6 A.M.	12 M.		Unsat.-Poor	Fair	7400 K.C.
0600	7 A.M.	1 A.M.		Unsat.-Poor	Fair-Poor	7400 K.C.
0700	8 A.M.	2 A.M.		Poor-Fair	Poor	10800 K.C.
0800	9 A.M.	3 A.M.		Fair	Unsat.	13200 K.C.
0900	10 A.M.	4 A.M.		Fair	Nil	15200 K.C.
1000	11 A.M.	5 A.M.		Fair-Poor	Nil	17000 K.C.

Fig. 122—Schenectady-Germany transmission chart. Winter season (November 1 to February 1). Distance from Schenectady to Berlin 3850 miles (approx.)

TIME			DAYLIGHT-DARKNESS DISTRIBUTION OVER GREAT CIRCLE PATH	PROBABLE RECEPTION OBTAINABLE FROM		PROBABLE OPTIMUM
GMT	Germany	Local		W2XAD	W2XAF	FREQUENCY
				13660 K.C.	9550 K.C.	Short Path
1100	12 N.	6 A.M.		Unsat.	Nil	20000 K.C.
1200	1 P.M.	7 A.M.		Unsat.	Nil	20000 K.C.
1300	2 P.M.	8 A.M.		Unsat.	Nil	20000 K.C.
1400	3 P.M.	9 A.M.		Unsat.	Nil	20000 K.C.
1500	4 P.M.	10 A.M.		Unsat.	Nil	20000 K.C.
1600	5 P.M.	11 A.M.		Unsat.	Nil	20000 K.C.
1700	6 P.M.	12 N.		Unsat.	Nil	20000 K.C.
1800	7 P.M.	1 P.M.		Unsat.	Nil	19400 K.C.
1900	8 P.M.	2 P.M.		Unsat.-Poor	Nil	18600 K.C.
2000	9 P.M.	3 P.M.		Poor	Nil	17600 K.C.
2100	10 P.M.	4 P.M.		Fair	Unsat.	16100 K.C.
2200	11 P.M.	5 P.M.		Fair-Good	Poor-Fair	14700 K.C.
2300	12 M.	6 P.M.		Fair-Good	Poor-Fair	12600 K.C.
0000	1 A.M.	7 P.M.		Good	Fair	11400 K.C.
0100	2 A.M.	8 P.M.		Good-Fair	Fair-Good	7400 K.C.
0200	3 A.M.	9 P.M.		Fair-Poor	Fair-Good	7400 K.C.
0300	4 A.M.	10 P.M.		Fair-Poor	Fair-Good	7400 K.C.
0400	5 A.M.	11 P.M.		Poor	Fair	7400 K.C.
0500	6 A.M.	12 M.		Poor-Fair	Fair-Poor	7400 K.C.
0600	7 A.M.	1 A.M.		Poor-Fair	Poor	12600 K.C.
0700	8 A.M.	2 A.M.		Fair	Nil	14600 K.C.
0800	9 A.M.	3 A.M.		Fair	Nil	16200 K.C.
0900	10 A.M.	4 A.M.		Fair-Poor	Nil	17400 K.C.
1000	11 A.M.	5 A.M.		Poor-Unsat.	Nil	19200 K.C.

Fig. 123—Schenectady-Germany transmission chart. Spring season (February 1 to May 1). Distance from Schenectady to Berlin 3850 miles (approx.)

TIME			DAYLIGHT-DARKNESS DISTRIBUTION OVER GREAT CIRCLE PATH	PROBABLE RECEPTION OBTAINABLE FROM		PROBABLE OPTIMUM FREQUENCY
GMT	Germany	Local		W2XAD	W2XAF	
				13600 K.C.	9550 K.C.	Short Path
1100	12 N.	6 A.M.		Unsat.	Nil	20000 K.C.
1200	1 P.M.	7 A.M.		Unsat.	Nil	20000 K.C.
1300	2 P.M.	8 A.M.		Unsat.	Nil	20000 K.C.
1400	3 P.M.	9 A.M.		Unsat.	Nil	20000 K.C.
1500	4 P.M.	10 A.M.		Unsat.	Nil	20000 K.C.
1600	5 P.M.	11 A.M.		Unsat.	Nil	20000 K.C.
1700	6 P.M.	12 N.		Unsat.	Nil	20000 K.C.
1800	7 P.M.	1 P.M.		Unsat.	Nil	20000 K.C.
1900	8 P.M.	2 P.M.		Unsat.-Poor	Nil	19800 K.C.
2000	9 P.M.	3 P.M.		Poor	Nil	19000 K.C.
2100	10 P.M.	4 P.M.		Poor-Fair	Nil	17800 K.C.
2200	11 P.M.	5 P.M.		Fair	Unsat.	16000 K.C.
2300	12 M.	6 P.M.		Fair	Unsat.-Poor	14400 K.C.
0000	1 A.M.	7 P.M.		Fair-Poor	Poor	12000 K.C.
0100	2 A.M.	8 P.M.		Fair-Poor	Poor-Fair	7400 K.C.
0200	3 A.M.	9 P.M.		Fair-Poor	Fair	7400 K.C.
0300	4 A.M.	10 P.M.		Poor-Fair	Fair	7400 K.C.
0400	5 A.M.	11 P.M.		Poor-Fair	Fair-Poor	11200 K.C.
0500	6 A.M.	12 M.		Fair	Poor	13000 K.C.
0600	7 A.M.	1 A.M.		Fair	Unsat.	14800 K.C.
0700	8 A.M.	2 A.M.		Fair-Poor	Nil	16800 K.C.
0800	9 A.M.	3 A.M.		Poor	Nil	18800 K.C.
0900	10 A.M.	4 A.M.		Unsat.	Nil	19800 K.C.
1000	11 A.M.	5 A.M.		Unsat.	Nil	20000 K.C.

Fig. 124—Schenectady-Germany transmission chart. Summer season (May 1 to August 1). Distance from Schenectady to Berlin 3850 miles (approx.)

TIME			DAYLIGHT-DARKNESS DISTRIBUTION OVER GREAT CIRCLE DISTANCE	PROBABLE RECEPTION OBTAINABLE FROM		PROBABLE OPTIMUM FREQUENCY
GMT	Germany	Local		W2XAD	W2XAF	
				13660 K.C.	9550 K.C.	Short Path
1100	12 N.	6 A.M.		Unsat.	Nil	20000 K.C.
1200	1 P.M.	7 A.M.		Unsat.	Nil	20000 K.C.
1300	2 P.M.	8 A.M.		Unsat.	Nil	20000 K.C.
1400	3 P.M.	9 A.M.		Unsat.	Nil	20000 K.C.
1500	4 P.M.	10 A.M.		Unsat.	Nil	20000 K.C.
1600	5 P.M.	11 A.M.		Unsat.	Nil	20000 K.C.
1700	6 P.M.	12 N.		Unsat.	Nil	20000 K.C.
1800	7 P.M.	1 P.M.		Unsat.	Nil	19400 K.C.
1900	8 P.M.	2 P.M.		Unsat.-Poor	Nil	18600 K.C.
2000	9 P.M.	3 P.M.		Poor	Nil	17600 K.C.
2100	10 P.M.	4 P.M.		Fair	Unsat.	16100 K.C.
2200	11 P.M.	5 P.M.		Fair-Good	Poor-Fair	14700 K.C.
2300	12 P.M.	6 P.M.		Fair-Good	Poor-Fair	12600 K.C.
0000	1 A.M.	7 P.M.		Good	Fair	11400 K.C.
0100	2 A.M.	8 P.M.		Good-Fair	Fair-Good	7400 K.C.
0200	3 A.M.	9 P.M.		Fair-Poor	Fair-Good	7400 K.C.
0300	4 A.M.	10 P.M.		Fair-Poor	Fair-Good	7400 K.C.
0400	5 A.M.	11 P.M.		Poor	Fair	7400 K.C.
0500	6 A.M.	12 M.		Poor-Fair	Fair-Poor	7400 K.C.
0600	7 A.M.	1 A.M.		Poor-Fair	Poor	12500 K.C.
0700	8 A.M.	2 A.M.		Fair	Nil	14600 K.C.
0800	9 A.M.	3 A.M.		Fair	Nil	16200 K.C.
0900	10 A.M.	4 A.M.		Fair-Poor	Nil	17400 K.C.
1000	11 A.M.	5 A.M.		Poor-Unsat.	Nil	19200 K.C.

Fig. 125—Schenectady-Germany transmission chart. Fall season (August 1 to November 1). Distance from Schenectady to Berlin 3850 miles (approx.)

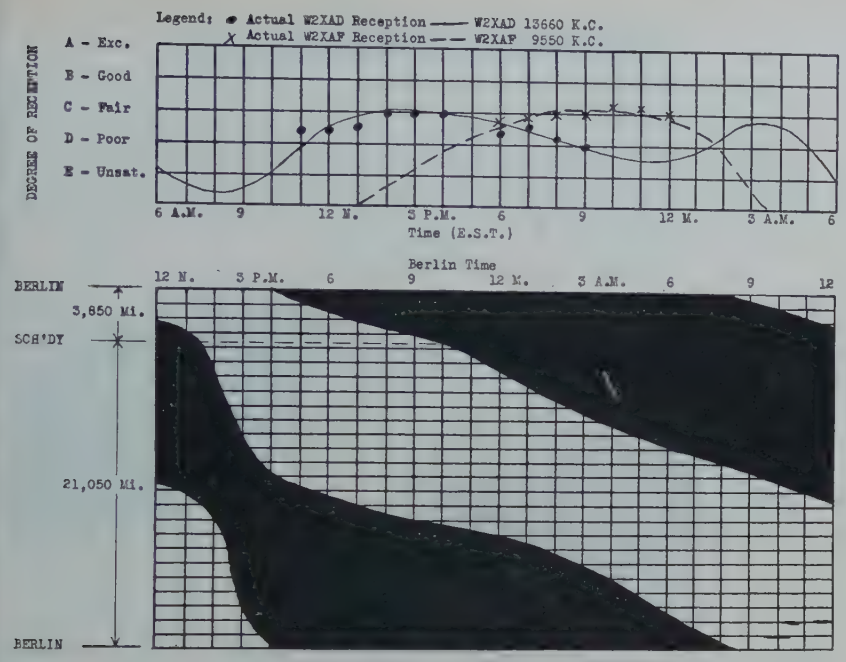

Fig. 126—Reception in Berlin from November 1 to February 1. Daylight-darkness distribution over great circle distance from Schenectady to Berlin, Germany, as of December 20.

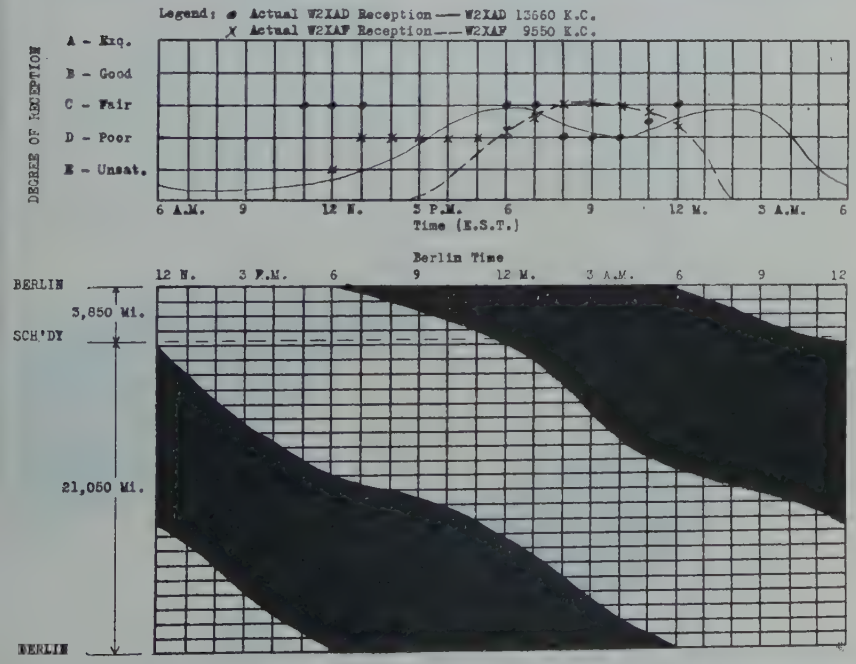

Fig. 127—Reception in Berlin from February 1 to May 1. Daylight-darkness distribution over great circle distance from Schenectady to Berlin, Germany, as of March 20.

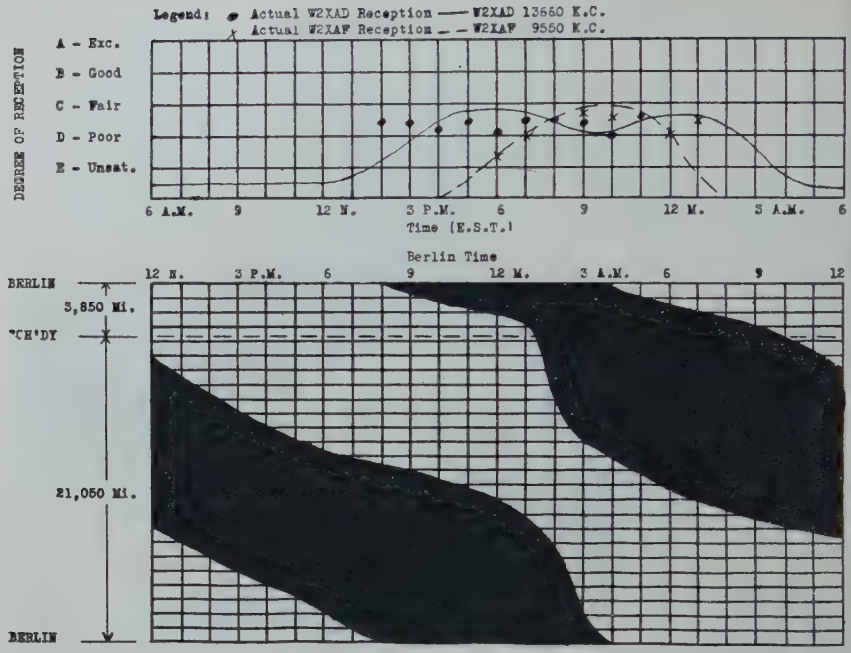

Fig. 128—Reception in Berlin from May 1 to August 1. Daylight-darkness distribution over great circle distance from Schenectady to Berlin, Germany, as of June 20.

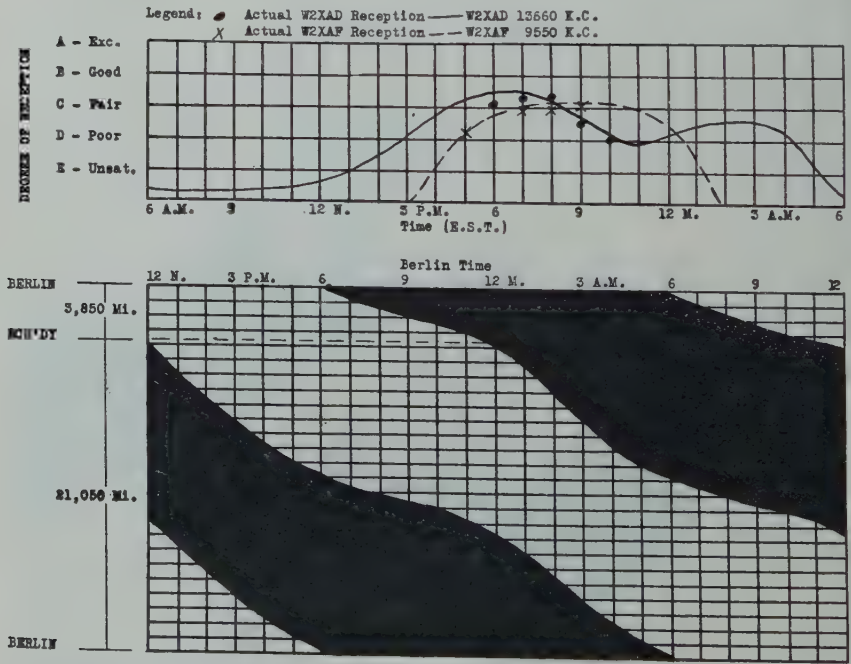

Fig. 129—Reception in Berlin from August 1 to November 1. Daylight-darkness distribution over great circle distance from Schenectady to Berlin, Germany, as of September 20.

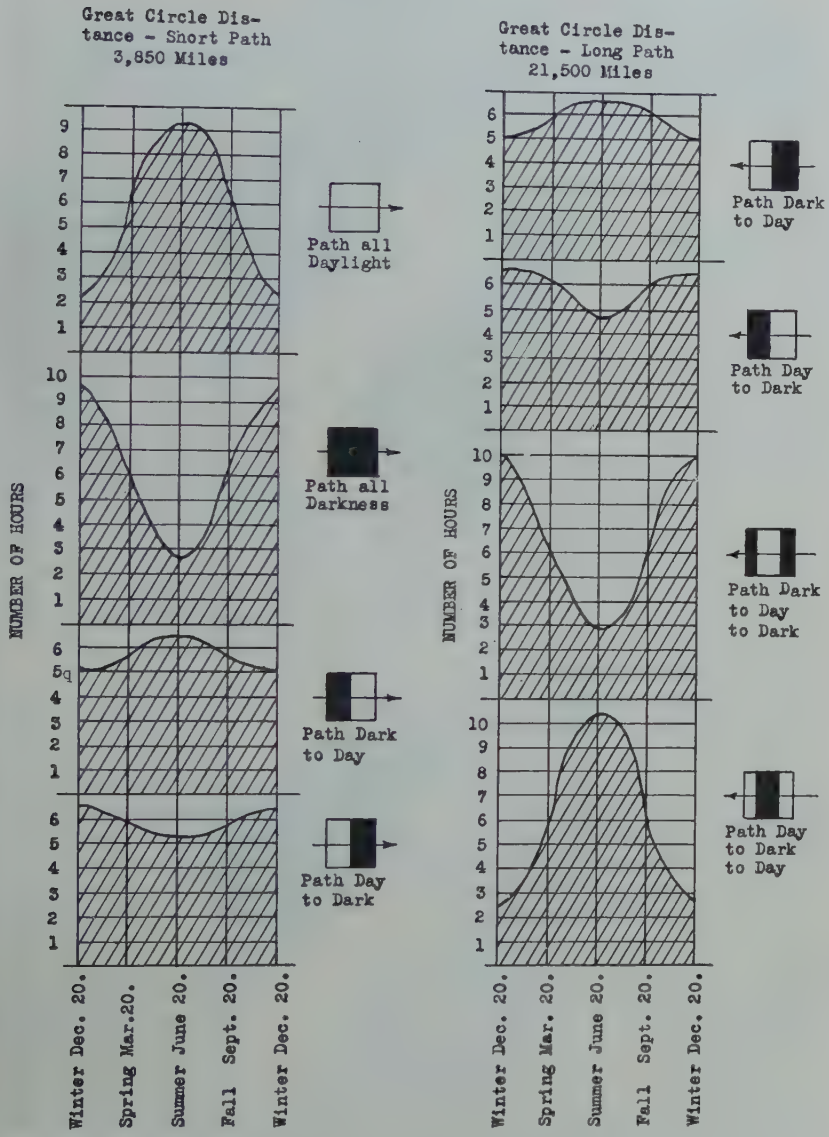

Fig. 130—Daylight-darkness distribution between Schenectady and Berlin, Germany.

The extent of the diurnal and seasonal variation can be determined by referring to Figs. 126, 127, 128, and 129. In this connection it will be noted that such variation is only moderate.

The chart shown on Fig. 131 gives the value of the optimum frequency to use over the Schenectady-Berlin circuit for any hour of the day and for the different seasons of the year.

Schenectady–Paris (France) Circuit

In most respects this circuit is similar to the Schenectady-Berlin circuit. Its length, of course, is different being approximately 3500

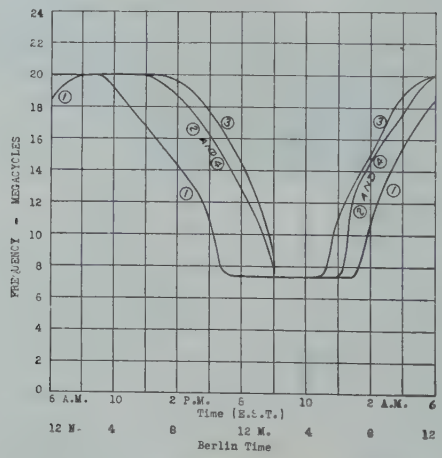

Fig. 131—Optimum frequency chart—Schenectady to Berlin.
(1) Winter—November 1 to February 1.
(2) and (4) Spring and Fall—February 1 to May 1 and August 1 to November 1.
(3) Summer—May 1 to August 1.

miles. Figs. 132, 133, 134, and 135 present a tabulation of W2XAD and W2XAF degree of reception data and, also, the optimum frequency data for this circuit.

From a survey of Figs. 136, 137, 138, and 139, a further understanding of the type of reception obtainable from the transmissions of W2XAD and W2XAF may be obtained. These figures also show the magnitude of the seasonal variation.

TIME			DAYLIGHT-DARKNESS DISTRIBUTION OVER GREAT CIRCLE PATH	PROBABLE RECEPTION OBTAINABLE FROM		PROBABLE OPTIMUM FREQUENCY
GMT	France	Local		W2XAD	W2XAF	
				13660 K.C.	9550 K.C.	Short Path
1100	11 A.M.	6 A.M.		Fair-Poor	Poor-Unsat.	17000 K.C.
1200	12 N.	7 A.M.		Poor	Unsat.	18800 K.C.
1300	1 P.M.	8 A.M.		Poor-Unsat.	Nil	19200 K.C.
1400	2 P.M.	9 A.M.		Unsat.	Nil	19200 K.C.
1500	3 P.M.	10 A.M.		Unsat.	Nil	19200 K.C.
1600	4 P.M.	11 A.M.		Unsat.	Nil	19200 K.C.
1700	5 P.M.	12 N.		Unsat.-Poor	Nil	18800 K.C.
1800	6 P.M.	1 P.M.		Poor	Unsat.	17600 K.C.
1900	7 P.M.	2 P.M.		Poor-Fair	Unsat.	15000 K.C.
2000	8 P.M.	3 P.M.		Fair	Unsat.-Poor	12800 K.C.
2100	9 P.M.	4 P.M.		Fair	Poor	10800 K.C.
2200	10 P.M.	5 P.M.		Fair-Poor	Poor-Fair	7200 K.C.
2300	11 P.M.	6 P.M.		Fair-Poor	Poor-Fair	7200 K.C.
0000	12 M.	7 P.M.		Fair-Poor	Fair	7200 K.C.
0100	1 A.M.	8 P.M.		Poor	Fair	7200 K.C.
0200	2 A.M.	9 P.M.		Poor-Unsat.	Fair	7200 K.C.
0300	3 A.M.	10 P.M.		Poor-Unsat.	Fair	7200 K.C.
0400	4 A.M.	11 P.M.		Poor-Unsat.	Fair	7200 K.C.
0500	5 A.M.	12 M.		Unsat.-Poor	Fair-Poor	7200 K.C.
0600	6 A.M.	1 A.M.		Poor	Fair-Poor	7200 K.C.
0700	7 A.M.	2 A.M.		Poor	Fair-Poor	10500 K.C.
0800	8 A.M.	3 A.M.		Poor-Fair	Fair-Poor	12500 K.C.
0900	9 A.M.	4 A.M.		Fair	Poor	14000 K.C.
1000	10 A.M.	5 A.M.		Fair-Poor	Poor-Unsat.	15500 K.C.

Fig. 132—Schenectady-France transmission chart. Winter season (November 1 to February 1). Distance from Schenectady to Paris 3500 miles (approx.)

TIME			DAYLIGHT-DARKNESS DISTRIBUTION OVER GREAT CIRCLE PATH	PROBABLE RECEPTION OBTAINABLE FROM		PROBABLE OPTIMUM FREQUENCY
GMT	France	Local		W2XAD	W2XAF	
				13660 K.C.	9550 K.C.	Short Path
1100	11 A.M.	6 A.M.		Unsat.	Nil	19200 K.C.
1200	12 N.	7 A.M.		Unsat.	Nil	19200 K.C.
1300	1 P.M.	8 A.M.		Unsat.	Nil	19200 K.C.
1400	2 P.M.	9 A.M.		Unsat.	Nil	19200 K.C.
1500	3 P.M.	10 A.M.		Unsat.	Nil	19200 K.C.
1600	4 P.M.	11 A.M.		Unsat.	Nil	19200 K.C.
1700	5 P.M.	12 M.		Unsat.-Poor	Nil	19200 K.C.
1800	6 P.M.	1 P.M.		Poor-Fair	Nil	18500 K.C.
1900	7 P.M.	2 P.M.		Fair	Nil	17500 K.C.
2000	8 P.M.	3 P.M.		Fair	Nil	16000 K.C.
2100	9 P.M.	4 P.M.		Fair	Unsat.	14600 K.C.
2200	10 P.M.	5 P.M.		Fair	Unsat.-Poor	12900 K.C.
2300	11 P.M.	6 P.M.		Fair-Poor	Poor-Fair	10400 K.C.
0000	12 M.	7 P.M.		Fair-Poor	Fair	7200 K.C.
0100	1 A.M.	8 P.M.		Fair-Poor	Fair-Good	7200 K.C.
0200	2 A.M.	9 P.M.		Poor	Fair-Good	7200 K.C.
0300	3 A.M.	10 P.M.		Poor	Good-Fair	7200 K.C.
0400	4 A.M.	11 P.M.		Poor	Good-Fair	7200 K.C.
0500	5 A.M.	12 M.		Poor-Fair	Fair	7200 K.C.
0600	6 A.M.	1 A.M.		Poor-Fair	Fair-Poor	11000 K.C.
0700	7 A.M.	2 A.M.		Poor-Fair	Poor	13000 K.C.
0800	8 A.M.	3 A.M.		Fair	Poor	15600 K.C.
0900	9 A.M.	4 A.M.		Fair-Poor	Poor-Unsat.	17300 K.C.
1000	10 A.M.	5 A.M.		Poor-Unsat.	Unsat.	18700 K.C.

Fig. 133—Schenectady-France transmission chart. Spring season (February 1 to May 1). Distance from Schenectady to Paris 3500 miles (approx.)

TIME			DAYLIGHT-DARKNESS DISTRIBUTION OVER GREAT CIRCLE PATH	PROBABLE RECEPTION OBTAINABLE FROM		PROBABLE OPTIMUM FREQUENCY
GMT	France	Local		W2XAD	W2XAF	
				13660 K.C.	9550 K.C.	Short Path
1100	11 A.M.	6 A.M.		Unsat.	Nil	19200 K.C.
1200	12 N.	7 A.M.		Unsat.	Nil	19200 K.C.
1300	1 P.M.	8 A.M.		Unsat.	Nil	19200 K.C.
1400	2 P.M.	9 A.M.		Unsat.	Nil	19200 K.C.
1500	3 P.M.	10 A.M.		Unsat.	Nil	19200 K.C.
1600	4 P.M.	11 A.M.		Unsat.	Nil	19200 K.C.
1700	5 P.M.	12 N.		Unsat.	Nil	19200 K.C.
1800	6 P.M.	1 P.M.		Unsat.	Nil	19200 K.C.
1900	7 P.M.	2 P.M.		Unsat.	Nil	19200 K.C.
2000	8 P.M.	3 P.M.		Unsat.	Nil	19200 K.C.
2100	9 P.M.	4 P.M.		Unsat.-Poor	Nil	19000 K.C.
2200	10 P.M.	5 P.M.		Unsat.-Poor	Nil	18300 K.C.
2300	11 P.M.	6 P.M.		Poor-Fair	Unsat.	17000 K.C.
0000	12 M.	7 P.M.		Poor-Fair	Unsat.-Poor	15000 K.C.
0100	1 A.M.	8 P.M.		Fair	Poor-Fair	13000 K.C.
0200	2 A.M.	9 P.M.		Fair	Fair	10200 K.C.
0300	3 A.M.	10 P.M.		Fair-Poor	Fair	7200 K.C.
0400	4 A.M.	11 P.M.		Fair-Poor	Fair	10400 K.C.
0500	5 A.M.	12 M.		Poor	Poor	12500 K.C.
0600	6 A.M.	1 A.M.		Poor	Poor-Unsat.	16000 K.C.
0700	7 A.M.	2 A.M.		Poor	Unsat.	17500 K.C.
0800	8 A.M.	3 A.M.		Poor-Unsat.	Unsat.	18600 K.C.
0900	9 A.M.	4 A.M.		Unsat.	Nil	19000 K.C.
1000	10 A.M.	5 A.M.		Unsat.	Nil	19200 K.C.

Fig. 134—Schenectady-France transmission chart. Summer season (May 1 to August 1). Distance from Schenectady to Paris 3500 miles (approx.)

TIME			DAYLIGHT-DARKNESS DISTRIBUTION OVER GREAT CIRCLE PATH	PROBABLE RECEPTION OBTAINABLE FROM		PROBABLE OPTIMUM FREQUENCY
GMT	France	Local		W2XAD	W2XAF	
				13660 K.C.	9550 K.C.	Short Path
1100	11 A.M.	6 A.M.		Unsat.	Nil	19200 K.C.
1200	12 N.	7 A.M.		Unsat.	Nil	19200 K.C.
1300	1 P.M.	8 A.M.		Unsat.	Nil	19200 K.C.
1400	2 P.M.	9 A.M.		Unsat.	Nil	19200 K.C.
1500	3 P.M.	10 A.M.		Unsat.	Nil	19200 K.C.
1600	4 P.M.	11 A.M.		Unsat.	Nil	19200 K.C.
1700	5 P.M.	12 N.		Unsat.	Nil	19200 K.C.
1800	6 P.M.	1 P.M.		Unsat.-Poor	Nil	19200 K.C.
1900	7 P.M.	2 P.M.		Poor-Fair	Nil	18500 K.C.
2000	8 P.M.	3 P.M.		Fair	Nil	17500 K.C.
2100	9 P.M.	4 P.M.		Fair	Nil	16000 K.C.
2200	10 P.M.	5 P.M.		Fair	Unsat.	14600 K.C.
2300	11 P.M.	6 P.M.		Fair	Unsat.-Poor	12900 K.C.
0000	12 M.	7 P.M.		Fair-Poor	Poor-Fair	10400 K.C.
0100	1 A.M.	8 P.M.		Fair-Poor	Fair	7200 K.C.
0200	2 A.M.	9 P.M.		Fair-Poor	Fair-Good	7200 K.C.
0300	3 A.M.	10 P.M.		Poor	Fair-Good	7200 K.C.
0400	4 A.M.	11 P.M.		Poor	Good-Fair	7200 K.C.
0500	5 A.M.	12 M.		Poor	Good-Fair	7200 K.C.
0600	6 A.M.	1 A.M.		Poor-Fair	Fair	7200 K.C.
0700	7 A.M.	2 A.M.		Poor-Fair	Fair-Poor	11000 K.C.
0800	8 A.M.	3 A.M.		Poor-Fair	Poor	13000 K.C.
0900	9 A.M.	4 A.M.		Fair	Poor	15600 K.C.
1000	10 A.M.	5 A.M.		Fair-Poor	Poor-Unsat.	17300 K.C.
				Poor-Unsat.	Unsat.	18700 K.C.

Fig. 135—Schenectady-France transmission chart. Fall season (August 1 to November 1). Distance from Schenectady to Paris 3500 miles (approx.)

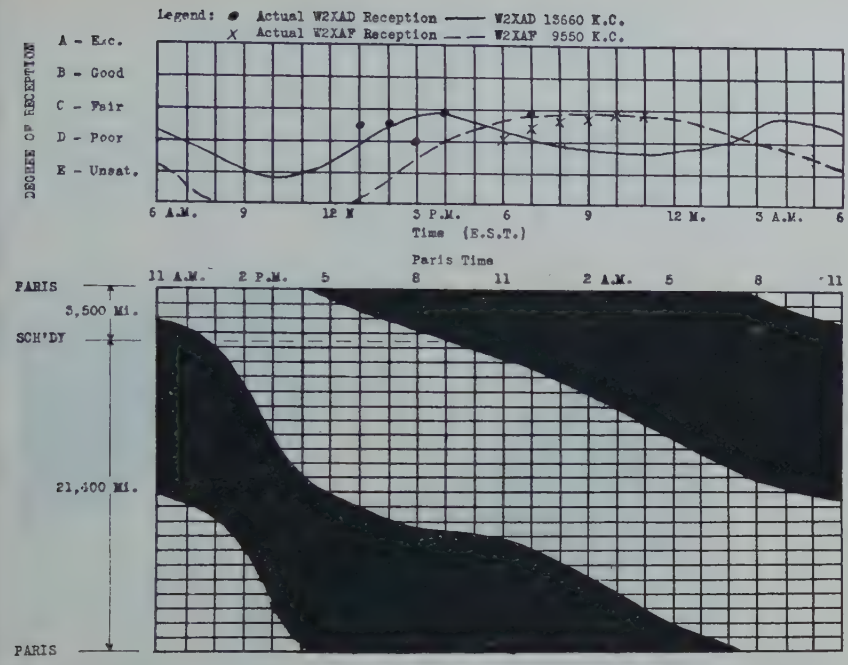

Fig. 136—Reception in Paris from November 1 to February 1. Daylight-darkness distribution over great circle distance from Schenectady to Paris, France, as of December 20.

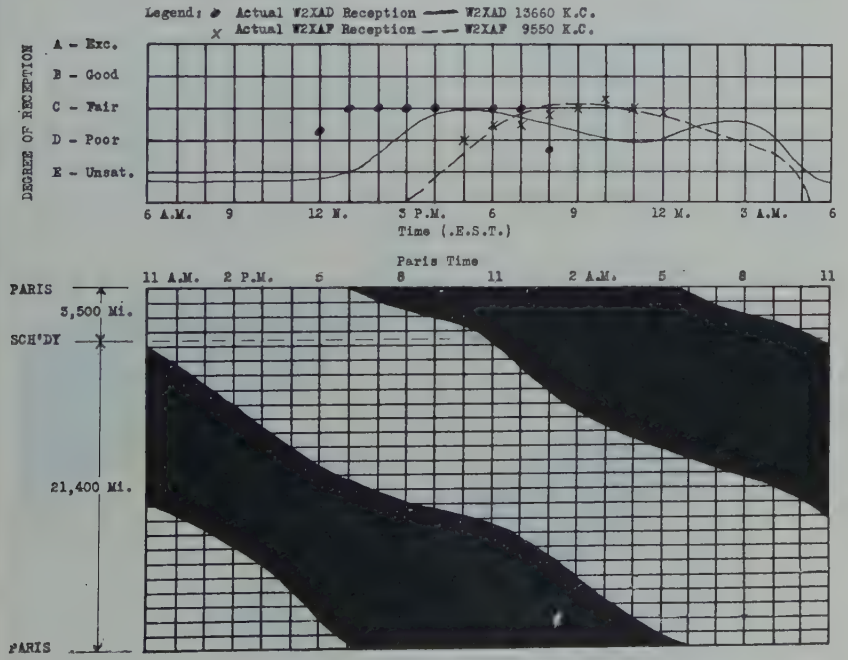

Fig. 137—Reception in Paris from February 1 to May 1. Daylight-darkness distribution over great circle distance from Schenectady to Paris, France, as of March 20.

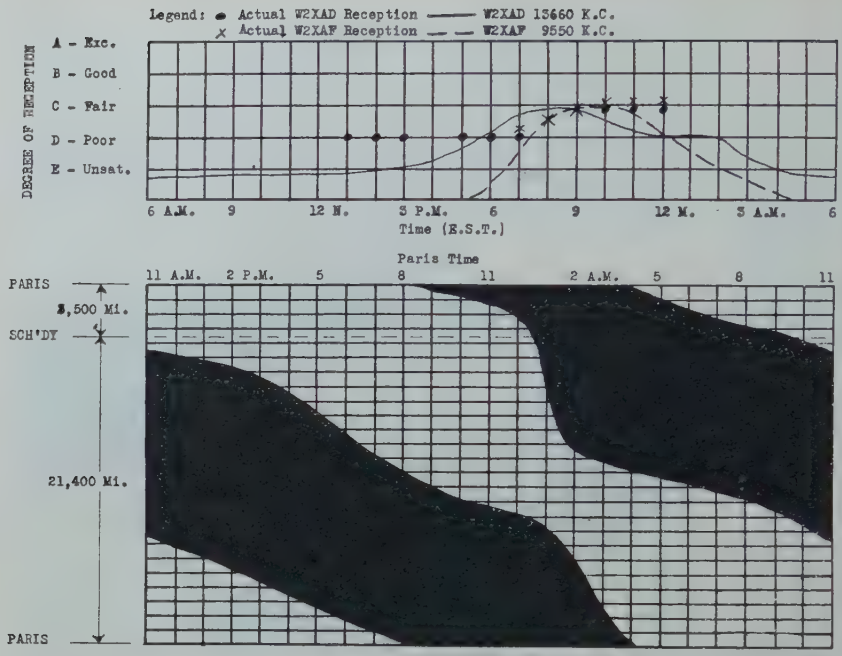

Fig. 138—Reception in Paris from May 1 to August 1. Daylight-darkness distribution over great circle distance from Schenectady to Paris, France, as of June 20.

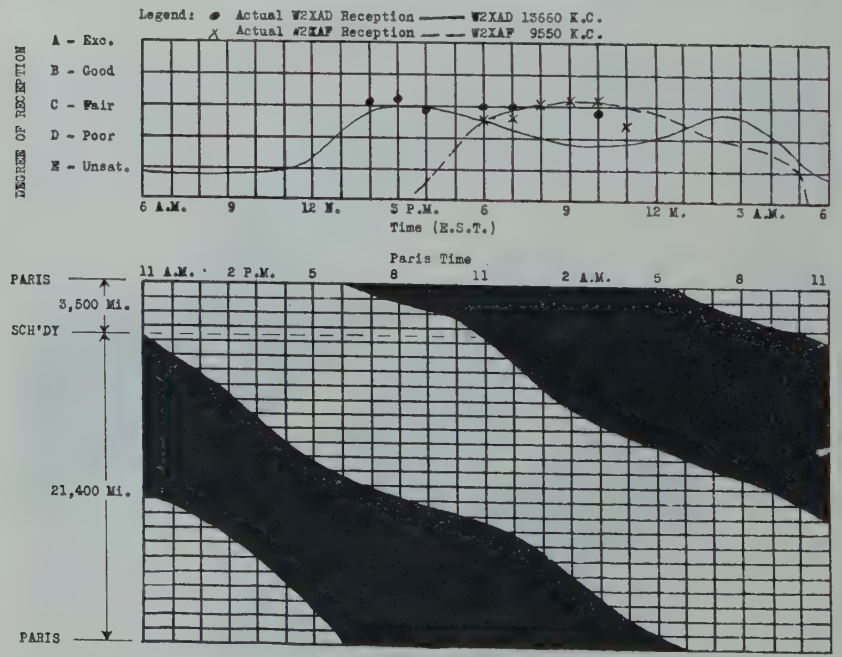

Fig. 139—Reception in Paris from August 1 to November 1. Daylight-darkness distribution over great circle distance from Schenectady to Paris, France, as of September 20.

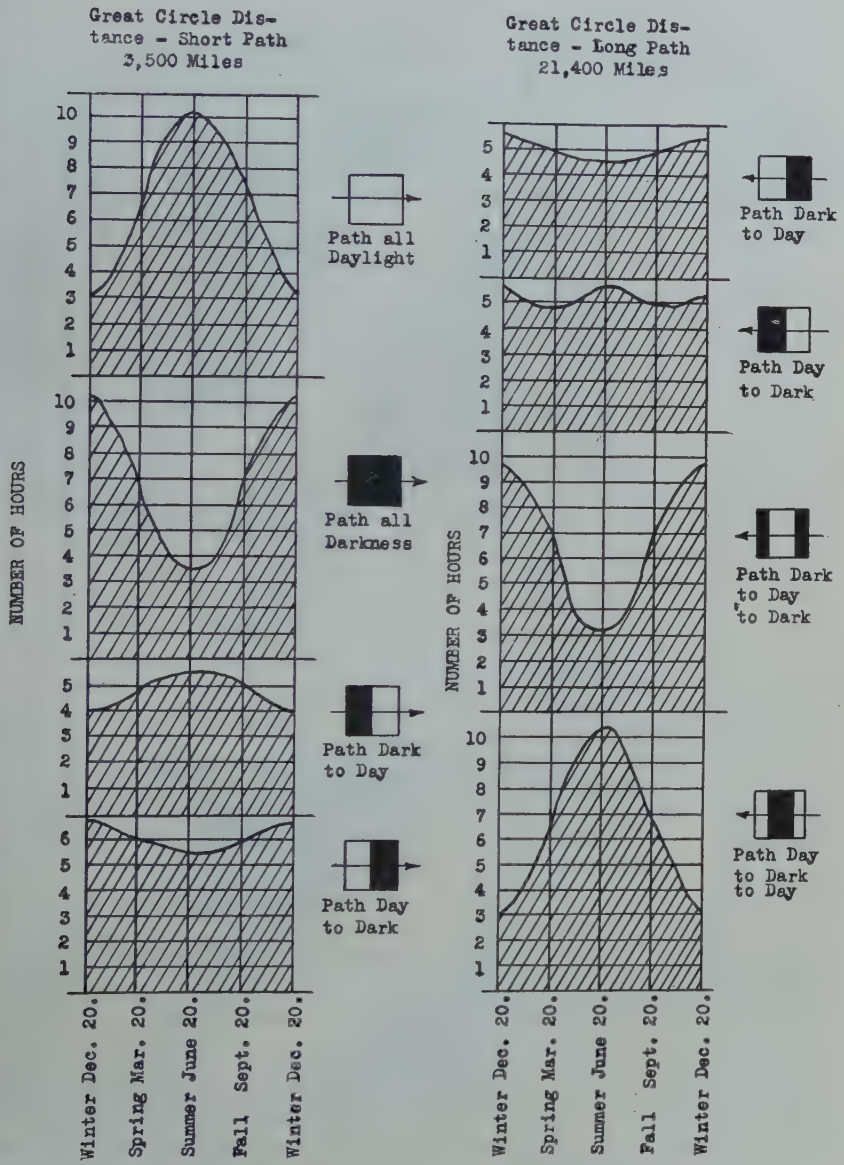

Fig. 140—Daylight-darkness distribution between Schenectady and Paris, France.

Figs. 140 and 141 present the daylight-darkness distribution and optimum frequency data in graphical form.

Schenectady–London (British Isles) Circuit

As might be expected, this circuit is somewhat similar to the Schenectady-Berlin and Schenectady-Paris circuits which have been discussed previously. The distance from Schenectady to London is 3400 miles (approx.) as compared with 3850 to Berlin and 3500 to Paris.

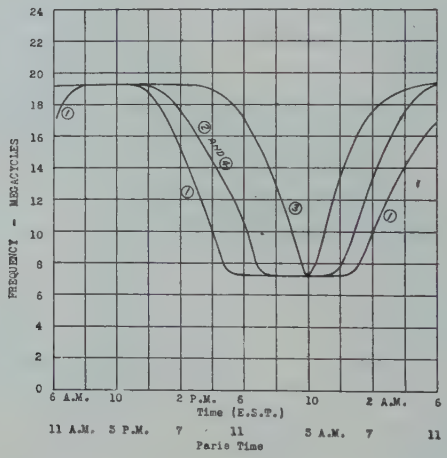

Fig. 141—Optimum frequency chart—Schenectady to Paris.
(1) Winter—November 1 to February 1.
(2) and (4) Spring and Fall—February 1 to May 1 and August 1 to November 1.
(3) Summer—May 1 to August 1.

More actual transmission and reception data are available for this circuit than for any of the others treated herein, with the possible exception of the Schenectady-Oakland (California) circuit.

Figs. 142, 143, 144, and 145 present a tabulation of W2XAD and W2XAF reception data and optimum frequency data. From Figs. 146, 147, 148, and 149, which incorporate a part of the above data, the degree of reception normally obtained from W2XAD and W2XAF transmissions will be more clearly understood. It will be observed that the afternoon transmissions of W2XAD, particularly during the period from 2:00 to 4:00 P.M., E.S.T., serve the British Isles quite

TIME			DAYLIGHT-DARKNESS DISTRIBUTION OVER GREAT CIRCLE PATH	PROBABLE RECEPTION OBTAINABLE FROM		PROBABLE OPTIMUM FREQUENCY
GMT	British Isles	Local		W2XAD	W2XAF	
				13660 K.C.	9550 K.C.	Short Path
1100	11 A.M.	6 A.M.		Poor	Nil	15500 K.C.
1200	12 N.	7 A.M.		Poor-Unsat.	Nil	17000 K.C.
1300	1 P.M.	8 A.M.		Unsat.	Nil	19300 K.C.
1400	2 P.M.	9 A.M.		Unsat.	Nil	19300 K.C.
1500	3 P.M.	10 A.M.		Unsat.-Poor	Nil	18500 K.C.
1600	4 P.M.	11 A.M.		Poor	Nil	17500 K.C.
1700	5 P.M.	12 N.		Poor-Fair	Nil	16400 K.C.
1800	6 P.M.	1 P.M.		Poor-Fair	Nil	15500 K.C.
1900	7 P.M.	2 P.M.		Fair-	Nil	14200 K.C.
2000	8 P.M.	3 P.M.		Fair-Good	Nil	13100 K.C.
2100	9 P.M.	4 P.M.		Fair	Unsat.	11800 K.C.
2200	10 P.M.	5 P.M.		Fair-Poor	Unsat.-Poor	10600 K.C.
2300	11 P.M.	6 P.M.		Fair-Poor	Poor	8000 K.C.
0000	12 M.	7 P.M.		Fair-Poor	Poor-Fair	7100 K.C.
0100	1 A.M.	8 P.M.		Fair-Poor	Fair	7100 K.C.
0200	2 A.M.	9 P.M.		Poor	Fair	7100 K.C.
0300	3 A.M.	10 P.M.		Poor	Fair	7100 K.C.
0400	4 A.M.	11 P.M.		Poor	Fair	7100 K.C.
0500	5 A.M.	12 M.		Poor-Unsat.	Fair-Poor	7100 K.C.
0600	6 A.M.	1 A.M.		Poor-Unsat.	Fair-Poor	7100 K.C.
0700	7 A.M.	2 A.M.		Poor-Unsat.	Poor	7100 K.C.
0800	8 A.M.	3 A.M.		Poor	Poor-Unsat.	11000 K.C.
0900	9 A.M.	4 A.M.		Poor-Fair	Unsat.	12500 K.C.
1000	10 A.M.	5 A.M.		Poor-Fair	Nil	14200 K.C.

Fig. 142—Schenectady-British Isles transmission chart. Winter season (November 1 to February 1). Distance from Schenectady to London 3400 miles (approx.)

TIME			DAYLIGHT-DARKNESS DISTRIBUTION OVER GREAT CIRCLE PATH	PROBABLE RECEPTION OBTAINABLE FROM		PROBABLE OPTIMUM FREQUENCY
GMT	British Isles	Local		W2XAD	W2XAF	
				13660 K.C.	9550 K.C.	Short Path
1100	11 A.M.	6 A.M.		Poor-Unsat.	Nil	16600 K.C.
1200	12 N.	7 A.M.		Unsat.	Nil	19300 K.C.
1300	1 P.M.	8 A.M.		Unsat.	Nil	19300 K.C.
1400	2 P.M.	9 A.M.		Unsat.	Nil	19300 K.C.
1500	3 P.M.	10 A.M.		Unsat.	Nil	19300 K.C.
1600	4 P.M.	11 A.M.		Unsat.	Nil	19300 K.C.
1700	5 P.M.	12 N.		Unsat.-Poor	Nil	18900 K.C.
1800	6 P.M.	1 P.M.		Poor	Nil	18000 K.C.
1900	7 P.M.	2 P.M.		Poor-Fair	Nil	17200 K.C.
2000	8 P.M.	3 P.M.		Fair-Good	Nil	16000 K.C.
2100	9 P.M.	4 P.M.		Fair-Good	Nil	14400 K.C.
2200	10 P.M.	5 P.M.		Fair-Good	Unsat.	13400 K.C.
2300	11 P.M.	6 P.M.		Fair	Unsat.-Poor	11500 K.C.
0000	12 M.	7 P.M.		Fair-Poor	Poor-Fair	7100 K.C.
0100	1 A.M.	8 P.M.		Fair-Poor	Fair	7100 K.C.
0200	2 A.M.	9 P.M.		Poor	Fair	7100 K.C.
0300	3 A.M.	10 P.M.		Poor	Fair	7100 K.C.
0400	4 A.M.	11 P.M.		Poor-Unsat.	Fair-Poor	7100 K.C.
0500	5 A.M.	12 M.		Poor-Unsat.	Fair-Poor	7100 K.C.
0600	6 A.M.	1 A.M.		Unsat.-Poor	Poor-Unsat.	10300 K.C.
0700	7 A.M.	2 A.M.		Poor	Unsat.	12200 K.C.
0800	8 A.M.	3 A.M.		Poor-Fair	Nil	14000 K.C.
0900	9 A.M.	4 A.M.		Fair-Poor	Nil	15000 K.C.
1000	10 A.M.	5 A.M.		Fair-Poor	Nil	16000 K.C.

Fig. 143—Schenectady-British Isles transmission chart. Spring season (February 1 to May 1). Distance from Schenectady to London 3400 miles (approx.)

TIME			DAYLIGHT-DARKNESS DISTRIBUTION OVER GREAT CIRCLE PATH	PROBABLE RECEPTION OBTAINABLE FROM		PROBABLE OPTIMUM FREQUENCY
GMT	British Isles	Local		W2XAD 13660 K.C.	W2XAF 9550 K.C.	Short Path
1100	11 A.M.	6 A.M.	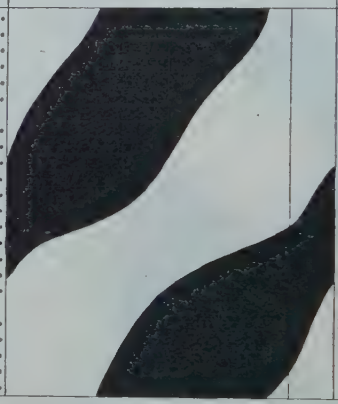	Unsat.	Nil	19300 K.C.
1200	12 N.	7 A.M.		Unsat.	Nil	19300 K.C.
1300	1 P.M.	8 A.M.		Unsat.	Nil	19300 K.C.
1400	2 P.M.	9 A.M.		Unsat.	Nil	19300 K.C.
1500	3 P.M.	10 A.M.		Unsat.	Nil	19300 K.C.
1600	4 P.M.	11 A.M.		Unsat.	Nil	19300 K.C.
1700	5 P.M.	12 N.		Unsat.	Nil	19300 K.C.
1800	6 P.M.	1 P.M.		Unsat.	Nil	19300 K.C.
1900	7 P.M.	2 P.M.		Unsat.-Poor	Nil	19300 K.C.
2000	8 P.M.	3 P.M.		Unsat.-Poor	Nil	18000 K.C.
2100	9 P.M.	4 P.M.		Poor-Fair	Nil	16400 K.C.
2200	10 P.M.	5 P.M.		Poor-Fair	Nil	15000 K.C.
2300	11 P.M.	6 P.M.		Fair-Poor	Unsat.	12500 K.C.
0000	12 M.	7 P.M.		Fair-Poor	Unsat.-Poor	11500 K.C.
0100	1 A.M.	8 P.M.		Poor	Poor-Fair	7100 K.C.
0200	2 A.M.	9 P.M.		Poor	Fair	7100 K.C.
0300	3 A.M.	10 P.M.		Poor-Unsat.	Fair	7100 K.C.
0400	4 A.M.	11 P.M.		Unsat.-Poor	Fair-Poor	7100 K.C.
0500	5 A.M.	12 M.		Poor-Fair	Poor	10500 K.C.
0600	6 A.M.	1 A.M.		Poor-Fair	Unsat.	12800 K.C.
0700	7 A.M.	2 A.M.		Poor-Fair	Nil	14000 K.C.
0800	8 A.M.	3 A.M.		Fair-Poor	Nil	16000 K.C.
0900	9 A.M.	4 A.M.		Poor	Nil	17600 K.C.
1000	10 A.M.	5 A.M.		Unsat.	Nil	19300 K.C.

Fig. 144—Schenectady-British Isles transmission chart. Summer season (May 1 to August 1). Distance from Schenectady to London 3400 miles (approx.)

TIME			DAYLIGHT-DARKNESS DISTRIBUTION OVER GREAT CIRCLE PATH	PROBABLE RECEPTION OBTAINABLE FROM		PROBABLE OPTIMUM FREQUENCY
GMT	British Isles	Local		W2XAD 13660 K.C.	W2XAF 9550 K.C.	Short Path
1100	11 A.M.	6 A.M.		Poor-Unsat.	Nil	16600 K.C.
1200	12 N.	7 A.M.		Unsat.	Nil	19300 K.C.
1300	1 P.M.	8 A.M.		Unsat.	Nil	19300 K.C.
1400	2 P.M.	9 A.M.		Unsat.	Nil	19300 K.C.
1500	3 P.M.	10 A.M.		Unsat.	Nil	19300 K.C.
1600	4 P.M.	11 A.M.		Unsat.	Nil	19300 K.C.
1700	5 P.M.	12 N.		Unsat.-Poor	Nil	18900 K.C.
1800	6 P.M.	1 P.M.		Poor	Nil	18000 K.C.
1900	7 P.M.	2 P.M.		Poor-Fair	Nil	17200 K.C.
2000	8 P.M.	3 P.M.		Fair-Good	Nil	16000 K.C.
2100	9 P.M.	4 P.M.		Fair-Good	Nil	14400 K.C.
2200	10 P.M.	5 P.M.		Good-Fair	Unsat.	13400 K.C.
2300	11 P.M.	6 P.M.		Fair	Unsat.-Poor	11500 K.C.
0000	12 M.	7 P.M.		Fair-Poor	Poor-Fair	7100 K.C.
0100	1 A.M.	8 P.M.		Fair-Poor	Fair	7100 K.C.
0200	2 A.M.	9 P.M.		Poor	Fair	7100 K.C.
0300	3 A.M.	10 P.M.		Poor	Fair	7100 K.C.
0400	4 A.M.	11 P.M.		Poor-Unsat.	Fair-Poor	7100 K.C.
0500	5 A.M.	12 M.		Poor-Unsat.	Fair-Poor	7100 K.C.
0600	6 A.M.	1 A.M.		Unsat.-Poor	Poor-Unsat.	10300 K.C.
0700	7 A.M.	2 A.M.		Poor	Unsat.	12200 K.C.
0800	8 A.M.	3 A.M.		Poor-Fair	Nil	14000 K.C.
0900	9 A.M.	4 A.M.		Fair-Poor	Nil	15000 K.C.
1000	10 A.M.	5 A.M.		Fair-Poor	Nil	16000 K.C.

Fig. 145—Schenectady-British Isles transmission chart. Fall season (August 1 to November 1). Distance from Schenectady to London 3400 miles (approx.)

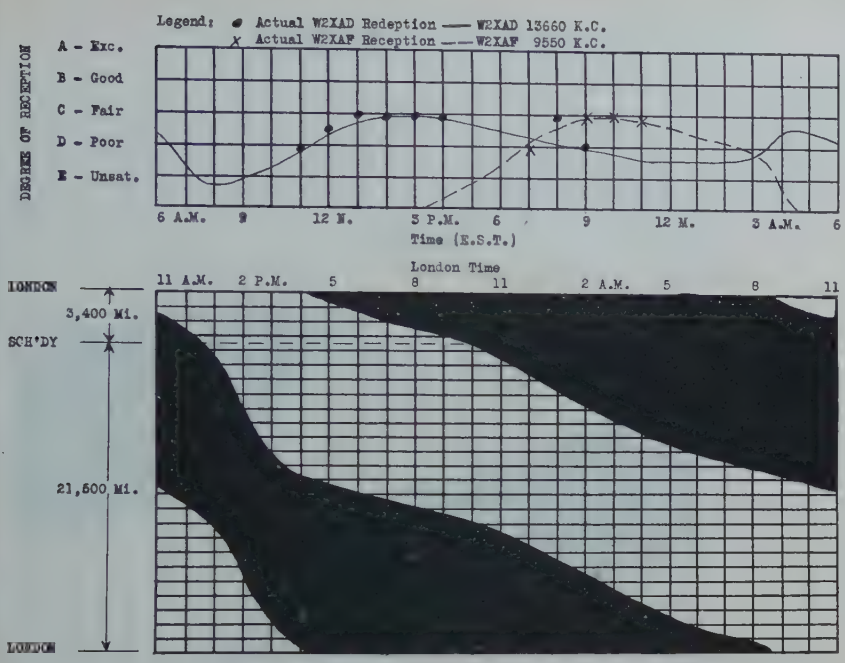

Fig. 146—Reception in British Isles from November 1 to February 1. Daylight-darkness distribution over great circle distance from Schenectady to London England, as of December 20.

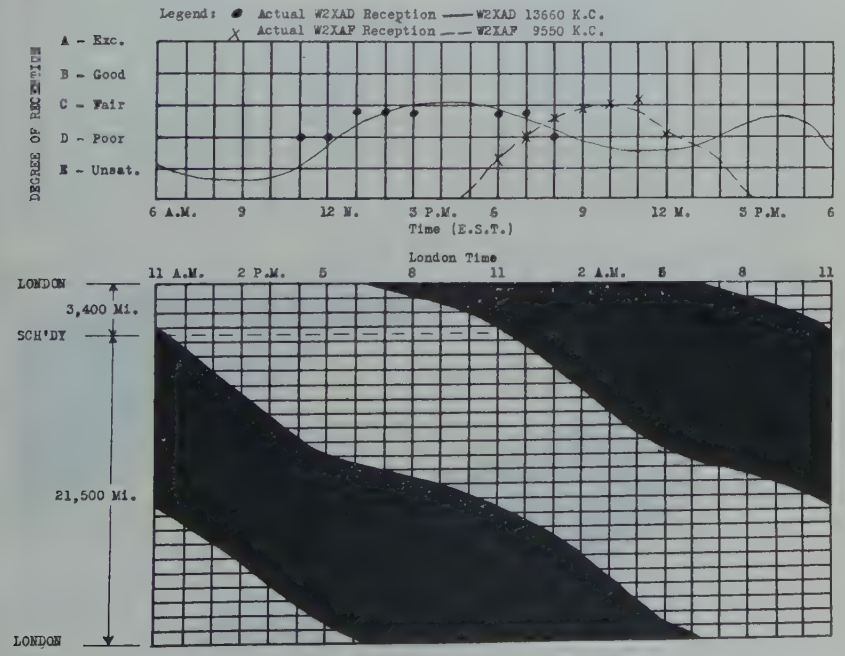

Fig. 147—Reception in British Isles from February 1 to May 1. Daylight-darkness distribution over great circle distance from Schenectady to London, England, as of March 20.

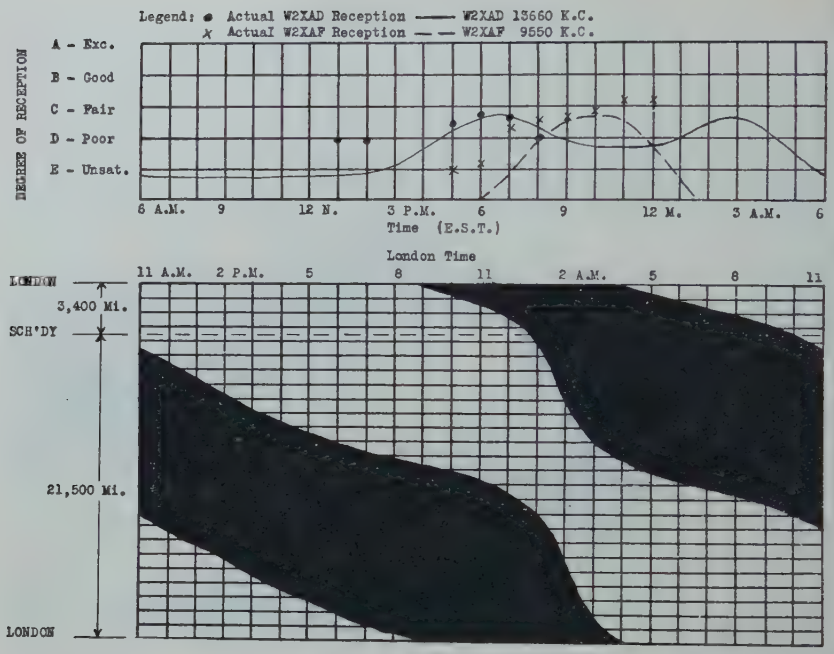

Fig. 148—Reception in British Isles from May 1 to August 1. Daylight-darkness distribution over great circle distance from Schenectady to London, England, as of June 20.

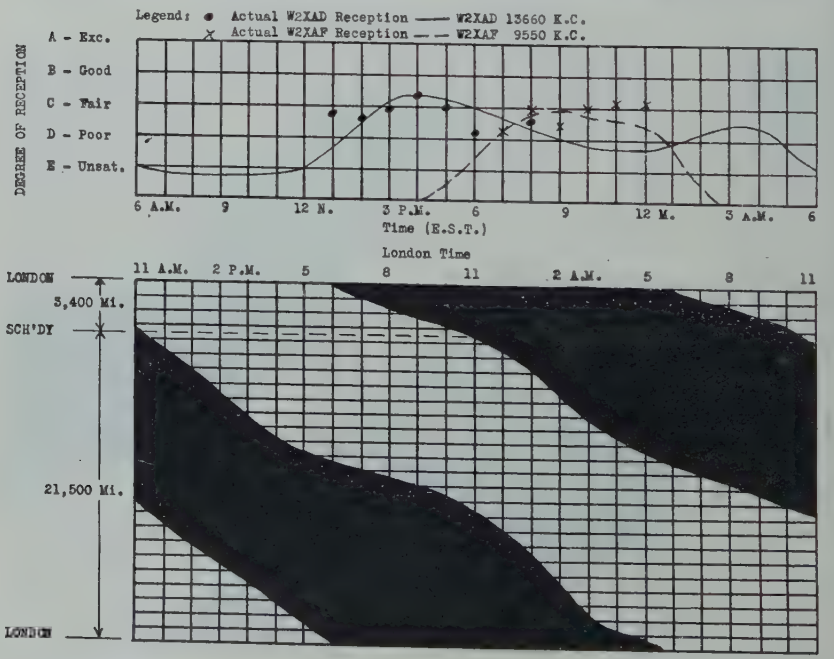

Fig. 149—Reception in British Isles from August 1 to November 1. Daylight-darkness distribution over great circle distance from Schenectady to London, England, as of September 20.

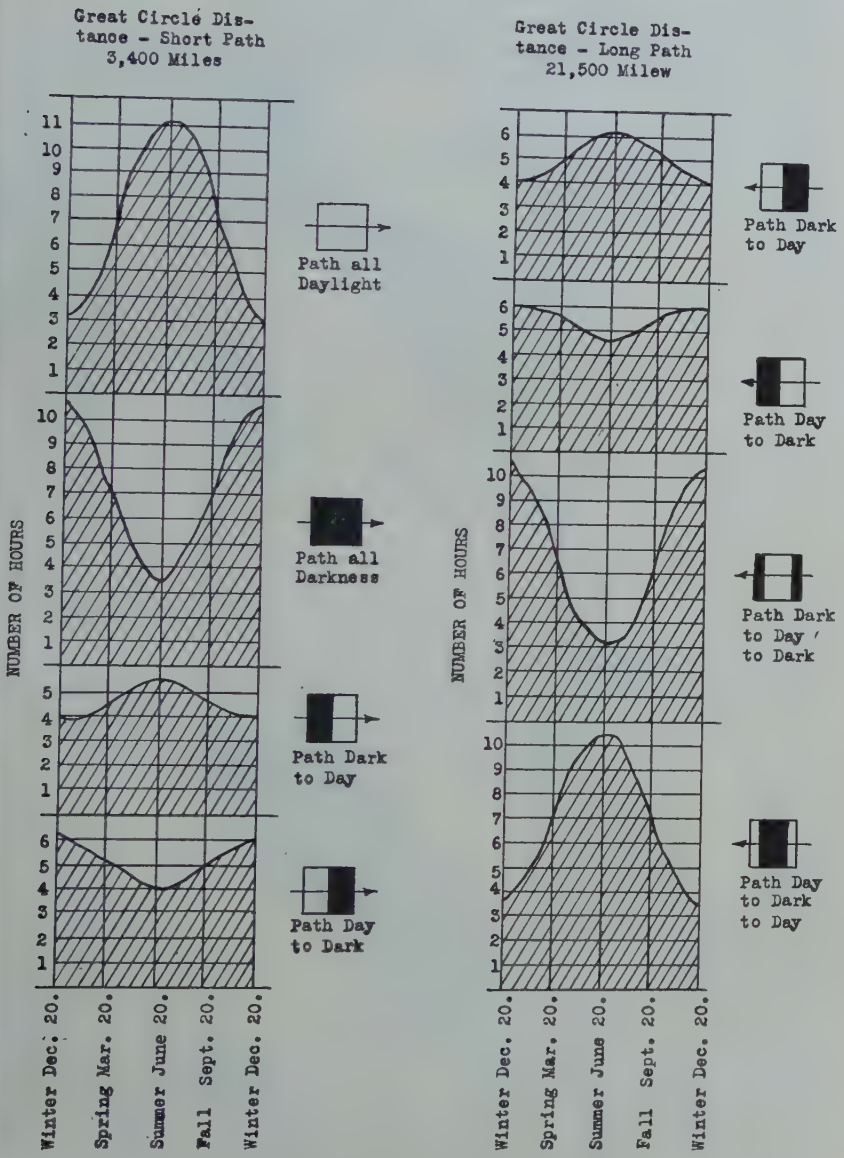

Fig. 150—Daylight-darkness distribution between Schenectady and London, England.

effectively. The transmissions occurring around this time have been relayed by the British Broadcasting Corporation. The W2XAF transmissions are well received from 8:00 to 11:00 P.M., E.S.T., but on account of the lateness of the hour (London time) reception is very inconvenient.

Fig. 150 gives the daylight-darkness data for this circuit, while Fig. 151 shows the optimum frequency data.

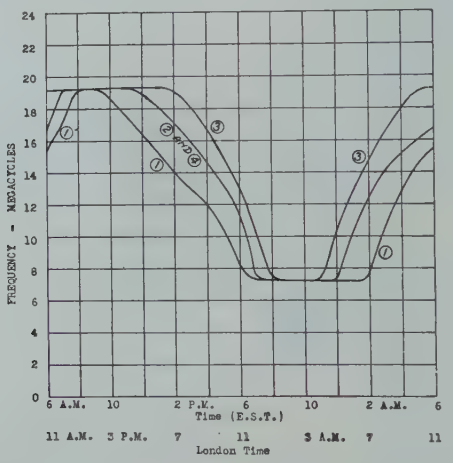

Fig. 151—Optimum frequency chart—Schenectady to London.
(1) Winter—November 1 to February 1.
(2) and (4) Spring and Fall—February 1 to May 1 and August 1 to November 1.
(3) Summer—May 1 to August 1.

Schenectady–Fairbanks (Alaska) Circuit

The length of this circuit, as measured in the plane of the great circle passing through Schenectady and Fairbanks is approximately 3100 miles.

Due to the proximity of Fairbanks to the Artic region where six months of daylight and darkness alternately prevail, the seasonal variation over this circuit is very pronounced. In this connection it is observed that during the winter season there is a period of almost 12 1/2 hours duration when the circuit is covered by darkness and a period of less than two hours of daylight; on the other hand, during the summer, complete darkness is to be had only for a period of about 1 hour

TIME			DAYLIGHT-DARKNESS DISTRIBUTION OVER GREAT CIRCLE PATH	PROBABLE RECEPTION OBTAINABLE FROM		PROBABLE OPTIMUM FREQUENCY
GMT	Alaska	Local		W2XAD	W2XAF	
				13660 K.C.	9550 K.C.	Short Path
1100	1 A.M.	6 A.M.		Poor	Fair-Poor	7200 K.C.
1200	2 A.M.	7 A.M.		Poor	Fair-Poor	7200 K.C.
1300	3 A.M.	8 A.M.		Poor-Fair	Poor	8500 K.C.
1400	4 A.M.	9 A.M.		Fair	Unsat.	12800 K.C.
1500	5 A.M.	10 A.M.		Fair	Unsat.	14200 K.C.
1600	6 A.M.	11 A.M.		Fair	Nil	15500 K.C.
1700	7 A.M.	12 N.		Fair-Poor	Nil	17000 K.C.
1800	8 A.M.	1 P.M.		Poor	Nil	18000 K.C.
1900	9 A.M.	2 P.M.		Poor-Unsat.	Nil	19000 K.C.
2000	10 A.M.	3 P.M.		Poor-Unsat.	Nil	19600 K.C.
2100	11 A.M.	4 P.M.		Unsat.-Poor	Nil	19600 K.C.
2200	12 N.	5 P.M.		Unsat.-Poor	Unsat.	18400 K.C.
2300	1 P.M.	6 P.M.		Poor-Fair	Unsat.	16000 K.C.
0000	2 P.M.	7 P.M.		Fair-Good	Unsat.-Poor	14000 K.C.
0100	3 P.M.	8 P.M.		Fair-Good	Poor-Fair	12000 K.C.
0200	4 P.M.	9 P.M.		Fair-Good	Fair-Good	10200 K.C.
0300	5 P.M.	10 P.M.		Fair-Good	Fair-Good	8500 K.C.
0400	6 P.M.	11 P.M.		Fair-Poor	Good	7200 K.C.
0500	7 P.M.	12 M.		Fair-Poor	Good	7200 K.C.
0600	8 P.M.	1 A.M.		Fair-Poor	Good-Fair	7200 K.C.
0700	9 P.M.	2 A.M.		Fair-Poor	Good-Fair	7200 K.C.
0800	10 P.M.	3 A.M.		Fair-Poor	Good-Fair	7200 K.C.
0900	11 P.M.	4 A.M.		Poor	Fair	7200 K.C.
1000	12 M.	5 A.M.		Poor	Fair-Poor	7200 K.C.

Fig. 152—Schenectady-Alaska transmission chart. Winter season (November 1 to February 1). Distance from Schenectady to Fairbanks 3100 miles (approx.)

TIME			DAYLIGHT-DARKNESS DISTRIBUTION OVER GREAT CIRCLE PATH	PROBABLE RECEPTION OBTAINABLE FROM		PROBABLE OPTIMUM FREQUENCY
GMT	Alaska	Local		W2XAD	W2XAF	
				13660 K.C.	9550 K.C.	Short Path
1100	1 A.M.	6 A.M.		Poor	Fair	7200 K.C.
1200	2 A.M.	7 A.M.		Poor-Fair	Fair-Poor	10500 K.C.
1300	3 A.M.	8 A.M.		Poor-Fair	Unsat.	12800 K.C.
1400	4 A.M.	9 A.M.		Fair	Nil	14400 K.C.
1500	5 A.M.	10 A.M.		Fair-Poor	Nil	16000 K.C.
1600	6 A.M.	11 A.M.		Poor-Unsat.	Nil	17500 K.C.
1700	7 A.M.	12 N.		Unsat.	Nil	19000 K.C.
1800	8 A.M.	1 P.M.		Unsat.	Nil	19600 K.C.
1900	9 A.M.	2 P.M.		Unsat.	Nil	19600 K.C.
2000	10 A.M.	3 P.M.		Unsat.	Nil	19600 K.C.
2100	11 A.M.	4 P.M.		Unsat.	Nil	19600 K.C.
2200	12 N.	5 P.M.		Unsat.	Nil	19600 K.C.
2300	1 P.M.	6 P.M.		Unsat.-Poor	Nil	19000 K.C.
0000	2 P.M.	7 P.M.		Poor-Fair	Nil	17000 K.C.
0100	3 P.M.	8 P.M.		Fair-Good	Unsat.	15000 K.C.
0200	4 P.M.	9 P.M.		Good	Poor	13600 K.C.
0300	5 P.M.	10 P.M.		Good	Fair	12000 K.C.
0400	6 P.M.	11 P.M.		Good-Fair	Fair-Good	11000 K.C.
0500	7 P.M.	12 M.		Fair	Good	9500 K.C.
0600	8 P.M.	1 A.M.		Fair-Poor	Good	7200 K.C.
0700	9 P.M.	2 A.M.		Fair-Poor	Good-Fair	7200 K.C.
0800	10 P.M.	3 A.M.		Fair-Poor	Good-Fair	7200 K.C.
0900	11 P.M.	4 A.M.		Poor	Good-Fair	7200 K.C.
1000	12 M.	5 A.M.		Poor	Fair	7200 K.C.

Fig. 153—Schenectady-Alaska transmission chart. Spring season (February 1 to May 1). Distance from Schenectady to Fairbanks 3100 miles (approx.)

TIME			DAYLIGHT-DARKNESS DISTRIBUTION OVER GREAT CIRCLE PATH	PROBABLE RECEPTION OBTAINABLE FROM		PROBABLE OPTIMUM FREQUENCY
GMT	Alaska	Local		W2XAD	W2XAF	
				13660 K.C.	9550 K.C.	Short Path
1100	1 A.M.	6 A.M.		Poor-Unsat.	Nil	17800 K.C.
1200	2 A.M.	7 A.M.		Poor-Unsat.	Nil	19000 K.C.
1300	3 A.M.	8 A.M.		Unsat.	Nil	19600 K.C.
1400	4 A.M.	9 A.M.		Unsat.	Nil	19600 K.C.
1500	5 A.M.	10 A.M.		Unsat.	Nil	19600 K.C.
1600	6 A.M.	11 A.M.		Unsat.	Nil	19600 K.C.
1700	7 A.M.	12 N.		Unsat.	Nil	19600 K.C.
1800	8 A.M.	1 P.M.		Unsat.	Nil	19600 K.C.
1900	9 A.M.	2 P.M.		Unsat.	Nil	19600 K.C.
2000	10 A.M.	3 P.M.		Unsat.	Nil	19600 K.C.
2100	11 A.M.	4 P.M.		Unsat.	Nil	19600 K.C.
2200	12 N.	5 P.M.		Unsat.	Nil	19600 K.C.
2300	1 P.M.	6 P.M.		Unsat.	Nil	19600 K.C.
0000	2 P.M.	7 P.M.		Unsat.-Poor	Nil	19000 K.C.
0100	3 P.M.	8 P.M.		Unsat.-Poor	Nil	18200 K.C.
0200	4 P.M.	9 P.M.		Poor	Nil	17000 K.C.
0300	5 P.M.	10 P.M.		Fair	Nil	15500 K.C.
0400	6 P.M.	11 P.M.		Fair-Good	Unsat.	14500 K.C.
0500	7 P.M.	12 M.		Fair-Good	Unsat.	13500 K.C.
0600	8 P.M.	1 A.M.		Fair-Good	Unsat.	12500 K.C.
0700	9 P.M.	2 A.M.		Fair	Unsat.-Poor	11500 K.C.
0800	10 P.M.	3 A.M.		Fair-Poor	Fair	10500 K.C.
0900	11 P.M.	4 A.M.		Fair-Poor	Fair-Good	7200 K.C.
1000	12 M.	5 A.M.		Fair-Poor	Poor	15000 K.C.

Fig. 154—Schenectady-Alaska transmission chart. Summer season (May 1 to August 1). Distance from Schenectady to Fairbanks 3100 miles (approx.)

TIME			DAYLIGHT-DARKNESS DISTRIBUTION OVER GREAT CIRCLE PATH	PROBABLE RECEPTION OBTAINABLE FROM		PROBABLE OPTIMUM FREQUENCY
GMT	Alaska	Local		W2XAD	W2XAF	
				13660 K.C.	9550 K.C.	Short Path
1100	1 A.M.	6 A.M.		Poor	Fair	7200 K.C.
1200	2 A.M.	7 A.M.		Poor-Fair	Fair-Poor	10500 K.C.
1300	3 A.M.	8 A.M.		Poor-Fair	Unsat.	12800 K.C.
1400	4 A.M.	9 A.M.		Fair	Nil	14400 K.C.
1500	5 A.M.	10 A.M.		Fair-Poor	Nil	16000 K.C.
1600	6 A.M.	11 A.M.		Poor-Unsat.	Nil	17500 K.C.
1700	7 A.M.	12 N.		Unsat.	Nil	19000 K.C.
1800	8 A.M.	1 P.M.		Unsat.	Nil	19600 K.C.
1900	9 A.M.	2 P.M.		Unsat.	Nil	19600 K.C.
2000	10 A.M.	3 P.M.		Unsat.	Nil	19600 K.C.
2100	11 A.M.	4 P.M.		Unsat.	Nil	19600 K.C.
2200	12 N.	5 P.M.		Unsat.	Nil	19600 K.C.
2300	1 P.M.	6 P.M.		Unsat.-Poor	Nil	19000 K.C.
0000	2 P.M.	7 P.M.		Poor-Fair	Nil	17000 K.C.
0100	3 P.M.	8 P.M.		Fair-Good	Unsat.	15000 K.C.
0200	4 P.M.	9 P.M.		Good	Poor	13600 K.C.
0300	5 P.M.	10 P.M.		Good	Fair	12000 K.C.
0400	6 P.M.	11 P.M.		Good-Fair	Fair-Good	11000 K.C.
0500	7 P.M.	12 M.		Fair	Good	9500 K.C.
0600	8 P.M.	1 A.M.		Fair-Poor	Good	7200 K.C.
0700	9 P.M.	2 A.M.		Fair-Poor	Good-Fair	7200 K.C.
0800	10 P.M.	3 A.M.		Fair-Poor	Good-Fair	7200 K.C.
0900	11 P.M.	4 A.M.		Poor	Good-Fair	7200 K.C.
1000	12 M.	5 A.M.		Poor	Fair	7200 K.C.

Fig. 155—Schenectady-Alaska transmission chart. Fall season (August 1 to November 1). Distance from Schenectady to Fairbanks 3100 miles (approx.)

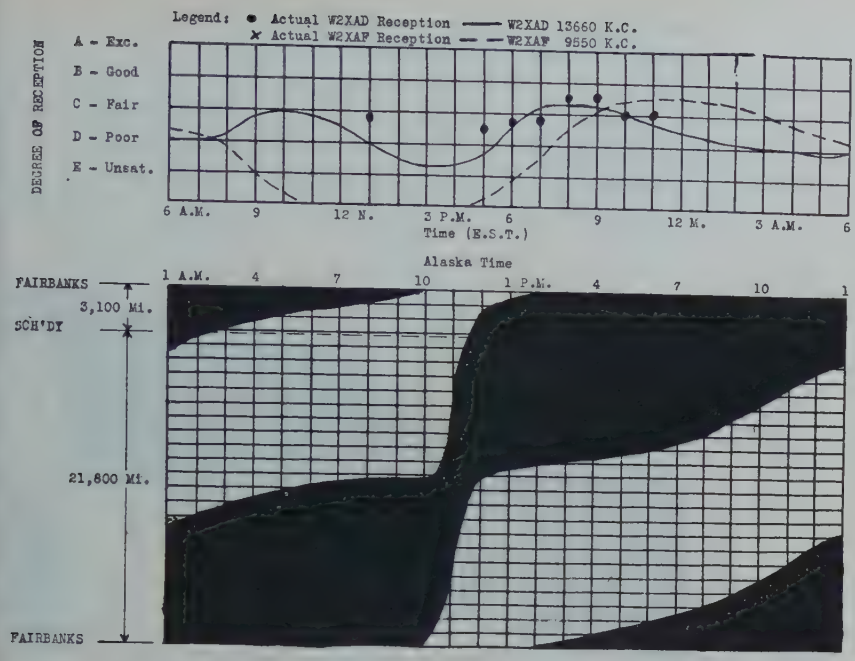

Fig. 156—Reception in Alaska from November 1 to February 1. Daylight-darkness distribution over great circle distance from Schenectady to Fairbanks, Alaska, as of December 20.

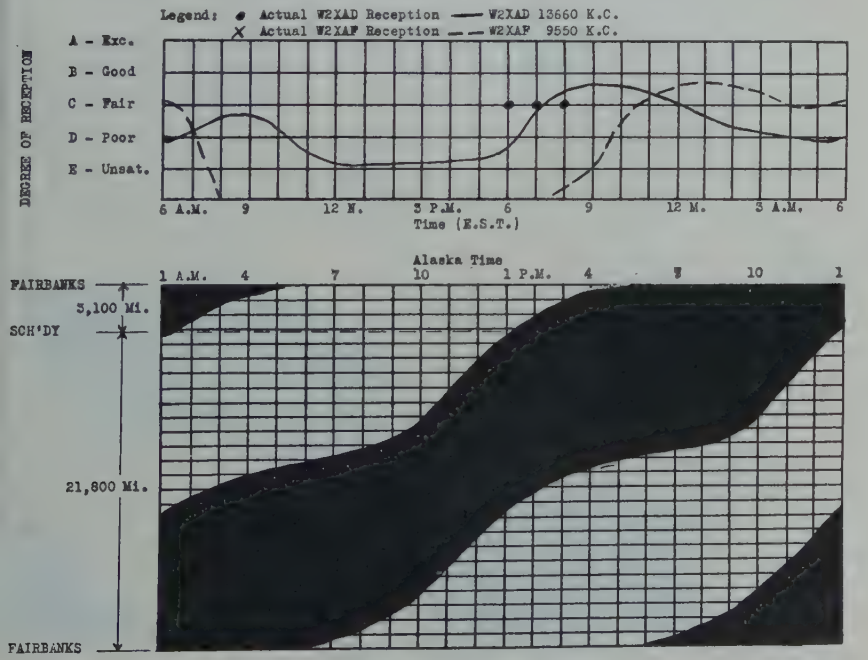

Fig. 157—Reception in Alaska from February 1 to May 1. Daylight-darkness distribution over great circle distance from Schenectady to Fairbanks, Alaska, as of March 20.

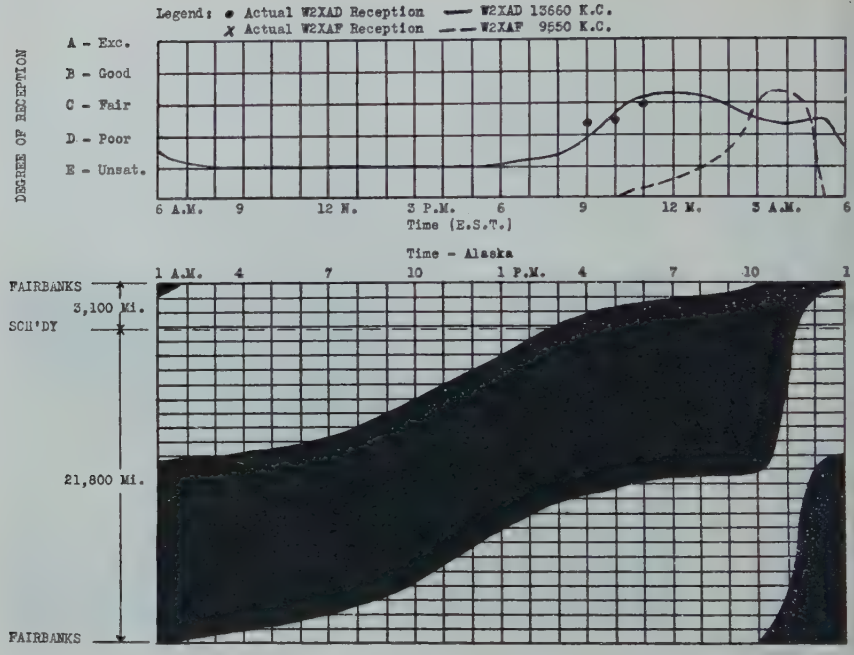

Fig. 158—Reception in Alaska from May 1 to August 1. Daylight-darkness distribution over great circle distance from Schenectady to Fairbanks, Alaska, as of June 20.

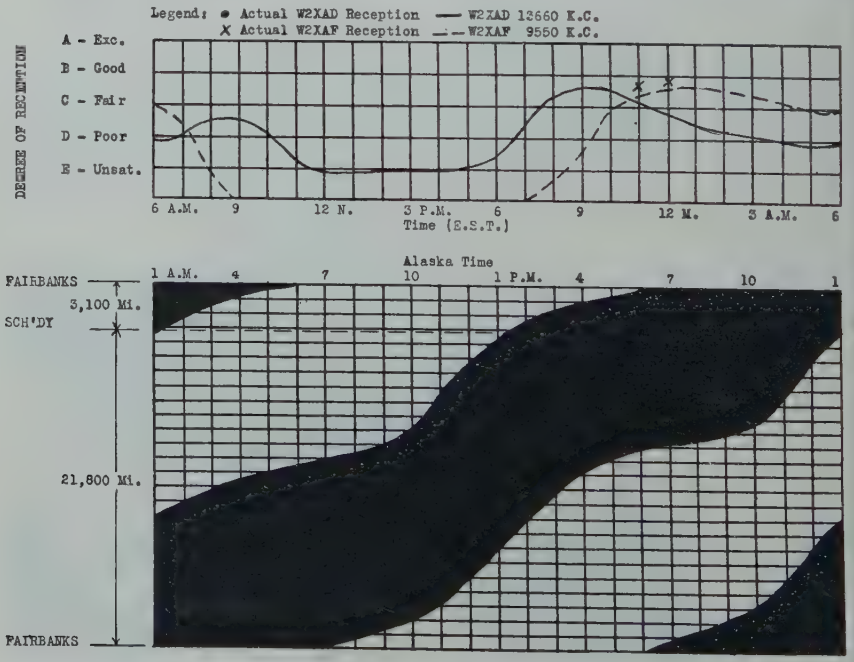

Fig. 159—Reception in Alaska from August 1 to November 1. Daylight-darkness distribution over great circle distance from Schenectady to Fairbanks, Alaska, as of September 20.

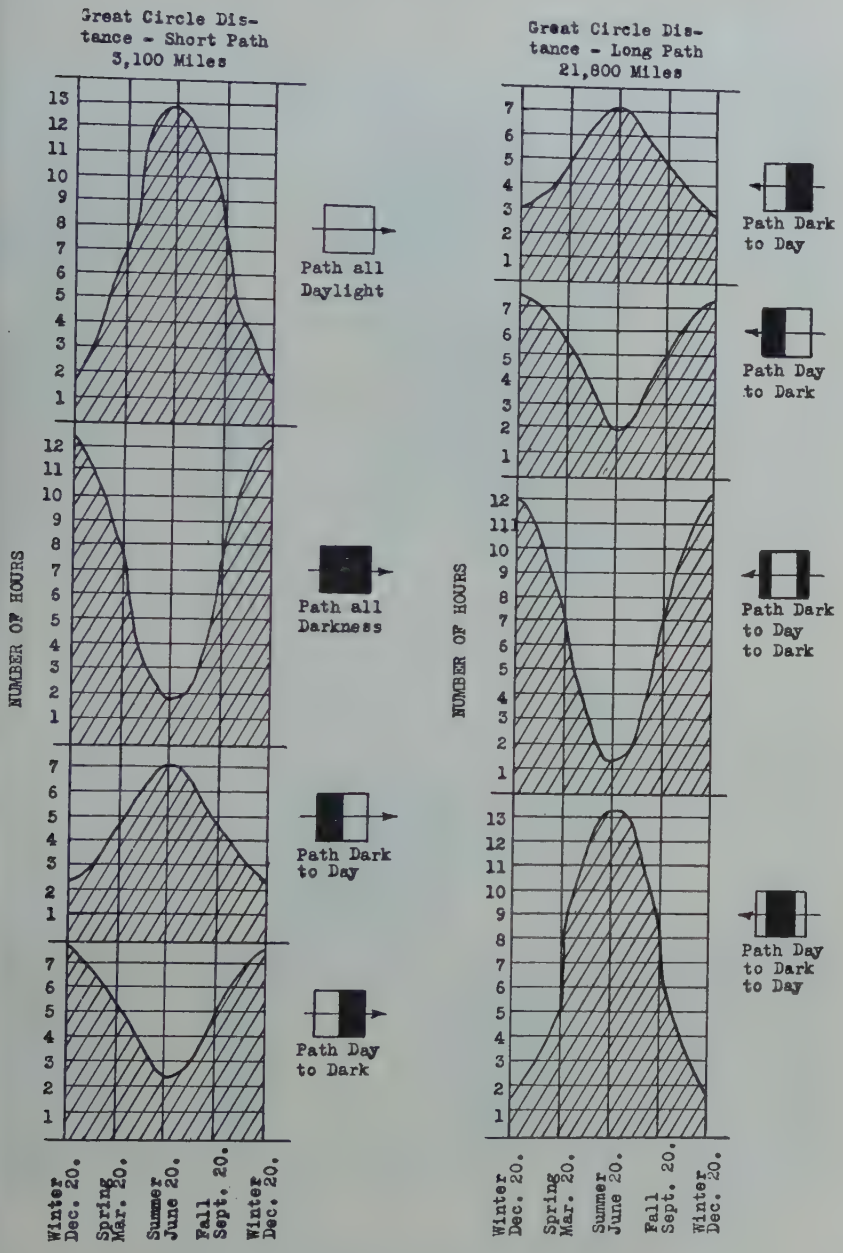

Fig. 160—Daylight-darkness distribution between Schenectady and Fairbanks, Alaska.

and 45 minutes while complete daylight prevails for a period of about 13 hours. (See Fig. 160.)

Furthermore, on account of the fact that the earth's north magnetic pole is not far removed from the path of this circuit, it is believed that the concentration of the earth's magnetic field will cause greater signal attenuation and more irregularities than are normally present where the circuit involved is longer and passes nearer to the equator.

Figs. 152 to 159, inclusive, show the optimum frequency and W2XAD-W2XAF reception data for the Schenectady-Fairbanks

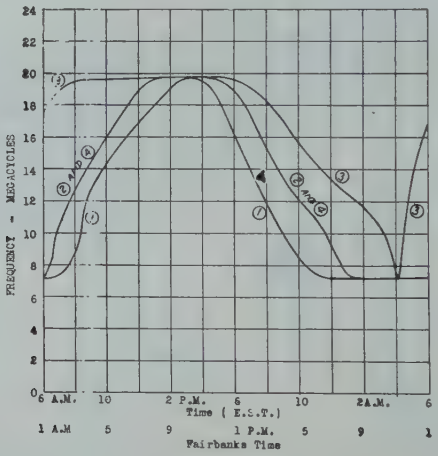

Fig. 161—Optimum frequency chart—Schenectady to Fairbanks.
(1) Winter—November 1 to February 1.
(2) and (4) Spring and Fall—February 1 to to May 1 and August 1 to November 1.
(3) Summer—May 1 to August 1.

circuit. By utilizing the W2XAD-W2XAF combination it will be noted that usable reception may be had in Fairbanks and vicinity throughout the duration of WGY's evening program (Usually considered as being from 6:00 P.M. to midnight, E.S.T.), except during the period from May to August. However, since Alaskan time is five hours slower than E.S.T., the WGY evening program (as relayed by W2XAD and W2XAF) occurs during the afternoon and early evening in Alaska, thereby making the time for listening somewhat inconvenient.

Schenectady–Bogotá (Colombia) Circuit

The length of this circuit is about 2700 miles and the direction of Bogotá from Schenectady is due south.

TIME			DAYLIGHT-DARKNESS DISTRIBUTION OVER GREAT CIRCLE PATH	PROBABLE RECEPTION OBTAINABLE FROM		PROBABLE OPTIMUM
GMT	Bogota	Local		W2XAD	W2XAF	FREQUENCY
1100	6 A.M.	6 A.M.		13660 K.C.	9550 K.C.	Short Path
1200	7 A.M.	7 A.M.		Poor	Fair-Poor	7200 K.C.
1300	8 A.M.	8 A.M.		Poor	Nil	17000 K.C.
1400	9 A.M.	9 A.M.		Poor-Unsat.	Nil	19000 K.C.
1500	10 A.M.	10 A.M.		Poor-Unsat.	Nil	20000 K.C.
1600	11 A.M.	11 A.M.		Poor-Unsat.	Nil	20000 K.C.
1700	12 A.M.	12 A.M.		Unsat.-Poor	Nil	20000 K.C.
1800	1 P.M.	1 P.M.		Unsat.-Poor	Nil	20000 K.C.
1900	2 P.M.	2 P.M.		Unsat.-Poor	Nil	20000 K.C.
2000	3 P.M.	3 P.M.		Unsat.-Poor	Nil	20000 K.C.
2100	4 P.M.	4 P.M.		Unsat.-Poor	Nil	19000 K.C.
2200	5 P.M.	5 P.M.		Unsat.-Poor	Nil	18200 K.C.
2300	6 P.M.	6 P.M.		Poor	Nil	17200 K.C.
0000	7 P.M.	7 P.M.		Poor-Fair	Unsat.	16000 K.C.
0100	8 P.M.	8 P.M.		Poor-Fair	Unsat.-Poor	15000 K.C.
0200	9 P.M.	9 P.M.		Fair	Poor-Fair	14000 K.C.
0300	10 P.M.	10 P.M.		Fair	Poor-Fair	12800 K.C.
0400	11 P.M.	11 P.M.		Fair-Poor	Poor-Fair	11000 K.C.
0500	12 M.	12 M.		Fair-Poor	Fair	7200 K.C.
0600	1 A.M.	1 A.M.		Poor	Fair	7200 K.C.
0700	2 A.M.	2 A.M.		Poor-Unsat.	Fair-Poor	7200 K.C.
0800	3 A.M.	3 A.M.		Poor-Unsat.	Fair-Poor	7200 K.C.
0900	4 A.M.	4 A.M.		Poor-Unsat.	Fair-Poor	7200 K.C.
1000	5 A.M.	5 A.M.		Unsat.-Poor	Fair-Poor	7200 K.C.
				Unsat.-Poor	Poor-Fair	7200 K.C.

Fig. 162—Schenectady-Bogotá transmission chart. Winter season (November 1 to February 1). Distance from Schenectady to Bogotá 2700 miles (approx.)

TIME			DAYLIGHT-DARKNESS DISTRIBUTION OVER GREAT CIRCLE PATH	PROBABLE RECEPTION OBTAINABLE FROM		PROBABLE OPTIMUM
GMT	Bogota	Local		W2XAD	W2XAF	FREQUENCY
1100	6 A.M.	6 A.M.		13660 K.C.	9550 K.C.	Short Path
1200	7 A.M.	7 A.M.		Unsat.-Poor	Nil	16000 K.C.
1300	8 A.M.	8 A.M.		Poor	Nil	20000 K.C.
1400	9 A.M.	9 A.M.		Poor	Nil	20000 K.C.
1500	10 A.M.	10 A.M.		Poor	Nil	20000 K.C.
1600	11 A.M.	11 A.M.		Poor	Nil	20000 K.C.
1700	12 N.	12 N.		Poor	Nil	20000 K.C.
1800	1 P.M.	1 P.M.		Poor	Nil	20000 K.C.
1900	2 P.M.	2 P.M.		Poor	Nil	20000 K.C.
2000	3 P.M.	3 P.M.		Poor	Nil	19400 K.C.
2100	4 P.M.	4 P.M.		Poor	Nil	18200 K.C.
2200	5 P.M.	5 P.M.		Poor	Nil	17000 K.C.
2300	6 P.M.	6 P.M.		Poor-Fair	Unsat.	15500 K.C.
0000	7 P.M.	7 P.M.		Fair-	Poor	13800 K.C.
0100	8 P.M.	8 P.M.		Fair-Good	Poor-Fair	12500 K.C.
0200	9 P.M.	9 P.M.		Good-Fair	Fair	11000 K.C.
0300	10 P.M.	10 P.M.		Fair	Fair-Good	9200 K.C.
0400	11 P.M.	11 P.M.		Fair-Poor	Fair	7200 K.C.
0500	12 M.	12 M.		Poor	Fair-Poor	7200 K.C.
0600	1 A.M.	1 A.M.		Poor-Unsat.	Fair-Poor	7200 K.C.
0700	2 A.M.	2 A.M.		Poor-Unsat.	Fair-Poor	7200 K.C.
0800	3 A.M.	3 A.M.		Unsat.	Fair-Poor	7200 K.C.
0900	4 A.M.	4 A.M.		Unsat.-Poor	Fair-Poor	7200 K.C.
1000	5 A.M.	5 A.M.		Unsat.-Poor	Poor	10500 K.C.

Fig. 163—Schenectady-Bogotá transmission chart. Spring season (February 1 to May 1). Distance from Schenectady to Bogotá 2700 miles (approx.)

TIME			DAYLIGHT-DARKNESS DISTRIBUTION OVER GREAT CIRCLE PATH	PROBABLE RECEPTION OBTAINABLE FROM		PROBABLE OPTIMUM FREQUENCY
GMT	Bogota	Local		W2XAD	W2XAF	
				13660 K.C.	9650 K.C.	Short Path
1100	6 A.M.	6 A.M.		Fair-Poor	Nil	18000 K.C.
1200	7 A.M.	7 A.M.		Poor	Nil	19600 K.C.
1300	8 A.M.	8 A.M.		Poor-Unsat.	Nil	20000 K.C.
1400	9 A.M.	9 A.M.		Poor-Unsat.	Nil	20000 K.C.
1500	10 A.M.	10 A.M.		Poor-Unsat.	Nil	20000 K.C.
1600	11 A.M.	11 A.M.		Unsat.-Poor	Nil	20000 K.C.
1700	12 N.	12 N.		Unsat.-Poor	Nil	20000 K.C.
1800	1 P.M.	1 P.M.		Unsat.-Poor	Nil	20000 K.C.
1900	2 P.M.	2 P.M.		Unsat.-Poor	Nil	20000 K.C.
2000	3 P.M.	3 P.M.		Unsat.-Poor	Nil	19600 K.C.
2100	4 P.M.	4 P.M.		Unsat.-Poor	Nil	19000 K.C.
2200	5 P.M.	5 P.M.		Poor	Nil	18000 K.C.
2300	6 P.M.	6 P.M.		Poor-Fair	Unsat.	16300 K.C.
0000	7 P.M.	7 P.M.		Poor-Fair	Unsat.-Poor	15000 K.C.
0100	8 P.M.	8 P.M.		Fair	Poor-Fair	13000 K.C.
0200	9 P.M.	9 P.M.		Fair-Poor	Poor-Fair	10800 K.C.
0300	10 P.M.	10 P.M.		Fair-Poor	Fair	7200 K.C.
0400	11 P.M.	11 P.M.		Poor	Fair	7200 K.C.
0500	12 M.	12 M.		Poor-Unsat.	Fair-Poor	7200 K.C.
0600	1 A.M.	1 A.M.		Poor-Unsat.	Fair-Poor	7200 K.C.
0700	2 A.M.	2 A.M.		Unsat.-Poor	Fair-Poor	7200 K.C.
0800	3 A.M.	3 A.M.		Unsat.-Poor	Poor-Fair	7200 K.C.
0900	4 A.M.	4 A.M.		Poor	Poor-Fair	7200 K.C.
1000	5 A.M.	5 A.M.		Poor-Fair	Poor	12800 K.C.

Fig. 164—Schenectady-Bogotá transmission chart. Summer season (May 1 to August 1). Distance from Schenectady to Bogotá 2700 miles (approx.)

TIME			DAYLIGHT-DARKNESS DISTRIBUTION OVER GREAT CIRCLE PATH	PROBABLE RECEPTION OBTAINABLE FROM		PROBABLE OPTIMUM FREQUENCY
GMT	Bogota	Local		W2XAD	W2XAF	
				13660 K.C.	9550 K.C.	Short Path
1100	6 A.M.	6 A.M.	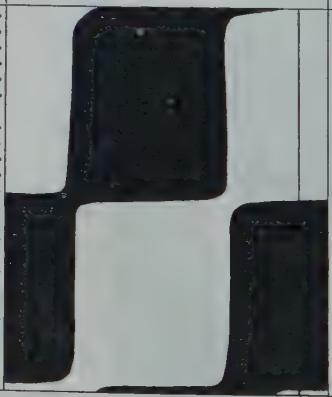	Unsat.-Poor	Nil	16000 K.C.
1200	7 A.M.	7 A.M.		Poor	Nil	20000 K.C.
1300	8 A.M.	8 A.M.		Poor	Nil	20000 K.C.
1400	9 A.M.	9 A.M.		Poor	Nil	20000 K.C.
1500	10 A.M.	10 A.M.		Poor	Nil	20000 K.C.
1600	11 A.M.	11 A.M.		Poor	Nil	20000 K.C.
1700	12 N.	12 N.		Poor	Nil	20000 K.C.
1800	1 P.M.	1 P.M.		Poor	Nil	20000 K.C.
1900	2 P.M.	2 P.M.		Poor	Nil	20000 K.C.
2000	3 P.M.	3 P.M.		Poor	Nil	19400 K.C.
2100	4 P.M.	4 P.M.		Poor	Nil	18200 K.C.
2200	5 P.M.	5 P.M.		Poor-Fair	Nil	17000 K.C.
2300	6 P.M.	6 P.M.		Fair	Unsat.	15500 K.C.
0000	7 P.M.	7 P.M.		Fair-Good	Poor	13800 K.C.
0100	8 P.M.	8 P.M.		Good-Fair	Poor-Fair	12500 K.C.
0200	9 P.M.	9 P.M.		Good-Fair	Fair	11000 K.C.
0300	10 P.M.	10 P.M.		Fair	Fair-Good	9200 K.C.
0400	11 P.M.	11 P.M.		Fair-Poor	Fair	7200 K.C.
0500	12 M.	12 M.		Poor	Fair-Poor	7200 K.C.
0600	1 A.M.	1 A.M.		Poor-Unsat.	Fair-Poor	7200 K.C.
0700	2 A.M.	2 A.M.		Poor-Unsat.	Fair-Poor	7200 K.C.
0800	3 A.M.	3 A.M.		Unsat.	Fair-Poor	7200 K.C.
0900	4 A.M.	4 A.M.		Unsat.	Fair-Poor	7200 K.C.
1000	5 A.M.	5 A.M.		Unsat.-Poor	Poor	10500 K.C.

Fig. 165--Schenectady-Bogotá transmission chart. Fall season (August 1 to November 1). Distance from Schenectady to Bogotá 2700 miles (approx.)

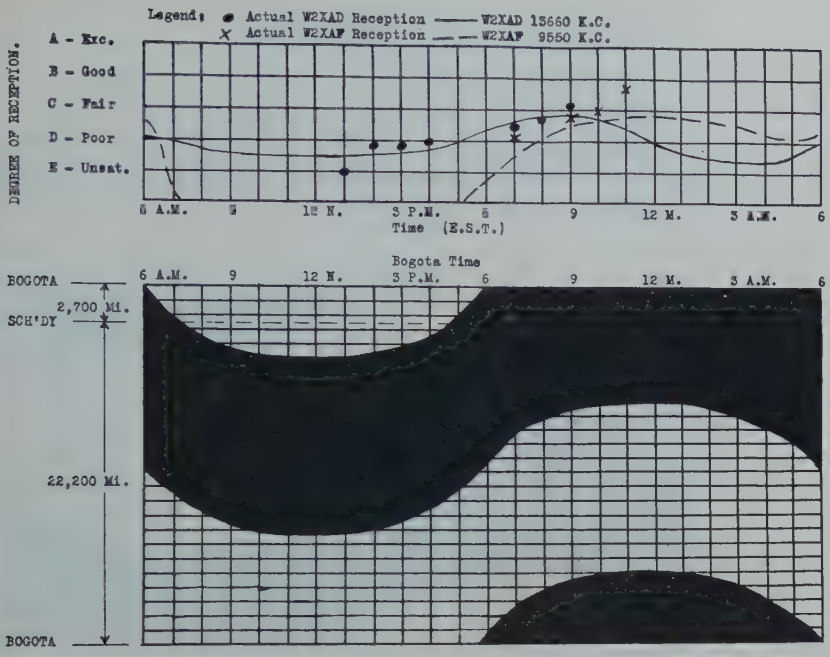

Fig. 166—Reception in Bogotá from November 1 to February 1. Daylight-darkness distribution over great circle distance from Schenectady to Bogotá, South America, as of December 20.

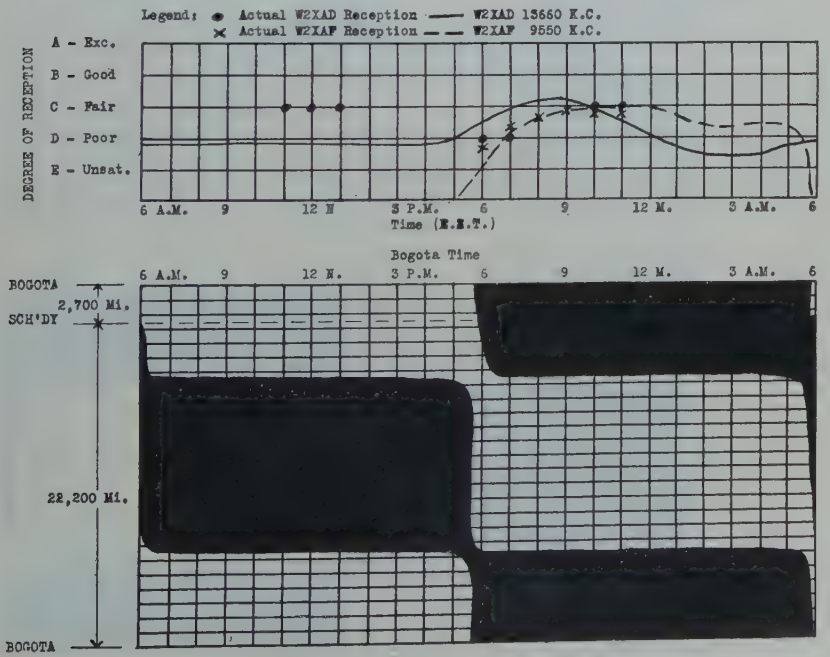

Fig. 167—Reception in Bogotá from February 1 to May 1. Daylight-darkness distribution over great circle distance from Schenectady to Bogotá, South America, as of March 20.

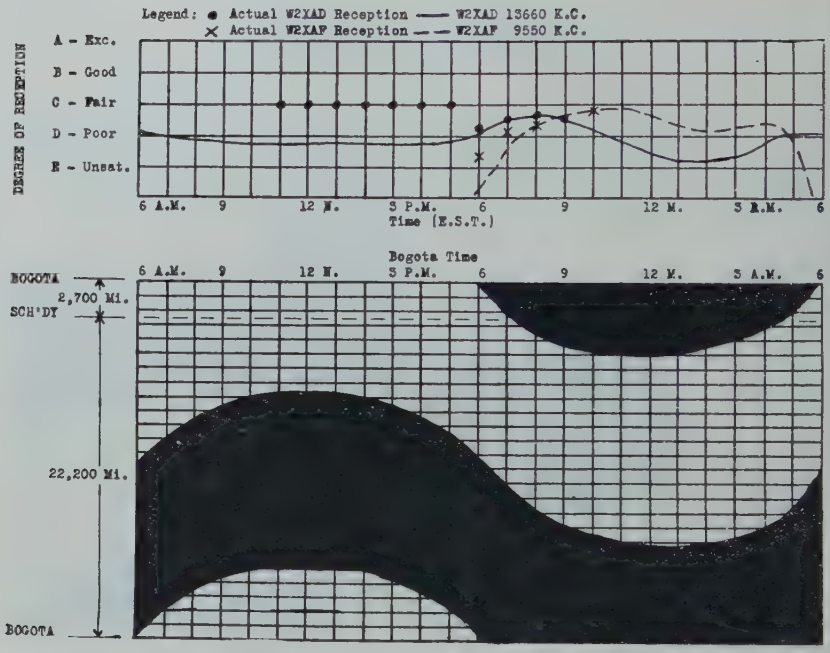

Fig. 168—Reception in Bogotá from May 1 to August 1. Daylight-darkness distribution over great circle distance from Schenectady to Bogotá, South America, as of June 20.

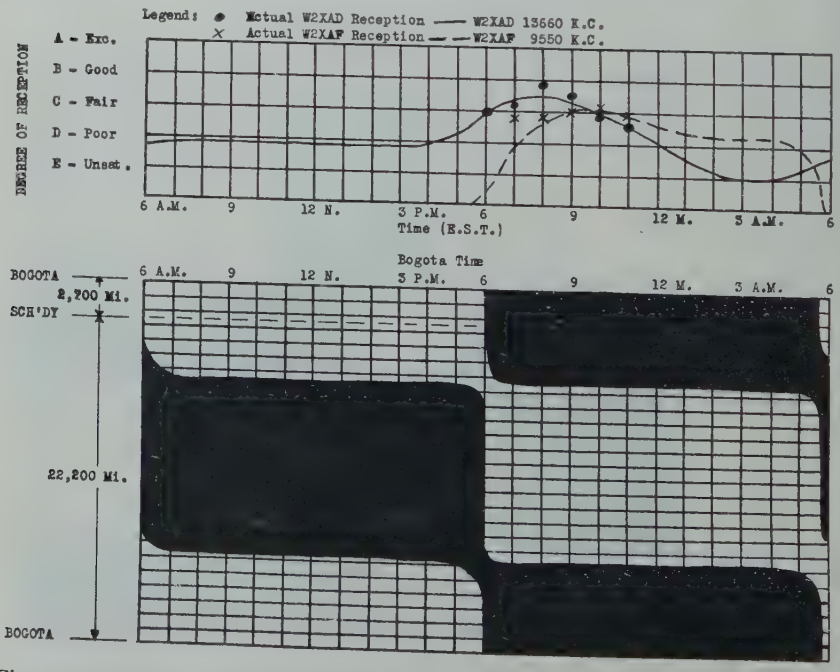

Fig. 169—Reception in Bogotá from August 1 to November 1. Daylight-darkness distribution over great circle distance from Schenectady to Bogotá, South America, as of September 20.

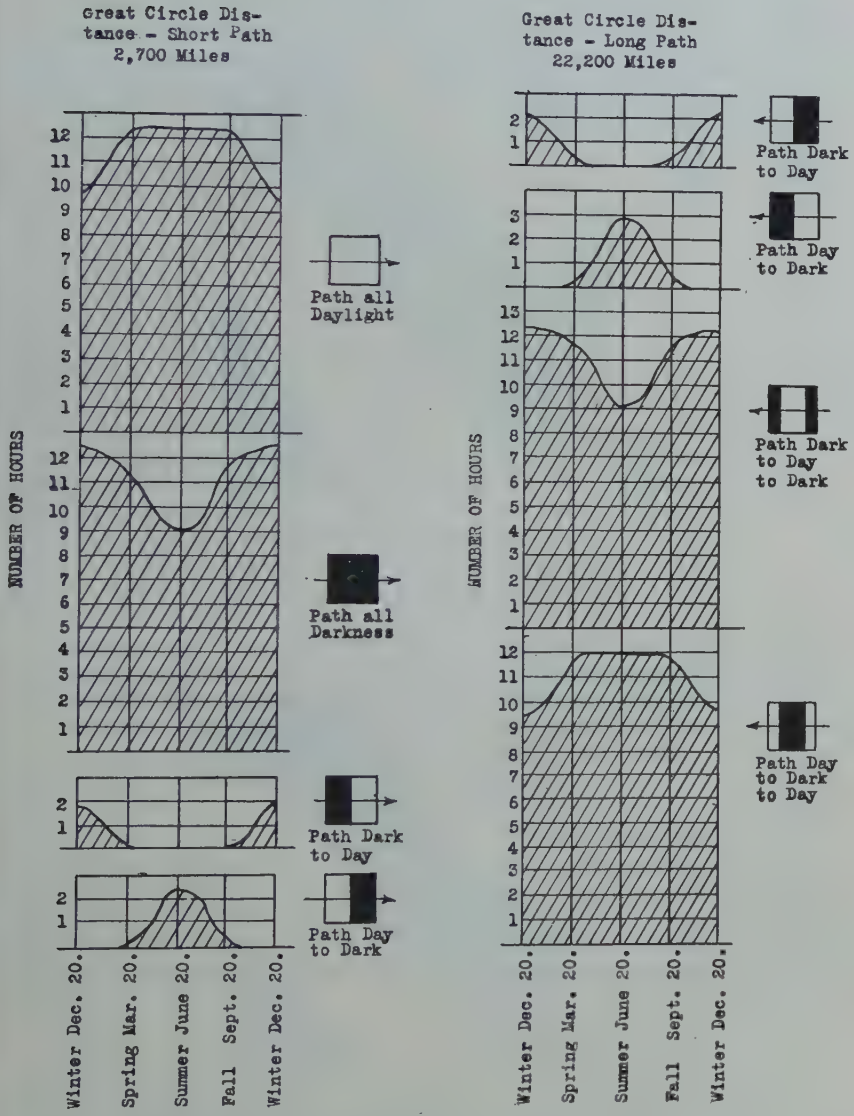

Fig. 170—Daylight-darkness distribution between Schenectady and Bogotá, South America.

Since Bogotá is situated in a tropical region not far from the Equator, it follows that a high atmospheric interference level normally prevails. As is true with most localities in northern South America and Central America, reception of American broadcast stations (550–1500 kc) in Bogotá and vicinity is almost impossible on account of atmospheric disturbances on these frequencies. As a consequence, practically all of the reception of American programs is effected at high frequencies.

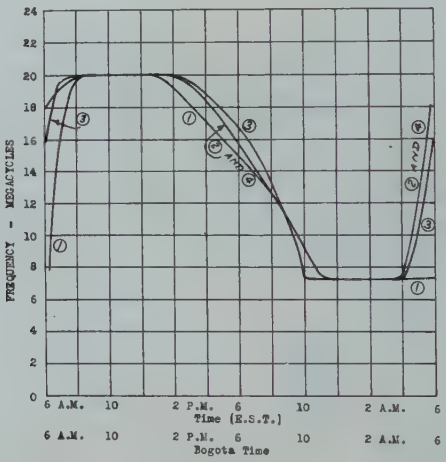

Fig. 171—Optimum frequency chart—Schenectady to Bogotá.
(1) Winter—November 1 to February 1.
(2) and (4) Spring and Fall—February 1 to May 1 and August 1 to November 1.
(3) Summer—May 1 to August 1.

The transmission and reception data available for the Schenectady-Bogotá circuit will be found on Figs. 162 to 169. Daylight-darkness distribution data are given on Fig. 170 while Fig. 171 shows a plot of the optimum frequency data which are given in tabulation form on Figs. 162, 163, 164, and 165.

Schenectady–Oakland (Calif.) Circuit

As a consequence of the relatively large amount of radio developmental work carried on between Schenectady and Oakland, a con-

TIME		DAYLIGHT-DARKNESS DISTRIBUTION OVER GREAT CIRCLE PATH	PROBABLE RECEPTION OBTAINABLE FROM		PROBABLE OPTIMUM FREQUENCY
GMT	Oakland Local		W2XAD	W2XAF	
			13660 K.C.	9550 K.C.	Short Path
1100	3 A.M. 6 A.M.		Unsat.-Poor	Poor-Unsat.	6400 K.C.
1200	4 A.M. 7 A.M.		Unsat.-Poor	Unsat.	6400 K.C.
1300	5 A.M. 8 A.M.		Poor-Fair	Unsat.	12600 K.C.
1400	6 A.M. 9 A.M.		Fair	Nil	15200 K.C.
1500	7 A.M. 10 A.M.		Fair-Poor	Nil	16800 K.C.
1600	8 A.M. 11 A.M.		Fair-Poor	Nil	17800 K.C.
1700	9 A.M. 12 N.		Poor	Nil	17800 K.C.
1800	10 A.M. 1 P.M.		Poor	Nil	17800 K.C.
1900	11 A.M. 2 P.M.		Poor-Fair	Nil	17800 K.C.
2000	12 N. 3 P.M.		Fair	Nil	17200 K.C.
2100	1 P.M. 4 P.M.		Fair-Good	Nil	16000 K.C.
2200	2 P.M. 5 P.M.		Good	Nil	15000 K.C.
2300	3 P.M. 6 P.M.		Good-Fair	Unsat.	14000 K.C.
0000	4 P.M. 7 P.M.		Good-Fair	Unsat.-Poor	13000 K.C.
0100	5 P.M. 8 P.M.		Good-Fair	Fair	11500 K.C.
0200	6 P.M. 9 P.M.		Fair	Fair-Good	9800 K.C.
0300	7 P.M. 10 P.M.		Fair-Poor	Fair-Good	6400 K.C.
0400	8 P.M. 11 P.M.		Poor	Good	6400 K.C.
0500	9 P.M. 12 M.		Poor-Unsat.	Good-Fair	6400 K.C.
0600	10 P.M. 1 A.M.		Unsat.	Good-Fair	6400 K.C.
0700	11 P.M. 2 A.M.		Unsat.	Good-Fair	6400 K.C.
0800	12 M. 3 A.M.		Unsat.	Fair-Poor	6400 K.C.
0900	1 A.M. 4 A.M.		Unsat.	Fair-Poor	6400 K.C.
1000	2 A.M. 5 A.M.		Unsat.	Poor-Unsat.	6400 K.C.

Fig. 172—Schenectady-Oakland transmission chart. Winter season (November 1 to February 1). Distance from Schenectady to Oakland 2545 miles (approx.)

TIME		DAYLIGHT-DARKNESS DISTRIBUTION OVER GREAT CIRCLE PATH	PROBABLE RECEPTION OBTAINABLE FROM		PROBABLE OPTIMUM FREQUENCY
GMT	Oakland Local		W2XAD	W2XAF	
			15660 K.C.	9550 K.C.	Short Path
1100	3 A.M. 6 A.M.		Unsat.	Poor-Unsat.	6400 K.C.
1200	4 A.M. 7 A.M.		Poor	Unsat.	12600 K.C.
1300	5 A.M. 8 A.M.		Fair	Nil	15200 K.C.
1400	6 A.M. 9 A.M.		Fair	Nil	16800 K.C.
1500	7 A.M. 10 A.M.		Fair-Poor	Nil	17800 K.C.
1600	8 A.M. 11 A.M.		Fair-Poor	Nil	17800 K.C.
1700	9 A.M. 12 N.		Poor	Nil	17800 K.C.
1800	10 A.M. 1 P.M.		Poor	Nil	17800 K.C.
1900	11 A.M. 2 P.M.		Poor-Fair	Nil	17800 K.C.
2000	12 N. 3 P.M.		Poor-Fair	Nil	17800 K.C.
2100	1 P.M. 4 P.M.		Fair	Nil	17200 K.C.
2200	2 P.M. 5 P.M.		Fair-Good	Nil	16000 K.C.
2300	3 P.M. 6 P.M.		Good-Fair	Nil	15000 K.C.
0000	4 P.M. 7 P.M.		Good-Fair	Unsat.	14000 K.C.
0100	5 P.M. 8 P.M.		Good-Fair	Unsat.-Poor	13000 K.C.
0200	6 P.M. 9 P.M.		Fair	Fair	11500 K.C.
0300	7 P.M. 10 P.M.		Fair-Poor	Fair-Good	9800 K.C.
0400	8 P.M. 11 P.M.		Fair-Poor	Good	6400 K.C.
0500	9 P.M. 12 M.		Fair-Poor	Good	6400 K.C.
0600	10 P.M. 1 A.M.		Poor	Good-Fair	6400 K.C.
0700	11 P.M. 2 A.M.		Poor-Unsat.	Good-Fair	6400 K.C.
0800	12 M. 3 A.M.		Poor-Unsat.	Fair	6400 K.C.
0900	1 A.M. 4 A.M.		Poor-Unsat.	Fair-Poor	6400 K.C.
1000	2 A.M. 5 A.M.		Unsat.	Poor-Unsat.	6400 K.C.

Fig. 173—Schenectady-Oakland transmission chart. Spring season (February 1 to May 1). Distance from Schenectady to Oakland 2545 miles (approx.)

TIME			DAYLIGHT-DARKNESS DISTRIBUTION OVER GREAT CIRCLE DISTANCE	PROBABLE RECEPTION OBTAINABLE FROM		PROBABLE OPTIMUM FREQUENCY
GMT	Oakland	Local		W2XAD	W2XAF	
				13660 K.C.	9550 K.C.	Short Path
1100	3 A.M.	6 A.M.		Poor-Fair	Nil	12600 K.C.
1200	4 A.M.	7 A.M.		Fair	Nil	15200 K.C.
1300	5 A.M.	8 A.M.		Fair-Poor	Nil	16800 K.C.
1400	6 A.M.	9 A.M.		Poor	Nil	17800 K.C.
1500	7 A.M.	10 A.M.		Poor	Nil	17800 K.C.
1600	8 A.M.	11 A.M.		Poor	Nil	17800 K.C.
1700	9 A.M.	12 N.		Poor	Nil	17800 K.C.
1800	10 A.M.	1 P.M.		Poor	Nil	17800 K.C.
1900	11 A.M.	2 P.M.		Poor	Nil	17800 K.C.
2000	12 N.	3 P.M.		Poor	Nil	17800 K.C.
2100	1 P.M.	4 P.M.		Poor-Fair	Nil	17800 K.C.
2200	2 P.M.	5 P.M.		Poor-Fair	Nil	17200 K.C.
2300	3 P.M.	6 P.M.		Fair-Good	Nil	16000 K.C.
0000	4 P.M.	7 P.M.		Fair-Good	Nil	15000 K.C.
0100	5 P.M.	8 P.M.		Fair-Good	Nil	14000 K.C.
0200	6 P.M.	9 P.M.		Good-Fair	Unsat.	13000 K.C.
0300	7 P.M.	10 P.M.		Good-Fair	Unsat.-Poor	11500 K.C.
0400	8 P.M.	11 P.M.		Fair	Fair	9800 K.C.
0500	9 P.M.	12 M.		Fair-Poor	Fair-Good	6400 K.C.
0600	10 P.M.	1 A.M.		Fair-Poor	Good-Fair	6400 K.C.
0700	11 P.M.	2 A.M.		Poor-Unsat.	Good-Fair	6400 K.C.
0800	12 M.	3 A.M.		Poor-Unsat.	Good-Fair	6400 K.C.
0900	1 A.M.	4 A.M.		Unsat.	Fair	6400 K.C.
1000	2 A.M.	5 A.M.		Unsat.-Poor	Poor	6400 K.C.

Fig. 174—Schenectady-Oakland transmission chart. Summer season (May 1 to August 1). Distance from Schenectady to Oakland 2545 miles (approx.)

TIME			DAYLIGHT-DARKNESS DISTRIBUTION OVER GREAT CIRCLE PATH	PROBABLE RECEPTION OBTAINABLE FROM		PROBABLE OPTIMUM FREQUENCY
GMT	Oakland	Local		W2XAD	W2XAF	
				13660 K.C.	9550 K.C.	Short Path
1100	3 A.M.	6 A.M.		Unsat.	Poor-Unsat.	6400 K.C.
1200	4 A.M.	7 A.M.		Poor	Unsat.	12600 K.C.
1300	5 A.M.	8 A.M.		Fair	Nil	15200 K.C.
1400	6 A.M.	9 A.M.		Fair	Nil	16800 K.C.
1500	7 A.M.	10 A.M.		Fair-Poor	Nil	17800 K.C.
1600	8 A.M.	11 A.M.		Fair-Poor	Nil	17800 K.C.
1700	9 A.M.	12 N.		Poor	Nil	17800 K.C.
1800	10 A.M.	1 P.M.		Poor	Nil	17800 K.C.
1900	11 A.M.	2 P.M.		Poor-Fair	Nil	17800 K.C.
2000	12 N.	3 P.M.		Poor-Fair	Nil	17800 K.C.
2100	1 P.M.	4 P.M.		Fair	Nil	17200 K.C.
2200	2 P.M.	5 P.M.		Fair-Good	Nil	16000 K.C.
2300	3 P.M.	6 P.M.		Good-Fair	Nil	15000 K.C.
0000	4 P.M.	7 P.M.		Good-Fair	Unsat.	14000 K.C.
0100	5 P.M.	8 P.M.		Good-Fair	Unsat.-Poor	13000 K.C.
0200	6 P.M.	9 P.M.		Fair	Fair	11500 K.C.
0300	7 P.M.	10 P.M.		Fair-Poor	Fair-Good	9800 K.C.
0400	8 P.M.	11 P.M.		Fair-Poor	Good	6400 K.C.
0500	9 P.M.	12 M.		Fair-Poor	Good	6400 K.C.
0600	10 P.M.	1 A.M.		Poor	Good-Fair	6400 K.C.
0700	11 P.M.	2 A.M.		Poor-Unsat.	Good-Fair	6400 K.C.
0800	12 M.	3 A.M.		Poor-Unsat.	Fair	6400 K.C.
0900	1 A.M.	4 A.M.		Poor-Unsat.	Fair-Poor	6400 K.C.
1000	2 A.M.	5 A.M.		Unsat.	Poor-Unsat.	6400 K.C.

Fig. 175—Schenectady-Oakland transmission chart. Fall season (August 1 to November 1). Distance from Schenectady to Oakland 2545 miles (approx.)

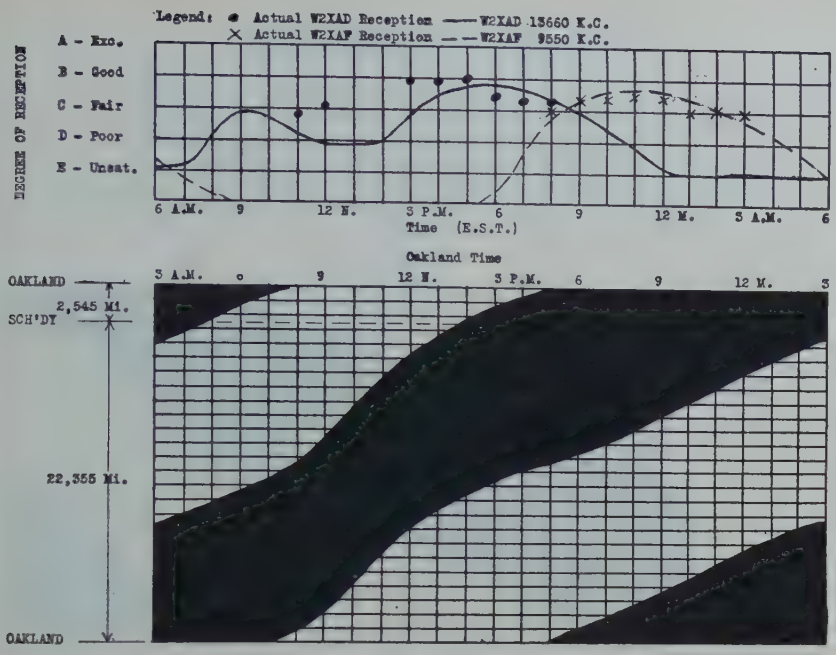

Fig. 176—Reception in Oakland from November 1 to February 1. Daylight-darkness distribution over great circle distance from Schenectady to Oakland, California, as of December 20.

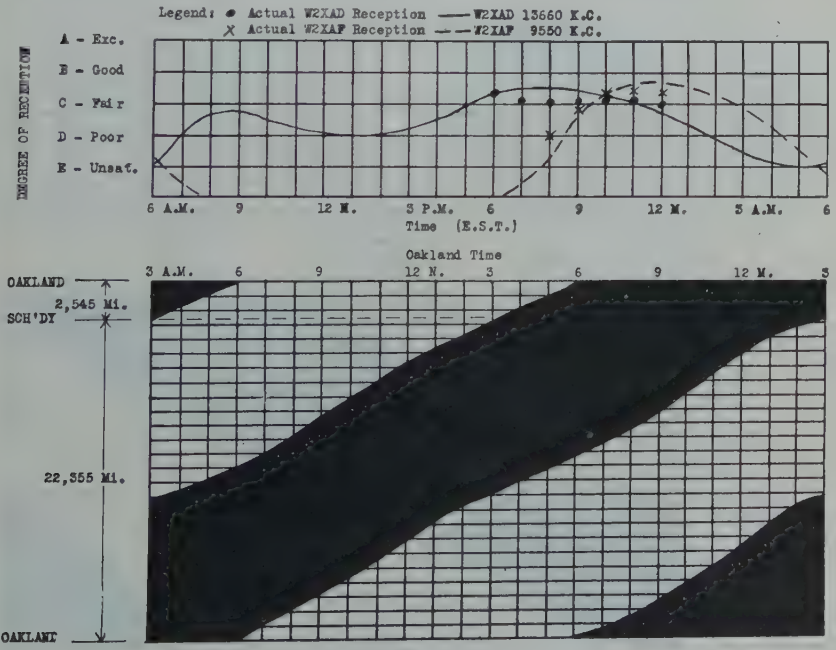

Fig. 177—Reception in Oakland from February 1 to May 1. Daylight-darkness distribution over great circle distance from Schenectady to Oakland, California, as of March 20.

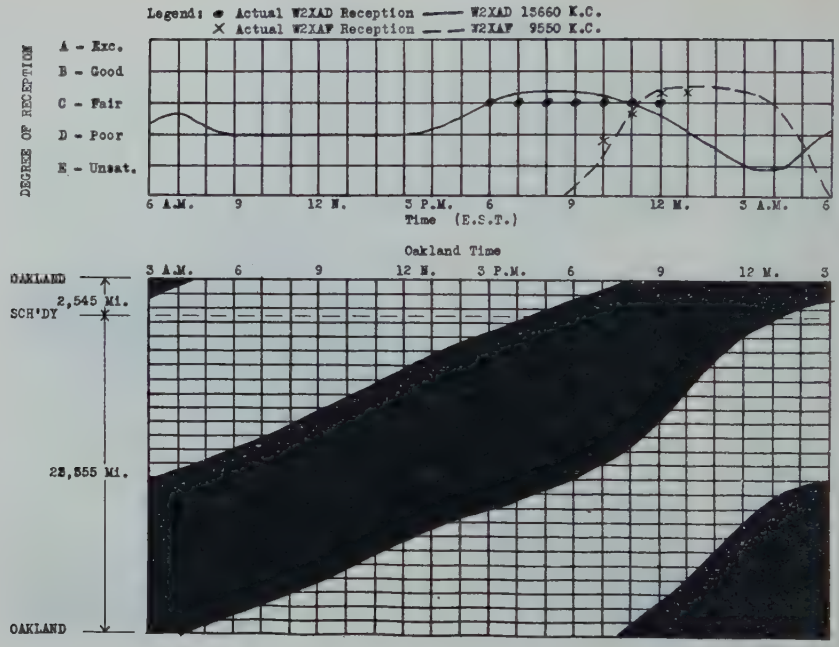

Fig. 178—Reception in Oakland from May 1 to August 1. Daylight-darkness distribution over great circle distance from Schenectady to Oakland, California, as of June 20.

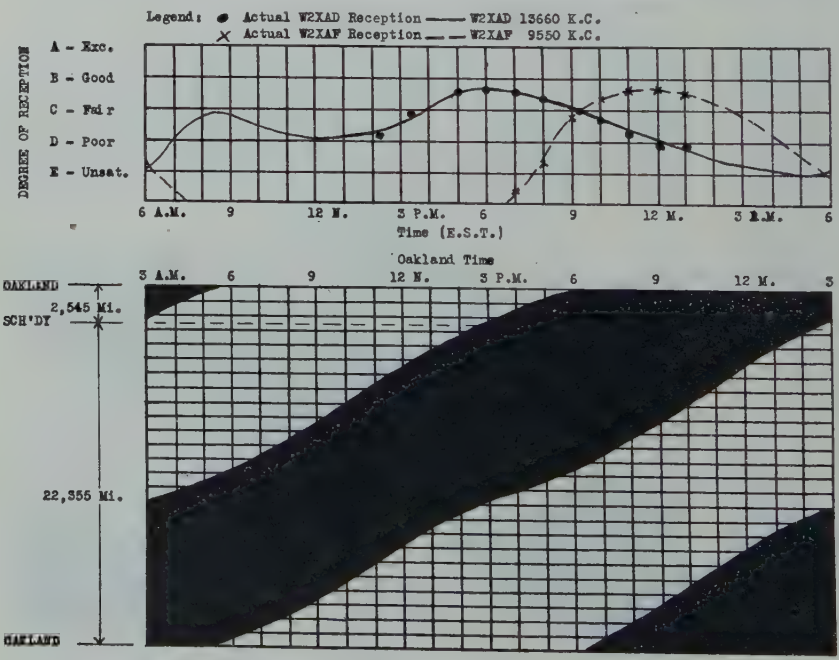

Fig. 179—Reception in Oakland from August 1 to November 1. Daylight-darkness distribution over great circle distance from Schenectady to Oakland, California, as of September 20.

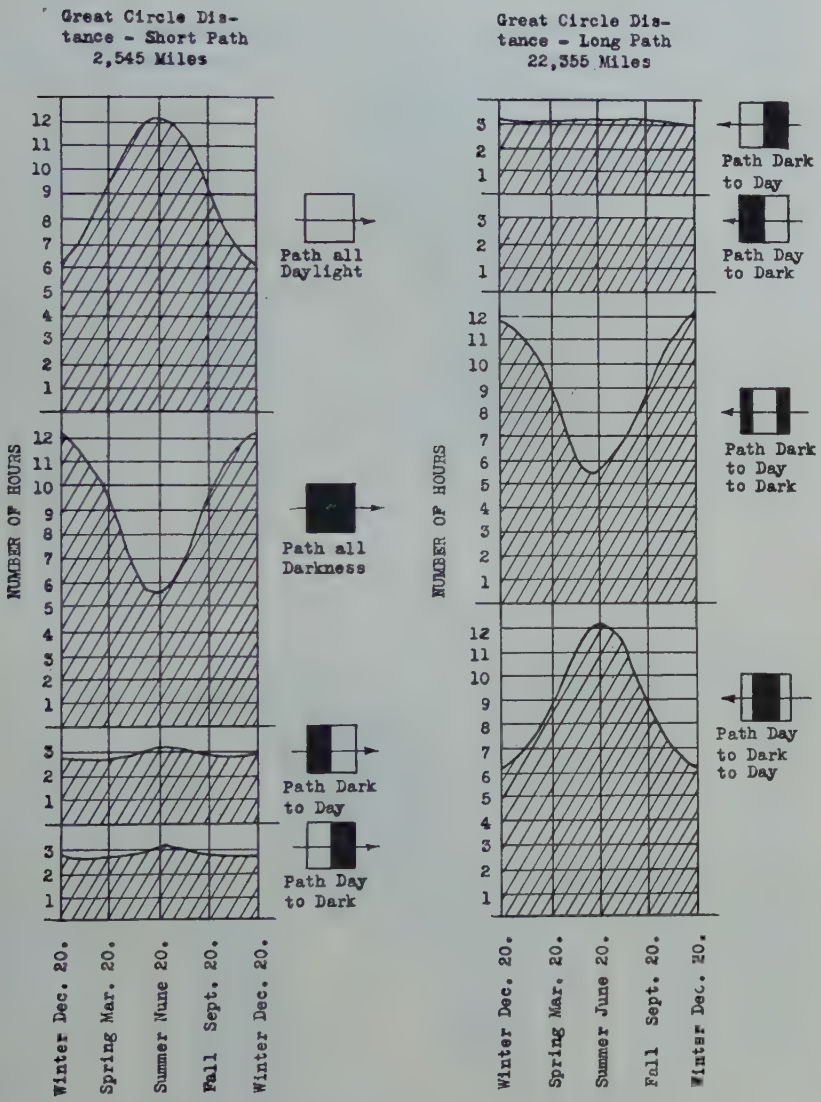

Fig. 180—Daylight-darkness distribution between Schenectady and Oakland, California.

siderable amount of radio propagation data are available for this circuit. However, not all of these data are presented herein as a part of them are not particularly adapted for use in a paper of this type.

The length of the Schenectady–Oakland circuit, as calculated along the plane of the great circle, is 2545 miles. The bearing of Oakland from Schenectady is N 81 deg. W-(approx.).

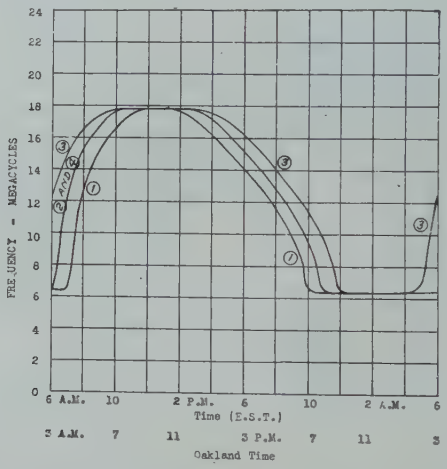

Fig. 181—Optimum frequency chart-Schenectady to Oakland.
(1) Winter—November 1 to February 1.
(2) and (4) Spring and Fall—February 1 to May 1 and August 1 to November 1.
(3) Summer—May 1 to August 1.

Figs. 172, 173, 174, and 175 show the degree of reception obtainable at Oakland from W2XAD and W2XAF transmissions. Also, these figures give the value of the optimum frequency for this circuit. On Figs. 176, 177, 178, and 179 will be found curves which show the diurnal and seasonal degree of reception obtainable from W2XAD and W2XAF.

Optimum frequency data are given on Fig. 181.

Schenectady–Colón (Panama) Circuit

Since Panama is located in a tropical region a high interference level normally prevails, particularly during the rainy season. This

TIME		DAYLIGHT-DARKNESS DISTRIBUTION OVER GREAT CIRCLE PATH	PROBABLE RECEPTION OBTAINABLE FROM		PROBABLE OPTIMUM FREQUENCY
GMT	Panama Local		W2XAD	W2XAF	
			13660 K.C.	9550 K.C.	Short Path
1100	6 A.M. 6 A.M.		Unsat.	Nil	6600 K.C.
1200	7 A.M. 7 A.M.		Unsat.-Poor	Nil	11000 K.C.
1300	8 A.M. 8 A.M.		Unsat.-Poor	Nil	15700 K.C.
1400	9 A.M. 9 A.M.		Poor	Nil	18000 K.C.
1500	10 A.M. 10 A.M.		Poor-Fair	Nil	19000 K.C.
1600	11 A.M. 11 A.M.		Poor-Fair	Nil	19000 K.C.
1700	12 N. 12 N.		Poor-Fair	Nil	19000 K.C.
1800	1 P.M. 1 P.M.		Poor-Fair	Nil	19000 K.C.
1900	2 P.M. 2 P.M.		Poor-Fair	Nil	19000 K.C.
2000	3 P.M. 3 P.M.		Fair	Nil	18000 K.C.
2100	4 P.M. 4 P.M.		Fair-Good	Nil	16000 K.C.
2200	5 P.M. 5 P.M.		Good-Fair	Unsat.	13200 K.C.
2300	6 P.M. 6 P.M.		Fair	Unsat.-Poor	10800 K.C.
0000	7 P.M. 7 P.M.		Fair-Poor	Poor	6600 K.C.
0100	8 P.M. 8 P.M.		Fair-Poor	Poor-Fair	6600 K.C.
0200	9 P.M. 9 P.M.		Poor	Fair	6600 K.C.
0300	10 P.M. 10 P.M.		Poor-Unsat.	Fair	6600 K.C.
0400	11 P.M. 11 P.M.		Poor-Unsat.	Fair	6600 K.C.
0500	12 M. 12 M.		Poor-Unsat.	Fair-Poor	6600 K.C.
0600	1 A.M. 1 A.M.		Unsat.	Poor	6600 K.C.
0700	2 A.M. 2 A.M.		Unsat.	Poor-Unsat.	6600 K.C.
0800	3 A.M. 3 A.M.		Unsat.	Unsat.	6600 K.C.
0900	4 A.M. 4 A.M.		Nil	Unsat.	6600 K.C.
1000	5 A.M. 5 A.M.		Nil	Unsat.	6600 K.C.

Fig. 182—Schenectady-Panama transmission chart. Winter season (November 1 to February 1). Distance from Schenectady to Colón 2300 miles (approx.)

TIME		DAYLIGHT-DARKNESS DISTRIBUTION OVER GREAT CIRCLE PATH	PROBABLE RECEPTION OBTAINABLE FROM		PROBABLE OPTIMUM FREQUENCY
GMT	Panama Local		W2XAD	W2XAF	
			13660 K.C.	9550 K.C.	Short Path
1100	6 A.M. 6 A.M.		Unsat.	Nil	6600 K.C.
1200	7 A.M. 7 A.M.		Unsat.-Poor	Nil	6600 K.C.
1300	8 A.M. 8 A.M.		Unsat.-Poor	Nil	11000 K.C.
1400	9 A.M. 9 A.M.		Unsat.-Poor	Nil	15700 K.C.
1500	10 A.M. 10 A.M.		Unsat.-Poor	Nil	18000 K.C.
1600	11 A.M. 11 A.M.		Unsat.-Poor	Nil	19000 K.C.
1700	12 N. 12 N.		Poor	Nil	19000 K.C.
1800	1 P.M. 1 P.M.		Poor-Fair	Nil	19000 K.C.
1900	2 P.M. 2 P.M.		Fair	Nil	19000 K.C.
2000	3 P.M. 3 P.M.		Fair-Good	Nil	18000 K.C.
2100	4 P.M. 4 P.M.		Fair-Good	Unsat.	16000 K.C.
2200	5 P.M. 5 P.M.		Good-Fair	Unsat.	12800 K.C.
2300	6 P.M. 6 P.M.		Good-Fair	Poor-Fair	10800 K.C.
0000	7 P.M. 7 P.M.		Fair	Poor-Fair	6600 K.C.
0100	8 P.M. 8 P.M.		Fair-Poor	Poor-Fair	6600 K.C.
0200	9 P.M. 9 P.M.		Fair-Poor	Fair	6600 K.C.
0300	10 P.M. 10 P.M.		Poor	Fair	6600 K.C.
0400	11 P.M. 11 P.M.		Poor-Unsat.	Fair	6600 K.C.
0500	12 M. 12 M.		Unsat.	Fair	6600 K.C.
0600	1 A.M. 1 A.M.		Unsat.	Fair-Poor	6600 K.C.
0700	2 A.M. 2 A.M.		Unsat.	Fair-Poor	6600 K.C.
0800	3 A.M. 3 A.M.		Nil	Poor	6600 K.C.
0900	4 A.M. 4 A.M.		Nil	Unsat.	6600 K.C.
1000	5 A.M. 5 A.M.		Nil	Unsat.	6600 K.C.

Fig. 183—Schenectady-Panama transmission chart. Spring season (February 1 to May 1). Distance from Schenectady to Colón 2300 miles (approx.)

TIME			DAYLIGHT-DARKNESS DISTRIBUTION OVER GREAT CIRCLE PATH	PROBABLE RECEPTION OBTAINABLE FROM		PROBABLE OPTIMUM FREQUENCY
GMT	Panama	Local		W2XAD	W2XAF	
				13660 K.C.	9550 K.C.	Short Path
1100	6 A.M.	6 A.M.		Unsat.	Nil	11800 K.C.
1200	7 A.M.	7 A.M.		Poor	Nil	12700 K.C.
1300	8 A.M.	8 A.M.		Poor-Fair	Nil	18000 K.C.
1400	9 A.M.	9 A.M.		Poor-Fair	Nil	19000 K.C.
1500	10 A.M.	10 A.M.		Poor-Fair	Nil	19000 K.C.
1600	11 A.M.	11 A.M.		Poor-Fair	Nil	19000 K.C.
1700	12 N.	12 N.		Poor-Fair	Nil	19000 K.C.
1800	1 P.M.	1 P.M.		Poor-Fair	Nil	19000 K.C.
1900	2 P.M.	2 P.M.		Fair	Nil	19000 K.C.
2000	3 P.M.	3 P.M.		Fair	Nil	19000 K.C.
2100	4 P.M.	4 P.M.		Fair	Unsat.	18000 K.C.
2200	5 P.M.	5 P.M.		Fair	Unsat.	16000 K.C.
2300	6 P.M.	6 P.M.		Fair	Poor	12800 K.C.
0000	7 P.M.	7 P.M.		Fair-Poor	Poor-Fair	10800 K.C.
0100	8 P.M.	8 P.M.		Fair-Poor	Poor-Fair	6600 K.C.
0200	9 P.M.	9 P.M.		Fair-Poor	Poor-Fair	6600 K.C.
0300	10 P.M.	10 P.M.		Fair-Poor	Fair	6600 K.C.
0400	11 P.M.	11 P.M.		Fair-Poor	Fair	6600 K.C.
0500	12 M.	12 M.		Poor	Fair	6600 K.C.
0600	1 A.M.	1 A.M.		Poor-Unsat.	Fair	6600 K.C.
0700	2 A.M.	2 A.M.		Poor-Unsat.	Fair-Poor	6600 K.C.
0800	3 A.M.	3 A.M.		Unsat.	Fair-Poor	6600 K.C.
0900	4 A.M.	4 A.M.		Nil	Poor-Unsat.	6600 K.C.
1000	5 A.M.	5 A.M.		Unsat.	Unsat.	7500 K.C.

Fig. 184—Schenectady-Panama transmission chart. Summer season (May 1 to August1). Distance from Schenectady to Colón 2300 miles (approx.)

TIME			DAYLIGHT-DARKNESS DISTRIBUTION OVER GREAT CIRCLE PATH	PROBABLE RECEPTION OBTAINABLE FROM		PROBABLE OPTIMUM FREQUENCY
GMT	Panama	Local		W2XAD	W2XAF	
				13660 K.C.	9550 K.C.	Short Path
1100	6 A.M.	6 A.M.		Unsat.	Nil	6600 K.C.
1200	7 A.M.	7 A.M.		Unsat.-Poor	Nil	6600 K.C.
1300	8 A.M.	8 A.M.		Unsat.-Poor	Nil	11000 K.C.
1400	9 A.M.	9 A.M.		Unsat.-Poor	Nil	15700 K.C.
1500	10 A.M.	10 A.M.		Unsat.-Poor	Nil	18000 K.C.
1600	11 A.M.	11 A.M.		Unsat.-Poor	Nil	19000 K.C.
1700	12 N.	12 N.		Poor	Nil	19000 K.C.
1800	1 P.M.	1 P.M.		Poor-Fair	Nil	19000 K.C.
1900	2 P.M.	2 P.M.		Fair	Nil	19000 K.C.
2000	3 P.M.	3 P.M.		Fair-Good	Nil	18000 K.C.
2100	4 P.M.	4 P.M.		Fair-Good	Nil	16000 K.C.
2200	5 P.M.	5 P.M.		Good-Fair	Unsat.	12800 K.C.
2300	6 P.M.	6 P.M.		Good-Fair	Unsat.	10800 K.C.
0000	7 P.M.	7 P.M.		Fair	Poor	6600 K.C.
0100	8 P.M.	8 P.M.		Fair-Poor	Poor-Fair	6600 K.C.
0200	9 P.M.	9 P.M.		Fair-Poor	Poor-Fair	6600 K.C.
0300	10 P.M.	10 P.M.		Poor	Fair	6600 K.C.
0400	11 P.M.	11 P.M.		Poor-Unsat.	Fair	6600 K.C.
0500	12 M.	12 M.		Unsat.	Fair	6600 K.C.
0600	1 A.M.	1 A.M.		Unsat.	Fair	6600 K.C.
0700	2 A.M.	2 A.M.		Unsat.	Fair-Poor	6600 K.C.
0800	3 A.M.	3 A.M.		Nil	Poor	6600 K.C.
0900	4 A.M.	4 A.M.		Nil	Unsat.	6600 K.C.
1000	5 A.M.	5 A.M.		Nil	Unsat.	6600 K.C.

Fig. 185—Schenectady-Panama transmission chart. Fall season (August 1 to November 1). Distance from Schenectady to Colón 2300 miles (approx.)

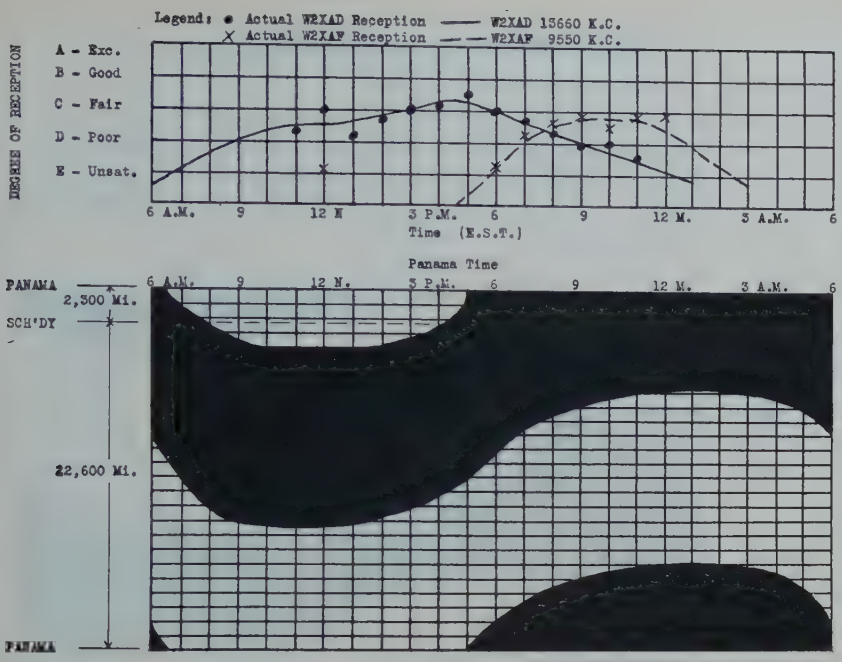

Fig. 186—Reception in Panama from November 1 to February 1. Daylight-darkness distribution over great circle distance from Schenectady to Colón, Panama, as of December 20.

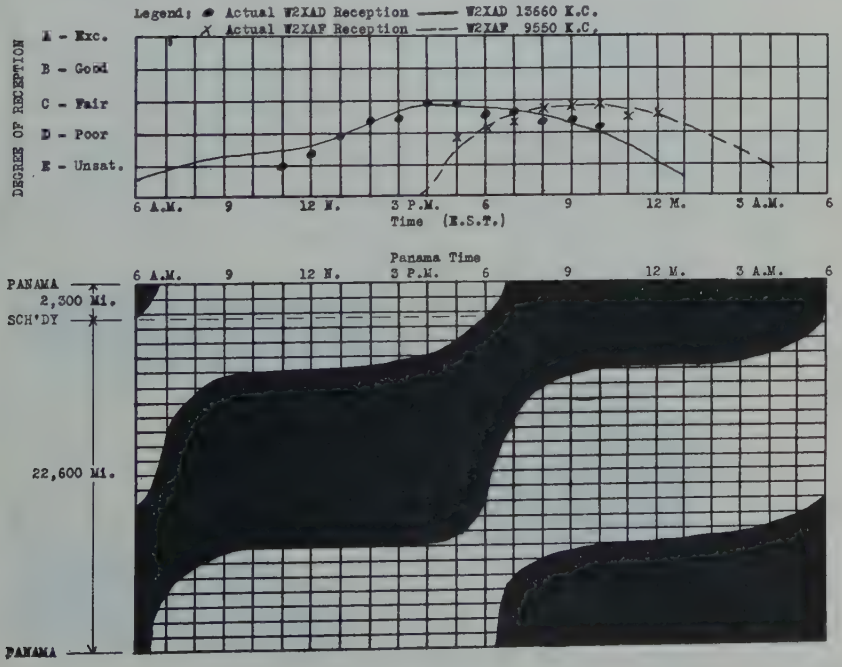

Fig. 187—Reception in Panama from February 1 to May 1. Daylight-darkness distribution over great circle distance from Schenectady to Colón, Panama, as of March 20.

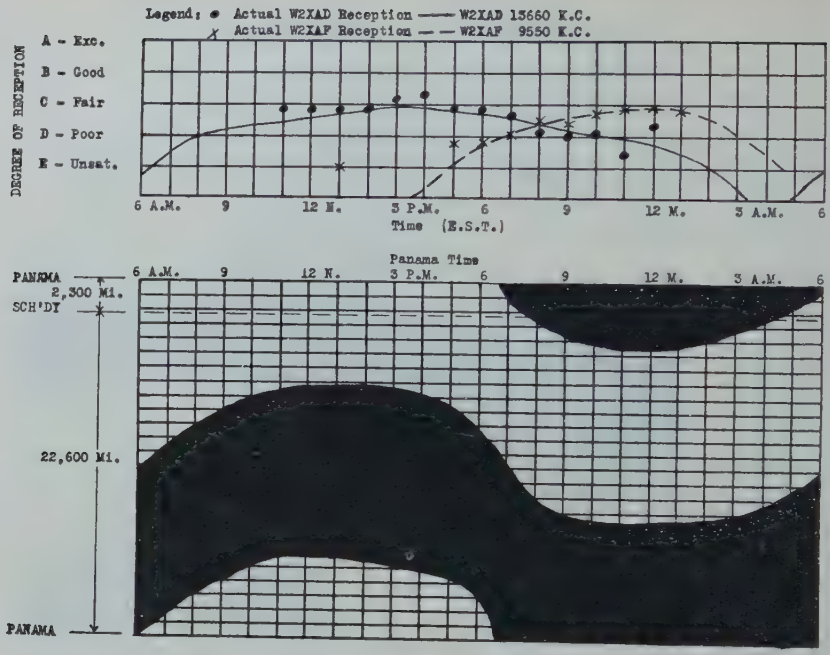

Fig. 188—Reception in Panama from May 1 to August 1. Daylight-darkness distribution over great circle distance from Schenectady to Colón, Panama, as of June 20.

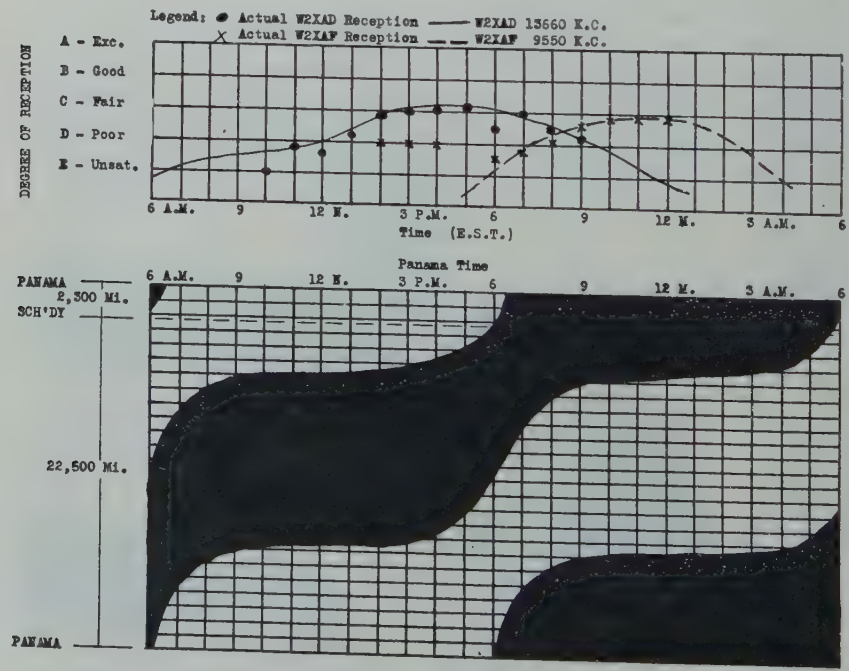

Fig. 189—Reception in Panama from August 1 to November 1. Daylight-darkness distribution over great circle distance from Schenectady to Colón, Panama, as of September 20.

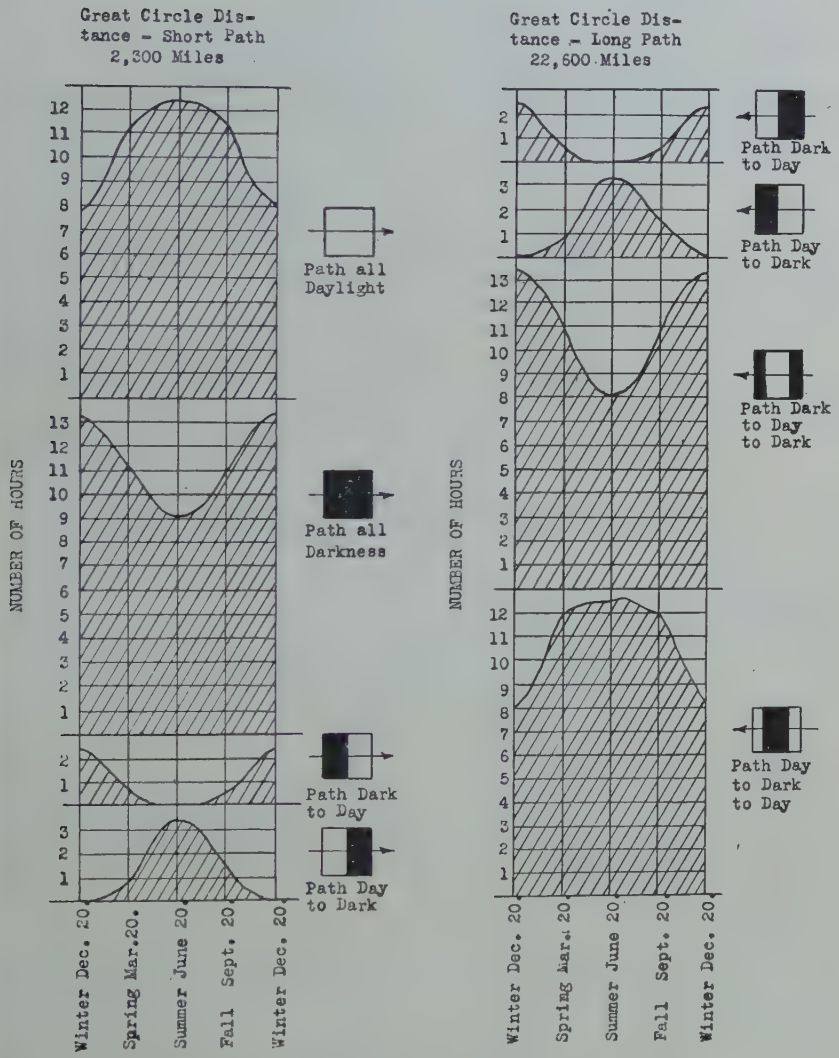

Fig. 190—Daylight-darkness distribution between Schenectady and Colón, Panama.

high interference level almost wholly prevents the reception of American broadcast stations operating within the frequency band from 550 to 1500 kc. As a consequence, many people residing in Panama depend on high-frequency broadcast transmissions for their radio entertainment.

As the Schenectady–Colón circuit is relatively short it follows that the night skip distance of W2XAD and W2XAF is such as to render

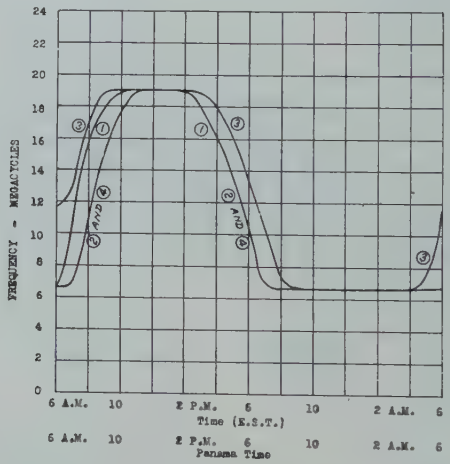

Fig. 191—Optimum frequency chart—Schenectady to Colón, Panama.
(1) Winter—November 1 to February 1.
(2) and (4) Spring and Fall—February 1 to May 1 and August 1 to November 1.
(3) Summer—May 1 to August 1.

very poor reception in Panama after about 12:00 o'clock midnight. Prior to this time W2XAD is well received from 3:00 to 7:00 P.M., E.S.T., while W2XAF is received best from 8:00 to 11:00 P.M., E.S.T. (See Figs. 182 to 189.)

The daylight-darkness distribution data for the Schenectady–Colón circuit are given on Fig. 190. Fig. 191 shows in graphical form the optimum frequency data which are tabulated on Figs. 182, 183, 184, and 185.

Proceedings of the Institute of Radio Engineers
Volume 18, Number 11 *November, 1930*

THE VAN DER POL FOUR-ELECTRODE TUBE RELAXATION OSCILLATION CIRCUIT*

By

R. M. Page and W. F. Curtis

(Naval Research Laboratory, "Bellevue", Anacostia, D. C.)

Summary—*Relaxation oscillations of an electrical nature are defined, and the operation of a tetrode relaxation circuit is described in detail. The mechanism of frequency division is explained, and oscillograms of the oscillations in this circuit are shown, both of the free oscillation and of the oscillation as controlled in frequency division.*

The characteristics of the oscillator are discussed with reference to frequency drift and stability of frequency division. The period of the oscillator is shown to be approximately RC log V_1/V_2, where V_1 and V_2 are initial and final voltages on the condenser, respectively, during the discharge. V_1/V_2 is shown to change very steeply with average internal grid resistance.

Modifications are shown for increasing the frequency stability and over-all efficiency of the system, and for controlling the ratio of charging time to discharging time of the condenser. A further modification is suggested for making the internal grid resistance independent of filament voltage when the grid is positive.

THE THERMIONIC vacuum tube, when connected in a circuit with the proper combination of electrical impedances and electromotive forces, will give rise to alternating-current energy. There are many known circuits in which such a tube will produce electrical oscillations, the most common of which is the inductance-capacity oscillator with a sinusoidal output. Of less renown, but destined to become of importance in several new fields is another type of oscillator, the oscillations of which consist of aperiodic pulses of e.m.f. occurring in cyclic order, and whose output, therefore, is far removed from sine wave form. Such an oscillation occurs when the electric or magnetic field of a capacity or an inductance is built up until a set of limiting conditions is reached, the field then being dissipated until a second set of limiting conditions causes a second reversal and the field is built up again. The action of the field in building up to a potential applied through an impedance or dissipating itself through an impedance may be referred to as relaxation,[1] and since the period of the oscillation in question is determined by the time of relaxations, the circuit producing such action is called a relaxation oscillator.

Among the known circuits of this type is one accredited to Balth.

* Decimal classification: R133. Original manuscript received by the Institute, March 12, 1930. Presented before Fifth Annual Convention of the Institute, August 19, 1930.

[1] Balth. van der Pol, "Relaxation oscillations," *Phil. Mag. and Jour. of Sci.*, **2**, 978–992; November, 1926.

van der Pol utilizing a two-grid or four-electrode tube associated with resistance and capacity only.[2] Like other relaxation oscillators, its frequency can be controlled on a submultiple of another periodic e.m.f. The fact that its output frequency, while of considerable amplitude, can be controlled by a higher frequency of extremely small amplitude has given great promise for the use of the circuit in frequency division. So sensitive is it to higher frequencies that it will successfully "divide" these frequencies in ratios up to several hundred to one. Attempts to apply the circuit in this field, however, have shown it to drift in discreet steps from one submultiple of the input to another while in operation, remaining on any one step for only a relatively short time. A study was therefore undertaken to discover the operating

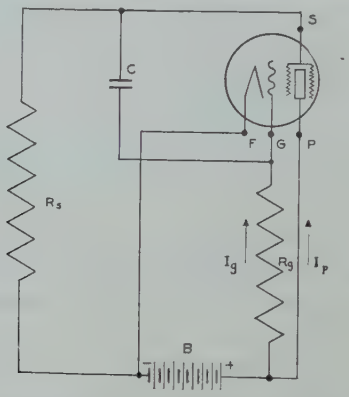

Fig. 1—Original relaxator circuit as given by van der Pol.

characteristics of the system and to produce, if possible, modifications to increase the stability for frequency division.

The original circuit as given by van der Pol is shown in Fig. 1. As screen-grid tubes available in this country give excessive current values and are unstable for frequency division in this arrangement, the grid voltage was reduced to a fraction of the plate voltage, and resistance was inserted in the plate circuit. These modifications are shown in Fig. 2, where the direct-current characteristics of the

[2] Ibid. Among the literature on relaxation oscillations and frequency division are the following articles: (a) Abraham and Bloch, "The multivibrateur," *Annal de Physique*, **12**, 237, 1919. (b) van der Pol and van der Mark "Some experiments with triodes and relaxation oscillation," *L'Onde Electrique*, **6**, 69; September, 1927. (c) van der Pol and van der Mark, "The beating of the heart considered as relaxation oscillation and an electric model of the heart," *L'Onde Electrique*, **7**, 365; September, 1928. (d) J. K. Clapp, "Universal frequency standardization from a single frequency source." *Jour. Opt. Soc. and Rev. Sci. Instr.*, **15**, 25; July, 1927. (e) L. M. Hull and J. K. Clapp, "A convenient method for referring secondary frequency standards to a standard time interval," Proc. I. R. E., **12**, 252, February, 1929.

modified system are also shown. A typical type –22 tube was used in this case, although the 7½-watt screen-grid tube is equally applicable. Since the screen voltage may be considered the independent variable in the normal functioning of the circuit, the various currents are plotted as functions of it. The operation of the circuit may be described as follows, with reference to Fig. 1:

The voltage on the condenser is equal to the difference between grid and screen voltages. The grid voltage is the impressed battery voltage less the IR drop through R_g. The screen voltage is merely the IR drop through R_s. Suppose the filament to be turned off. The condenser voltage will then assume a value

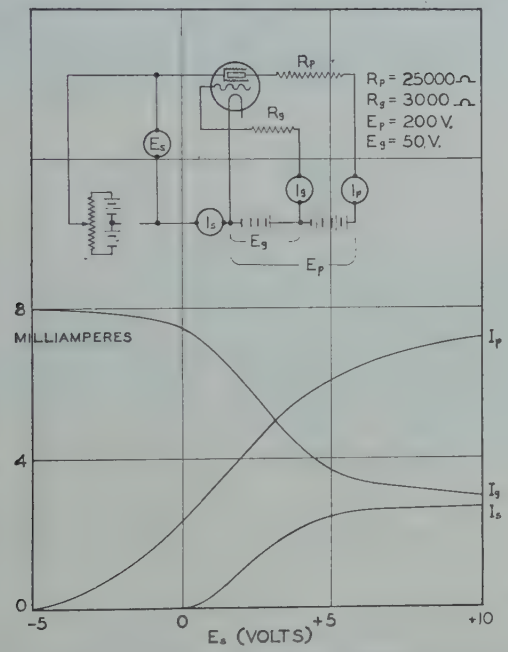

Fig. 2—Direct-current characteristics of a type –22 tube in the circuit as shown in the insert. With 200,000-ohms resistance in the place of milliammeter I_s, and a suitable condenser between grid and screen, this becomes substantially the circuit studied.

equal to that of the battery B. Now let the filament be turned on. The high grid current that follows will reduce the positive potential at G to less than half its initial value, causing the condenser to discharge. The discharge current through R_s causes a high negative potential at s, which decreases as the discharge current decreases. As the potential at s approaches filament potential it reaches the value at which plate current begins to flow

and grid current is decreased. (Fig. 2.) The accompanying increase in positive potential at G causes the condenser to begin to charge, the charging current through R_s putting the potential at s at a positive value. By virtue of the positive potential thus placed on the shield, the grid current is further reduced and therefore the potential at G is further increased so that the condenser is caused to charge at a higher rate. The resulting high charging current through R_s causes a very high positive potential at s, which now decreases as the condenser becomes charged and the charging current decreases. As the screen potential approaches filament potential now from the positive direction, it reaches the value at which plate current is reduced and grid current increased. The resulting decrease in potential at G soon

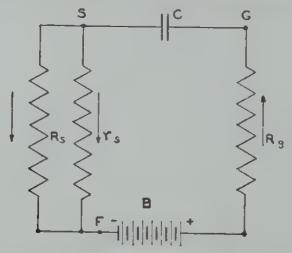

Fig. 3—The equivalent condenser circuit during the charging portion of the cycle. r_s = internal screen resistance. During the discharging portion of the cycle, the current is reversed and r_s becomes practically infinite.

causes the condenser to discharge, the high discharge current through R_s causing a high negative potential at s, and the cycle is repeated. The tube works continuously on saturation current (considering the sum of I_p, I_s, and I_g) and the shifts in grid voltage from one extreme to the other may be considered to take place instantaneously.

As shown in Fig. 3, the condenser is charged through the external and internal screen resistances in parallel. The external resistance being on the order of 100,000 to 200,000 ohms, is much greater than the internal resistance during the charging portion of the cycle, when the screen is positive. The condenser therefore becomes charged very quickly through the comparatively low internal resistance. During the discharge portion of the cycle, however, the internal resistance to the reverse current is of the order of megohms, and the condenser discharges more slowly through the external resistance. Consequently, the discharge period of the condenser and resistances R_s and R_g in series constitutes the major portion of the period of oscillations in the circuit. Oscillograms of this oscillation are shown in Fig. 4.

The charging period can be lengthened with respect to the discharge period for facilitating the study of operation. This is accomplished by the simple expedient of inserting a suitable resistance directly in series with the condenser. The new wave form thereby produced is shown in Fig. 5.

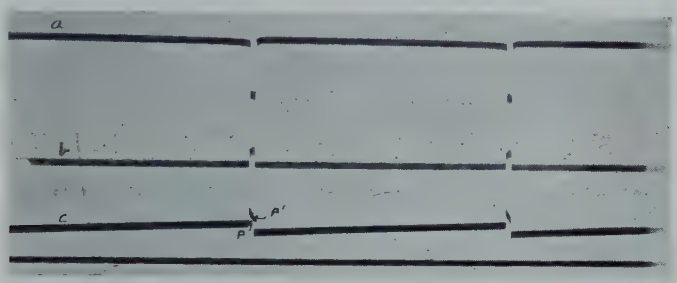

Fig. 4—An oscillogram of the oscillator in operation. a = plate voltage, b = grid voltage, c = screen voltage, P and P^1 indicate the critical screen voltages, at which the direction of condenser current is reversed.

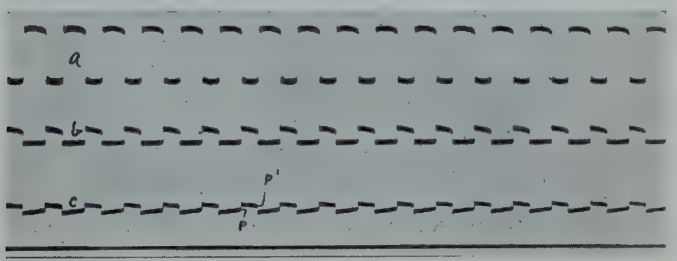

Fig. 5—Same as Fig. 4, but with resistance in series with the condenser. This resistance is seen to speed the discharge and slow up the charge, thus operating to equalize the two parts of the cycle.

From the foregoing discussion and illustrations, it is at once evident that oscillations in this system take place about two critical values of screen voltage, one that initiates the decrease in high grid current and one that initiates the increase in low grid current.[3] These

[3] Strictly speaking, this is only approximately true. The critical voltages on the screen are actually those at which the time differential of screen voltage is equal to the time differential of grid voltage; i.e., $de_s/dt = de_g/dt$. This represents an unstable condition except when $de_s/dt = e_s = 0$, for when $de_s/dt = de_g/dt$, $e_g - e_s$ is constant and the condenser is neither charging nor discharging; but the condenser never becomes fully charged or fully discharged at any point in the cycle, therefore it must always be either charging or discharging. The oscillator can be made to "stick" or fail to "kick over" from discharge to the charging condition by so adjusting circuit constants that as the screen voltage approaches zero from the negative direction, $\frac{de_g}{dt} - de_s/dt$ will not become zero until $e_s = 0$. This is equivalent to removing one set of limiting conditions.

two values are shown at the points P and P^1, respectively, in Fig. 4. If an alternating e.m.f. of higher frequency be superimposed on the screen voltage, it will be instrumental in determining the time at which the resultant screen voltage will reach the critical value, and so may control the period of the oscillation. The tendency is for the period of oscillation to assume a value equal to an integral multiple of the period of the superimposed e.m.f., as shown in the oscillogram of Fig. 6. When this condition exists the oscillator frequency is controlled by the input frequency on a submultiple of the input frequency, and will follow in exact proportion any moderate changes in the input fre-

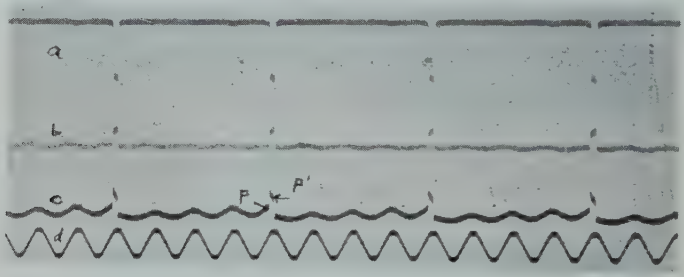

Fig. 6.—An oscillogram of the oscillator operating under control by a higher frequency. a, b, c, p, and p^1 are as in Fig. 4. d is the input frequency from a separate source. The order of "division" is 4-to-1. It will be noted that the first three cycles of input e.m.f. in each cycle of the oscillator fail to boost the screen voltage up to the critical value denoted by P, while the fourth cycle is more than sufficient to "trip" the discharge. The charge of the condenser is so rapid that the second critical voltage, at P^1, is reached very quickly in spite of the coincident peak of input e.m.f.

quency, while small changes in the frequency-determining factors of the oscillator will produce no change in frequency. A progressive change in any of the frequency-determining factors, however, that would cause the oscillator frequency to shift in discrete steps from one submultiple to the next would in the absence of the control voltage produce a continuous frequency drift in the same direction. Upon investigation the frequency drift in this circuit was found to be very pronounced. It would not be difficult at this juncture to guess the cause of this drift, but the following considerations leave no doubt as to its origin.

The period of condenser discharge, which is nearly equal to the period of oscillations in this circuit, may be expressed as follows:

$$T = \overline{R}C \log \frac{V_1}{V_2} \qquad (1)$$

where C is the total capacity in the oscillating circuit, $\overline{R}$ is the total effective resistance in series with that capacity, and V_1 and V_2 are

the initial and final voltages, respectively, across the condenser. Experimental curves verify exactly the relation

$$T = K_1 C \tag{2}$$

and approximately the relation

$$T = K_2(R_s + R_g) \tag{3}$$

when R_s is varied and R_g constant. When R_s is left constant and R_g is varied, (3) does not hold, due to the influence of R_g on the factor

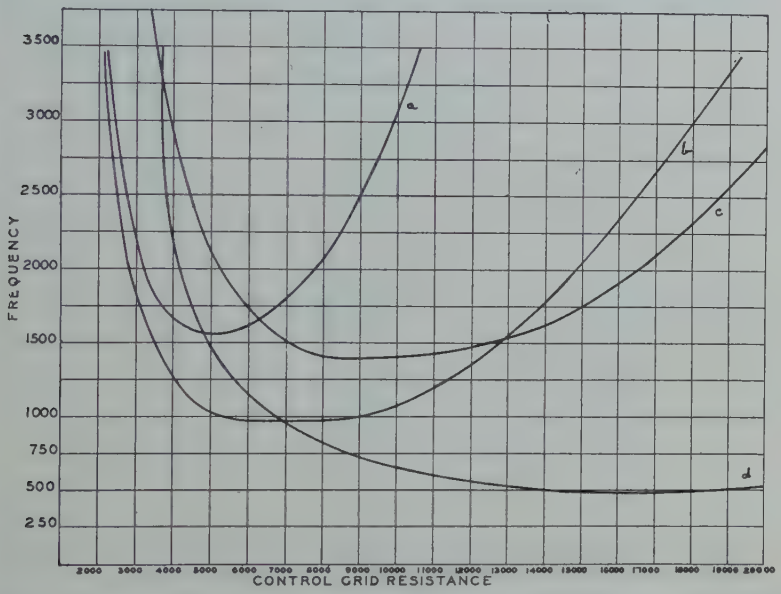

Fig. 7.—Curves of frequency plotted against external grid resistance. The different curves were taken with different values of applied grid voltage, the total plate voltage remaining constant at 200 v. *a*, $E_g = 30$ v. *b*, $E_g = 40$ v. *c*, $E_g = 50$ v. *d*, $E_g = 72$ v.

V_1/V_2. The curve of frequency plotted against R_g is shown in Fig. 7. The value of R_g corresponding to minimum frequency must be that value which produces a maximum V_1/V_2. Since V_1/V_2 depends on the magnitude of voltage variation on the grid, it will be influenced by the matching of external and internal grid resistances. It is the changing ratio, therefore, of external to internal grid resistance that is responsible for the frequency curve shown in Fig. 7.

A somewhat similar curve should obtain from variation of internal grid resistance. A near approximation is produced by variation of filament voltage, and the striking result is shown in Fig. 8. These

curves indicate pretty well that the positive potential on the grid is sufficient to draw most of the space-charge electrons from the vicinity of the filament so that the current passed by the tube is at all times limited only by the electron emission of the filament, and that small changes from any cause whatsoever in filament emission effect changes in internal tube resistances that cause large changes in the frequency of the oscillator. Even when the filament voltage is maintained constant with great precision, the excessive emission current causes rapid aging of the filament and continuous decrease of emission.

These effects can be minimized by the use of high resistance in grid and plate circuits and adjustment of filament voltage and grid

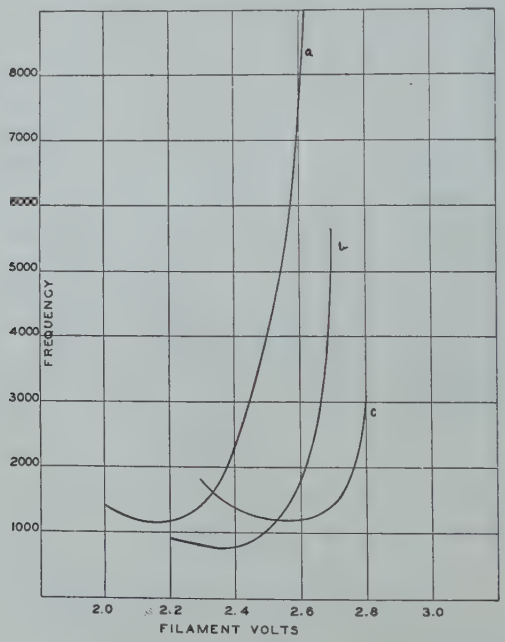

Fig. 8.—Curves of frequency plotted against filament voltage. *a*, $R_g = 20{,}000$ ohms. *b*, $R_g = 10{,}000$ ohms. *c*, $R_g = 5{,}000$ ohms. In all cases $E_g = 40$ v, $E_p = 200$ v, $R_s = 188{,}000$ ohms, $R_p = 10{,}000$ ohms, and $c = 0.05$ μf.

resistance to obtain maximum V_1/V_2, but at best the drift is objectionable. Undoubtedly there are ways to make the frequency of this oscillator insensitive to the most likely changes in tube constants. When such are developed, this circuit should prove one of the most satisfactory for frequency division.

One modification suggested involves a change in tube design. The current flow could be limited by a third grid interposed between filament and present inner grid. Such a grid, if biased so as to allow

only sufficient current to sustain strong oscillations, would effect a marked increase in tube life, reduction of drift in filament emission, and elimination of the dependence of internal resistances on filament voltage. The result would be more nearly constant frequency, far greater stability for frequency division, and greater over-all efficiency of the oscillator. It is hoped that tubes will be available in the near future with three grids, applicable to this circuit.

Proceedings of the Institute of Radio Engineers
Volume 18, Number 11 *November, 1930*

AN INTERNATIONAL COMPARISON OF FREQUENCY BY MEANS OF A LUMINOUS QUARTZ RESONATOR*

By
S. Jimbo

(Electrotechnical Laboratory, Tokyo, Japan)

Summary—*The international comparison of frequency standards made with the luminous quartz resonator shows the different laboratories,—Physikalisch-technische Reichsanstalt, National Physical Laboratory, Bureau of Standards, and Electrotechnical Laboratory,—to be in agreement to one part in 10^5 when used to calibrate the resonator at its flexural fundamental of about 10 kc, due allowance being made for the temperature coefficient of the resonator in this mode, namely, about 1 part in 10^5 and negative. The observed agreement seems limited by the luminous glow resonator used rather than by any difference between the laboratory standards compared.*

LAST year the writer had an opportunity of making an international comparison of frequency by means of a luminous quartz resonator.

The quartz resonator (No. 108/77.9) was made by the Loewe Radio Company of Germany. The quartz bar, as illustrated in Fig. 1, is enclosed in a partially evacuated bulb, and is a bar of Curie cut (X-cut).

The thickness of the quartz bar along the X axis (electrical axis) is 0.15 cm, its length along the Y axis is 8 cm, and its breadth along the Z axis (optical axis) is 0.4 cm. The bar is held in position by silk threads at a distance of 1 cm from each end and has four electrodes, the lengths of which are approximately 2.4 cm each. Terminals (1) and (4) of the resonator are connected to one of the terminals of the coupling coil provided, and terminals (2) and (3) to the other terminal of the coil. The coupling coil has an inductance of 158 mh and a resistance of 88 ohms.

The frequency f_b of flexural vibration of the bar in the direction of the Z axis is theoretically

$$f_b = \frac{k^2\sqrt{v}}{4\pi\sqrt{3}} \cdot \frac{z}{y^2}$$

in cycles per second where k is $(m+\frac{1}{2})\pi$; y and z are the lengths of the bar in cm along the Y and Z axes respectively; v denotes the propagation velocity of elastic waves in quartz in cm per sec. Putting $v=5.4$

* Decimal classification: R214. Original manuscript received by the Institute, May 2, 1930.

$\times 10^5$ and $m=2$, we obtain, as the approximate value of f_b, 9300 cycles per second. This mode of vibration was used in the international comparisons. m is an integer designating the mode of vibration.

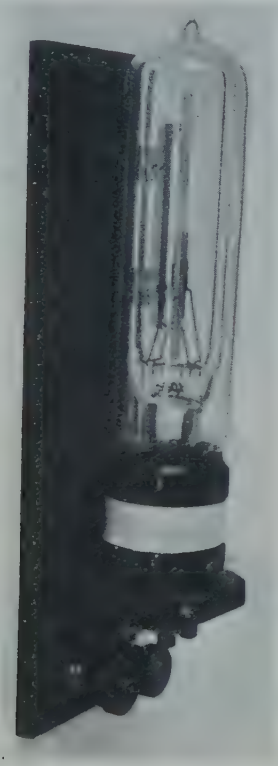

Fig. 1.

At resonance, the luminous regions[1] on the quartz bar appear at two points about 2.3 cm apart from each end, while the glow under the electrodes is not so clear. The coil is loosely coupled to the output coil of a tube generator, and by increasing the frequency of the generator, the glow appears at a frequency f_a and disappears at a frequency f_b. Upon decreasing the frequency of the generator, the glow appears at a frequency f_a' and disappears at a frequency f_b'. As the sharpness of resonance of the quartz resonator is comparatively small for such a low frequency as 10 kc, the interval between fa and fa', or f_b and f_b' may consequently amount to several cycles. All the

[1] E. Giebe und A. Sheibe: *E. T. Z.*, **4**, 380–385, 1926. *Zeitschrift für Physik*, **46**, 607–652, 1928.

above frequencies are somewhat ambiguous owing to the nature of the glow discharge, especially since the frequencies f_b and f_b' are unsteady by reason of the residual vibration of the quartz after the cessation of resonance.

As the response frequency of the resonator, we can take the mean of all the above frequencies, or the mean of f_a and f_a'.

In March, 1929, the measurement on this resonator was made at the Physikalisch-technische Reichsanstalt, using the standard tuning fork oscillator,[2] the frequency f_0 of which is 1560 cycles per second, and the standard wave meter.[3] We can assume that a value as great as 51 times the frequency of the tuning fork is nearly equal to 8 times the response frequency of the quartz; then first, with the 51st harmonic of the tuning fork oscillator, the wave meter was calibrated, its reading on the condenser being C_0; second, the 8th harmonic of the local oscillator, which had been set at the response frequency of the quartz, was measured by the wave meter, its reading on the condenser being C_x. ΔC denotes the difference between C_0 and C_x, and ΔC is very small compared to C_0. Then the response frequency of the quartz is given by

$$f = \frac{51}{8} f_0 \sqrt{\frac{C_0}{C_x}} = \frac{51}{8} f_0 \left(1 + \frac{\Delta C}{2C_0}\right),$$

where $\Delta C/C_0$ can be obtained from the calibration of the condenser. The tuning fork is made of nickel-chrome steel and its frequency f_0 was measured against the standard clock by the chronograph and synchronous motor used in the Siemens-Karolus telephotography. A large number of such measurements were made and the following final result was found:

$$f = 9960.7 \pm 0.1 \text{ cycles per second at 20 deg. C.}$$

Temperature correction $f = -0.08$ cycles per second per degree Centigrade.

In August, 1929, the resonator was measured at the National Physical Laboratory by the multivibrator method.[4] The auxiliary oscillator was finely calibrated by means of the subharmonics of the A-multivibrator, and the frequency of the local oscillator, set at the response frequency of the quartz resonator, was measured by means of the calibrated auxiliary oscillator. The tuning fork was measured against the Shortt clock by means of the high speed phonic motor and the chronograph. A large number of measurements of the response

[2] *Zeitschr. f. Instrumentenkunde*, p. 222, 1929.
[3] E. Giebe und E. Alberti: *Zietschr. f. techn. Physik*, Nos. 3 and 4, 1925.
[4] D. W. Dye, *Proc. Royal Soc.* (London), **224**, 1924.

frequency were made at 19.5 deg. C. After applying the temperature correction obtained at the P.T.R., the following result was obtained:

$$f = 9960.7 \pm 0.1_5 \text{ cycles per second at 20 deg. C.}$$

In September, 1929, the quartz resonator was measured at the Bureau of Standards. A quartz oscillator having a frequency of 25 kc and controlled thermostatically was used as a working standard. Its frequency was calibrated against the radio time signals by a phonic motor, after having been lowered to an audio frequency by the use of subharmonics. The beat frequency between the 5th harmonic of the local oscillator coupled to the quartz resonator and the 25 kc of the working standard, was measured against the standard clock by means of a special oscillograph. A large number of measurements were made at various temperatures from 23.0 deg. C to 24.0 deg. C. Applying the temperature correction above described, the response frequency was found as follows:

$$f = 9960.7 \pm 0.1 \text{ cycles per second at 20 deg. C.}$$

In January, 1930, the quartz resonator was measured at the Electrotechnical Laboratory, by means of the multivibrator method as well as by the modified multivibrator method.

In the case of the multivibrator method, an auxiliary oscillator was finely calibrated by means of the 40th harmonic and subharmonics of the A-multivibrator, and the 4th harmonic of the local oscillator, set at the response frequency of the quartz resonator, was measured by the calibrated auxiliary oscillator. The tuning fork, controlled thermostatically, was measured against the radio time signals by a phonic motor.

In the case of the modified multivibrator method,[5] the beat frequency between the 20th harmonic of the tuning fork and the 2nd harmonic of the local oscillator coupled to the quartz resonator was measured by a frequency bridge, which has such a precision that one cycle corresponds to 14 scale divisions on the condenser. The tuning fork, the frequency of which is 1024 cycles per second, was calibrated against the standard clock by means of a high speed phonic motor and a chronograph. The coupling between the local oscillator and the resonator was made so loose that the interval between f_a and f_a' was 0.5 cycle per second.

A large number of measurements were made, and the response

[5] S. Jimbo, "Measurement of frequency," Proc. I. R. E., 17, 2011–2033; November, 1929.

frequencies of the resonator at various temperatures were obtained as follows:

Temperature	Cycles per Second
13.3 deg. C	9961.3_0
14.6 deg. C	9961.0_6
16.6 deg. C	9961.0_1
18.5 deg. C	9960.8_5
23.6 deg. C	9960.3_7

The final value of the response frequency at 20 deg. C was found to be

$$f = 9960.7 \pm 0.1 \text{ cycles per second},$$

where the last term denotes the maximum deviation of any single observation from the probable value.

Conclusion

Summarizing the above data, we arrive at the conclusion that the present result shows a satisfactory agreement between the international comparisons. Such an order of agreement as $\pm 1.5 \times 10^{-5}$ has not been attained hitherto. This satisfactory result is due in part to the consideration of the temperature correction and the superiority of the luminous quartz resonator, although there are still some difficulties in determining precisely the response frequency, owing to the unsteadiness of the luminous glow.

The writer wishes to render his thanks to E. Giebe, A. Scheibe, D. W. Dye, J. E. P. L. Vigoureux, E. L. Hall, E. Yokoyama, and Y. Namba for their kind help in carrying out this international comparison.

Proceedings of the Institute of Radio Engineers
Volume 18, Number 11 *November, 1930*

CHARACTERISTICS OF PIEZO-ELECTRIC QUARTZ OSCILLATORS*

By

Issac Koga

(Assistant Professor, Tokyo University of Engineering, Tokyo, Japan)

Summary—*It goes without saying that piezo-electric quartz oscillators are very satisfactory in their stability of frequency, but their frequencies are obviously somewhat influenced by several factors associated with the circuits. Starting from the Barkhausen equation their behavior could be almost completely explained together with their amplitudes of oscillations.*

1. Circuital Equations

THERE may be several ways of treatment in which the characteristics of piezo-electric quartz oscillators can be explained. We have found that the Barkhausen equation[1] is a most convenient basis for this matter, because not only the frequencies of oscillators can be examined, but also the amplitudes of oscillations can be roughly estimated at the same time.

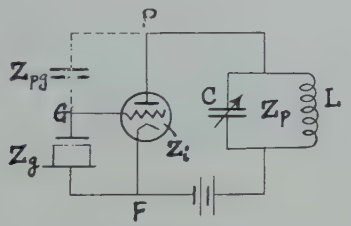

Fig. 1

In the first place we shall treat the circuit shown in Fig. 1., the Pierce circuit,[2] which seems to be the simplest both in practice and in theory. Several other circuits can be deduced from this case. For the sake of convenience we shall start by developing the Barkhausen formula.

Let $\omega/2\pi$ = frequency of the oscillating current

Z_g = impedance of the circuit between grid and filament

Z_{pg} = impedance of the circuit between plate and grid

* Decimal classification: R214. Original manuscript received by the Institute, November 11, 1929. This paper appeared in Japanese, *Jour. I. E. E.* (Japan), No. 494, 1031; September 1929.

[1] H. Barkhausen, "Wie weit kann bei Elektronenröhren allein durch die natürliche Kapazität zwischen Gitter und Anode Selbsterregung eintreten?" *Z. f. H. T.*, 21, 198, April 1923; Elektronenröhren, 1925. Bd. I., 98, Bd. II, 75.

[2] G. W. Pierce, "Piezo-electric crystal resonators and crystal oscillators applied to the precision calibration of wave meters," *Proc. Amer. Acad.*, 59, 81, 1923.

$\boldsymbol{Z}_p$ = impedance of the circuit between plate and filament outside the vacuum tube

$\boldsymbol{Z}_i$ = impedance between plate and filament inside the valve, i.e., the internal impedance of the valve

$\boldsymbol{E}$ = a-c component of the potential difference between grid and filament

μ = amplification constant of the three electrode valve.

Symbols in bold-face type are considered as vector quantities. Direct-current components of currents and voltages are not considered. Fig.

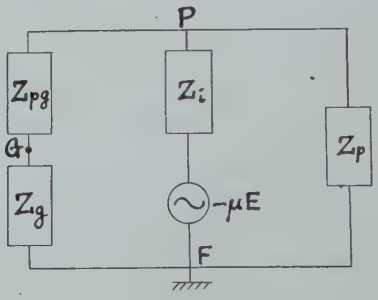

Fig. 2

2 is an equivalent circuit corresponding to Fig. 1. If we assume that the current oscillates with steady amplitude and frequency, the following relations hold. Since the potential difference $\boldsymbol{E}$ existing in the grid circuit introduces an imaginary e.m.f. $\mu\boldsymbol{E}$ in the phase opposite to $\boldsymbol{E}$, the terminal voltage across $\boldsymbol{Z}_p$ becomes

$$-\mu\boldsymbol{E} \times \frac{\boldsymbol{Z}_p}{\boldsymbol{Z}_i + \boldsymbol{Z}_p},$$

since the current in the circuit $\boldsymbol{Z}_{pg}+\boldsymbol{Z}_g$ may be neglected in comparison with that in $\boldsymbol{Z}_p$. Under this potential difference the terminal voltage $\boldsymbol{E}$ across grid and filament becomes

$$\boldsymbol{E} = -\mu\boldsymbol{E} \times \frac{\boldsymbol{Z}_p}{\boldsymbol{Z}_i + \boldsymbol{Z}_p} \times \frac{\boldsymbol{Z}_g}{\boldsymbol{Z}_g + \boldsymbol{Z}_{pg}}$$

or

$$\frac{1}{\boldsymbol{Z}_g} + \frac{1}{\boldsymbol{Z}_{pg}} + \frac{\mu}{\boldsymbol{Z}_{pg}(1 + \boldsymbol{Z}_i/\boldsymbol{Z}_p)} = 0. \qquad (1)$$

This is the Barkhausen equation, which is the necessary and sufficient condition for the sustained continuous oscillation.

In our problem the $\boldsymbol{Z}_g$ of this equation is that of the equivalent circuit[3] shown in Fig. 3, in which N, K, and S are respectively the

[3] D. W. Dye, "Piezo-electric quartz resonator and equivalent electrical circuit," *Proc. Phys. Soc.* (London), **38**, 399, 1926.

equivalent inductance, capacity, and resistance of the oscillating crystal (simply termed "quartz" hereafter), K_1 is very nearly the capacity of a quartz plate as a simple dielectric material, K_2 represents an air-gap between an upper electrode and the surface of the quartz, the

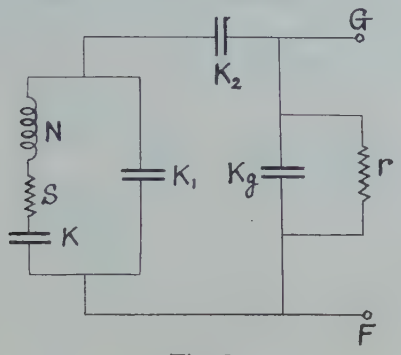

Fig. 3

latter being supposed to lie between two horizontal electrodes. K_g and r are respectively the capacity and average resistance between grid and filament, the latter being nearly equal to the grid-leak resistance if a leak is used. Hence

$$\frac{1}{Z_g} = K_g\alpha + \frac{1}{r} + \frac{S + N\alpha + \dfrac{1}{K\alpha} + \dfrac{1}{K_1\alpha}}{S + N\alpha + \dfrac{1}{K\alpha} + \dfrac{1}{(K_1 + K_2)\alpha}} \times \frac{K_1K_2}{K_1 + K_2}\alpha \quad (2)$$

where

$$\alpha = j\omega = \sqrt{-1}\omega.$$

Rearranging we get

$$\frac{1}{Z_g} = \frac{1}{r} + \left(\frac{K_2}{K_1+K_2}\right)^2 \frac{S}{S^2 + \left\{N\omega - \dfrac{1}{K\omega} - \dfrac{1}{(K_1+K_2)\omega}\right\}^2} + j\omega\left(K_g + \frac{K_1K_2}{K_1+K_2}\right) - j\left(\frac{K_2}{K_1+K_2}\right)^2 \frac{N\omega - \dfrac{1}{K\omega} - \dfrac{1}{(K_1+K_2)\omega}}{S^2 + \left\{N\omega - \dfrac{1}{K\omega} - \dfrac{1}{(K_1+K_2)\omega}\right\}^2} \quad (3)$$

It is well known that N is enormously large and consequently the damping factor of the NSK circuit is extremely small in comparison

with the ordinary electrical circuit, while K is extremely small compared with K_1, K_2, K_g, and K_{pg}. These relations are very essential in the simplification of the formulas.

The plate circuit of the vacuum tube is composed of a coil of appropriate inductance usually with or without a condenser in parallel. If we neglect the resistance component existing in this circuit, which does not seriously affect the result, since

$$\frac{1}{\boldsymbol{Z}_p} = \frac{1}{L\alpha} + C\alpha, \qquad \frac{1}{\boldsymbol{Z}_{pg}} = K_{pg}\alpha, \tag{4}$$

we have

$$\frac{\mu}{\boldsymbol{Z}_{pg}(1 + \boldsymbol{Z}_i/\boldsymbol{Z}_p)} = -\mu K_{pg}\omega \frac{r_i\left(\frac{1}{L\omega} - C\omega\right)}{1 + r_i^2\left(\frac{1}{L\omega} - C\omega\right)^2} + j\mu K_{pg}\omega \frac{1}{1 + r_i^2\left(\frac{1}{L\omega} - C\omega\right)^2} \tag{5}$$

where Z_i is replaced by its resistance component.

Introducing (3), (4), (5) into (1), we get

$$\left(\frac{K_2}{K_1+K_2}\right)^2 \frac{S}{S^2 + \left\{N\omega - \frac{1}{K\omega} - \frac{1}{(K_1+K_2)\omega}\right\}^2} + \frac{1}{r} - \mu K_{pg}\omega \frac{r_i\left(\frac{1}{L\omega} - C\omega\right)}{1 + r_i^2\left(\frac{1}{L\omega} - C\omega\right)^2} = 0 \tag{6}$$

$$\frac{N\omega - \frac{1}{K\omega} - \frac{1}{(K_1+K_2)\omega}}{S^2 + \left\{N\omega - \frac{1}{K\omega} - \frac{1}{(K_1+K_2)\omega}\right\}^2} = \left(\frac{K_1+K_2}{K_2}\right)^2 \left\{K_g + \frac{K_1K_2}{K_1+K_2} + K_{pg} + \mu K_{pg} \frac{1}{1 + r_i^2\left(\frac{1}{L\omega} - C\omega\right)^2}\right\}\omega \tag{7}$$

Equation (7) gives the oscillating frequency, while (6) discriminates as to whether the circuit can sustain the continuous oscillation or not.

2. Oscillating Frequency of the Circuit

We shall first solve (7). Let us write this equation in the form

$$\phi = H\omega \tag{8}$$

where

$$\phi = \frac{N\omega - \dfrac{1}{K\omega} - \dfrac{1}{(K_1+K_2)\omega}}{S^2 + \left\{N\omega - \dfrac{1}{K\omega} - \dfrac{1}{(K_1+K_2)\omega}\right\}^2} \tag{9}$$

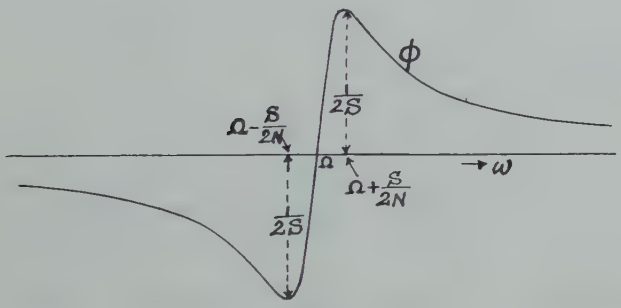

Fig. 4

Fig. 4 represents ϕ in the neighborhood of zero or at

$$\omega^2 = \frac{1}{N}\left\{\frac{1}{K} + \frac{1}{K_1+K_2}\right\} = \Omega^2. \tag{10}$$

The maximum and minimum values are

$$\phi = \pm\frac{1}{2S} = \pm\frac{1}{2\left\{N\omega - \dfrac{1}{K\omega} - \dfrac{1}{(K_1+K_2)\omega}\right\}} \tag{11}$$

which occur at the points

$$\omega \approx \Omega \pm \frac{S}{2N} \tag{12}$$

In Fig. 5, ϕ and $H\omega$ are represented approximately to scale for an actual example, in which the maximum value of ϕ has some 25 times

the height of point marked m. Strictly speaking, the quantity $H\omega$ increases very slightly with ω, but the inclination of the curve is so small that it cannot be represented in the figure. Practically, $H\omega$ is a straight line parallel to the abscissa ω, and its height depends only upon H; the curve ϕ may also be taken as a straight line in the neighborhood of Q.

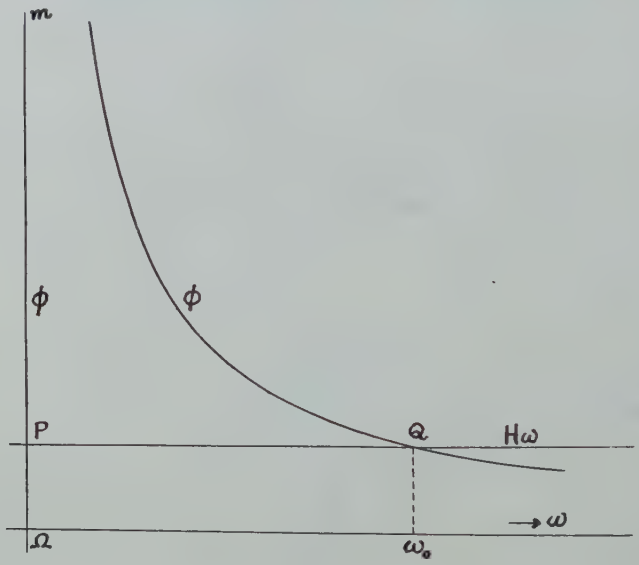

Fig. 5

The curves ϕ and $H\omega$ meet in points P and Q, but P, which corresponds approximately to the frequency of quartz as a resonator, cannot satisfy (6) as will be proved later on, hence the oscillating frequency is always given by the abscissa ω_0 of point Q. At this point, since

$$S^2 \ll \left\{ N\omega_0 - \frac{1}{K\omega_0} - \frac{1}{(K_1 + K_2)\omega_0} \right\}^2 \tag{13}$$

the equation (8) can be simplified as

$$\omega_0^2 = \frac{1}{N}\left\{ \frac{1}{K} + \frac{1}{K_1 + K_2} + \frac{1}{H} \right\} \tag{14}$$

Practically, as the value ω_0 in the expression of H can be assumed constant throughout our treatment without introducing any significant error, we shall write p instead of ω_0, thus

$$H = \left(\frac{K_1+K_2}{K_2}\right)^2 \left\{ \frac{K_1K_2}{K_1+K_2} + K_g + K_{pg} + \mu K_{pg} \frac{1}{1+r_i^2\left(\frac{1}{Lp} - Cp\right)^2} \right\} \tag{15}$$

Further, if we put

$$K_s = K_g + K_{pg} + \mu K_{pg} \frac{1}{1+r_i^2\left(\frac{1}{Lp} - Cp\right)^2} \tag{16}$$

the equation (14) can be transformed as

$$\omega_0^2 = \frac{1}{NK} + \frac{1}{NK_1}\left\{1 - \frac{1}{\frac{K_1+K_s}{K_s} + \frac{K_1}{K_2}}\right\} \tag{17}$$

To treat the frequency problems we may employ (16) and (17) or (8), (9), (15), and Fig. 5, according to circumstances.

We see from the above relationship that both the total grid circuit and the equivalent electrical circuit of quartz itself behave as inductive impedances at the oscillation frequency.

3. Dependence of Frequency upon Air Gap of the Quartz Holder

The length of air gap determines the value of K_2. To observe how the frequency depends upon K_2, let ϵ, D, A, be the dielectric constant, thickness and the surface area of quartz, and d be the length of air gap, then, since

$$K_1 = \frac{\epsilon A^*}{4\pi D} \quad \text{and} \quad K_2 = \frac{A}{4\pi d} \tag{18}$$

We have from (17)

$$\omega_0^2 = \frac{1}{NK} + \frac{1}{NK_1}\left\{1 - \frac{1}{\frac{K_1+K_s}{K_s} + \frac{\epsilon}{D}d}\right\} \tag{19}$$

From this equation, we can immediately understand that the oscillation frequency increases from the value corresponding to zero gap length

$$\omega_1^2 = \frac{1}{N}\left\{\frac{1}{K} + \frac{1}{K_1+K_s}\right\} \tag{20}$$

* Here we neglect the effect of polarization due to piezo-electricity.

to that corresponding to an infinitely large air gap

$$\omega_2^2 = \frac{1}{N}\left(\frac{1}{K} + \frac{1}{K_1}\right) \tag{21}$$

as shown experimentally in Fig. 6[4] following the variation of d, and also that the smaller the value K_s, the smaller the difference between two extreme values.

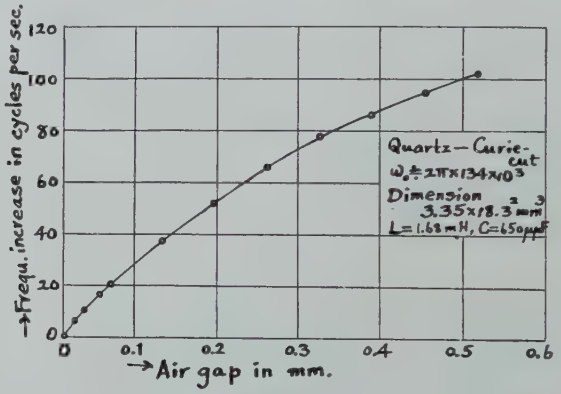

Fig. 6

The rate of the change of frequency by the air gap at zero gap is from (19) and (20)

$$\gamma = \left(\frac{\partial \omega_0/\omega_0}{\partial d}\right)_{d=0} = \frac{1}{2}\,\frac{1}{NK_1}\,\frac{\epsilon}{D}\left(\frac{K_s}{K_1+K_s}\right)^2 \frac{1}{\omega_1^2}$$
$$\approx \frac{1}{2}\,\frac{\epsilon}{D}\,\frac{K}{K_1}\left(\frac{K_s}{K_1+K_s}\right)^2. \tag{22}$$

If, in Curie-cut quartz, the vibration is due to the longitudinal or the transverse piezo-electric effect,[5]

$$K = \frac{8\delta^2}{\pi^2} \times \frac{A}{D}E \tag{23}$$

[4] The explanation of the method of observation is omitted in this paper as being no longer necessary, since during the time of the author's experiment R. S. Strout published the same method. R. S. Strout, "The temperature coefficient of quartz crystal oscillators," *Phys. Rev.*, **32**, 829; November, 1928. I. Koga, "Carrier frequency variations of transmitters," (in Japanese), Reports of the Electrical Research Institute, Tokyo Municipality, **1**, 180; August, 1927; *Elec. Rev.* (Japan), **15**, 865; October, 1927.

[5] K. S. Van Dyke, "The piezo-electric resonator and its equivalent network," Proc. I. R. E., **16**, 742; June, 1928. P. Vigoureux, "Development of formulae for the constants of the equivalent electrical circuit of a quartz resonator in terms of the elastic and piezo-electric constants," *Phil. Mag.*, **6**, 1140; December 1928.

where δ and E are piezo-electric modulus and modulus of elasticity of quartz, so that (22) becomes

$$\gamma = 16\frac{\delta^2 E}{\pi}\left(\frac{K_s}{K_1+K_s}\right)^2\frac{1}{D}. \tag{24}$$

As there are frequently the cases

$$\left(\frac{K_s}{K_1+K_s}\right)^2 \approx 1$$

we can say that

$$\gamma D \text{ or } \left\{\frac{\partial\omega_0/\omega_0}{\partial(d/D)}\right\}_{d=0}$$

is approximately constant. In the same way there will be similar constants for each different cut of crystal and for each mode of vibration. Table 1 shows some of these. In the table, the 1st and 3rd figures of dimensions are the lengths in the direction of electrical and optical axes, respectively, and the italicized figures are the thickness D.

TABLE I

Dimension (cm³)	$\omega_0/2\pi\times 10^3$	γ	γD
1.31 $\times$ *0.131* $\times$ 1.33	1540	0.091	0.012
1.34 $\times$ *0.303* $\times$ 1.33	715	0.042	0.013
0.195 $\times$ 1.32 $\times$ 1.33	1470	0.026	0.0051
0.498 $\times$ 1.31 $\times$ 1.31	575	0.0089	0.0041
0.335 $\times$ 1.83 $\times$ 1.83	865	0.017	0.0055

When Curie-cut quartz is in vibration due to the longitudinal piezo-electric effect, the frequency and current vary somewhat, as shown in Fig. 7. The reason for such frequency variations is clearly explained, for example, by Rayleigh.[6] Here the air-gap is a dependent system which reacts upon the frequency of quartz; the air column in the gap is stopped up at both ends, therefore, the air is set into vigorous vibrations and absorbs a large amount of energy from the vibrating system when the length of air-gap becomes some multiples of half a wavelength of aerial wave corresponding to the frequency of quartz. In the proximity of this special point, if the natural wavelength of air column is little less than that of the source of vibration, the frequency of the system will be decreased, and vice versa as shown in Fig. 8. For these reasons the resulting frequency characteristic is obtained by superposing the curve of Fig. 8 upon the curve given by (19).

[6] Lord Rayleigh, "Reaction of a dependent system," *Theory of Sound*, Vol. 1, 166, 1926.

On the other hand, the amplitude of oscillation is greatly decreased or may even become zero at this region because the equivalent re-

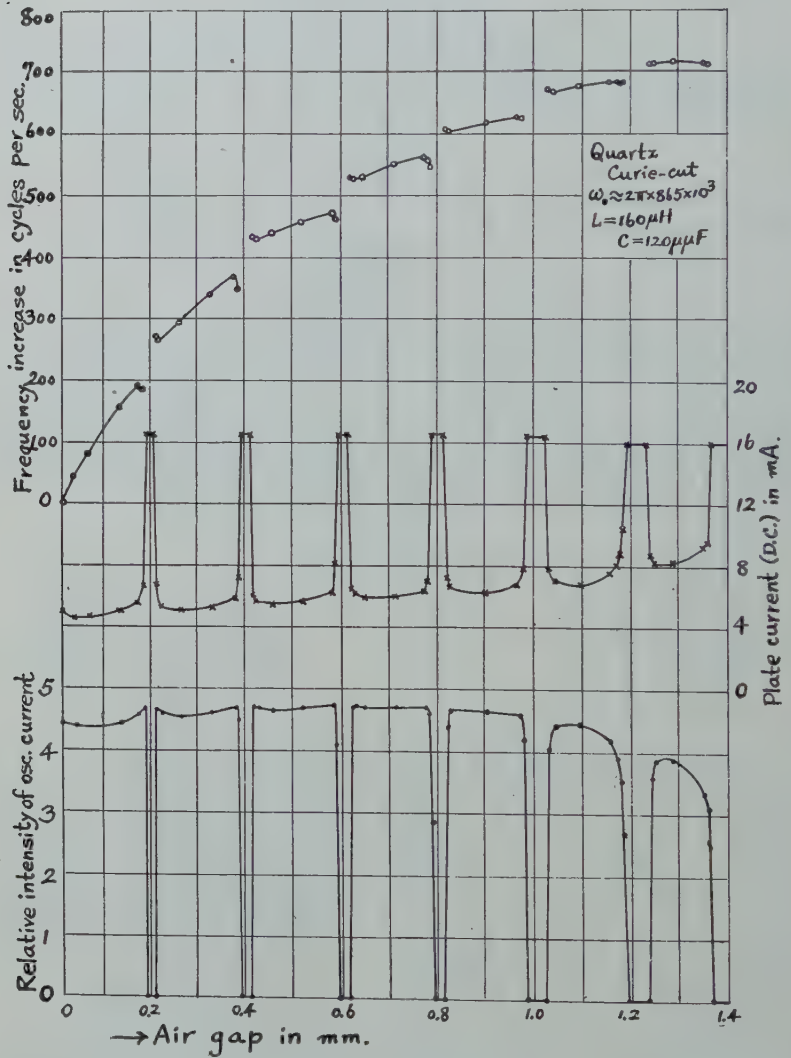

Fig. 7

sistance S of quartz is enormously increased as the damping coefficient of the aerial wave is very small. The dependence of amplitude upon S will later become clear.

When this phenomenon is not conspicuous it is convenient to notice

the direct current in the plate circuit, which increases generally as the amplitude of oscillation decreases. Fig. 9 is another example in which the single-frequency quartz oscillating crystal† is used. As the ampli-

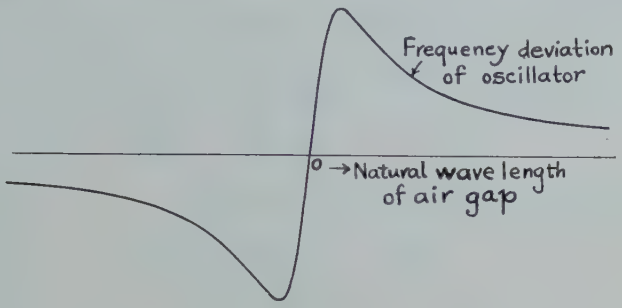

Fig. 8

tude of oscillation is rather large, the aerial resonance is observed even though the quartz is in the shear mode of vibration.

If the Curie-cut quartz vibrates due to the transverse piezo-electric effect, these phenomena cannot be observed because the value of K_2

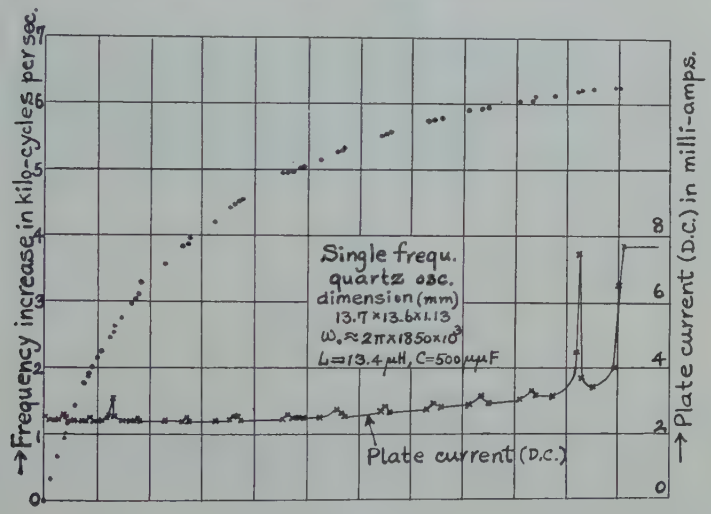

Fig. 9

becomes insufficient to maintain the continuous oscillation before the first resonance point of the aerial wave is reached, since the oscillation frequency is generally low in this case.

† Presented for the author by H. Nagaoka at the meeting of the U. R. S. I., 1928 in Brussels.

4. Temperature Effect upon Oscillating Frequency

In this section we shall prove that the frequency variation due to the temperature is practically due to the change of physical constants of quartz alone, and independent of any other constants. In (17) let

$$\xi^2 = \frac{1}{NK}, \qquad (\Delta\xi)^2 = \frac{1}{NK_1}\left\{1 - \frac{1}{\dfrac{K_1 + K_s}{K_s} + \dfrac{K_1}{K_2}}\right\} \tag{25}$$

Differentiating (17) with temperature, we have

$$\omega_0 \frac{\partial \omega_0}{\partial T} = \xi \frac{\partial \xi}{\partial T} + \Delta\xi \frac{\partial \Delta\xi}{\partial T} \tag{26}$$

or

$$\frac{\partial \omega_0/\omega_0}{\partial T} = \frac{\xi^2}{\omega_0{}^2} \frac{\partial \xi/\xi}{\partial T} + \frac{(\Delta\xi)^2}{\omega_0{}^2} \frac{\partial \Delta\xi/\Delta\xi}{\partial T}. \tag{27}$$

In case of longitudinal vibrations

$$\xi^2 = \frac{\pi^2}{l^2} \frac{E}{\rho} \tag{28}$$

where l, E, ρ are the length of quartz in the direction of vibration, the modulus of elasticity, and the density of quartz. From (25) the temperature coefficient $(\partial\Delta\xi/\Delta\xi)/\partial T$ is obviously of the order of linear expansion coefficients of solid materials, while $(\partial\xi/\xi)/\partial T$ is at least of the same order, as ξ contains the terms of linear dimension, hence remembering that

$$\xi \gg \Delta\xi \tag{29}$$

we can simplify (27) to

$$\frac{\partial \omega_0/\omega_0}{\partial T} = \frac{\partial \xi/\xi}{\partial T} \tag{30}$$

which shows the fact stated above.

Formally it is also possible to calculate the temperature coefficient of the variation of elastic constant E from (28) and (30) but the result is not reliable since the mode of vibration may not be so simple as we have imagined, even in Curie-cut quartz.

5. Frequency Variation with Tube Constants

This problem consists in the investigation of H in (15). In the first place there is no considerable influence upon the frequency by the variation of elements comprising H within the limits where continuous oscillation is possible.

If the valve be replaced by valves of other types, K_g, K_{pg}, μ, r_i will assume different values and consequently give rise to a slight variation of frequency. We shall first treat the case in which the same valve is used throughout.

When K_{pg} or K_g is increased by shunting the condenser, H will be increased and hence ω_0 varies as shown in the practical example of Fig. 10, which is as expected from Fig. 5, until the oscillation finally stops when (6) is no longer satisfied.

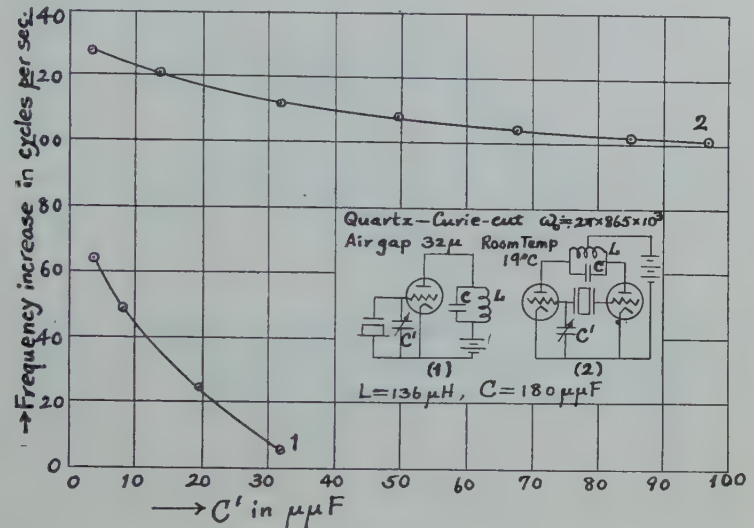

Fig. 10

Next we consider the plate circuit. Let

$$\psi = \mu K_{pg} \frac{1}{1 + r_i^2\left(\frac{1}{Lp} - Cp\right)^2}. \tag{31}$$

This is represented in Fig. 11. ψ is maximum at

$$\frac{1}{Lp} - Cp = 0 \tag{32}$$

where $p/2\pi$ is very nearly equal to the oscillating frequency $\omega_0/2\pi$.

Now that the height of $H\omega$ in Fig. 5 varies linearly with ψ, the oscillating frequency $\omega_0/2\pi$ determined by the intersection of ϕ and $H\omega$ decreases as ψ increases, so that if we plot the value ψ in proper scale, Fig. 11 represents the decrease of frequency influenced by the change

of capacity C. But we shall see later on that the oscillation stops just before (32) is satisfied, thus the frequency varies as shown in Fig. 12. Figs. 13 and 14 are practical examples. If we disconnect the grid

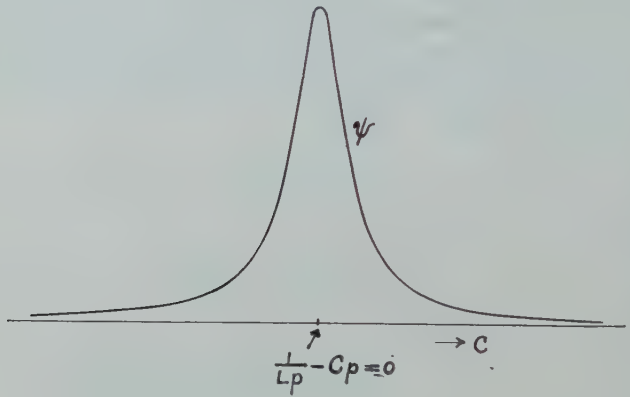

Fig. 11

leak, as in the case of Fig. 14, the resulting increase in r_i causes the curve of ψ to be very steep near the point satisfied by (32), but the region of almost constant frequency becomes broad.

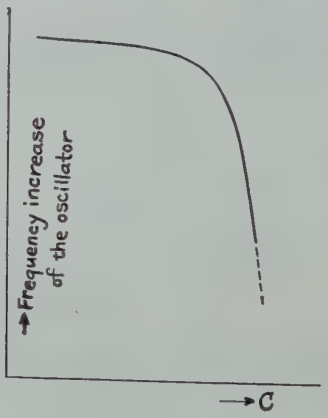

Fig. 12

The internal resistance of the valve also varies with the filament and plate voltages. If other things are unaltered, the frequency will be increased through the decreases of H when r_i is increased by the diminution of plate voltage or of filament current. Table II is an example which verifies this reasoning. In this example the oscillation

stopped at plate voltages below 45 volts and at filament currents of 420 ma. The quartz used is that described in the last row of Table I.

TABLE II

Plate Voltage Volts	Filament Current ma	Frequency Increase
99	500	0
99	540	0
99	420	9
45	420	21
45	540	21

$\omega_0 \approx 2\pi \times 186 \times 10^3$, air gap $= 6.4\mu$, $L = 376\mu H$, $C = 1700\mu\mu f$
Valve—Radiotron UX-201-A. Room temperature = 18.5 deg. C.

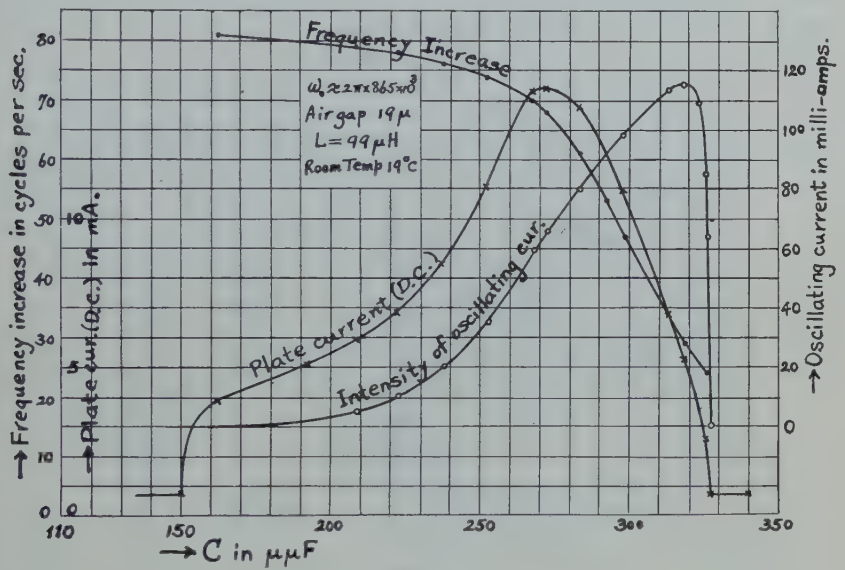

Fig. 13

The grid leak has no effect upon the oscillating frequency as given by (7) or (17). To determine in which sense the frequency is altered by the grid-leak resistance variation we must start from a more precise equation than (1), which is obtained by neglecting the current in the circuit $Z_{pg}+Z_g$ as being small compared with that in Z_p. If we proceed without neglecting this current the fundamental equation corresponding to (1) becomes

$$\frac{1}{Z_g}+\frac{1}{Z_{pg}}+\frac{\mu}{Z_{pg}\left\{1+Z_i\left(\frac{1}{Z_p}+\frac{1}{Z_g+Z_{pg}}\right)\right\}}=0\cdot \qquad (33)$$

As the frequency given by this equation does not materially differ

from $\omega_0/2\pi$ by (1), we put ω_0 in place of ω in the third term of (33) and let

$$V = \frac{\mu}{Z_{pg}\left\{1 + Z_i\left(\frac{1}{Z_p} + \frac{1}{Z_g + Z_{pg}}\right)\right\}} = jK_{pg}\omega\frac{\mu}{r_i}U \qquad (34)$$

where

$$\frac{1}{U} = \frac{1}{r_i} + \frac{1}{Z_p} + \frac{1}{Z_g + Z_{pg}} \qquad (35)$$

then the impedance U is the resultant of four impedances r_i, Z_p, Z_g, and Z_{pg} connected as shown in Fig. 15.

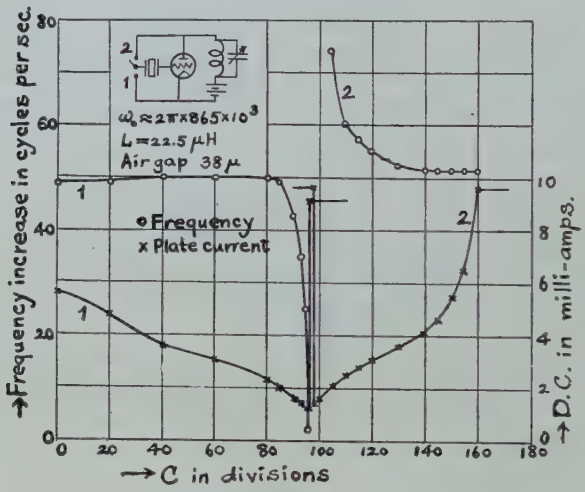

Fig. 14

As we found with (1), the imaginary parts of the second and third terms are positive, and their sum is equal in magnitude and opposite in sign to that of the first term, so that it is readily seen that the inductive reactance of Z_g is smaller than the condensive reactance of Z_{pg}, and that the reactance of Z_g+Z_{pg} is condensive. Moreover if r is gradually decreased the resultant effective reactance of Z_g+Z_{pg} becomes more and more condensive, because the impedance Z_g becomes smaller and smaller compared with Z_{pg}. But the impedance U cannot be turned from the inductive to condensive reactance as a whole, as the impedance Z_p is much less than Z_g+Z_{pg}.

Summarizing the above relations, to decrease r is to increase condensive reactance of the arm Z_g+Z_{pg} and bring the circuit U towards the tuning point against the oscillating frequency $\omega_0/2\pi$,

and to increase the effective resistance of the circuit U, thus the positive imaginary value of V, and finally the height of line $H\omega$ in Fig. 5, which means the depression of oscillating frequency.

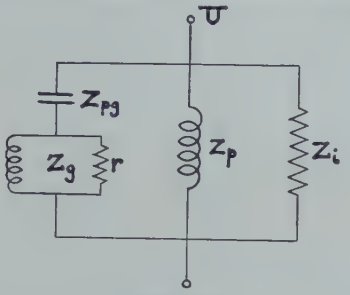

Fig. 15

This conclusion is consistent in sense with an experiment shown in Fig. 16. Too small values of r stop the oscillation as is clear from (6).

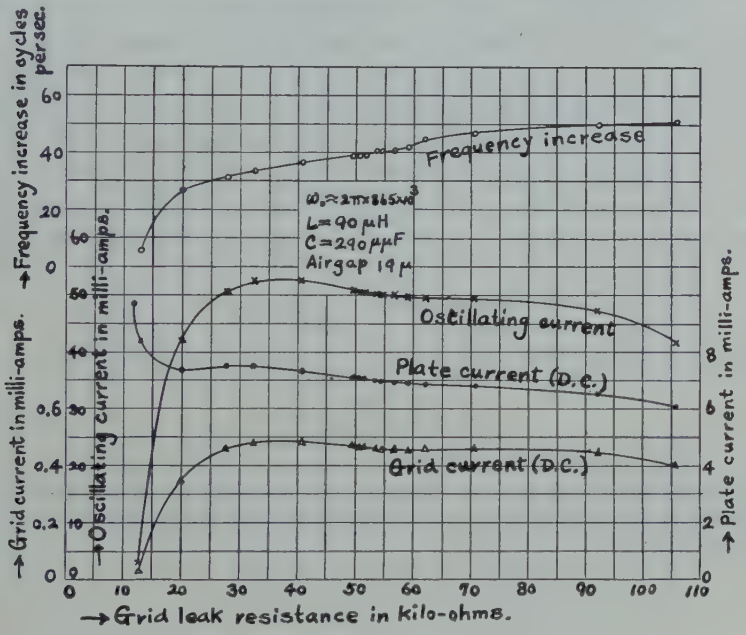

Fig. 16

6. Effective Resistance of the Oscillatory Circuit

In order that the sustained continuous oscillation should exist, the total effective resistance of the circuit or the sum of the real parts of (1) must vanish. This condition is expressed in (6). But when the

oscillation is in the process of starting, the real part of (1) is less than zero, that is

$$\left(\frac{K_2}{K_1+K_2}\right)^2 \frac{S}{S^2+\left\{N\omega-\frac{1}{K\omega}-\frac{1}{(K_1+K_2)\omega}\right\}^2} + \frac{1}{r} < \mu K_{pg}\omega \frac{r_i\left(\frac{1}{L\omega}-C\omega\right)}{1+r_i^2\left(\frac{1}{L\omega}-C\omega\right)^2}, \tag{36}$$

owing to the fact that the value of r_i is much less than that in the steady state of oscillation. After starting, the amplitude of oscillation builds up until the value of r_i satisfies (6). In other words, the oscillation can only be sustained in the condition of (36), if the value of r_i be taken as the internal resistance of the vacuum tube at its starting condition of oscillation. This relation also shows that the more extreme the inequality of (36), the larger the steady amplitude of oscillation, so that for the sake of convenience we assume that the excess of the value of the right-hand side compared with the left-hand side of (36) is proportional to the steady amplitude of the oscillation. (We shall see later that this assumption is not unreasonable.)

We have already said that of the two roots of (7) that one corresponding to P in Fig. 5 cannot satisfy (6); for, since at this point

$$S^2 \gg \left\{N\omega-\frac{1}{K\omega}-\frac{1}{(K_1+K_2)\omega}\right\}^2$$

the first term of (6), for instance Φ, becomes approximately

$$\Phi = \left(\frac{K_2}{K_1+K_2}\right)^2 \frac{1}{S} \tag{37}$$

which is obviously a very large quantity compared with the second and third terms. But at Q in Fig. 5, remembering the relation (13), (14), and (15),

$$\Phi_0 = \left(\frac{K_2}{K_1+K_2}\right)^2 \frac{S}{S^2+\left\{N\omega_0-\frac{1}{K\omega_0}-\frac{1}{(K_1+K_2)\omega_0}\right\}^2} = \left(\frac{K_2}{K_1+K_2}\right)^2 SH^2\omega_0^2 = Sp^2\left(\frac{K_1+K_2}{K_2}\right)^2 \left\{\frac{K_1K_2}{K_1+K_2} + K_g + K_{pg} + \mu K_{pg}\frac{1}{1+r_i^2\left(\frac{1}{Lp}-Cp\right)^2}\right\}^2. \tag{38}$$

This quantity is possible to satisfy (6) according to circumstances. Thus if we take hereafter that r_i is the internal resistance of the vacuum tube at the starting moment of oscillation, we may conclude that the amplitude of oscillation in the steady state, say A, is given by the equation

$$\Psi - \{\Phi_0 + 1/r\} = \alpha A \tag{39}$$

where

$$\Psi = \mu K_{pg} p \frac{r_i\left(\frac{1}{Lp} - Cp\right)}{1 + r_i^2\left(\frac{1}{Lp} - Cp\right)^2} . \tag{40}$$

Φ_0—see (38)

and α = proportionality constant.

From these equations we see that to start easily and to get large amplitude of oscillation it is necessary to keep S and K_g as small as possible, but K_2 as large as possible. To keep S small, we must choose a so-called good oscillating crystal obtained from good raw crystal and careful cutting. All sources which are apt to increase the value of S, such as the aerial resonance explained before and mechanical damping due to the poor construction of the quartz holder, should be avoided. Any value of K_g greater than zero is objectionable, but as K_{pg} appears in both Ψ and Φ_0, there will be some value of K_{pg} which will yield large amplitude. There is thus some reason to connect a small variable condenser across plate and grid.[7,8] To increase K_2 it is often the practice to rest the upper electrode upon the quartz, but it seems to introduce some uncertainty as to the constancy of oscillating frequency, so that this method is not recommended in precision work.

As to the term $1/r$ in (39) it is almost unnecessary to explain. Really the grid-leak resistance r should be as high as possible in so far as it is sufficient to keep the d-c grid potential in legitimate value.

The plate circuit has a considerable influence upon the amplitude. Fig. 17 shows graphically the relation expressed by (39) for a certain fixed value of L. Ψ reaches its maximum value

$$\frac{1}{2}\mu K_{pg} p \text{ at } \frac{1}{r_i} = \frac{1}{Lp} - Cp \tag{41}$$

that is, where the impedance (or the admittance) of the plate circuit

[7] Y. Watanabe, "Piezo-electric oscillators and piezo-electric frequency stabilizers," (in Japanese), *Jour. I. E. E.* (Japan), No. 469, p. 835; August, 1927.

[8] Gebhard, American Patent No. 1, 683, 130.

is equal to the internal resistance (or admittance) of the valve. At the point where (32) is satisfied Ψ becomes zero, while Φ_0 reaches its maximum value. The curve G in Fig. 17 shows the value Φ_0+1/r. Thus the curve αA is obtained by taking the difference of height between the curves Ψ and G. As is easily seen from this figure, the sustained oscillation is possible only when the plate circuit is an inductive impedance against the oscillating frequency, and the maximum amplitude is obtained near the point where (41) is satisfied. It is rather interesting that the curve αA is very similar to the actual oscillating amplitude experimentally obtained in Fig. 13. The smallest value of C to

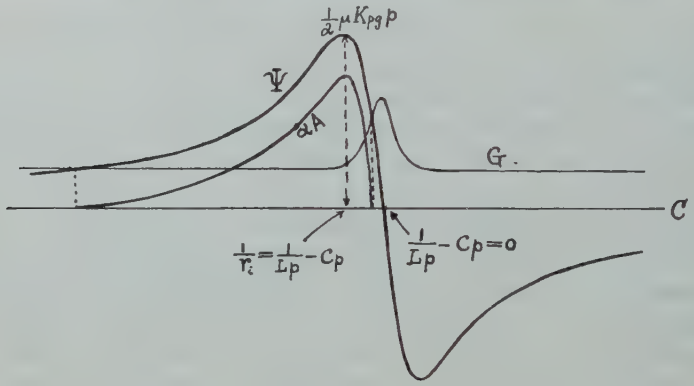

Fig. 17

start the oscillation is not distinct, as is well known, because here the angle of intersection between Ψ and G is so small, that the value of C corresponding to their intersecting point is apt to change by a slight variation of the height of the line G or the shape of Ψ caused by the circuit condition. The largest value of C necessary to maintain the oscillation is very near to but by no means can arrive at the point where (32) is satisfied.

The sharpness of Ψ varies considerably with the value of r_i and resistances in the L-C circuit, the latter being neglected in (1) for the sake of simplicity.

Fig. 18 is an example in which a thermoammeter* of high resistance is connected in series with the condenser C in the plate circuit. In this case the resistance is so high that the impedance of the plate circuit cannot become inductive for any of the value of C, and at the same time all the characteristic features are changed as the fundamental equation (1) is no longer suitable.

* Weston portable thermomilliammeter, Model 412, Series No. 317, Range 2ma, Resistance 750 ohms at 25 deg. C.

As was briefly explained above, the sustained oscillation can be realized as long as the height of the line G is less than the maximum value of Ψ. This condition is satisfied without much difficulty for

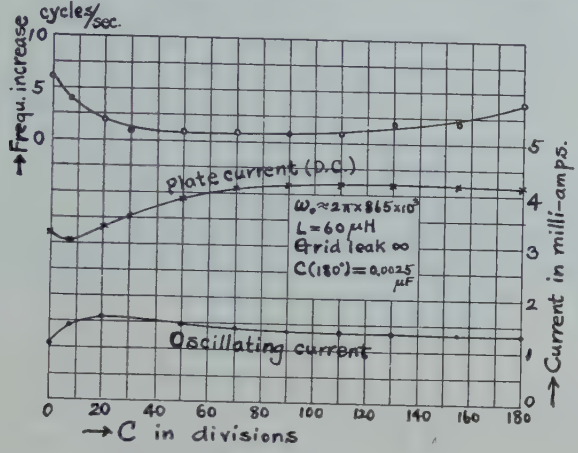

Fig. 18

medium frequencies as is readily verified by checking the order of their values. But as the values Φ_0 and Ψ are proportional to p^2 and p respectively, there are upper and lower limits of frequency within which the maximum value of Ψ can be larger than the height of G.

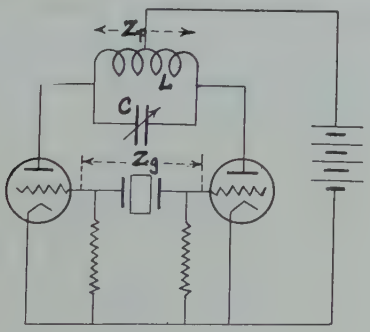

Fig. 19

For this reason the quartz oscillator of extremely high or low frequency is not easily made. At very high frequencies, in which the quartz to be used is very thin, the difficulty is increased as it is hard on the constructional side to make K_2 large compared with K_1 and to make K_g small.

7. Quartz Oscillator of Push-Pull Connection

An oscillator,[9,10] in which a quartz is connected between two grids of valves as shown in Fig. 19 is often employed as it is very satisfactory in practice. We now examine why it is superior to that shown in Fig. 1. The fundamental equation (1) is seen to be readily applicable also to the present case, by replacing only the values r_i, K_g, K_{pg} and r of the single valve by $2r_i$, $\frac{1}{2}K_g$, $\frac{1}{2}K_{pg}$, and $2r$; $\boldsymbol{Z}_g$ and $\boldsymbol{Z}_p$ are now taken to be the impedance between both grids and plates respectively. The above replacement shows directly why the present oscillator is superior to that of Fig. 1. This increase in r_i and r, and decrease in K_g and K_{pg} are effective in reducing the frequency variation and in increasing the amplitude of oscillation as was formerly explained in detail. In Fig. 10 the frequency variations due to the capacity K_g are compared with two types of oscillators.

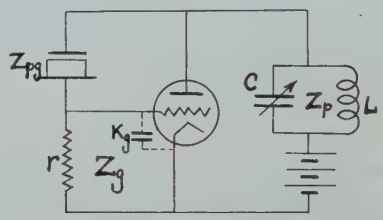

Fig. 20

8. Quartz Oscillator having Quartz Between Grid and Plate

An oscillator connected as shown in Fig. 20 was also presented by Pierce,[11] the characteristics of which are also explained by the Barkhausen equation (1). Here

$$\frac{1}{\boldsymbol{Z}_{pg}} = K_{pg}\alpha + \frac{S + N\alpha + \dfrac{1}{K\alpha} + \dfrac{1}{K_1\alpha}}{S + N\alpha + \dfrac{1}{K\alpha} + \dfrac{1}{(K_1 + K_2)\alpha}} \times \frac{K_1K_2}{K_1 + K_2}\alpha \qquad (42)$$

$$\frac{1}{\boldsymbol{Z}_g} = K_g\alpha + \frac{1}{r}, \qquad \boldsymbol{Z}_i = r_i, \qquad \frac{1}{\boldsymbol{Z}_p} = \frac{1}{L\alpha} + C\alpha. \qquad (43)$$

We need not treat again the problems for which the results are similar to those for Fig. 1, so that we shall chiefly attend to the characteristics

[9] Thomson Houston, British Patent No. 277,008.
[10] I. Koga, Japanese Patent No. 72,815.
[11] See footnote 2.

different from the foregoing cases. To this end we may neglect the term K_{pg} and r, whose influences are already understood. Writing the equation (1) as

$$Z_{pg} + Z_g + \frac{\mu Z_g}{1 + Z_i/Z_p} = 0 \tag{44}$$

and introducing (42) and (43) we have

$$\left(\frac{1}{K_1\omega}\right)^2 \frac{S}{S^2 + \left\{N\omega - \frac{1}{K\omega} - \frac{1}{K_1\omega}\right\}^2} + \frac{\mu}{K_g\omega} \times \frac{r_i\left(\frac{1}{L\omega} - C\omega\right)}{1 + r_i^2\left(\frac{1}{L\omega} - C\omega\right)^2} = 0 \tag{45}$$

$$\frac{\frac{1}{K\omega} + \frac{1}{K_1\omega} - N\omega}{S^2 + \left\{N\omega - \frac{1}{K\omega} - \frac{1}{K_1\omega}\right\}^2} = K_1^2\left\{\frac{1}{K_1} + \frac{1}{K_2} + \frac{1}{K_g} + \frac{\mu}{K_g} \frac{1}{1 + r_i^2\left(\frac{1}{L\omega} - C\omega\right)^2}\right\}\omega. \tag{46}$$

These equations determine the oscillating frequency and amplitude of oscillation. Although there are two values of ω satisfying (46), only the smaller value ω_n can satisfy (45), and since at this value

$$S^2 \ll \left\{N\omega - \frac{1}{K\omega} - \frac{1}{K_1\omega}\right\}^2 \tag{47}$$

we have

$$\omega_n^2 = \frac{1}{N}\left\{\frac{1}{K} + \frac{1}{K_1} - \frac{1}{G}\right\} \tag{48}$$

where

$$G = K_1^2\left\{\frac{1}{K_1} + \frac{1}{K_2} + \frac{1}{K_g} + \frac{\mu}{K_g} \frac{1}{1 + r_i^2\left(\frac{1}{Lp} - Cp\right)^2}\right\} \tag{49}$$

and p is a certain fixed value written in place of ω_n.

Introducing the relation (47), (48), (49) to (45),

$$SK_1^2\left\{\frac{1}{K_1}+\frac{1}{K_2}+\frac{1}{K_g}+\frac{\mu}{K_g}\frac{1}{1+r_i^2\left(\frac{1}{Lp}-Cp\right)^2}\right\}^2$$

$$+\frac{\mu}{K_g p}\frac{r_i\left(\frac{1}{Lp}-Cp\right)}{1+r_i^2\left(\frac{1}{Lp}-Cp\right)^2}=0. \tag{50}$$

This equation determines the condition of sustained oscillation, and also the relative amplitude.

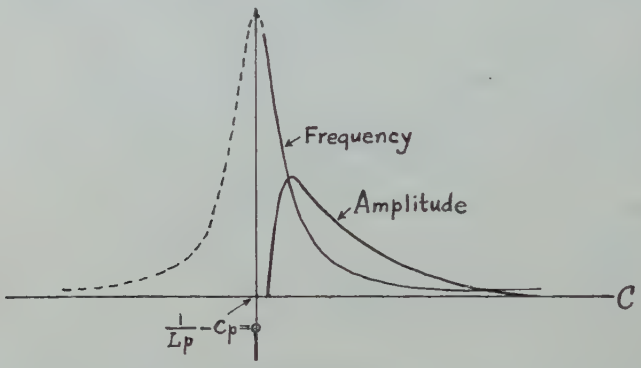

Fig. 21

The oscillation frequency increases and the amplitude of oscillation decreases with the length of air-gap of the holder. The plate circuit causes the frequency and amplitude variations as shown in Fig. 21, as is easily understood from (45) and (50). In the present case, the oscillation is maintained only when the frequency is such that the plate circuit impedance is condensive, hence the capacity C must be larger than that which satisfies (32).

Generally, in the working range the relation

$$\frac{1}{K_1}>\frac{1}{K_1+K_2}+\frac{1}{H}+\frac{1}{G} \tag{51}$$

holds, we can say that

$$\frac{1}{N}\left\{\frac{1}{K}+\frac{1}{K_1}\right\}>\frac{1}{N}\left\{\frac{1}{K}+\frac{1}{K_1}-\frac{1}{G}\right\}>\frac{1}{N}\left\{\frac{1}{K}+\frac{1}{K_1+K_2}+\frac{1}{H}\right\}$$
$$>\frac{1}{N}\left\{\frac{1}{K}+\frac{1}{K_1+K_2}\right\} \tag{52}$$

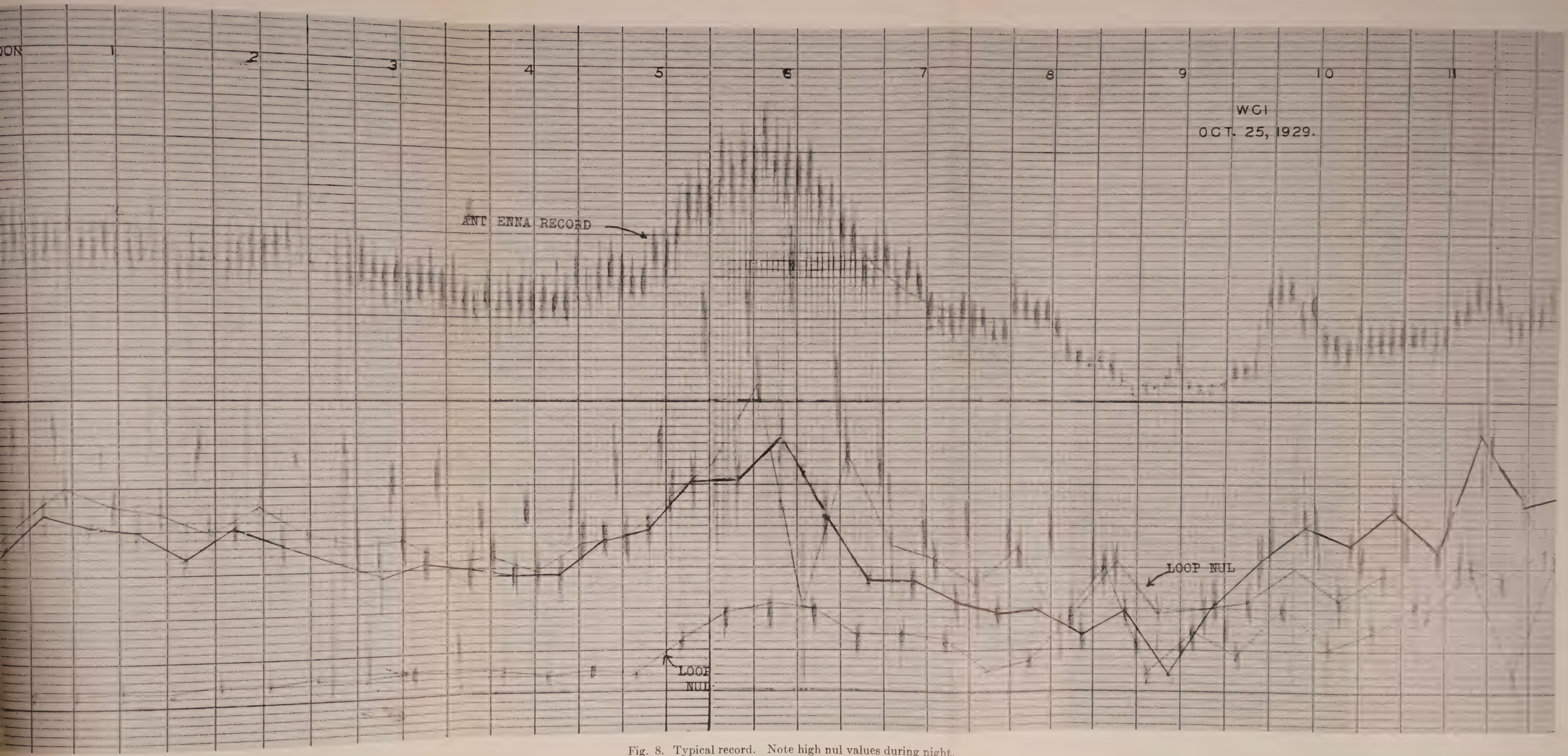

Fig. 8. Typical record. Note high nul values during night.

or

$$\omega_1 > \omega_n > \omega_0 > \Omega \tag{53}$$

In the limit at $K_2=0$, i.e., at infinite air-gap, both $1/H$ and $1/G$ vanish, so that all ω_n, ω_0, and Ω increase up to ω_1. At any rate, with a given quartz the frequency obtained by the connection of Fig. 20 is always higher than that of Fig. 1, and yet both are certainly greater than $\Omega/2\pi$, the response frequency as a piezo-electric quartz resonator.

9. Conclusion

1. Frequency variations due to the change of several circuital conditions are always very small, so that the total variation is obtained by summing up the variations due to the individual changes of condition.

2. Frequency of the quartz oscillator, as shown in Figs. 1, 19, and 20, is always higher than the response frequency as a piezo-electric quartz resonator, and the oscillation frequency of Fig. 20 is always higher than that of Fig. 1.

3. The oscillating frequency and the amplitude decrease when the capacity between grid and filament in Fig. 1 increases.

4. Increase in the length of air gap of the quartz holder reduces the amplitude and increases the frequency. The product of the two quantities, the thickness of quartz and the rate at which the frequency is varied by the air gap, is nearly constant with the same kind of quartz.

5. Aerial resonance occurs in the air gap of the quartz holder. The characteristic features in frequency and amplitude are explained by means of the theory of reaction of a dependent system.

6. Low plate voltage or filament current increases (decreases) the oscillating frequency through an increase of internal resistance of the valve.

7. Influence of temperature upon the oscillating frequency is localized in the change of physical constant of quartz proper.

8. In Fig. 1 (Fig. 20) the continuous oscillation is maintained only when the capacity C of the plate circuit is smaller (larger) than that which satisfies (32). The maximum amplitude of oscillation occurs when the plate circuit impedance is equal to the internal resistance of the valve.

9. Grid leak has almost no influence upon the oscillating frequency, but really the latter increases (decreases) with the former in Fig. 1 (Fig. 20).

10. There is a certain limit of frequency at which the oscillator can maintain its oscillation.

11. Oscillator of push-pull connection is superior in some respects upon that of Pierce.

Proceedings of the Institute of Radio Engineers
Volume 18, Number 11 *November, 1930*

FREQUENCY DIVISION*

By

Janusz Groszkowski

(Scientific Laboratory, Radio Institute, Warsaw, Poland)

Summary—*It is demonstrated that the division of frequencies, that is, the inverse process from frequency multiplication, is possible by using a triode arrangement. The requirements of such a circuit are analyzed theoretically and the conditions resulting from this study are tested experimentally. Curves are included showing the results of these experiments when the initial frequency bears a ratio to the final frequency equal to a small integer number.*

ALTHOUGH the problem of frequency multiplication is a simple and natural occurrence, the inverse problem, the division of the frequency is much more complicated and may be said to be "against nature."

We find higher harmonics as the result of distortions which occur in the various oscillating phenomena; furthermore, it is easier in general to obtain oscillations rich in harmonics than pure ones. With these conditions, therefore, no particular difficulties are found in exciting circuits whose frequency is an integral multiple of the exciting frequency.

The inverse process, however, that of exciting circuits with frequencies which are integral multiples of the natural frequency of the circuit is a phenomenon unknown in nature, and its realization requires artificial arrangements. It is logically evident that such a state exists since in the case of oscillations of constant amplitude each period has strength of action equivalent to the preceding as well as the succeeding period. And it is not unreasonable for every second, third, or in general n period, to have exciting qualities on a circuit the frequency of which is two, three, or in general n times, smaller.

In a mechanical analogy we can imagine the excitation of a shorter pendulum by a longer one, especially by making the oscillations of the latter rich in harmonics of the order of the fundamental of the former (by a suitable disposition of additional masses). The inverse condition, i.e., of exciting a longer pendulum by a shorter one is, however, not realizable in such a simple manner.

We have also in electrotechnics many examples of simple circuits for frequency multiplication. Numerous systems of radio-electrical arrangements for communication purposes are known in which the principle of frequency multiplication is used.

* Decimal classification: R139. Original manuscript received by the Institute, April 17, 1930.

The method of heterodyning with detection is considered to belong to a quite different domain. There exist to-day two published methods describing frequency division. These are first, the Balth. van der Pol arrangement[1] making use of the relaxation oscillations; and second, I. Koga's arrangement[2] with the generator synchronized with a greater frequency. In both arrangements we have to deal first with the phenomenon of the synchronization in some definite band of already existing oscillations. These bands correspond in van der Pol's circuit to $1/n$ times the synchronizing frequency, in that of I. Koga, to m/n times this frequency, m and n being integral numbers. The smaller these numbers are, the more distinct the effect.

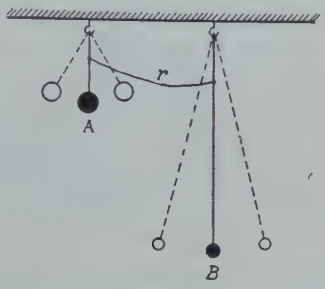

Fig. 1

An indispensable condition with these systems is the utilization of oscillations of a lower frequency in the process of maintaining these oscillations by a higher one, in other words, the previous existence of such oscillations with a period approaching a multiple of the exciting period.

An example of a longer pendulum excited by a shorter one by use of the arrangement represented schematically in Fig. 1, illustrates the analogical phenomenon. The exciting pendulum A is shorter and has a greater mass, and consequently, has a greater quantity of energy. It is coupled rather loosely by means of a thread of appropriate length with another pendulum B, which is four times as long. Normally the pendulum A during its oscillations cannot excite the pendulum B, because during one swing of pendulum B there are two swings of pendulum A and therefore the sum of exciting impulses is zero during one period of B. It is different, when the pendulum B is excited by an external power. In this case, the length of the thread being properly

[1] Balth. v. d. Pol, "Frequency demultiplication," *Nature*, September 10, 1927.

[2] I. Koga, "A new frequency transformer," Proc. I. R. E., 15, 669; August, 1927.

regulated, it is possible to obtain a reaction of the impulses of A on B, but only when the position of B is to the right and when the thread is short enough to transmit the impulses of A to B. It is evident that if the frequency of A is twice that of B, each second oscillation of A will act on B and the steady maintainance of oscillations of the latter can be obtained in this way.

The circuit of Fig. 2 is the electrical equivalent of the two pendulums. The a-c source S, which may be a vacuum tube generator, has a frequency F and excites by means of a triode the circuit LCR, tuned to the frequency $f<F$. The internal conductivity of the triode can be varied between wide limits by varying the grid bias.

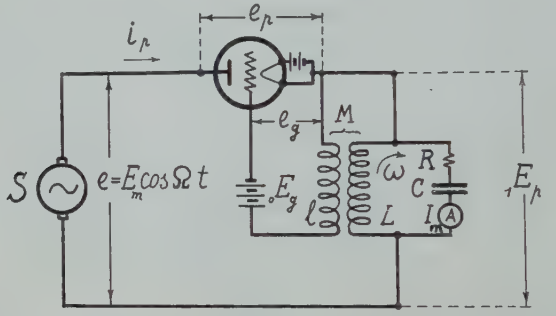

Fig. 2

If $M=0$, the current in the plate circuit in general will consist of unidirectional impulses of the frequency F, whose amplitude for a given E_m depends on the grid bias ${}_0E_g$. These impulses, when passing thru the circuit LCR will not produce any action, because this circuit is tuned to a much lower frequency f.

Suppose now, the sign and the value of the coupling to the coil l in the grid circuit, M, is properly chosen so that arbitrarily weak free oscillations are generated in the circuit LCR.

Then, with the suitable phase and amplitude of the induced e.m.f. in the coil l by the current in L, the grid potential will be less negative at certain instants causing a stronger impulse of the plate current to pass thru the triode, provided that the plate potential is also high at these instants. The coincidence of the above grid and plate potentials will occur only when F is a multiple of f, i.e., when $F=p \cdot f$ or in a certain degree even when $mF=nf$ (where p, m, and n are integer numbers).

The problem is to create conditions such that the transient plate current impulse passing through the triode each $1/f$ of a second, shall have a phase relation capable of maintaining the oscillations.

It appears that these conditions are always obtainable in a circuit which satisfies the condition of oscillation by regenerative coupling. Mathematically, the process is the following:

Referring to Fig. 2, let the a-c voltage of S be equal to

$$e = E_m \cos \Omega t = E_m \cos p\omega t. \tag{1}$$

The anode voltage is equal to

$$e_p = E_m \cos p\omega t - {}_1E_{pm} \cos \omega t \tag{2}$$

where

$${}_1E_{pm} = {}_1I_{pm} \cdot r \tag{3}$$

${}_1E_{pm}$ and ${}_1I_{pm}$ are fundamental voltage and current amplitudes, and

$$r = \frac{L}{RC} = \frac{\omega^2 L^2}{R} \tag{4}$$

for such frequency f of the circuit LCR, so that

$$\omega = 2\pi f = \frac{1}{\sqrt{LC}}. \tag{5}$$

The grid potential

$$e_g = {}_0E_g + I_m \omega M \cos \omega t = {}_0E_g + {}_1E_{pm} \frac{M}{L} \cos \omega t \tag{6}$$

where

$$I_m \leqq \frac{{}_1E_{pm}}{\omega L} \tag{7}$$

is the amplitude of the current of the frequency f in the circuit LCR. Now, let us assume the equation of the plate current characteristic is

$$i_p = \Phi\{e_g\} \tag{8}$$

and that the lumped potential

$$e_e = e_p + \mu e_g \geqq 0 \tag{9}$$

(μ being the amplification factor of the triode). Substituting (2) and (6) in (9), and (9) in (8) we obtain the expression

$$i_p = \Phi\left[E_m \cos p\omega t + \mu \cdot {}_0E_g + {}_1E_{pm}\left(\mu \frac{M}{L} - 1\right) \cos \omega t\right] \tag{10}$$

which is true when the quantity within the brackets $\geqq 0$. The form of the function determines the instantaneous values of the plate current. By analyzing (10), it is easy to deduce that the conditions will be realized conveniently by adjusting E_m, ${}_0E_g$, and M (${}_0E_g$ being negative). Then, in view of (9), the current i_p can pass only at instants determined

by the last expression within the brackets of (10). In such a way the action of the grid is analogous to the action of the loose coupling with a long thread in the former mechanical example. The plate current will then consist of impulses produced by the voltage of the frequency pf of the source S, but occurring with the frequency f, according to the action of the last expression of (10). An example of

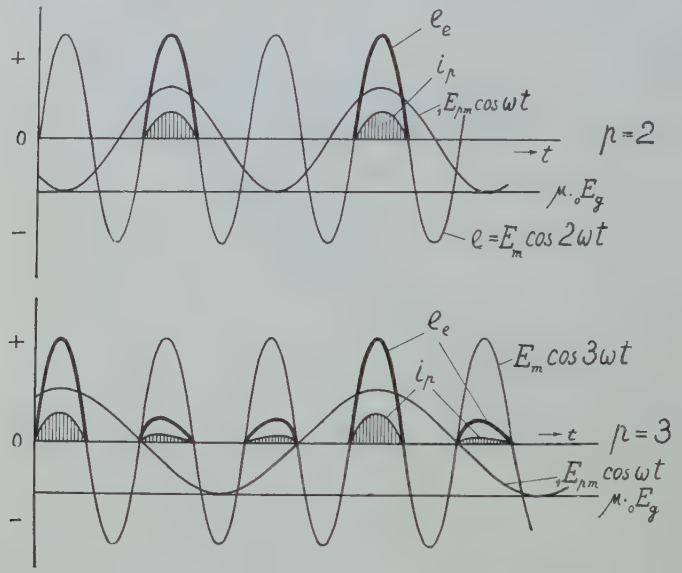

Fig. 3

the function $e_e=\Phi\{t\}$ and of its components for $p=2$ and 3, is represented in Fig. 3. If we adjust

$$_1E_{pm}\left(\mu\frac{M}{L}-1\right)\cong\mu_0 E_g \tag{11}$$

then the maximum instantaneous value of the lumped potential will be

$$e_{em}=E_m \tag{12}$$

which determines the maximum instantaneous value of the plate impulse

$$i_{pm}=\Phi\{E_m\} \tag{13}$$

This current is passing during a time approximately equal to

$$\frac{1}{2pf}. \tag{14}$$

The shape of the plate current depends on the shape of the grid-plate characteristic of the triode, i.e., the function Φ. Assuming for greater simplicity the shape of this function as

$$\begin{aligned} i_p &= \frac{e_e}{r} \quad \text{for} \quad e_e > 0 \\ i_p &= 0 \quad \text{for} \quad e_e < 0 \end{aligned} \tag{15}$$

the plate current results as a succession of impulses created by each p

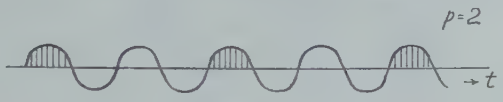

Fig. 4

half wave of one sign, selected from the sinusoid of the pulsation $p\omega$ (Fig. 4); the maximum instantaneous intensity of this impulse is

$$i_{pm} = \frac{E_m}{r}. \tag{16}$$

The plate current has undoubtedly a component of pulsation ω; which is able to maintain oscillations in the LCR circuit. With sufficient approximation it is given by

$${}_1I_{pm} \cong \frac{2E_m}{\pi r p} \tag{17}$$

where the greater the value of p, the smaller the error. The stricter values are given in Table I.

TABLE I

p	2	3	4
the component	$\frac{0.93}{\pi . r}E_m$	$\frac{0.66}{\pi . r}E_m$	$\frac{0.48}{\pi . r}E_m$

The steady component (the mean value of the current) is given by

$${}_0I_p \cong \frac{E_m}{\pi r p}. \tag{18}$$

The presence of p in the denominator of (17) indicates, that the action of the arrangement becomes poorer with the degree of the frequency division except when E_m is simultaneously increased, but this requires the use of high supply voltages.

For these reasons it is preferable to experiment with a smaller ratio p, because when p is increased the influence of capacitive currents of pulsation $p\omega$ obscures the results of the experiments.

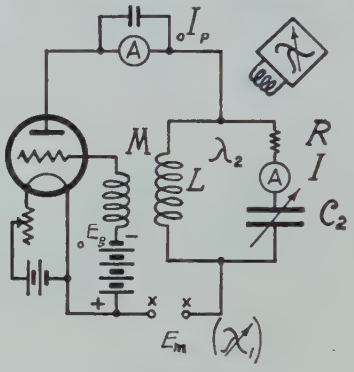

Fig. 5

We have assumed that the oscillations of the frequency f are supposed to exist already at the instant when the a-c voltage of the frequency pf begins its action. In these conditions we have to deal with a synchronization of oscillations of frequency f with those of frequency pf, with the difference that the synchronizing voltage is simultaneously the real source of the supplied energy.

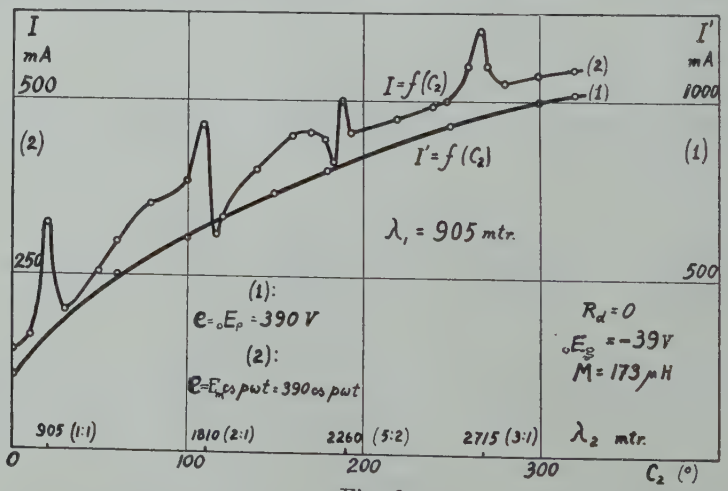

Fig. 6

These phenomena are well illustrated by the following example: A generator circuit with feed-back inductive coupling (Fig. 5) has the d-c supply across XX. Curve 1 of Fig. 6 represents the oscillatory

circuit current with various capacities (or wavelengths), and indicates that the current increases regularly with capacity.

However, when the supply voltage is alternating current of frequency $F = 333{,}300$ (λ about 900 meters) the curve has many peaks, which occur at the positions of the condenser C_2 corresponding to the

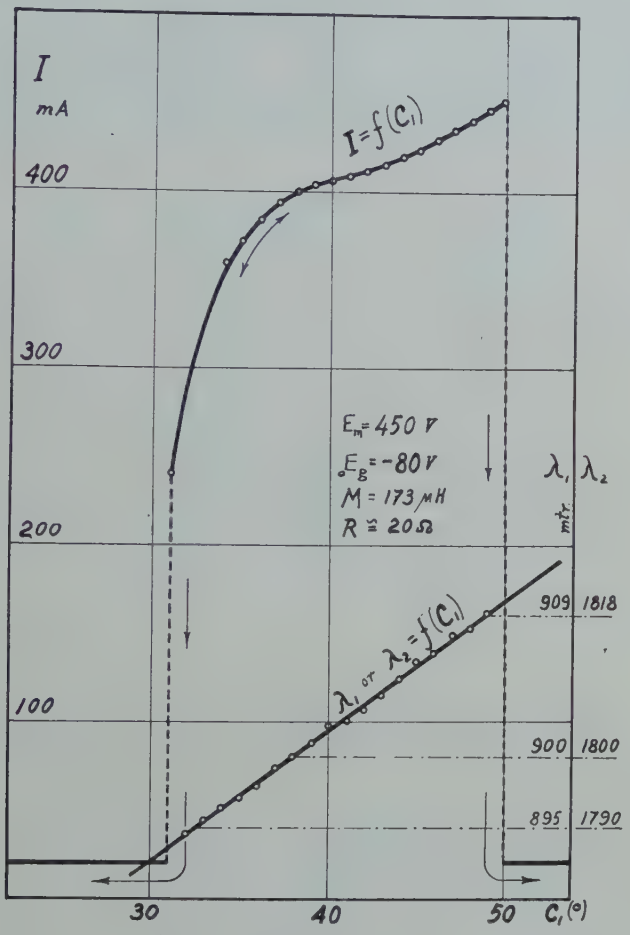

Fig. 7

natural wavelength of the circuit which is m/n times the wavelength λ, i.e., when $f = (m/n)F$, m and n being simple and small numbers.

The conclusion of a more detailed investigation of the synchronization bands is as follows: for exciting the oscillations ω in the system, a choice of electrical conditions in the circuit is possible so that the previous existence of the oscillations is not necessary at the instant

when the exciting voltage $p\omega$ is applied; i.e., in this kind of frequency division system the condition for self-excitation is also fulfilled.

Evidently, the first impulse of the applied voltage $p\omega$ on the circuit LCR is very important, especially, because the condition of the circuit required for these best conditions is very nearly the critical one for self-excitation. The circuit being regulated in this way, the oscillation circuit current detuning effect of the circuit curve is represented on Fig. 7 when the frequency is halved. Fig. 8 gives the values of the synchronization bands for various values of coupling M; in these bands the condition $\lambda_2 = 2\lambda_1$ or $f = F/2$ is strictly observed.

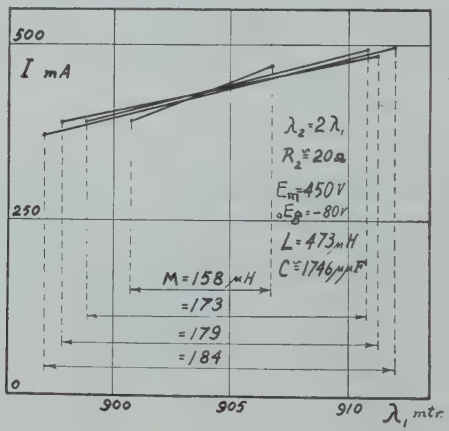

Fig. 8

The maximum permissable detuning without disturbing the synchronization is about 15 meters for a wavelength 900 meters, i.e., about 1.5 per cent.

If the circuit is not adjusted for the most critical condition, the action of the synchronizing voltage of the twice greater frequency on the circuit LCR is analogous to the case of equal frequencies. From the curves of Fig. 10, is obtained the curve of Fig. 9, giving the character of this action. The circuit LCR is tuned to the wavelength $\lambda_{20} = 1810$ meters and oscillates at that frequency, when supplied with a d-c voltage; when supplied, however, with an a-c voltage of variable frequency changed from $\lambda_1' < \lambda_{20}/2$ to $\lambda_1'' > \lambda_{20}/2$, the wavelength λ_2 of LCR deviates from the value $\lambda_{20} = 1810$ meters when λ_1 approaches the value $\lambda_{20}/2$. Then, after a sudden jump (the instant of entering into synchronization), we obtain $\lambda_2 = 2\lambda_1$. Then there occurs another sudden drop (the instant of falling out of synchronization) and the

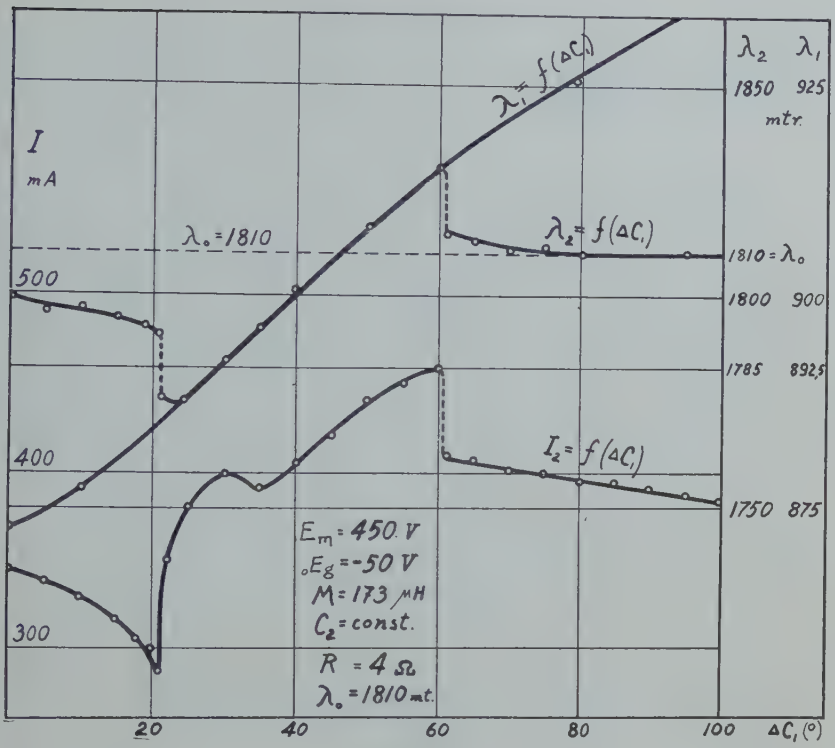
I
mA
500
400
300
$\lambda_0 = 1810$
$\lambda_1 = f(\Delta C_1)$
$\lambda_2 = f(\Delta C_1)$
$I_2 = f(\Delta C_1)$
$E_m = 450$ V
$E_g = -50$ V
$M = 173\ \mu H$
C_2 = const.
$R = 4\ \Omega$
$\lambda_0 = 1810$ mt.
20
40
60
80
100
ΔC_1 (°)
λ_2 λ_1
1850 925
mtr.
1810 = λ_0
1800 900
1785 892,5
1750 875

Fig. 9

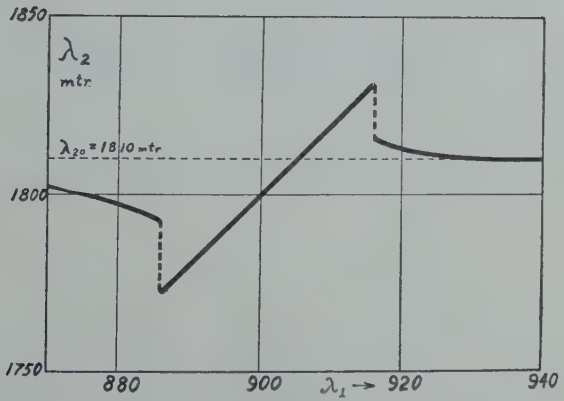
1850
λ_2
mtr.
$\lambda_{20} = 1810$ mtr.
1800
1750
880
900
$\lambda_1 \rightarrow$
920
940

Fig. 10

gradual approach to the wavelength $\lambda_{20} = 1810$ meters again. The lower curve of Fig. 10 gives the corresponding variations of the oscillating circuit current.

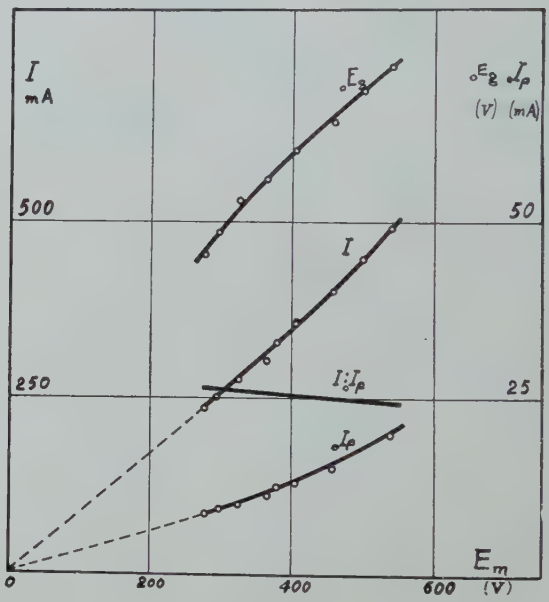

Fig. 11

In Fig. 11 the relation between the steady current component I_{ao} of the anode current and the oscillating circuit current I_m (or the alternating-current component), obtained from experimenting with the above arrangement ($\lambda_2 = 2\lambda_1$), is represented. The arrangement was adjusted to the limiting value of the grid bias $_0E_g$, the coupling M being constant. The variations of $_0E_g$ are also given. From the resulting curves the proportionality between $_0I_p$, I_m, and $_0E_g$ conform with (11), (17), and (19).

Proceedings of the Institute of Radio Engineers
Volume 18, Number 11 *November, 1930*

NOTE ON THE ACCURACY OF ROLF'S GRAPHS OF SOMMERFELD'S ATTENUATION FORMULA*

By

W. Howard Wise

(Engineer, Dept. of Development and Research, American Tel. and Tel. Co., New York City)

DR. BRUNO ROLF has recently published two papers giving graphs and tables for Sommerfeld's attenuation formula. No adequate discussion of the accuracy of this formula is given in his abbreviated communication to the Proceedings of the Institute of Radio Engineers.[1] In the original paper[2] but four sources of error are mentioned and it might be inferred that aside from them the graphs are rigorously applicable to vertical dipoles at the surface of a homogeneous earth.

It is the object of this note to point out that a number of approximations are not mentioned by Rolf and to discuss one of them. The other approximations not discussed by Rolf are not important enough to cause any great worry to an engineer trying to use the graphs; especially since they are all necessary in order that one may make a graph in the two parameters q and b.

The one approximation which it is the object of this note to discuss imposes a considerable restriction on the range of applicability of his graphs. In order to get the exponent $-\frac{1}{2}qe^{ib}$ in the ground wave it was necessary for Sommerfeld to write $i(k_1-s)r \approx \frac{1}{2}qe^{ib}$. With high frequencies and poorly conducting grounds the error so introduced is by no means negligible. The exact relation is

$$i(k_1 - s)r = \frac{\sqrt{1+\tau^2} - 1}{(\tau^2 - \tau^4)\sqrt{1+\tau^2}} qe^{ib} = (1+\zeta)\frac{1}{2}qe^{ib}$$

where $\tau = k_1 \div k_2$ and $s = k_1 \div \sqrt{1+\tau^2}$, and this defines a correction factor $\exp -\zeta\frac{1}{2}qe^{ib}$ which is lacking in the ground wave as computed by Rolf.

Taking Sommerfeld's figures for wet ground, $\epsilon = 10$ and $\sigma = 5 \times 10^{-14}$, and $\lambda = 16.6$ meters

* Decimal classification: R113. Original manuscript received by the Institute, June 3, 1930.

[1] Bruno Rolf, "Graphs to Prof. Sommerfeld's attenuation formula for radio Waves," Proc.I. R. E., **18**, 391–403; March, 1930.

[2] Numerical discussion of Sommerfeld's attenuation formula for radio waves. *Ingeniors Veterskaps Academien Handkingen*, Nr. 96, Svenska Bokhandelscentralen A.–B., Stockholm, 1929.

$$k_2^2/k_1^2 = 10 + i\,4.98$$

$$1 + \zeta = 1.02428 - i\,0.01586$$

$$b = \frac{\pi}{2} + \tan^{-1}\frac{4.98}{9} - 2\tan^{-1}\frac{4.98}{10} = 66^\circ\,0'\,38''$$

$$\tfrac{1}{2}(\cos b + i \sin b) = 0.012{,}180 + i\,0.007{,}870.$$

If $q = 28$ then $\zeta\tfrac{1}{2}qe^{ib} = 0.34103 + i\,0.22036$ and

$$\exp - \zeta\tfrac{1}{2}qe^{ib} = 0.71103/\overline{12^\circ\,37'\,33''}.$$

Thus the neglect of ζ here amounts to adding $12^\circ\,37'\,33''$ to the argument of the ground wave and increasing the modulus of the ground wave by 40.64 per cent.

If $\lambda = 50$ meters and the earth constants are unchanged

$$k_2^2/k_1^2 = 10 + i\,15$$

$$1 + \zeta = 1.006596 - i\,0.014029$$

$$b = \frac{\pi}{2} + \tan^{-1}\frac{15}{9} - 2\tan^{-1}\frac{15}{10} = 36^\circ\,24'\,59''$$

$$\tfrac{1}{2}(\cos b + i \sin b) = 0.006828 - i\,0.003700.$$

If $q = 30$ then $\zeta\tfrac{1}{2}qe^{ib} = 0.20483 - i0.11099$ and

$$\exp - \zeta\tfrac{1}{2}qe^{ib} = 0.81478\ \underline{/6^\circ\,21'\,33''}.$$

These numerical examples show that in the region of short waves and low conductivity Rolf's graphs may be considerably in error.

It is to be remarked that Sommerfeld derived the formula used by Rolf for two uses only; first, as an asymptotic formula, and observed that as such the ground wave part is uncertain; second, for the limiting case of a perfect conductor, or for short numerical distances.

Proceedings of the Institute of Radio Engineers
Volume 18, Number 11 *November, 1930*

BOOK REVIEWS

The Handbook of Chemistry and Physics, 14th edition. Published by the Chemical Rubber Publishing Company, 1900 W. 112th St., Cleveland, Ohio. 1386 pp., 4 1/4×6 3/4. Price $5.00.

"The Handbook of Chemistry and Physics" had been revised and enlarged again. The general features and scheme of arrangement which have been used in former editions have been retained. Material on all branches of chemistry and physics and the closely allied sciences which would be likely to find extended use has been included to the exclusion of material of use only in certain highly specialized lines of work.

There are fourteen main sections as follows: Mathematical Tables, General Chemical Tables, Properties of Matter, Heat, Hygrometric and Barometric Tables, Sound, Electricity and Magnetism, Light, Definitions and Formulas, Laboratory Arts and Recipes, Photographic Formulas, Measures and Units, Wire Tables, and Problems.

The mathematical tables will illustrate the general nature of the contents of the individual sections. These contain tables of: five-place logarithms, four-place logarithms, natural trigonometric functions of angles for each minute from 0 to 360 degrees, logarithms of the trigonometric functions for each minute from 0 to 360 degrees, Naperian logarithms of numbers from 1 to 1109, exponentials, hyperbolic functions, degrees-radians, reciprocals, powers and roots of numbers, circumferences and areas for numbers from 1 to 1000, formulas from algebra, geometry, trigonometry, analytical geometry, and short tables of differentials and integrals.

Purely radio data tables are not very plentiful. There are formulas for the calculation of inductance, capacitance, and high frequency resistance. Also there are frequency-wavelength-*LC* conversion tables.

This edition is printed on the same thin paper and has the same flexible binding as previous editions. Although it cannot be considered as a vest pocket handbook it is nevertheless a very manageable book in spite of its 1386 pages.

S. S. Kirby*

* Bureau of Standards, Washington, D. C.

Alternating-Current Rectification and Allied Problems, by L. B. W. Jolley. John Wiley & Sons Inc., New York, 1928, 521 pp., 374 figures. Price $6.00.

This is the third edition of this book since its original publication in 1925.

The treatment of the subject is comprehensive, Part I being devoted to the mathematical fundamentals, the next four parts to specific types of rectifiers and the concluding three parts to allied problems.

The many tables and schematic diagrams make the book useful to engineers for reference purposes.

One feature of the book is the grouping together of references at the end of each chapter or portion of a chapter devoted to a particular phase of the subject. This is convenient from the viewpoint of a study of a particular subject but not so convenient as the usual subscript form from the viewpoint of the reader interested in a certain detail.

The American engineer engaged in rectifier work is apt to be a little disappointed in the absence of descriptive material on recent American developments, such as the hot-cathode mercury-vapor rectifier, the thyratron, and the grid-glow tube. However, such material can hardly be expected in view of the date of the third edition.

The increased activity and interest in rectifiers in the broad field of electrical engineering coupled with the thoroughness of the plan of this book leads to the hope that it will be revised from time to time as the art progresses.

W. C. White†

† General Electric Co., Schenectady, N. Y.

BOOKLETS, CATALOGS, AND PAMPHLETS RECEIVED

Copies of the publications listed on this page may be obtained gratis by addressing a request to the manufacturer or publisher.

Type 404 test signal generator is described in catalog supplement F-200 of the General Radio Co., Cambridge, Mass.

Supplement No. 2 to Bulletin No. 100, of the Roller-Smith Co., 233 Broadway, New York City, describes their type PD direct-current voltammeters for signal systems and general testing.

A thirty-four page booklet, "The Photolytic Cell," published by the Arcturus Radio Tube Co., of Newark, N. J. describes photo-electric phenomenon, and gives information for the correct use of photo cells.

The Aerovox Wireless Corporation, 70–82 Washington St., Brooklyn, N. Y , publishes a thirty-two page manual on the uses, advantages and limitations of electrolytic condensers.

A six-page engineering bulletin giving characteristics of CX-326 and C-327 tubes is available from E. T. Cunningham, 370–7th Ave., New York.

Jenkins and Adair, 3333 Belmont Ave., Chicago, issue the following bulletins:

No. 14. A portable amplifier for broadcast pick-up work is described.

Transmitting condensers and inductances are described in bulletin 9A.

An audio amplifier for speech input, recording, and similar work is described in bulletin No. 15.

"Hum Must Go" is the title of a folder of the Sprague Specialities Co. of Quincy, Mass., describing electrolytic condensers.

Several types of vacuum thermocouples are described in an eight-page folder issued by the Thermal Instrument Co. 38 Woods Ave., Somerville, Mass.

The Supreme Instruments Corp. of Greenwood, Miss., publishes several folders describing broadcast receiver servicing equipment. One of these describes their complete line of service equipment. Another folder describes their model 90 set analyzer.

Several folders issued by the American Transformer Co. of 178 Emmet St., Newark, N. J., have recently been received:

Amertran audio transformers are described in bulletin 1065.

Bulletin 1066 describes filament heating transformers, and filter and modulation chokes.

A three-unit concert hall amplifier and power supply unit for relay rack mounting is described in bulletin 1077.

Bulletin 1078 describes type PA-51 and type PA-70 concert hall amplifiers for relay rack mounting.

Two- and three-stage audio amplifiers are described in bulletin 1079.

REFERENCES TO CURRENT RADIO LITERATURE

THIS IS a monthly list of references prepared by the Bureau of Standards, and is intended to cover the more important papers of interest to the professional radio engineer, which have recently appeared in periodicals, books, etc. The number at the left of each reference classifies the reference by subject, in accordance with the "Classification of Radio Subjects; an Extension of the Dewey Decimal System," a revised edition of Bureau of Standards Circular No. 138 which appeared in full on pp. 1433–1456 of the August, 1930, issue of the PROCEEDINGS of the Institute of Radio Engineers. The classification numbers are in some instances different from those used in the earlier version of this system (first edition of Circular 138) used in the issues of other PROCEEDINGS of the Institute of Radio Engineers before the October, 1930 issue.

The articles listed are not obtainable from the Government or the Institute of Radio Engineers, except when publications thereof. The various periodicals can be secured from their publishers and can be consulted at large public libraries.

R000. RADIO COMMUNICATION

R050 Dellinger, J. H. and Jolliffe, C. B. Classification of radio subjects; an extension of the Dewey decimal system. PROC. I. R. E., **18**, 1433–56; August, 1930.

A systematic scheme of classification of subjects in radio science and engineering is necessary in classifying references to current radio publications and also for classifying all sorts of radio material, such as reports, reprints, drawings, books, apparatus, etc. In an effort to fill the need for a radio classification this extension of the Dewey decimal system was prepared. Since the publication of the first edition of this circular, in 1923, the subject classification it presents has been used extensively by many radio research workers and engineers as well as by the radio section of the Bureau of Standards. The present edition brings the classification up to date and makes a few changes which use has shown to be necessary.

R100. RADIO PRINCIPLES

R113 deMars, P. A., Kenrick, G. W., Pickard, G. W. Low-frequency radio transmission. PROC. I. R. E., **18**, 1488–1501; September, 1930.

This paper presents the results of field intensity measurements on low-frequency transmission (17.8 kc) from the R.C.A. station WCI, located at Tuckerton, N.J. The results of observations made at Newton Centre and at Medford, Mass., are presented. Apparatus for alternating antenna observations with variously oriented loop observations is described and the results of such measurements are presented. The relation of the state of elliptical polarization of received signals to loop responses for various positions of the loop is investigated theoretically, and the results thus obtained are applied to an interpretation of the observations. The necessary approximations required to render this problem determinate are pointed out and their questionable validity emphasized. The mean of the received signal intensity in the absence of magnetic disturbances is lowest during the night, and strong sunrise and sunset peaks are found. An inversion of received signal intensity is noted during magnetic storm conditions. At such times the night field strength exceeds the day field.

R113.2 Austin, L. W. Long wave radio receiving measurements at the Bureau of Standards in 1929. PROC. I. R. E., **18**, 1481–87; September, 1930.

This paper gives monthly averages of daylight signal intensity at Washington for 1929, as received from a number of European and American low-frequency stations. Several of the stations formerly measured have ceased to transmit regularly at hours suitable for all-daylight transmission paths and their measurement has therefore been discontinued. The annual average field intensities of the European stations have not shown much change since last year, but the atmospheric disturbances have increased.

R113.6 Verman, Lal. C. Reflection of radio waves from the surface of the earth. Proc. I. R. E., **18**, 1396–1432; August, 1930.

The reflection of an elliptically polarized electromagnetic wave from partially conducting and perfectly conducting surfaces is studied in detail. It is shown that in either case the interference of incident and reflected waves gives rise to a pseudo stationary wave field above the surface of the reflector. This field is bodily propagated along the horizontal projection of the direction of the incoming wave at a velocity greater than that of light, i.e., $c/\sin \alpha$ where α is the angle of incidence. The resultant field at any given point lies in a plane whose orientation varies with height. This fact is made the basis of experimental measurements. It is found that the 43-meter wave from WIZ, located at New Brunswick, N.J. holds its polarization and angle of incidence constant during morning hours at Ithaca, N.Y. The rapid fading that accompanies the signal is attributed to purely amplitude fluctuations. Observations on this station are analyzed and it is shown on the basis of the above theory, how it is possible to obtain the angle of incidence as well as the complete information regarding the polarization of the incoming wave. Measurements on almost all other stations ranging from 25 to 50 meters wavelength show highly erratic conditions.

R114 Baümler, M. Gleichzeitige Luft und Kabelstörungen. (Simultaneous static interference in the air and in cables.) *Elek.-Nach. Technik*, **7**, 325–330; August, 1930.

A report on experiments in which a recording oscillograph was used to show that interference experienced in undersea cables and static interference in radio, are both caused by the same electrical disturbances.

R125 Southworth, G. C. Certain factors affecting the gain of directive antennas. Proc. I. R. E., **18**, 1502–1536; September, 1930.

An analysis is given of the performance of antenna arrays as influenced by certain variables within the control of the engineer. Starting with an extremely simple analysis of the interfering effects produced by two sources of waves of the same amplitude, and followed by an analysis of unidirectional couplets and linear arrays. Directional diagrams for various arrays are given and a mathematical appendix gives general equations for calculating directional diagrams and gains of linear arrays.

R131 Bligh, N. R. A note on an alternative equivalent circuit for the thermionic valve. *Exp. Wireless & W. Engr.* (London), **7**, 480–481; September, 1930.

A discussion of the advantages of an alternative equivalent circuit for the vacuum tube, which involves the replacement of the constant e.m.f. generator and series resistance by a constant current generator and shunt resistance.

R131 Caporale, P. A note on the mathematical theory of the multielectrode tube. Proc. I. R. E., **18**, 1593–99; September, 1930.

The expression for the a-c current (rather the change in current due to applied a-c voltages) in any electrode is expanded in an ascending power series in terms of all the applied a-c voltages. It is shown that the coefficients in these series must satisfy a number of systems of linear simultaneous equations (one system for each power and frequency of the currents), and that hence to obtain the coefficients in any particular case it is merely necessary to set up these equations and solve them. The solution of the equations of course increase in complexity as the number of electrodes increases. The development does not make any assumption of approximation, although in the discussion only the terms of the first and second degree are considered. It is shown, however, that however slow be the convergency of the series, the coefficients must always satisfy similar sets of algebraic equations.

R133 Möller, H. Der Mechanismus der Barkhausen Schwingungen. (The mechanism of Barkhausen oscillations.) *Elek. Nach. Technik*, **7**, 293–306; August, 1930.

A theoretical treatment of Barkhausen oscillations. Proceeding from the fundamental principals governing oscillating systems, the author derives formulas which explain how the three-electrode vacuum tube functions as an oscillator, when its grid is positive and its plate is negative or neutral. The author's conclusions have been experimentally verified.

R134 Herd, J. F. Some measurements on optimum heterodyne. *Exp. Wireless & W. Engr.* (London), **7**, 493–99; September, 1930.

Experimental results show, that when a triode tube is operating as an anode-curvature detector with local heterodyne, there is a value of heterodyne voltage for which the audio-frequency output, due to the formation of beats is a maximum. With this optimum value of heterodyne voltage, the audio-frequency output varies linearly with small input signal voltages, while the output from small signals may be several hundred

times that which would accrue with a heterodyne voltage equal to the small signal. The use of such an optimum heterodyne may tend to equalize the performance, as rectifiers, of tubes which appear different in details of their rectifying characteristics.

R142 Petrizilka, V. Zur Theorie zweier gekoppelter Schwingungskreisen. (A contribution to the theory of two mutually coupled circuits.) *Elek.-Nach. Technik*, **7**, 318–324; August, 1930.

The author advances a simplified method for the mathematical analysis of coupled circuits. This method enables the determination of resonance curves from a consideration of the energy added to the system containing two coupled circuits.

R148.1 Eckersley, T. L. Frequency modulation and distortion. *Exp. Wireless & W. Engr.* (London), **7**, 482–84; September, 1930.

The author offers an explanation of the distortion observed in short wave radio telephonic communication. Such distortion is known to occur only when frequency modulation occurs at the transmitter and is due to beat tones in the receiving set between the carrier and side bands arriving via one path and the carrier and side bands arriving via another path of two or three milliseconds delay.

R170 Ballantine, S. Fluctuation noise in radio receivers. Proc. I. R. E., **18**, 1377–87; August, 1930.

This paper discusses fluctuation noise in radio receivers due to shot and thermal effects (Schottky) in the radio-frequency circuits. The r-f noise components beat with the carrier when a signal is being received and are transformed to audio components, which are heard as a hissing noise. The mathematical theory for a receiver employing a square-law detector is given, and it is shown that the deflection of a meter measuring the average square of the voltage or current due to the noise is proportional to the area under the curve representing the square of the over-all transmission against frequency. The over-all transmission is somewhat analogous to the over-all fidelity of the receiver. This result is similar to the well known laws for simple linear networks without frequency transformation. The method of calculating the noise due to the shot and thermal effects is discussed. Finally a convenient method of measuring the specific noise (noise per frequency interval) in a radio receiver is described, and results for several typical commercial receivers are given. The method consists in comparing the noise, as referred to the antenna circuit, with the amplitudes of the side bands, mE_0, in a standard modulated signal.

R200. Radio Measurements and Standardization

R210 Case, N. P. A precise and rapid method of measuring frequencies from 5 to 200 cycles per second. *Bureau of Standards Jour. of Research*, **5**, 237–42; August, 1930. Proc. I. R. E., **18**, 1586–92; September, 1930.

A method of measuring frequencies from 0 to 200 cycles is described, which combines accuracy to within 1/10 of a cycle with ease and rapidity of use. The method depends on the fact, that if a condenser be discharged through a resistance f times per second (the condenser being charged to the same initial voltage each time), then the average voltage drop across the discharging resistance is directly proportional to f. The voltage drop is balanced, through a sensitive galvanometer and high resistance, against a known function of the total voltage drop along a slide wire resistance shunted around a storage cell. After calibration, it is possible to read unknown frequencies directly from the slide wire.

R213 Clapp, J. K. Interpolation methods for use with harmonic frequency standards. Proc. I. R. E., **18**, 1575–85; September, 1930.

Interpolation methods for determining the value of an unknown frequency in terms of harmonic standard frequencies are discussed under the four following classifications; (1) direct beating methods; (2) direct interpolation methods; (3) harmonic interpolation methods; (4) modifications of methods discussed under number 3. Advantages, disadvantages, and limitations of the various methods are considered.

R230 Wilmotte, R. M. Capacitative and inductive coupling including a method of measuring mutual inductance at radio frequencies. *Exp. Wireless & W. Engr.* (London), **7**, 485–92; September, 1930.

It is shown how inductive coupling may be replaced by an equivalent capacitive coupling and vice versa. The methods of transformation lead to a simple method of measuring the mutual inductance between two coils. Further applications and some limitations of the transformation method are discussed.

R243.1 Benecke, H. Hochempfindliches Röhren-Voltmeter. (A very sensitive vacuum-tube voltmeter.) *Zeits für Technische Physik*, **9**, 361, 1930.

A vacuum tube voltmeter, which uses an auxiliary alternating current is described. It has a strictly linear calibration curve and its sensitivity is such that a-c voltages of the order of a fraction of a millivolt may be read directly from the indicating instrument. The application of this device using a Wheatstone bridge circuit is also given.

R243.1 Moullin, E. B. Some developments of the thermionic voltmeter. *Jour. I. R. E.*, (London), **68**, 1039–51; August, 1930.

In this paper the various ways are considered in which a three-electrode tube may be used in a thermionic voltmeter, and the author's accumulated experience of several years' work in making vacuum tube voltmeters for various purposes is described. No one arrangement can possess every desirable property, and it is shown how to produce a voltmeter to fulfill specified requirements. The effective input resistance of the various arrangements, and the harmonic currents produced by grid current, are considered analytically and experimentally. The effect of range and sensitivity of providing additional batteries is also discussed, extra batteries being found to be an advantage only in very low range instruments. The effect on the calibration, of a change in the tube and in temperature is found to depend on the form of the rectifier used. In general a vacuum tube voltmeter cannot read r.m.s. values. The wave-form error of various systems is investigated; with one arrangement the reading is proportional to the peak voltage and in another to the mean. The possibility of a frequency error is negligible for frequencies up to 1000 kilocycles per second, whilst from indirect tests it would appear that the error is probably negligible for frequencies up to 30 times this value.

R243.1 King, R. A screen-grid voltmeter and its application as a resonance indicator. Proc. I. R. E., **18**, 1388–95; August, 1930.

A screen-grid voltmeter of high sensitivity is described and compared with a triode voltmeter. At low frequencies using either the 222 or the 224 tube, it effectively covers a range from 0.1 to 10 volts, r.m.s. At frequencies of the order of 10^8 cycles per second, it serves as a supersensitive indicator for a Lecher wire system. For this purpose a tuned input is used.

R261 Farnham, P. O., and Barber, A. W. Problems involved in design and use of apparatus for testing radio receivers. Proc. I. R. E., **18**, 1338–50; August, 1930.

This paper deals briefly with: (1) the desirable characteristics of measuring equipment employed in making the usual tests of radio receiver performance and (2), a description of apparatus and technique used in carrying out several special tests. Measuring equipment and methods are discussed with reference to the elements of the receiver, after which, are remarks on the usual tests of sensitivity, selectivity, and fidelity. Under special test is a discussion of measurement on hum, tube and circuit noise, modulation, distortion, intermodulation, audio harmonic analysis, and volume control. Some specimen curves showing results obtained on model receivers are presented.

R281 Brown, W. W. Properties and applications of mycalex to radio apparatus. Proc. I. R. E., **18**, 1307–15; August, 1930.

A description is given of a new type of molded insulation having a low dielectric loss, high dielectric strength, high tensile strength, and high resiliency. These properties, in combination found in mycalex in a higher degree than in any other one material, explain the rapid increase in applications of this material in radio apparatus, particularly transmitters.

R300. Radio Apparatus and Equipment

R325.31 Barfield, R. H. Recent developments in direction-finding apparatus. *Jour. I. E. E.*, (London), **68**, 1052–75; August, 1930.

Part 1 describes a four-aerial direction-finding system, based on the Adcock principle. Tests with this apparatus at wavelengths of 300 to 600 meters show that it is considerably superior to the closed loop system for conditions of "night effect," but indicate a residual instrumental error of the system in the presence of downcoming waves. Part 2 describes two distinct types of portable short wave direction finding apparatus working from 12 to 60 meters. The first is a totally screened closed loop type. The second is of the rotating Adcock type. Observations on the ground wave show both instruments equally satisfactory and similar in performance to the longer wave apparatus, while at ranges beyond the skip distance the Adcock type is superior to the other.

R339 Sashoff, S. P. The power grid-glow tube. Electric *Jour.*, **27**, 486–89; August, 1930.

On the characteristics of the power grid-glow tube. By means of this recent development of the grid-glow tube, engineers are able to control large amounts of power with a minimum number of relays.

R355.6 Gunn, R. A new frequency stabilized oscillator system. PROC. I. R. E., **18**, 1560–74; September, 1930.

Describing a new vacuum tube self-oscillating system having extraordinary frequency stability. It functions by virtue of reëntrant circulation of oscillations through tuned filter or coupling units. The methods and necessary precautions for attaining frequency stability are given. Frequency shifts due to ordinary variations of plate potentials, filament current, or keying are found to be of the order of one one thousandth of one per cent.

R365.2 Clarke, H. M. Moving coil loud speakers. Exp. *Wireless & W. Engr.* (London), **7**, 477–80; September, 1930.

A contribution to the theory involved in predicting the performance of a moving coil loud-speaker from its dimensions and operating conditions.

R381 Edelman, P. E. Dry electrolytic condensers. PROC. I. R. E., **18**, 1366–71; August, 1930.

Operating characteristics, of compact, dry, electrochemical, high voltage, filter condensers, comprising a dielectric plated sheet electrode contacting with a gummed spacer rolled with an untreated electrode sheet, show that such condensers are in all respects suitable for power-pack filter service and effect large reduction in cost. Commercial condensers of this type have working voltages up to 700 volts direct current. The leakage current, which determines the merit of an electrochemical condenser, is extremely small in the case of the gum condenser and affords a very long operating life. Gum condensers are operable in the extreme temperature range from −30 deg. F through +250 deg. F.

R500. APPLICATIONS OF RADIO

R561 Stoner, F. E. War Department message center. PROC. I. R. E., **18**, 1372–76; August, 1930.

A description of the new high-frequency beam transmitting station of the Signal Corps and the methods of handling heavy radio traffic for the 55 government bureaus it serves.

R590 Roters, H. C., and Paulding, H. L. Radio electric clock system. PROC. I. R. E., **18**, 1537–59; September, 1930.

This paper describes briefly a clock system, which employs radio time signals from a government station to correct automatically an electric clock system. As interference is the usual limitation of a system of this sort, special emphasis has been placed upon the pulse amplifier, by means of which pulses of a periodic character are amplified with an extremely high selectivity against interference. The mathematical theory of this amplifier is developed in detail, and response curves for several stages are drawn.

R700. RADIO MANUFACTURING

R700 Graham, V. M., and Olney, B. Engineering control of radio receiver production. PROC. I. R. E., **18**, 1351–65; August, 1930.

A brief discussion of a system of radio receiver production testing and inspection backed up by "proving" inspection and engineering laboratory checks, which gives close control of production quality to the radio engineering department, thereby enabling the quality and uniformity of the product to be continuously maintained at the high standards set by the engineers.

R800. NONRADIO SUBJECTS

538.11 Muzzey, D. S. Jr. Some measurements of the longitudinal elastic frequencies of cylinders using a magnetostriction oscillator. *Phys. Rev.*, **36**, 935–47; September 1, 1930.

Cylindrical rods cut from two samples of stainless steel were excited to longitudinal vibration in a magnetostriction oscillator and the resonant frequencies at which the rods control the oscillator were measured by beating with a crystal oscillator of known frequency. Many rods of each material were measured in order to test the theoretical relation given by Lord Rayleigh between the natural longitudinal frequency and the dimensions, in particular the effect of the diameter of the rod on its frequency.

621.385.96 Evans, P. H. A comparison of the engineering problems in broadcasting and audible pictures. PROC. I. R. E., 18, 1316–37; August, 1930.

Attention is called to the principal difference between the present success of audible pictures and the failures which preceded it. The similarities and differences between broadcasting and audible pictures are pointed out. This includes a comparison of the installation, a comparison of the pick-up and reproduction conditions, etc. Some of the advantages of disk recording are pointed out. Measurements of the acoustical characteristics of recording stages and theaters are given, as well as system frequency characteristic. The factors limiting the frequency range on this recording are discussed. Some of the problems in sound editing are mentioned and the elements in greatest need of improvement are pointed out.

CONTRIBUTORS TO THIS ISSUE

Curtis, F. W.: Born November 15, 1905. Received A. B. degree, Colorado College, 1928. Westinghouse Engineering School, August, 1928; junior physicist, Naval Research Laboratory, 1928 to date. Associate member, Institute of Radio Engineers, 1929.

Groszkowski, Janusz: Born 1898 at Warsaw, Poland. Received Doctor of Technical Science degree, Warsaw Polytechnical High School, 1927; professor, Warsaw Polytechnical High School, 1929. Director, Radio Institute, Poland. Nonmember, Institute of Radio Engineers.

Jimbo, Seikichi: Born February, 1896. Educated at Imperial University, Japan. Entered electrotechnical laboratory, Ministry of Communications, Tokyo, 1919; Japanese delegate, advisory committee of electrical standards, Paris, 1928. Associate member, A. I. E. E. Associate member, Institute of Radio Engineers, 1930.

Koga, Issac: Born December 5, 1899 at Kashii, near Fukuoka, Japan. Received E. E. degree, Tokyo Imperial University, 1923; University Hall student, Tokyo Imperial University, 1923–1925; lecturer, Tokyo Imperial University, 1925 to date; Electrical Research Institute, Tokio Municipality, 1926–1929; assistant professor, Tokyo University of Engineering, 1929 to date. Nonmember, Institute of Radio Engineers.

Page, Robert M.: Born June 2, 1903 at St. Paul, Minnesota. Received B. S. degree in physics, Hamline University, 1927. Engaged in radio research and precision measurements, U. S. Naval Research Laboratory, 1927 to date. Associate member, Institute of Radio Engineers, 1927.

Prescott, Maurice L.: Born August 8, 1900 at Antelope, Texas. Received B. S. degree, University of Oklahoma, 1924. Testing department, General Electric Company, 1924–1926; radio engineering department, 1926 to date. Member, Institute of Radio Engineers, 1928.

Wise, W. Howard: Received B. S. degree, Montana State College, 1921; M. A. degree, University of Oregon, 1923; Ph. D. degree, California Institute of Technology, 1926; Department of development and research, American Telephone and Telegraph Company, 1926 to date. Nonmember, Institute of Radio Engineers.